INSTITUT LAUE - LANGEVIN **ANNUAL REPORT** 2013

71, avenue des Martyrs - 38000 Grenoble - France - http://www.ill.eu
This report has been printed using FSC certified paper (http://www.fsc.org/)
SYNTHESE ECA - Tél. 04 76 90 02 73

The world's leading facility in neutron science and technology

CONTENTS

PUBLISHING INFORMATION

Editors: Giovanna Cicognani and Helmut Schober
Production team: Giovanna Cicognani, Alison Mader, Robert Corner and Susan Tinniswood
Design: www.synthese-eca.com - **Printing:** Imprimerie du Pont de Claix
Photography: ILL (unless otherwise specified)

Further copies can be obtained from Institut Laue-Langevin
Scientific Coordination Office (SCO)
BP 156 F-38042 Grenoble Cedex 9 (France)
Email: sco@ill.eu – web: www.ill.eu

NEUTRONS FOR SCIENCE®

DIRECTOR' FOREWORD

The latest cycle of reincarnation – the Millennium Programme - has brought astonishing gains, increasing the average detection rate across the instrument suite by a factor of more than 24 already, and transforming the scope and capacity of the science we support

It is now more than 40 years since the first neutron experiments were conducted at ILL, and although accounts vary over what was the first sample to be studied, and who carried out the measurement, there is no dispute that by the end of the 1970s the ILL had established itself as a world-leading centre for science. That remarkable success is a testament to the vision and skill of ILL's founding fathers and the band of pioneering scientists, engineers and technicians who created it. What is also remarkable is how well ILL has stood the test of time: it still leads the field of neutron science and technology and far from being an 'old' or even 'middle-aged institute', almost every technical component between the source and the detectors on our instruments has been upgraded at least once.

The latest cycle of reincarnation – the Millennium Programme - has brought astonishing gains, increasing the average detection rate across the instrument suite by a factor of more than 24 already, and transforming the scope and capacity of the science we support. 2012 saw first neutrons on the third small-angle instrument D33, optimised for magnetic studies from day one, and with a time-of-flight option that enables structure to be studied on an unprecedented range of length-scales in a single shot. We also welcomed back the greatly upgraded cold triple-axis CRG spectrometer IN12, which now contends with our public instrument IN14 as class-leader, and throws down the gauntlet to the team who will upgrade it to ThALES. And the cold-neutron Laue instrument LADI returns to a new position with a new guide, boosting its flux and pushing back the boundaries of biological crystallography way beyond what seemed reasonable 5 and more years ago.

The Millennium Programme still has two years to run, but the process of renewal should not end there. It is vital to the health both of our Institute and the broader scientific community that we continue to explore and exploit the limits of what is possible in instrumentation. To this end, four years of consultation and planning will deliver in 2013 the case for the next wave of our upgrade Programme, christened 'Endurance' to signal our aim to continue to lead for years to come. 2013 will therefore be crucial for ILL: approval and funding for the Endurance Programme will not only lever significant further improvements in performance, but much of the technical development we propose should also be applied further afield in other neutron centres. Not least among these will be the next-generation European Spallation Source in Lund as it ramps up to full scientific strength by the end of the next decade.

Elsewhere at the ILL other major projects abound. Post-Fukushima work is well underway to strengthen our defences further against yet more improbable circumstances: in this we are very fortunate to be able to receive prompt and generous additional funding from our Associates, strong political support from our host country, France, and tremendous expertise and determination on the part of many ILL staff to deliver this project. We will also soon have a new 'Science Building', funded by the city of Grenoble and the Rhône-Alpes region, to house facilities shared with the ESRF: a common theory group, joint chemistry laboratories and the Partnership for Soft Condensed Matter will all be housed therein, together with members of both institutes to establish a vigorous new scientific community, particularly for large-scale structures. Further afield, the rest of the 'Presqu'île Scientifique' is also in the midst of major reconstruction, with new facilities for research, innovation and education promised for the members of the GIANT partnership (ILL, ESRF, EMBL, with the laboratories of the CEA and CNRS as well as local universities). The accent on 'innovation' marks a new departure for ILL, with additional funding to establish with ESRF new interface facilities for industrial users.

Of course the real strength of ILL is human – represented both by expert staff and a vibrant user community – and we paid tribute to some of them in 2012. We celebrated two 80th birthdays in 2012: that of the neutron itself – or rather its first public announcement by James Chadwick – as well as Philippe Nozières, the first head of our theory group and still playing a key role in the intellectual life of the ILL. We feted the remarkable contribution of his successor, Efim Kats, as well the many and varied contributions of Alan Hewat – one of that original pioneering band referred to above – and Joe Zaccai, whose has done so much to bring biology to the ILL, and vice versa. We also saw the departure of José Luis Martínez Peña, who came to the end of his term of office as French Associate Director: José Luis brought great clarity and rigour to the planning and delivery of the Millennium Programme – indeed to all aspects of the life of ILL in which he was involved – and we salute him for that: muchas gracias y hasta pronto! He gives way to Charles Simon, a long-term user of ILL who brings much "savoir-faire" in matters scientific, technical and political. Finally, we note the passing of the "baton" from Martin Walter to Manuel Rodriguez-Castellano as Head of Administration. Martin held the fort magnificently during an unexpected interregnum period, while Manuel brings decades of experience working for our neighbours, the ESRF: bienvenido !

Of course this is all part of the much broader renewal of staff who have contributed in very different but no less crucial ways. This point is made most clearly each year at the General Assembly for retired ILL staff: looking out towards old friends and colleagues in our Chadwick Amphitheatre it is humbling to be reminded of the roles they have played in ILL's success. This success is all the more remarkable for the diversity of the actors, with very different skills and cultural backgrounds yet bound through the generations to a common purpose: truly an example of a 'Europe that works'.

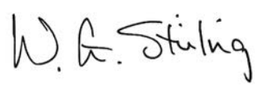

Prof. W.G. Stirling
Director of the ILL

ABOUT THE ILL

The Institut Laue-Langevin (ILL) is an international research centre at the leading edge of neutron science and technology, where neutrons are used to probe the microscopic structure and dynamics of a broad range of materials at molecular, atomic and nuclear level.

The ILL is owned by the three founding countries - France, Germany and the United Kingdom. The three Associate member countries contributed a total of about 63M€ to the Institute in 2013, a sum enhanced by significant contributions from the ILL's Scientific Member countries, Austria, Belgium, the Czech Republic, Denmark, Hungary, India, Italy, Poland, Spain, Slovakia, Sweden and Switzerland. ILL's overall budget in 2013 amounted to approximately 100.5M€.

The Institute operates the most intense neutron source in the world, based on a single-element, 58.3 MW nuclear reactor designed for high brightness. The reactor normally functions round-the-clock during four 50-day cycles per year, feeding neutrons to a suite of 40 high-performance instruments that are constantly upgraded.

As a service institute, the ILL makes its facilities and expertise available to visiting scientists. Our user community is world-wide: every year, about 2000 researchers from more than 30 countries visit the ILL to perform over 800 experiments selected by a scientific review committee.
The ILL monitors the papers published as a result of the use of our facilities, of which there are – on average – about 600 per year. We pay particular attention to papers published in high-impact journals. About 80 such papers are published per year from data taken on ILL instruments. This is a factor of two higher than the second most productive neutron source in the world.

The Institute has a Director and two Associate Directors who represent each of the Associate countries and are appointed on short-term contracts, normally for five years. A Scientific Council, comprising external scientists from the member countries, advises the Directors on scientific priorities for the Institute and how to develop the instrument suite and technical infrastructure in order to best meet the needs of the user research programme. It also assesses the scientific output of the Institute. Our governing body is the Steering Committee, which meets twice yearly and is made up of representatives of the Associates and the Scientific Members together with the Directors and Staff Representatives. Within the framework of the Intergovernmental Convention, the Steering Committee has the ultimate responsibility for determining operational and investment strategies for the Institute.

NEUTRONS AND SOCIETY

The scope of the research carried out at the ILL is very broad, embracing condensed matter physics, chemistry, biology, materials and earth sciences, engineering, and nuclear and particle physics. Much of it impacts on many of the challenges facing society today, from sustainable sources of energy, improved healthcare and a cleaner environment to new materials for information and computer technology.
For example, neutron scattering experiments have given us new insights into the structure and behaviour of biological and soft condensed matter, important in designing better drug delivery systems or improving polymer processing. They also provide a unique probe into the phenomena that underpin high-temperature superconductivity or the molecular magnetism that may provide the technology on which the computers of the future are based.

PREPARING FOR THE FUTURE

In 2001, the ILL launched an ambitious programme to modernise its instruments and infrastructure called the ILL Millennium Programme, whose aim was to optimise the ILL's instrument suite (Phase M0: 2001-2008; Phase M1: 2008-2014). We are now looking forward to and setting the scene – in the framework of our ENDURANCE programme - for developments still further into the future, in order to maintain the Institute's world-leading position for another 20 years.

WHY NEUTRON SCATTERING IS USEFUL

When used as a probe for small samples of materials, neutron beams have the power to reveal what is invisible using other radiations. Neutrons can appear to behave either as particles or as waves or as microscopic magnetic dipoles and it is these specific properties which enable them to uncover information which is often impossible to access using other techniques.

WAVELENGTHS OF TENTHS OF NANOMETERS

Neutrons have wavelengths varying from 0.01 to 100 nanometers, which makes them an ideal probe of atomic and molecular structures ranging from those consisting of single atomic species to complex biopolymers.

ENERGIES OF MILLIELECTRONVOLTS

The associated energies of millielectronvolts are of the same magnitude as the diffusive motions of atoms and molecules in solids and liquids, the coherent waves in single crystals (phonons and magnons) and the vibrational modes in molecules. An energy exchange between the incoming neutron and the sample of between 1μeV (even 1 neV with spin-echo) and 1eV can easily be detected.

MICROSCOPICALLY MAGNETIC

Neutrons possess a magnetic dipole moment which makes them sensitive to magnetic fields generated by unpaired electrons in materials. Precise details of the magnetic behaviour of materials at the atomic level can be investigated. In addition, the scattering power of a neutron by an atomic nucleus depends on the orientation of the spin of both the neutron and the atomic nuclei in a sample, thereby providing a powerful tool for detecting the nuclear spin order.

ELECTRICALLY NEUTRAL

Neutrons are electrically neutral and so can penetrate deep into matter, while remaining non-destructive. This makes them an ideal probe for studying, for example, biological samples or engineering components under extreme conditions of pressure, temperature or magnetic field, or within chemical-reaction vessels.

HIGH SENSITIVITY AND SELECTIVITY

The variation of scattering power from nucleus to nucleus in a sample varies in a quasi-random manner, even in different isotopes of the same atom. This means that light atoms are visible in the presence of heavy atoms and atoms that are close to one another in the periodic table may be distinguished from each other. This introduces the possibility of using isotopic substitution (for example deuterium for hydrogen or one nickel isotope for another) to allow contrast to be varied in certain samples thereby highlighting specific structural features.

In addition, neutrons are particularly sensitive to hydrogen atoms and therefore they are a powerful probe of hydrogen storage materials, organic molecular materials, and biomolecular samples or polymers.

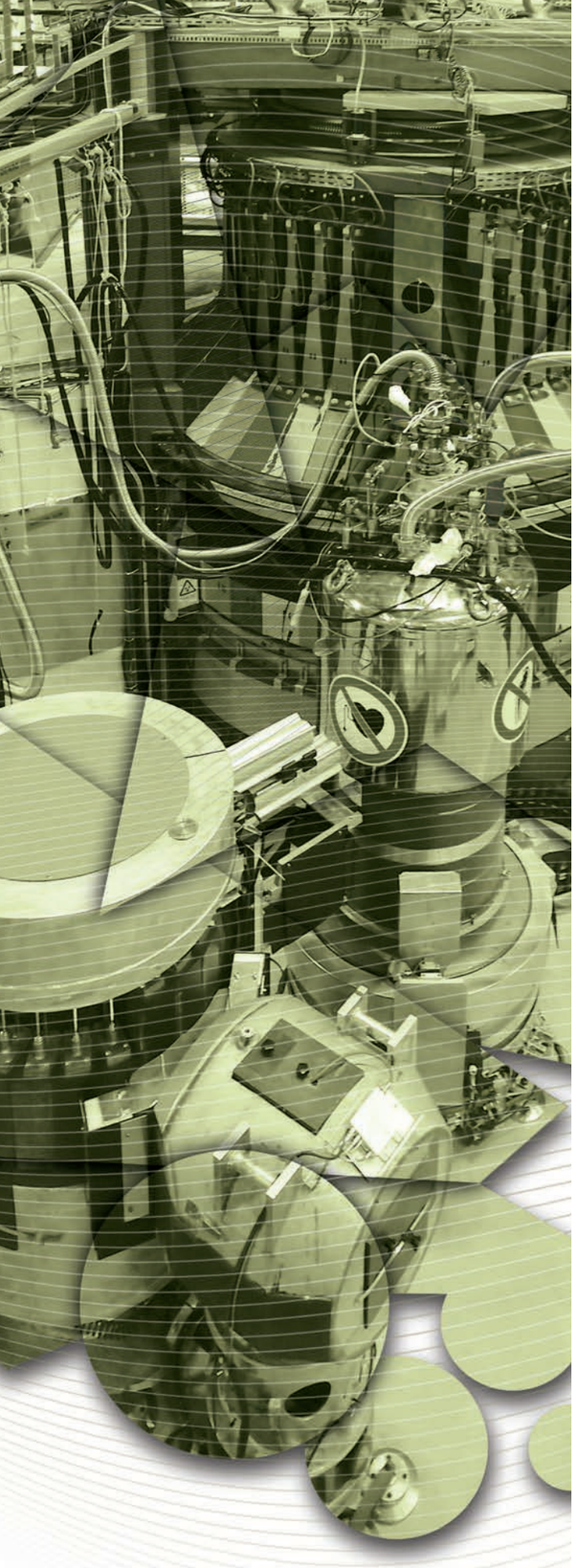

The scientific highlights presented in this year's annual report demonstrate how research with neutrons continues to push back the frontiers of science

If we had to draw up an organisation chart of human society, research facilities would most certainly occupy a prominent position. The importance of knowledge for human development has deeply penetrated our collective consciousness. The task of preserving and expanding this knowledge has been entrusted to a network of academic institutions which provides society with its rational intelligence. If, as is generally accepted, a high degree of interconnectivity is a sign of increased intellectual capacity, tremendous progress has been achieved in recent decades. Thanks to modern communication technologies and human mobility, researchers can now interact almost instantaneously on a global scale. This interaction has boosted the productive exchange of ideas and, among many other things, has broken down barriers between scientific disciplines. Large research infrastructures play a crucial role in the network of academic institutions. Offering unique services across a broad array of disciplines, they are an essential stopover destination for scientists of every stripe and can thus be considered the true crossroads of academic exchange.

The founding fathers of the ILL clearly anticipated the enormous potential of research infrastructures for interconnecting the scientific community. They insisted right from the start on an organisational structure that places collaboration with outside academic institutions at the very heart of the ILL's mode of operation. They also defined as broad a scope as possible for the science to be carried out at the Institute, thus laying the foundations for intense interdisciplinary cross-fertilisation. When reading the scientific highlights in this report, you will quickly realise that the ILL has remained true to its original vocation.

Like all infrastructure, roads are best when they are safe and easy to use. Knowledge-based infrastructure is no exception to this rule. It must be the aim of all responsible research to create knowledge that can be easily passed on and exploited outside its domain. In particular, for a scientific discipline to become a cross-cutting analytical tool, it has to reach a high degree of maturity. It is difficult to know whether the pioneers of neutron science anticipated the tremendous pace at which their research field would fulfil this requirement.
As 2014 has just been declared the International Year of Crystallography, what better way to illustrate this point than with this venerable discipline? Starting from the groundbreaking work of von Laue and Bragg (father and son), crystallography had by the start of the 21st century developed into an established analytical tool for structural investigation used in virtually every branch of natural science. Several of the highlights in this report bear testimony to the outstanding quality of today's structure determination by neutron crystallography.

The downside of maturity is the obvious loss of attractiveness for universities. Under the current paradigm, universities have to favour fields of investigation with a large potential for scientific discovery. This implies that, in addition to providing user services, research facilities must increasingly take on the role of safeguarding and developing methodology-related knowledge. The ILL Science Division is responding firmly to this dual challenge: by focusing particular efforts on the training of young scientists, we are guaranteeing the preservation and dissemination of know-how relating to neutron science, and by constantly striving to improve our instrumentation and services, we are helping to develop the techniques needed to meet the ever-growing demands of our users. It is these efforts that have made the fascinating scientific results presented in this report possible. The ILL is without doubt the world's leading provider, custodian and developer in neutron science.

The key to this enduring success has been the succession of modernisation programmes initiated by the ILL. 2012 and 2013 saw the commissioning of a number of highly innovative instruments, such as IN1-LAGRANGE, D33, and the new IN16B. The user experiments performed on these instruments have confirmed their tremendous potential. The last projects to be completed within the Millennium Programme will be the high-resolution spin-echo instrument IN15 and the wide-angle spin-echo instrument WASP. In this context, we very much appreciate the support we have received via third-party funding from the BMBF and FZ-Jülich.

With the Millennium Programme in its final phase, the ILL has spent the last few years preparing the successor programme. The "2020 Vision" user meeting in 2010 gave ILL scientists an opportunity to confront their ideas for modernisation with the expectations of the user community. Driven by the support of the community, the project teams then set out to elaborate their proposals, making them suitable for evaluation. The evaluation phase of what has since become the Endurance programme started in 2012 under the close scrutiny of the Instrument Subcommittee, with the programme taking final shape in 2013. Enthusiastically endorsed by the Scientific Council, Endurance has been proudly presented to the ILL Steering Committee and is now awaiting funding approval.

The scientific highlights presented in this report are a glowing testament to the success of the ongoing process of rejuvenation at the ILL. I am sure you will be as impressed as I am by the breadth and depth of the results achieved. Alongside articles on work dealing with very fundamental scientific questions, you will also find reports on investigations with immediate practical implications. I hope you enjoy reading them!

Helmut Schober

Helmut Schober
Associate Director

COLLEGE 1 - APPLIED METALLURGY, INSTRUMENTATION AND TECHNIQUES

AUTHOR: **G. Cuello** (College 1 Secretary)

This year was an excellent year for applied sciences at the ILL with more than 40 high-quality experiments being performed. The scope of applied sciences at the ILL is broad, varied and state-of-the-art, ranging from geophysics to engineering and from cultural heritage to biomaterials. A large proportion of experiments were in the field of engineering, for which SALSA, the dedicated instrument for residual stresses, is an extremely useful tool, capable of mapping large and complex samples. In just a few years, SALSA has established itself as a world-class instrument for the determination of bulk residual stresses. In College1, these experiments represent almost 50% of the experiments conducted. However, the number of cultural heritage and materials science experiments still remains healthy, involving a wide suite of ILL instruments. This year our College chose to focus on a flagship experiment in palaeontology and we are looking forward to reading about this fascinating experiment (which could confirm a new species of glyptodont) in future Annual Reports.
In the framework of the Endurance upgrade programme, our College has one flagship project: SuperSALSA. Although SALSA's performance is outstanding in terms of acquisition rate, precision, lateral resolution and flexibility of sample manipulation, stress is only one parameter in the spectrum of materials characterisation. The proposed new instrument will add the analysis of textures and phases, and the *in situ* distribution of elements in an object at a given stage in its manufacture, by offering a white beam option. By placing the sample in the white beam and analysing the scattered intensity using the two large crystal analyser units, selected parts of the diffractogram will be recorded in acquisition times of around 1s. This new instrument will provide new opportunities not only for materials scientists and engineers, but also for other user groups, such as geologists and archaeologists who also need to analyse complex, bulky samples non-destructively.
The life of the College is not only restricted to the conducting of experiments. Our users also come to give talks on their results or to present new techniques or instrumentation for neutron scattering. One particularly successful event this year saw Prof. Ferenc Mezei give an excellent talk on low-dimensional neutron moderators for enhanced source brightness. The seminar attracted an exceptional number of scientists interested in the development of new moderators for spallation sources.

COLLEGE 2 - THEORY

AUTHOR: **T. Ziman** (ILL Theory Group)

The Theory College has always covered a breadth of subjects relevant to neutron science and this year, following the retirement of Efim Kats, the structure of the College was modified somewhat in order to allow this to continue. For soft matter, in particular, J.-L. Barrat has joined M.-B. Lepetit (*ab initio* study of solids) and T. Ziman (hard condensed matter) to jointly run the Theory College. The move to the new Science Building should also encourage informal contacts with soft matter experimentalists on the site. In "hard" condensed matter, one of the continuing themes has been the effect of spin-orbit interactions and the highlight on ***p.72*** illustrates this. While spin-orbit interactions are relatively weak for all but the heaviest elements, their rather peculiar symmetry means they couple bulk properties - electrical and magnetic responses, for example - that otherwise are quite independent. In materials science, this form of multifunctionality is exactly what people are looking for in novel applications, both for bulk materials and in new nano-devices. In the highlight, which entailed close involvement in the neutron experiments on the multiferroic $YMnO_3$, a rigorous symmetry analysis was developed to bring to light the underlying mechanism of multiferroicity.
The presence of theorists at the ILL sometimes leads to the re-examination of older results obtained with neutrons. A very recent example is work by a former postdoc (G. Sordi) and a visitor to the ILL (M. Pezzoli) in collaboration with theorists from Rutgers, showing the effect of correlations on magnetic form factors across the α-γ transition in cerium, measured almost ten years ago by high-energy neutron inelastic scattering.

COLLEGE 3 - NUCLEAR AND PARTICLE PHYSICS

AUTHOR: **A. Blanc** (College 3 Secretary)

Activities in nuclear and particle physics cover a very wide range from fundamental to applied science. Combining the high-resolution Lohengrin spectrometer with two high-efficiency Germanium clover γ-ray detectors make this instrument ideal for detailed spectroscopy of very neutron-rich nuclei. In particular, the nuclei of the neutron-rich A≈100 region have been the subject of intense experimental and theoretical studies for many years, due to the observation of a rapid onset of strong prolate deformation in the ground states of the Sr, Y, and Zr nuclei when moving from 58 to 60 neutrons. An experiment conducted at Lohengrin to measure the delayed γ-rays and conversion electrons from neutron-rich A=97 fission fragments made it possible to observe and study for the first time decays of excited states in the neutron rich ^{97}Rb nucleus, helping elucidate the much discussed shape change around N=59.
At the end of 2012 and the beginning of 2013, a successful measurement campaign devoted to nuclear spectroscopy was conducted at the PF1B cold neutron instrument: the EXILL campaign. For the duration of 2 reactor cycles an array of 16 Germanium detectors was installed to perform γ-ray spectroscopy of neutron-induced reactions on both stable and fissile targets (^{235}U and ^{241}Pu). In addition, for a few weeks, 16 $LaBr_3$ scintillators were added to the set-up for ultrafast-timing measurements, thus broadening the scope of the study. A large user community of about 120 people participated in the data-taking, which produced a total of 60TB of data. The data analysis is ongoing and several years of work are expected to be devoted to this collaboration.
An experiment performed recently at the PF2-VCN instrument (polychromatic beam of very cold neutrons) has demonstrated the technical feasibility of a novel type of resonator: the "travelling wave" neutron spin resonator. Such resonators allow the complete decoupling of wavelength and time resolution, leading to precise wavelength selection and definition of the time structure of thermal, cold and very cold polarised neutron beams by purely electronic means. Such devices may become important for experiments searching for new physics beyond the Standard Model of particle physics, for which a perfect knowledge of the key beam parameters is needed. Another possibility is the implementation of the device as integrated monochromator and chopper for advanced neutron time-of-flight spectroscopy.

COLLEGE 4 - MAGNETIC EXCITATIONS

AUTHOR: **E. Wheeler** (College 4 Secretary)

In the study of magnetic excitation spectra, neutron scattering remains an essential tool. The breadth of instruments at the ILL allows for varied studies across a broad field using both triple-axis spectrometers (TAS) and time-of-flight instruments (TOF). 2013 saw continued research into the main topics of interest to the field of magnetism and the final experiments carried out on IN14 before it is updated to ThALES.
This year the work of Kempa *et al.* (***p.22***) continued research into Fe_2O_3, which has long been a source of scientific interest. Using the TOF instrument IN4, they worked on nanoparticles stabilised in the less commonly studied ε-Fe_2O_3 state in search of electromagnons. Observed in the spectra of various multiferroics, electromagnons are normally only identified in single crystals by complete polarisation analysis. The team showed that with a powder sample and unpolarised infrared and terahertz measurements combined with inelastic neutron scattering, they were able to identify an electromagnon and its origins.
Intense research into iron-pnictide superconductors also continued. We highlight work on the TOF instrument IN4 investigating the crystal field excitations of one such system. Looking at changes in the crystal field excitations in paramagnetic and antiferromagnetic phases has provided an insight into the differing exchange interactions in the system and consequently their electronic landscape. Progress was also made in the physics of layered oxides, which impacts developing theories of cuprate high-temperature superconductors. Komarek *et al.*, working on the TAS instrument IN8, investigated a lanthanum-doped cobalt oxide and showed that an hour-glass shaped spectrum is present even in the absence of charge-stripe order. Although some theories of high-temperature cuprate superconductors link charge-stripe order and an hour-glass spectrum, this work would suggest the hour-glass spectrum has other origins. By using the full capabilities of the TAS IN14, Raymond *et al.* (***p.24***) gained valuable insight into the spin-polarised spectrum of heavy-fermion superconductors. They used the instrument in the polarised neutron set-up to investigate the chirality of the excitation spectrum. Their measurement of the chiral proportion of a key mode goes towards explaining the spin-resonance mode of the unconventional superconducting phase in heavy fermion materials.

COLLEGE 5A - CRYSTALLOGRAPHY

AUTHOR: **T. Hansen** (College 5A Secretary)

The College deals with the study of the atomic-scale structures of crystalline solid matter, usually in the form of single crystals and polycrystalline powders, and considers applications for beamtime primarily on the ILL's diffractometer suite. The crystallography of biological matter, in particular proteins, is dealt with in College 8, and College 5B deals with the crystallography of magnetic structures. Neutron diffraction is a vital tool for the crystallographic study of many minerals and functional materials. Neutrons allow the accurate location of low atomic number elements in the presence of heavier elements, as well as the distinction between neighbouring elements in the periodic table, two tasks which are extremely difficult for X-ray diffraction. Moreover, neutrons penetrate most construction materials without substantial losses and allow complex sample environments to be produced easily. In this connection, neutrons are scattered by the bulk of the sample and not just by the surface and therefore provide a better picture of the whole sample. An example for the power of these techniques is the *in situ* high-resolution powder diffraction study of a new borosilicate, where a full *ab initio* structure solution at elevated temperature was successfully determined (***p.32***).
Nowadays, we can access not only the instantaneous structure, but also its evolution with thermodynamic conditions, *i.e.* temperature and pressure, as well with time, which is important for our understanding, among other things, of chemical reaction pathways, ion conduction, corrosion, and the uptake of gases. The proposal statistics show very clearly that neutron diffraction at the ILL is increasingly employed to study the activity and behaviour of materials under non-ambient and chemically active conditions. Studies of even the simplest of materials, such as oxygen in confined geometry or at high pressure, or water ice at certain temperatures and preparation conditions, lead to fundamental new insights. Here we report on the so-called Morin-transition of hematite under pressure (***p. 38***). Neutron diffraction is a vital tool for the characterisation of materials for emerging applications, such as energy conversion, which is of the utmost importance for humanity due to the need to eliminate or reduce the climatic and pollution impact of the various techniques available for the storage and "production" of energy, in particular in the light of decisions favouring or excluding certain techniques for political and social reasons. To this end, we need to determine oxygen ion positions in solid-oxide fuel cell materials, oxygen positions in the presence of metals, and the pathway of oxygen when ion conduction sets in. This must be done as a function of temperature and redox conditions, *i.e.* partial pressures of hydrogen and oxygen. The most promising rechargeable battery materials are based on the light element lithium. Such materials are already widely used, but their quality, reliability and use in other application domains, *e.g.* transportation, need to be improved. The economic and societal impact is and will be enormous. The position of these lithium ions in an oxide host can be determined by neutron diffraction, and the pathway of these ions during charge and discharge cycles can be traced in operation conditions (*in operando*): rapid data acquisition, combining detector technology and high neutron flux, allows time-resolved powder neutron diffraction to follow the chemistry. Also, for the formation and decomposition of hydrides, leading to the storage and release of hydrogen gas, the kinetics and reaction mechanisms can be efficiently mapped, making it possible to tailor the properties of these materials for future energy storage applications.
Similarly, single-crystal neutron diffraction studies of organo-metallic catalysts have revealed the precise details of chemical bonding in intricate coordination complexes.Here, we report on a multiferroic organometallic framework compound with a rich phase diagram which could be elucidated by the combined use of Laue-diffraction, monochromatic single crystal diffraction and powder diffraction (***p.30***).

COLLEGE 5B - MAGNETIC STRUCTURES

AUTHOR: **C. Ritter** (College 5B Secretary)

The scientific areas covered by College 5B have developed and changed significantly over the past few years. Originally – and as can still be seen from the College's name "Magnetic Structures" – College 5B experiments were devoted almost exclusively to studies aimed at the determination of long-range magnetic order and its parameter dependence using powder or single-crystal diffractometers. With the advent of Cu-superconductors, the study of flux line lattices using small-angle scattering opened up a new field of investigation, which quickly developed and is now becoming even more prolific thanks to the new possibilities of using high magnetic

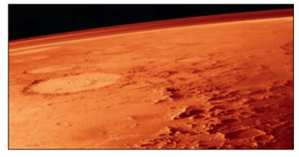

Applied metallurgy, instrumentation and techniques
cf. article "Morin transition in hematite (α-Fe_2O_3) under pressure"
p. 38

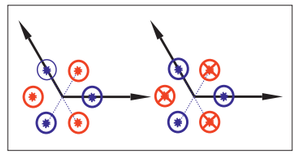

Theory
cf. article "Analysis of the multiferroicity in the hexagonal manganite $YMnO_3$"
p. 72

Nuclear and particle physics
cf. article "EXILL, a campaign of measurements devoted to nuclear spectroscopy"
p. 68

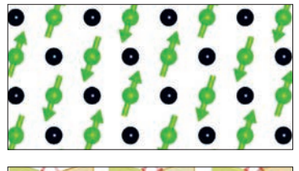

Magnetic excitations
cf. article "Hour-glass spectrum in a stripeless insulating transition metal oxide"
p. 18

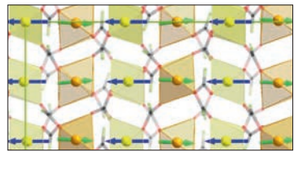

Crystallography
cf. article "Structural and Magnetic Neutron Studies of a molecular multiferroic compound: joining forces across the ILL's neutron diffraction instrument suite"
p. 30

fields and polarisation analysis offered by the recently commissioned SANS machine D33. An excellent example of what can be done using polarised neutrons in small-angle scattering is given by one of our highlights (***p. 16***), in which the distortion of the vortex lattice in Sr_2RuO_4 as function of the angle between the applied magnetic field and the Ru-O basal plane was determined to obtain the superconducting anisotropy.
In the past, studies on magnetic defects or short-range magnetic order or correlations were rare. Now things have changed dramatically thanks to the ILL's Millennium Programme with the upgrading of the diffuse scattering diffractometer D7. The development of a new supermirror spin-analyser array for this instrument has increased the detected flux of polarised neutrons drastically allowing, for example, the detection of magnetic monopoles (see ***Annual Report 2009***).
The availability of the dedicated reflectometers D17 and SuperADAM has had an even greater impact on the science conducted in College 5B: in parallel to a strong shift in scientific interest towards thin films, multilayers and nanoparticles, the newly developed polarisation analysis option on these two reflectometers has boosted the demand for studies of magnetic correlations, magnetic domain structures and magnetisation profiles. The example of the use of polarised neutrons to determine the field-dependent magnetic scattering density in multilayers of iron oxide nanoparticles on the reflectometer SuperADAM is presented on ***p. 26***.
This considerable increase in the importance of "non-traditional" areas of activity for College 5B has not, however, prevented the "classical" experiments on magnetic structure determination from continuing to thrive. In particular, work on multiferroic systems and low dimensional magnetism is flourishing with ever increasing demands being placed on the sample environment. In this context, we are delighted to announce that the first ever experiment using a 10 T cryomagnet has successfully taken place on the high-intensity powder diffractometer D20. A qualitative jump pushing back the limits in terms of the available magnetic field strength and pressure range is also expected from the single crystal and powder diffractometer XtremeD, which is part of the Endurance programme. The refurbishment of the very old neutron guide H24, together with the complete upgrade of the primary and secondary spectrometers, which are also part of Endurance, should enable our much sought-after single crystal diffractometer D10 to measure even smaller magnetic moments and reduce the limits for the magnetic structure determination of thin film samples down to a thickness of only 20 nm.

COLLEGE 6 – LIQUIDS AND GLASSES

AUTHOR: **V. Cristiglio** (College 6 Secretary)

Non-crystalline materials are characterised by the loss of long-range order. However, chemical short- and intermediate-range order can be identified by diffraction and dynamics observed by quasi-elastic and inelastic scattering. Neutron scattering has proved to be a powerful tool in this field. It complements other techniques based on X-ray measurements and is underpinned increasingly frequently by molecular dynamics simulations.
For structure characterisation, D4 and D20 are the most requested instruments. The measurement of the structure factor S(Q) allows the atomic arrangement in a material to be determined, with isotopic substitution often used for atomic labelling.
Major advances in instrument capabilities have resulted in a notable increase in the number of studies concerned with dynamics in aqueous solutions. The instruments most in demand for the study of dynamic behaviours are BRISP, IN5, IN6 and IN16. IN16, now IN16B, has recently been completely upgraded and now occupies a new beam position, which is optimised for the instrument. With the start of the new Endurance programme, the instruments IN5 and IN6 (christened RAMSES) will also undergo substantial upgrades. The improved signal quality will open up paths for studying more complex and more diluted systems.
In this Annual Report three highlights have been selected to show the capabilities offered by neutrons for responding to complex questions in a wide range of domains.
Our first highlight, by Martin *et al.* (***p. 46***), shows the impact of Ti incorporated into melt-quenched Bioglass. Bioactive glasses are known for their ability to bond chemically to bone and stimulate new bone growth. By adding different ions to their structure, properties such as bioactivity and antibacterial effects could be improved. Isotopic substitution has enabled the Ti–O coordination to be successfully isolated from a very complex total structure factor (6 chemical elements and 21 partial structure factors).
In our second highlight, by Guarini *et al.* (***p. 48***), the dynamic structure factor of liquid gold is determined by inelastic scattering, supported by *ab initio* simulations. Neutron measurements reveal the presence of underdamped ion density-fluctuation modes and the dynamic features show an overall Q behaviour globally similar to that already found for insulating liquids.
The third highlight, by Bove *et al.* (***p. 44***), shows for the first time self-dynamics measurements of liquid water in the GPa range. This study provides a criterion for estimating diffusion coefficients along melting lines at extreme pressures and temperatures which canno be predicted by conventional equations used for the dynamics of simple liquids.

COLLEGE 7 – SPECTROSCOPY AND MODELING

AUTHOR: **M. Zbiri** (College 7 Secretary)

The atomistic world is subject to perpetual dynamics that define its characteristics and shape its evolution in time and space. Neutron spectroscopy is a perfect tool for revealing the dynamic fingerprints of atoms and molecules on the meV and nanometre scales. This paves the way for a comprehensive understanding, at the microscopic level, of the chemical and physical principles underlying the properties of matter. In the solid-state phase, various interesting and societally relevant phenomena can be observed. These need to be studied and/or explored for their potential application. The activities of College 7 - "Spectroscopy in solid-state physics and chemistry" – are situated precisely within this framework and are aimed at dealing with topics at the boundaries of various domains ranging from materials science and condensed matter to energy and life sciences. This can be clearly seen from the highlights presented in this report. On the side of materials science and energy-related applications, the study by Ling and coworkers of the structure (single crystal diffraction) and dynamics (time-of-flight spectroscopy) of solid-state oxide-ion conductors is a good representative example (***p. 40***). These materials can be of tremendous use as membranes in solid oxide fuel cells. Such keen interest stems from the fact that oxide-ion conductors are a typical energy-related research area where the use of neutron scattering is vital for gaining new and deeper insights into the structure-dynamics-property relationships. On the life sciences side, Zaccai and collaborators show that neutrons are a promising non-invasive probe for studying the molecular dynamics of the protein populations of living cells. The authors used the backscattering technique to detect *in vivo* stress in cells by measuring the physical response of microorganisms to thermal stress (***p. 60***).
There is no doubt that the neutron-based research topics relevant to the activities of College 7 are constantly expanding to cover new areas of science. This was and is the result of the continuous efforts made by the ILL to renew and upgrade its suite of spectrometers in terms of performance and robustness.
As a part of the Endurance programme, we should mention the RAMSES project, whose main objective is to provide a solution for the spectroscopy of advanced materials in extreme environments. This requires high pressures and temperatures and therefore imposes strict limitations on the size of samples, which in turn means that a very high neutron flux is needed as we strive to achieve a wider dynamic range and phase space and greater flexibility in terms of energy resolution.

COLLEGE 8 – BIOLOGY

AUTHOR: **M. Blakeley** (College 8 Secretary)

The most complex and exciting chemical processes are found in living organisms. In order to better understand these processes, researchers use neutron scattering experiments to study the structure and dynamics of biological systems. Information obtained from experiments using crystals, solutions or partially ordered systems contributes to advances in areas such as medicine, health and biotechnology.
Crystallographic studies at high resolution, performed using the LADI-III or D19 diffractometers, provide unique structural details on protonation, hydration and hydrogen bonding.
This information is critical for our understanding of, for example, enzyme mechanisms or redox reactions, and can also aid in drug design to improve the effectiveness of modern medicines. The versatility of D16 allows studies of partially ordered systems, such as biological and model membrane multilayers under controlled humidity and vapour contrast. Neutron reflectometry is optimally suited for the study of biological interfaces, providing structural information on processes at cell surfaces. Interactions between membranes and small molecules can be investigated at a molecular length scale using the D17 and FIGARO reflectometers, enabling the characterisation of protein conformation in membrane environments, as well as specific drug interaction mechanisms.
Working with samples in aqueous solution, biological small-angle neutron scattering (BioSANS) investigations using the ILL's small-angle suite of instruments (D11, D22, D33) probe the gross structural features (*i.e.* shape, quaternary and tertiary structure) of different components of macromolecular complexes. For instance, BioSANS can provide structural information about each component of biological complexes, such as membrane proteins in complex with detergents, protein-protein complexes, or protein-nucleic acid complexes.
Biological molecules are not static objects - their atomic and molecular motions are essential for biological processes, and high-resolution neutron spectroscopy offers exactly the right time-window for observing these movements. In addition, incoherent neutron spectroscopy provides unambiguous access to the self-dynamics of biological molecules and important questions relating to macromolecular crowding, protein gelation, aggregation, denaturing, and internal fluctuations of proteins can be addressed. The ILL suite of spectrometers is today second-to-none, and now includes the recently commissioned backscattering spectrometer IN16B, which accesses biomolecular dynamics with unprecedented precision.
Finally, the importance of deuterium in sample preparation for biological studies cannot be overstated: from H_2O/D_2O exchange and contrast-variation methods to selectively or completely deuterated (*i.e.* perdeuterated) biological molecules produced in the D-Lab, researchers are able to perform ever more sophisticated experiments using neutrons that provide new and exciting insights for a vast array of biological processes.

COLLEGE 9 – SOFT CONDENSED MATTER

AUTHORS: **R. Campbell** (College 9 Secretary) and **L. Porcar** (vice secretary)

Soft condensed matter is a key growth area at the ILL with the number of experiments exceeding 20% of the total in 2013. Research areas cover a broad range of fundamental and applied sciences at the interface of physics, chemistry and biology. Topics under investigation include colloids, micelles, surfactants, polymers and bio-related systems. Neutrons are an ideal probe for the structure and dynamics of soft matter and contrast variation is of critical importance. Colloidal and polymeric systems continue to generate a great deal of research interest. For example, work on D11 has revealed the mechanism of deformation for liquid crystals formed by block copolymer micelles (***p. 50***). Also, electrochemical polymerisation of surface films has been characterised on FIGARO and related to the detection of invisible fingerprints (***p. 34***). Bio-related soft matter experiments continue to thrive and recent highlights include work on FIGARO and D17 concerning the anchoring of polymers into phospholipid monolayers and bilayers by ring-shaped cyclodextrin molecules (***p. 52***), as well as work on D17 linking the interactions between gold nanoparticles and floating lipid bilayers to the surface charge (***p. 66***). Findings from soft matter experiments at the ILL have featured in the popular press in articles dealing with such diverse topics as health and crime prevention. For example, work on understanding breathing difficulties from studying the effects of pollutants on the destruction of lung surfactant featured in the New Scientist and the new approach for fingerprint detection mentioned above was publicised on the BBC website. There continues to be emphasis on combined neutron experiments with *in situ* techniques, such as dynamic light scattering combined with small-angle neutron scattering (D11) and neutron reflectometry combined with infrared reflection absorption spectroscopy (D17). Furthermore, a great effort has been made to promote research into formulations under industrially relevant conditions to processing and applications with dynamic experiments under flow both in the bulk solution (D22) and at the air/water and solid/liquid interfaces (FIGARO). The soft matter research communities at the ILL and ESRF now rely on support from the Partnership for Soft Condensed Matter (PSCM). The organisation provides a key platform to assist scientific visitors in the pre-characterisation, analysis and interpretation of scattering data. At the start of 2014, the PSCM and chemistry laboratories will move into the new Science Building adjacent to ILL7, where they will provide modern, state-of-art facilities for future soft matter research using neutron, x-rays and complementary techniques carried out on the EPN campus.

Magnetic structures
cf. article "Magnetic correlations in multilayers and monolayers of iron oxide nanoparticles"
p. 26

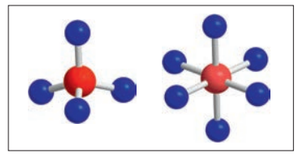

Liquids and glasses
cf. article "sotopic and isomorphic substitution applied to dilute glassy systems"
p. 46

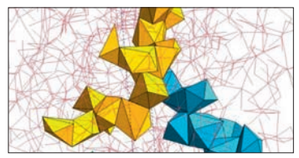

Spectroscopy and modeling
cf. article "Fragile glass-formers reveal their structural secrets"
p. 37

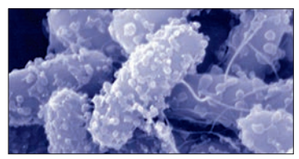

Biology
cf. article "Membrane thickness and the mechanism of action of the short antimicrobial peptide trichogin GA IV"
p. 56

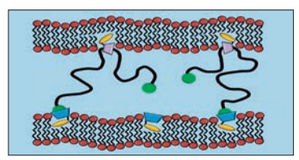

Soft condensed matter
cf. article "Achieving molecular control of bio-adhesive interactions through the design of spacer architecture"
p. 52

ILL IN THE PRESS

1 - *Published in Scientist Live on April 2013.*
2 - *Published in Laboratory News on 10 April 2013.*
3 - *Published in Sci-News.com on 12 April 2013.*
4 - *Published in BBC NEWS on 3 July 2013.*
5 - *Published in The Guardian on 3 July 2013.*

1

SCIENTISTLIVE

Drug Discovery/Development

Neutrons help explain why antibiotics prescribed for chemotherapy cause kidney failure

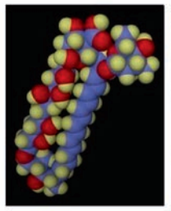

Analysis will help development of new treatments to protect vulnerable patients undergoing chemotherapy or suffering from HIV

IMAGE: This is a molecular model of the antibiotic - Amphotericin B.

Neutron scattering experiments have provided new insights into the origin of the side effects of an antifungal drug prescribed all over the world. The analysis conducted by scientists at King's College London and the Institut Laue-Langevin in Grenoble, and published in Scientific Reports, follows 40 years of debate and could help drug developers reduce these harmful complications.

Wherever you are in the world, indoors or outdoors, the air you breathe contains fungal spores. Though occasionally linked with allergies, asthma or skin irritations, the majority are easily dealt with by the body's immune system.A far greater risk is posed to individuals whose immune systems are already compromised such as those infected with HIV, severe burn victims or those having just undergone chemotherapy.

2

LaboratoryNews

HOME | NEWS | FEATURES | PRODUCTS | COMMENT | DIRECTORY | VIDEOS | COMPANIO

BRAIN PRESERVATION TECHNIQUE COULD LEAD TO UNRELIABLE AUTOPSIES

April 10, 2013 LaboratoryNews No comments

For the first time, scientists have conducted neutron scattering experiments on brain tissue. They have found that formaldehyde preservation is not as reliable as initially thought, as it significantly affects the process of water diffusion.

These findings are the first stage in the Institut Laue-Langevin-based group's research where neutrons are used to understand the movement of cellular water within brain tissue. Water movement forms the basis of diffusion magnetic resonance imaging (dMRI) which is used in analysis of several brain pathologies.

Lead research Dr Francesca Natali said: "This is the first evidence that water diffusion, a key process in the modelling and diagnosis of brain pathologies is significantly affected by common tissue sample preservation techniques."

Cellular water is the major constituent of our bodies and its content varies in brain regions depending on their specific composition. As this water plays a key role in cell regulation, its distribution is an accurate indicator of cellular structure as it interacts with different tissue components such as membranes and nerve fibres.

dMRI and other imaging techniques rely on water diffusion as a contrast method to reveal and characterise various brain pathologies, such as ischaemia and tumours on the micron scale. But concerns over the impact of preservation processes used for imaging on the brain's fundamental structural and compositional properties have reduced confidence in dMRI as an accurate technique.

To address these concerns, the researchers compared the behaviour of cellular water in *ex vivo* bovine tissue preserved using two common preservation techniques: chemical fixation with formaldehyde and cryopreservation. The samples were investigated using incoherent quasi-elastic neutrons scattering (QENS) experiments carried out on the high-resolution IN5 spectrometer at the ILL.

3

Ozone Exposure Linked to Thousands of Premature Deaths Annually

Apr 12, 2013 by Sci-News.com « PREVIOUS | NEXT »

Published in Medicine
Tagged as ozone
Follow
Like 10k
Share
Tweet 6
Like 5
+1 7

You Might Like

Air quality signboard indicating an ozone watch in Guffton, Houston

An international team of scientists has used world-leading neutron sources at the Institute Laue-Langevin in Grenoble, France, and at the Rutherford Appleton Laboratory in the UK, to explain how ozone causes severe respiratory problems and thousands of cases of premature death each year by attacking the fatty lining of our lungs.

Scientists Discover Odor Receptors in Human Lungs

Molecular Pathway Discovery May Help Treat Psoriasis, Crohn's

In a study, published in the journal *Langmuir*, the team observed how even a relatively low dose of ozone attacks lipid molecules that line the lung's surface.

4

BBC NEWS SCIENCE & ENVIRONMENT

News Sport Weather Capital Culture Shop

Home UK Africa Asia Europe Latin America Mid-East US & Canada Business Health

3 July 2013 Last updated at 16:21 GMT

Share

Glowing tags to reveal hidden prints

By Paul Rincon
Science editor, BBC News website

Scientists have described a new system for visualising "hidden" crime scene fingerprints.

Despite several enhancement techniques already in use, only about 10% of fingerprints from crime scenes are of sufficient quality to be used in court.

The technique is based around fluorescent chemical "tags" and works on metal surfaces, meaning it could be used on knives, guns or bullet casings.

Details were outlined at the **Faraday Discussions** lecture series in Durham.

"Notwithstanding DNA, fingerprints are still the major source of identification in criminal investigations," co-author Prof Robert Hillman, from the University of Leicester, told BBC News.

The technique, demonstrated here on stainless steel, produces a negative image of the print

Related Stories

5

theguardian

News | Sport | Comment | Culture | Business | Money | Life & style | Travel | Environment

News › Science › Forensic science

SHORTCUTSBLOG
TRENDING TOPICS AND NEWS ANALYSIS

Previous Blog home Next

New fingerprint technology that means evidence can no longer be wiped away

A hankie used to be enough to remove traces of a person's presence from a crime scene. Now scientists have come up with an ingenious way to recover latent prints – but will it work?

Share 35 Tweet 2 +1 8 Pin it Share 1 Email

'Make sure you've got your turties on ...' Photograph: Alamy

Posted by Duncan Campbell Wednesday 3 July 2013 17.18 BST The Guardian
Jump to comments (14)

We all know the scene in the movies where the criminal wipes his gun and the door handles with his hankie so as not to leave any trace of his presence. Now scientists claim to have invented a method that could identify his fingerprints, regardless of how much wiping has taken place. So how much of a difference will it make?

Article history

Science
Forensic science

More from Shortcuts on

6

DIE WELT zur Startseite machen

Home Politik Wirtschaft Geld Sport Wissen Panorama Kultur ICON Reise

IN DEN NACHRICHTEN: Freizügigkeit | Michael Schumacher | Thomas Hitzlsperger | Wetter-Extreme

Home › Wissen › Fingerabdrücke werden jetzt besser sichtbar

16.07.13 | Forensik

Fingerabdrücke werden jetzt besser sichtbar

Innovation aus England: Polymere statt Puder bei der Spurensicherung am Tatort. Forscher wenden dazu fluoreszierende Schichten an, die ihre Farben je nach Leitfähigkeit des Materials verändern. *Von Bernd Schöne*

Foto: University of Leicester

Dieser Fingerabdruck auf dem Schaft eines Messers wurde dank der neuen Technik sichtbar

Bild teilen

WEITERFÜHRENDE LINKS

Forensik: So entlarvt die Blutspur einen Täter

Raum-Zeit-Analyse:

Fingerabdrücke gehören auch im Zeitalter der DNA-Analyse immer noch zu den wichtigsten Tatortspuren. Bislang sind aber nur zehn Prozent der Fingerabdrücke am Tatort von ausreichender Qualität und Größe, um sie vor Gericht auch tatsächlich verwerten zu können.

7

chemicals-technology.com

News, views and contacts from the global Chemicals industry

Home | Products & Services | Company A - Z | Projects | Features | Videos | White

Latest Features | Features A - Z | Contributors

Neutron beams: key to a deeper understanding of surface properties

17 July 2013

While several probes allow for the characterization of formulations in great detail, only neutron beams can generate a truly detailed pictures of surface composition. Richard A. Campbell explains why, when it comes to optimising the performance of complex formulations in the chemical industry, neutron beams are rather special.

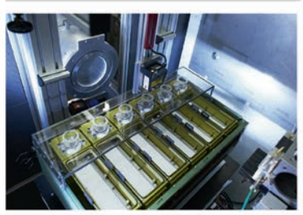

Adsorption troughs.

Solid / liquid / solid interface cells.

Overflowing cylinder.

8

physicsworld.com

Home | News | Blog | Multimedia | In depth | Events

News archive
› 2014
▾ 2013
› December 2013
› November 2013
› October 2013
› September 2013
› August 2013
› July 2013
› June 2013
› May 2013
› April 2013
› March 2013
› February 2013
› January 2013
› 2012
› 2011
› 2010
› 2009
› 2008
› 2007
› 2006
› 2005
› 2004
› 2003
› 2002
› 2001
› 2000
› 1999
› 1998

Neutron study aims to improve HIV drugs

Aug 21, 2013 1 comment

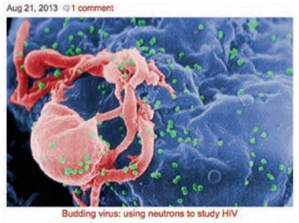

Budding virus: using neutrons to study HIV

A neutron study of a common component of HIV drugs has revealed that the component is not as good at bonding as had been thought. The study, performed by an international group of researchers, highlights aspects of the drug component that could be improved to make it better at mitigating the effects of HIV.

HIV is a virus that replicates through use of a person's immune system. HIV implants genetic information into the immune system's T-cells, which then produce copies of the virus until they die. Once enough T-cells have died from churning out HIV, the person is unable to ward off other infections and they are said to be suffering from AIDS.

9

London Evening Standard

HOME | NEWS | SPORT | FOOTBALL | BUSINESS | COMMENT | ARTS | GOING

Hot Topics Michael Schumacher | Cycling | Ashes Series | Ed Miliband

Tropical tree seeds 'purify water'

Scientists believe the seed proteins could be used in large and small water treatment plants in both industrialised and developing countries

Published: 09 December 2013

Share

Seeds from a tropical tree could provide a more efficient way to purify drinking water, say scientists.

Related Articles

6 - *Published in DIE WELT on 16 July 2013.*
7 - *Published in Chemicals-technology on 17 July 2013.*
8 - *Published in Physics World on 21 August 2013.*
9 - *Published in London Evening Standard on 9 December 2013.*

MORE ARTICLES ON:

http://www.ill.eu/news-events/press-room/ill-in-the-media/

Small-angle diffractometers D11, D22 and D33

Anisotropy of the superconducting state in Sr_2RuO_4

While superconductors continue to find an increasing range of practical applications, they still hold an even greater, untapped potential. In this regard, it appears that some of the most significant advances will be precisely in those materials that are the most complex to understand and control. Strontium ruthenate (Sr_2RuO_4) can in many ways be considered a paradigm for unconventional superconductivity. We have measured the anisotropy of the superconducting state in Sr_2RuO_4, providing significant constraints on models of superconductivity in this material.

The superconducting state emerges due to the formation and condensation of Cooper pairs made from charge carriers (electrons and/or holes). That said, the exact microscopic mechanism responsible for the pairing in different materials varies and, in many cases, remains elusive.
A prominent example of this is found in Sr_2RuO_4, where the two carrier spins in the Cooper pairs are believed to form a triplet that introduces an additional degree of freedom and complexity [1,2]. As a result, the exact nature of the order parameter in this compound remains unresolved despite being studied extensively for almost 20 years.

We have used the D11, D22 and D33 small-angle neutron scattering (SANS) instruments to study the vortex lattice (VL) in Sr_2RuO_4 [3]. The distortion of the VL, arising when the field is applied parallel to the Ru-O planes, provides a direct measure of the anisotropy, Γ_{ac}, of the superconducting state. This anisotropy is of particular interest in comparison to earlier measurements of the upper critical field (H_{c2}) ratio for magnetic fields applied parallel and perpendicular to the basal plan. This H_{c2} ratio ($\approx$ 20) is much smaller than expected from the Fermi surface anisotropy ($\geq$ 60), suggesting a suppression of the upper critical field perpendicular to the basal plane, possibly due to Pauli limiting, that in turn would raise questions concerning triplet pairing in Sr_2RuO_4 [2].

While measurements with the field parallel to the basal plane are conceptually simple, they require a novel approach to SANS VL studies. This is evident from a simple estimate of the VL scattering intensity that turns out to be several orders of magnitude too weak to be measurable, even at a high intensity neutron facility such as the ILL. However, due to the large anisotropy of Sr_2RuO_4, applying the field close to, but not perfectly within, the Ru-O planes causes a significant current to run in the basal plane along the field direction [4].

Figure 1

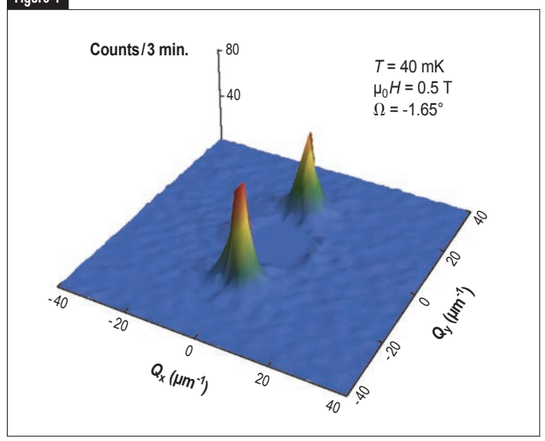

Diffraction pattern showing spin-flip scattering from the VL due to the transverse field modulation. Two Bragg peaks at Q_x = 0 and Q_y = ±18 μm^{-1} are observed. Other Bragg reflections exist but are not observable since the scattering vector Q is essentially parallel to the magnetisation. No background subtraction was performed, but a small remnant of the undiffracted beam close to Q = 0 due to the finite flipping ratio (about 8) is masked off.

This greatly enhances the field modulation and hence the scattered intensity, making the VL Bragg reflections easily observable as shown in **figure 1**. The increased magnetisation is perpendicular to the field directions (and hence the neutron spin) causing spin-flip scattering and a Zeeman splitting of the VL rocking curves as shown in **figure 2**.

Figure 2

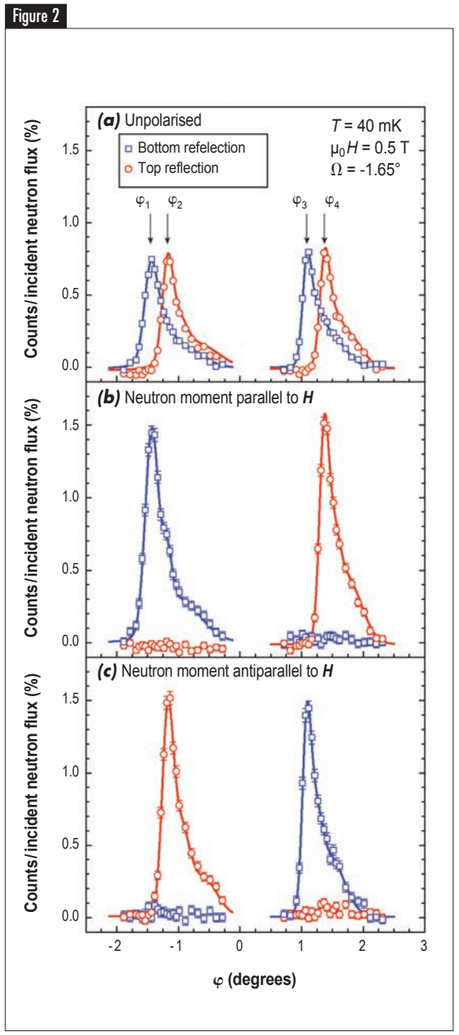

*Vortex lattice rocking curves showing the scattered intensity as a function of tilt angle, φ. With an unpolarised neutron beam, two maxima are observed for both the bottom (negative Q_y) and top (positive Q_y) VL Bragg reflections. Using incident neutrons polarised with their magnetic moment parallel **(b)** or antiparallel **(c)** to the applied field selects a single maximum for each reflection. In all cases the intensity was normalised to the incident neutron flux. As expected, the scattering rate doubled when a polarised beam was used.*

Altogether, our SANS measurements required the combination of a number of technical abilities: (i) availability of high magnetic fields and low (millikelvin) temperatures, (ii) a rotation stage which allowed a precise angular positioning of the dilution refrigerator insert for precise field alignment relative to the crystalline axes, and (iii) a polarised neutron beam and spin analysis of the scattered neutrons. Presently the simultaneous availability of these techniques only exists at the ILL.
Both the position (Q_y) of the VL Bragg peaks in **figure 1**, as well as the peak positions (φ) and splitting of the split rocking curves in **figure 2**, can be used to determine the VL anisotropy.

Figure 3 summarises the measured VL anisotropy as a function of the angle (Ω) between the field and the Ru-O basal planes for 2 different values of the magnetic field. This shows how the VL anisotropy rises quickly as the field gets closer to the basal plane, even if measurements with perfect alignment (Ω = 0) are not possible due to a vanishing intensity. Instead we used a fit to the data to obtain the intrinsic superconducting anisotropy Γ_{ac} = 58.5 ± 2.3 as shown by the dashed line. In comparison the H_{c2}-anisotropy of 20 (dotted line) yields a very poor fit to our measurements.

In conclusion we have used SANS to measure the anisotropy of the superconducting state in Sr_2RuO_4, in a narrow range of field angles close to, but not perfectly aligned with, the Ru-O basal plane. The superconducting anisotropy greatly exceeds that of the upper critical field and imposes significant constraints on the possible pairing of carriers in this material. Any model aimed at describing the superconducting phase must provide a satisfactory explanation for this observation.

Figure 3

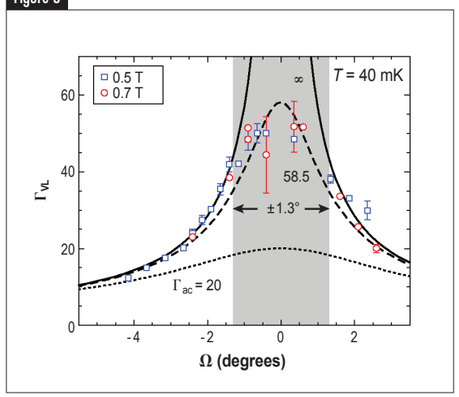

*Vortex lattice anisotropy as a function of the angle between the applied magnetic field and the crystalline a-axis (**Ω**). The lines show the calculated VL anisotropy for Γ_{ac} = 20 (dotted line), 58.5 (dashed line), and ∞ (full line). Only within ±1.3° does the measured anisotropy deviate from that expected for a perfectly two-dimensional system (∞).*

AUTHORS & REFERENCES

M.R. Eskildsen, **C. Rastovski** and **S.J. Kuhn** (University of Notre Dame, USA)
C.D. Dewhurst (ILL)
Y. Maeno (Kyoto University, Japan)
K. Machida (Okayama University, Japan)

[1] A.P. Mackenzie and Y. Maeno, Rev. Mod. Phys. 75 (2003) 657
[2] Y. Maeno *et al.*, J. Phys. Soc. Jpn. 81 (2012) 011009
[3] C. Rastovski *et al.*, Phys. Rev. Lett. 111 (2013) 087003
[4] S.L. Thiemann, Z. Radovic and V.G. Kogan, Phys. Rev. B 39 (1989) 11406

Three-axis spectrometer IN8

Hour-glass spectrum in a stripeless insulating transition metal oxide

The magnetic excitations in high-temperature copper oxide superconductors are believed to be crucial for superconductivity. The most promising models able to describe these "hour-glass"-shaped magnetic excitation spectra are currently based either on models where the charges within the copper oxygen planes segregate into stripes or on purely itinerant models where Fermi surface effects are significant. However, a recent observation of this type of magnetic excitation spectrum in an insulating cobalt oxide showed that Fermi surface effects are not necessarily needed for an understanding of the hour-glass spectrum [1]. We have now been able to synthesise an insulating cobalt oxide with this spectral shape that does not exhibit charge stripes either, thus suggesting that "hour-glass"-shaped magnetic excitations may have a completely different origin [2].

AUTHORS & REFERENCES

Y. Drees and **A.C. Komarek** (Max Planck Institute for Chemical Physics of Solids, Germany)
D. Lamago (LLB, France)
A. Piovano (ILL)

[1] A.T. Boothroyd, P. Babkevich, D. Prabhakaran and P.G. Freeman, Nature 471 (2011) 341
[2] Y. Drees, D. Lamago, A. Piovano and A.C. Komarek, Nature Communication 4 (2013) 2449

In this work, we studied a 40 % hole-doped single-layer perovskite cobaltate, $La_{1.6}Sr_{0.4}CoO_4$, which is isostructural to the high-temperature superconducting cuprates. In the ideal half-doped "parent compound", the charges are known to order in an alternating Co^{2+}/Co^{3+} arrangement with an antiferromagnetic structure that resembles a checkerboard (see **figure 1a**). In contrast, the incommensurate magnetic peak positions in our 40% hole-doped cobaltate should, in principle, be compatible with a phase where the charges arrange into diagonal stripes. Due to the comparably high sharpness of the magnetic peaks in our high-quality single crystals, we would also expect relatively sharp charge-stripe ordering superstructure reflections. (It should be noted that magnetic-stripe phases cannot easily be decoupled from charge-stripe phases in this insulating and localised system containing non-magnetic Co^{3+} ions. The movement of one electron from a Co^{2+} to a Co^{3+} site would require several 100 meV).

However, in detailed neutron scattering experiments, we were not able to detect any indication of charge-stripe ordering reflections in our 40% hole-doped cobaltate material [2]. Instead, we observed superstructure reflections located at half-integer positions in reciprocal space and indicative of the checkerboard charge ordering exhibited by the half-doped "parent compound". In fact, this is not entirely surprising, because the half-doped compound exhibits a very robust checkerboard charge order that persists up to very high temperatures (above 800K). It would therefore seem quite natural that such an extremely stable checkerboard charge order also persists in a certain doping regime around half-doping. In addition, it is unlikely for these stripes to occur at lower temperatures, since the charges cannot easily re-arrange themselves once they are frozen in a disordered checkerboard arrangement due to their insulating properties ("spin blockade" mechanism). Finally, the results of the study we performed at the spectrometer IN8 of high-energy cobalt-oxygen bond-stretching phonon modes in these cobaltates are consistent with our checkerboard charge ordering scenario and support our elastic studies (see **figure 2a**). This kind of bond-stretching phonon mode can be expected to exhibit an anomalous softening at the charge ordering propagation vector of the underlying charge order in this system. Whereas an isostructural nickel oxide with the same hole concentration exhibits such behaviour due to electron-phonon coupling, the same phonon modes in our cobaltate indicate almost the opposite behaviour, very similar to the behaviour in the optimum half-doped cobaltate with robust checkerboard charge ordering.

Figure 1

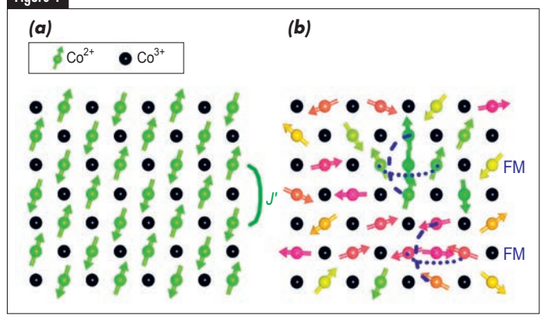

*Taken from [2]. **(a)** Antiferromagnetic structure of the ideal checkerboard charge-ordered half-doped cobaltate. Co^{3+} (black) ions are in the non-magnetic low spin state, whereas Co^{2+} ions (green) couple antiferromagnetically across these non-magnetic hole-doped Co-sites with a weak exchange interaction J'. **(b)** Our frustration scenario for our 40% Sr-doped cobaltate. The doping of one additional electron at a Co^{3+} site introduces extremely strong nearest-neighbour exchange interactions J that are also antiferromagnetic and therefore turn originally antiferromagnetic couplings ferromagnetic, as indicated by the blue dashed lines. This results in strong frustration effects and chiral magnetic structures that most likely arise locally in order to release the frustration. The different spin directions are emphasised by the colour change.*

Surprisingly, our study of the magnetic excitation spectrum in our 40% hole-doped cobaltate revealed the presence of an hour-glass-shaped feature, as can be seen in **figure 2b** and **2c**. As a consequence, the emergence of these hour-glass-shaped magnetic excitations in this insulating cobalt oxide is apparently not connected either to the existence of Fermi surface effects or to the appearance of charge-stripe phases in these layered insulators. Another, third mechanism must therefore be responsible for triggering the onset of these hour-glass spectra. We propose a frustration scenario based on disordered checkerboard charge-ordered structures, which is shown in **figure 1b**. The doping of one additional electron could turn two originally antiferromagnetic exchange interactions within the original checkerboard charge-ordered matrix ferromagnetic. This is due to the formation of stronger nearest neighbour exchange interactions *J* compared to the existing weak exchange interactions *J'*. This strong degree of frustration most likely induces non-collinear magnetic structures, as shown schematically in **figure 2b**, demonstrating the high significance of frustration for "hour-glass" spectra.

In conclusion, we have shown that, like Fermi surface effects, charge stripes are not needed for the emergence of an "hour-glass" dispersion.

Figure 2

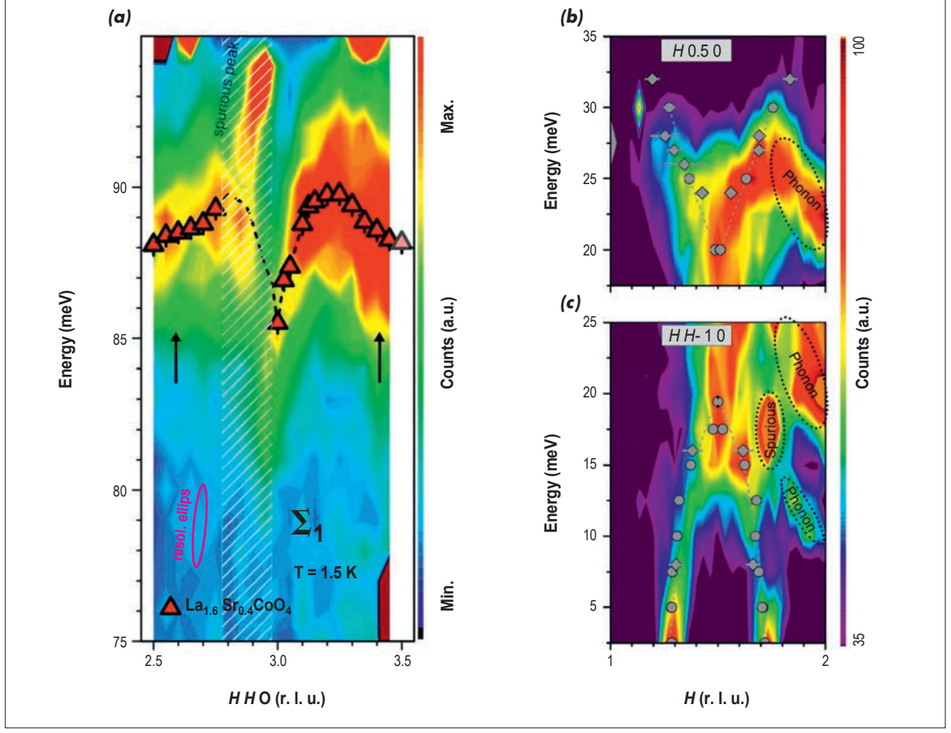

*Taken from [2]. **(a)** Neutron scattering intensity as a function of energy and momentum transfer obtained at the spectrometer IN8. Red triangles denote the high-frequency Co-O bond-stretching phonon dispersion. A distinct softening at Q = (2.5 2.5 0) becomes apparent. **(b,c)** Inelastic neutron scattering intensities obtained from constant-energy scans across the planar antiferromagnetic wavevector in **(b)** the [100]-direction and **(c)** the [110]-direction. All basic features of a so-called "hour-glass" dispersion are visible: the inward-dispersing branches that merge with increased intensity ("neck" of the hour-glass) and the outward-dispersing branches at higher energies.*

Time-of-flight spectrometer IN4

Crystal field excitations in NdFeAsO: another magnetic aspect of the Fe-pnictides

The discovery of high-temperature superconductivity in Fe-based oxy-arsenides has triggered extensive research on the physical properties of Fe-based superconductors in general. Magnetically, the interplay between the Fe 3d and rare-earth 4f electrons plays a key role in determining the physical aspects of these materials. For the specific case of NdFeAsO, the Fe spin-density-wave (SDW) transition at ~ 137 K is found to be preceded closely by a high-temperature paramagnetic tetragonal to a low temperature antiferromagnetic orthorhombic structural phase transition at ~ 142 K. Further, a spin-reorientation of the Fe magnetic sublattice takes place upon the ordering of the Nd moments below 2 K. Therefore this system offers a rich magnetic case where different magnetic and magneto-structural interactions can be observed at different temperature scales.

AUTHORS & REFERENCE

M. Zbiri and **T. Chatterji** (ILL)
Y. Xiao and **Th. Brückel** (JCNS and PGI, Germany)
R. Downie and **J.-W.G. Bos** (Heriot-Watt University, Edinburgh, UK)

[1] Y. Xiao, M. Zbiri, R.A. Downie, J.-W. G. Bos, Th. Brückel, and T. Chatterji, Phys. Rev. B 88 (2013) 214419

As a major interaction in rare earth compounds, the crystalline electric field (CEF) reflects directly the electrical and magnetic potential on the rare-earth site, which is created by the neighbouring ions. Interestingly, in the case of NdFeAsO, the neighbouring ions are more than just a point charges since they include the magnetic Fe cations. The determination of structure and parameters of CEF is therefore an attractive issue to be addressed for a better understanding of the physical properties of these systems.

We have studied the CEF excitations of Nd^{3+} in NdFeAsO by performing detailed temperature-dependent (1.6 to 200 K) inelastic neutron scattering (INS) measurements on IN4, using two neutron incident wavelengths (1.11 and 2.22 Å). Simulations based on a single ion crystal field model Hamiltonian were carried out to help analysis and interpretation of the INS data. The structure of the crystal field levels are constructed for both the high-temperature paramagnetic tetragonal (local point group symmetry C_{4v}) and the low-temperature antiferromagnetic orthorhombic (local point group symmetry C_{2v}) phases. The crystal field parameters are obtained from the analysis of the CEF interactions [1].
The local structure surrounding the Nd^{3+} ion is illustrated in **figure 1a**. A schematic diagram of the obtained splitting of the Nd^{3+} ground multiplet, at 5 and 160 K, is presented in **figure 1b**. We note that the ground state at 5 and at 160 K is a magnetic singlet and doublet, respectively.
The obtained CEF spectra at 5 and 160 K are shown in **figure 2a** and **figure 2b**, respectively. The solid lines represent a relevant modeling based on a crystal field model Hamiltonian. The simulations allowed extracting reliable CEF parameters which are used to describe the behaviour of the CEF excitations. Good agreement is found between the results of the fits and the experimental data. With increasing temperature, the intensities of all peaks decrease, indicating that these features are excitations occurring between the ground state and the excited states. Moreover, few new peaks are observed and can be assigned to the CEF transitions between the populated excited states. Further, the de-excitation transition from the excited states to the ground state can be also observed on the neutron energy gain side (negative energies) of the spectra in **figure 2b**. The assignment of the peaks is depicted in **figure 1b**. We notice that, while four CEF excitation peaks were expected at 5 K, we observe in fact five (*A* - *E*). The additional splitting of CEF peaks in the low-temperature orthorhombic phase indicates that the molecular field, *i.e.* the effective exchange magnetic field induced by the Fe magnetic sublattice, is correlated with the magnetism of Nd^{3+}, leading to a further lifting of the degeneracy.

The interplay between Nd and Fe magnetism in NdFeAsO is complex and becomes significant as the order-order transition of the Fe magnetic sublattice exhibits a close proximity to the onset of the Nd magnetic order. In order to gain deeper insights into the effect of the molecular field of the magnetic Fe sublattice on the CEF excitations, we consider the temperature-dependent INS measurements presented in **figure 3a**. Two peaks are clearly observed at 7.24 (labeled as *B*) and 8.59 meV (labeled as *C*). We define the splitting parameter, $P=[E(C)-E(B)]/[E(C)+E(B)]$, whose temperature dependence is shown in **figure 3b**. The SDW transition temperature is found at ~ 140 K, which is associated with a long-range antiferromagnetic order of the Fe moments. Further, the splitting parameter reaches its maximum at 2 K and its amplitude is reduced below 2 K (inset of **figure 3b**).

This highlights that the local potential at the Nd^{3+} sites has changed due to the change of the Fe molecular field upon the spin-reorientation transition of the Fe cations [1].

In summary, combining INS measurements and crystal field modeling, the crystal field levels and parameters were extracted for both the high-temperature paramagnetic tetragonal and the low-temperature antiferromagnetic orthorhombic phases of NdFeAsO. The revealed variation of the CEF excitations reflects not only the change of local symmetry but also the change of the magnetic ordered state of the Fe sublattice. A significant variation of the high order CEF parameters is found to occur upon the magnetic phase transition, indicating a pronounced difference in the exchange interaction between the rare-earth 4*f* and conduction electrons [1]. This highlights the importance of the magnetic interplay between the rare-earth and the Fe atoms, as well as the very similar Fe magnetism in the rare-earth iron oxy-arsenides.

While this work concerned the non-superconducting parent compound NdFeAsO, we plan to pursue the study in the light of the present findings and the conclusions we have drawn. We would therefore extend the combined experimental and numerical INS approach to treat CEF in the related superconducting doped counterpart systems. Further interesting insights could then be gained into other relevant characteristics, like the superconducting energy gap.

Figure 1

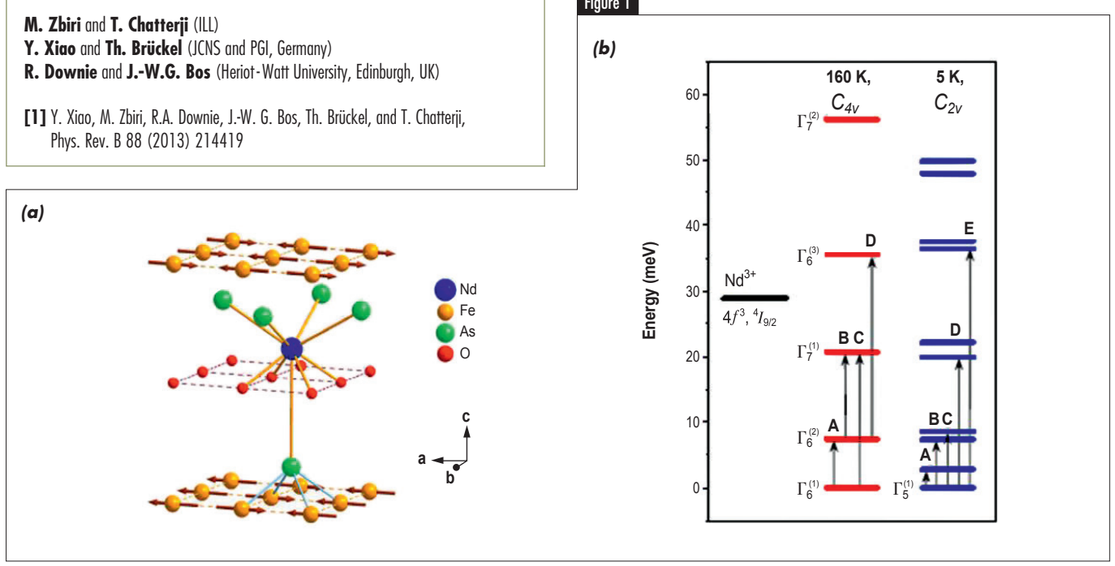

(a) *Illustration of the local structure of the Nd^{3+} ion at 5 K.* ***(b)*** *Scheme of the energy-levels diagram of Nd^{3+} in NdFeAsO for the lowest J-multiplets, under the tetragonal (C_{4v}) and orthorhombic (C_{2v}) structural environments. The arrows denote a few representative CEF transitions as extracted from our inelastic neutron spectra.*

Figure 2

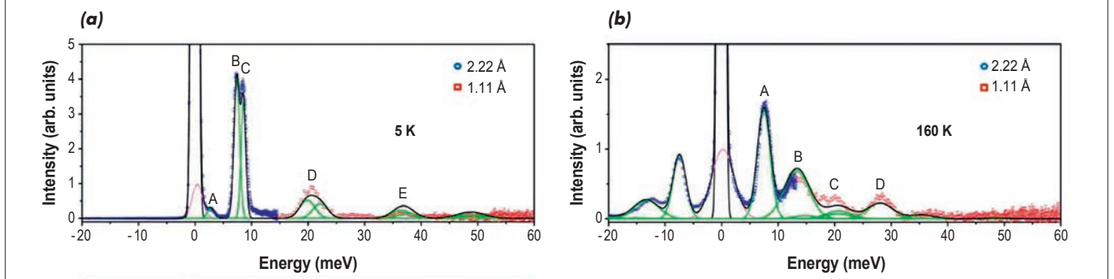

(a) *and* ***(b)*** *Energy spectra of CEF excitations for NdFeAsO at 5 and 160 K, respectively. The solid lines are results of the fit. The labeled peaks correspond to representative CEF transitions marked in* ***figure 1b****.*

Figure 3

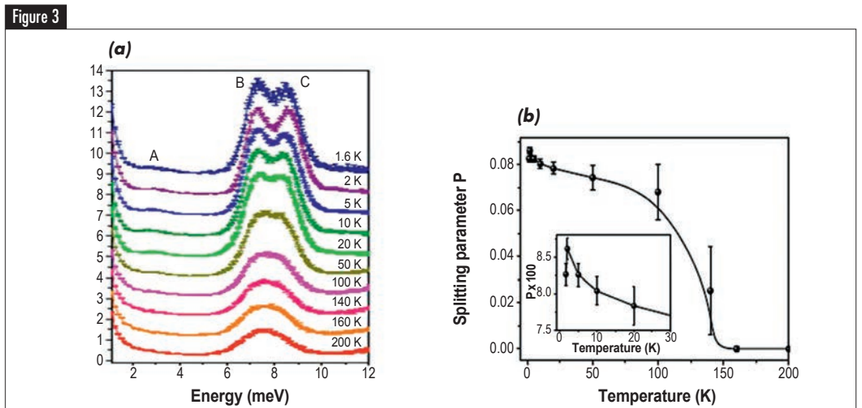

(a) *Temperature dependence (1.6 – 200 K) of the CEF excitations within the energy range 2-12 meV.*
(b) *Evolution of the related splitting parameter, $P = [E(C)-E(B)]/[E(C)+E(B)]$, as a function of temperature. The lines are guides to the eyes. The inset shows the enlarged view between 0 and 30 K.*

Time-of-flight spectrometer IN4

Electromagnon in ferrimagnetic ε-Fe_2O_3 nanograin ceramics

There has been increasing interest in so-called multiferroic materials, which simultaneously display spontaneous ferroelectric polarisation and (anti) ferromagnetic ordering. Electromagnons are spin waves excited by the electric component of electromagnetic radiation due to dynamic magnetoelectric coupling in multiferroics. Here we report on the discovery of an electromagnon in ε-Fe_2O_3 appearing below 110 K, where the ferrimagnetic structure becomes incommensurately modulated. This is the first time that electromagnons have been observed in a polycrystalline material through a combination of infrared reflectivity, time-domain THz spectroscopy and inelastic neutron scattering.

C. Kadlec, **F. Kadlec**, **V. Goian**, **M. Kempa**, **M. Savinov** and **S. Kamba** (Institute of Physics, ASCR, Prague, Czech Republic)
M. Gich (Institut de Ciència de Materials de Barcelona, Spain)
S. Rols (ILL)
J. Prokleška (Charles University, Prague, Czech Republic)
M. Orlita (High Magnetic Field Lab, CNRS, Grenoble, France)

AUTHORS & REFERENCES

[1] A. Pimenov, A. Mukhin, V. Ivanov, V. Travkin, A. Balbashov and A. Loidl, Nat. Phys. 2 (2006) 97
[2] R. Valdés Aguilar, A.B. Sushkov, C.L. Zhang, Y.J. Choi, S.-W. Cheong and H.D. Drew, Phys. Rev. B 76 (2007) 060404
[3] C. Kadlec, F. Kadlec, V. Goian, M. Gich, M. Kempa, S. Rols, M. Savinov, J. Prokleška, M. Orlita and S. Kamba, Phys. Rev. B 88 (2013) 104301

Terahertz (THz) studies of multiferroics have revealed a new kind of electric-field active spin excitations contributing to the dielectric permittivity $\varepsilon = \varepsilon' - i\varepsilon''$, known as electromagnons (EMs) [1]. They were first discovered in $TbMnO_3$ and $GdMnO_3$ and then confirmed in many other multiferroics [1].They couple with polar phonons, which manifests itself in the spectra by a transfer of dielectric strength from phonons to EMs on cooling [2]. In contrast to (anti) ferromagnetic resonances, which are magnons from the Brillouin zone (BZ) centre contributing to magnetic permeability, EMs can also be activated outside the BZ centre. The understanding of this fact is not trivial, because the photons which excite EMs have wave vectors much smaller than the EMs.
To date, there are several different theories attempting to explain the observed properties of EMs in various materials.

Our experiments show [3] that an EM can appear in the pyroelectric and ferrimagnetic ε phase of Fe_2O_3. While ε-Fe_2O_3 is quite rare and less known than the α (hematite) or γ (maghemite) phases of Fe_2O_3, its properties make it attractive for applications such as electromagnetic wave absorbers and memories. Owing to a limited phase stability, it can only be synthesised in the form of nanoparticles, epitaxial thin films or nanowires. Below 480–495 K, it is ferrimagnetic; at room-temperature, it has a collinear spin structure and exhibits a coercive field of $H_c \approx 2$ T, the highest known value among metal oxides.

Figure 1

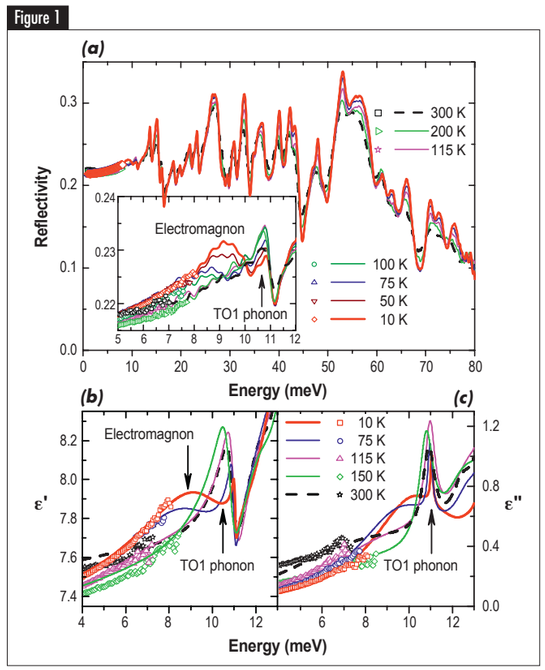

(a) *Lines: IR reflectivity spectra showing polar phonons. Symbols below 8 meV: data calculated from THz spectra. The inset shows in detail the low-energy part where, below 100 K and 10 meV, a new reflection band appears due to the EM.* ***(b)***, ***(c)****: Complex permittivity in the far IR region, obtained from the fit of IR reflectivity spectra using a sum of harmonic oscillators (lines), compared to data obtained from THz spectroscopy (symbols).*

The crystal lattice has a temperature-independent non-centrosymmetric orthorhombic structure with the $Pna2_1$ space group. Its low-temperature phase diagram is complex - below 150 K, a series of magnetic phase transitions occur. Below $T_m = 110$ K, an incommensurate magnetic ordering appears, where the magnetic structure modulation has a periodicity of about 10 unit cells.

The results of our infrared (IR) and THz measurements are given in **figure 1**, showing polar optical phonons. Upon cooling, all phonons above 12 meV exhibit the usual behaviour: their intensity increases due to reduced phonon damping at low temperatures.
In contrast, the phonon near 11 meV exhibits an anomalous behaviour: on cooling, its intensity only increases down to 115 K. Below this temperature, it weakens notably, while a supplementary broad reflectivity peak develops below $E \approx 10$ meV and becomes more intense upon cooling. This transfer of strengths evidences a coupling between these two polar modes.

At the same time, we confirmed that the crystal symmetry of ε-Fe_2O_3 does not change with temperature. In other words, no new polar phonons should appear.

As the nanopowder does not allow us to determine directly the phonon and magnon dispersion branches in the BZ, we used the time-of-flight technique on IN4. The resulting intensity maps of inelastic neutron scattering (INS) taken at selected temperatures are depicted in **figure 2a**, **2b** and **2c**.

The data reveal a steep column of intense scattering, emanating from magnetic Bragg peaks at $Q = 1.4$ Å^{-1} and extending up to $E \approx 10$ meV. The weaker columns at $Q > 2$ Å^{-1} are due to scattering in higher-order BZs. The fact that the area of most intense scattering is located at low Q shows unambiguously that the dominant contribution to the low-Q scattering comes from spin waves. Around 10 meV, a distinct scattering peak persists down to low temperatures, corresponding to the maximum of the magnon density of states (DOS). Moreover, the energy at the maximum magnon DOS, as well as its temperature evolution, correspond to that of the newly IR-activated mode (see **figure 2d**).

Since the observed spin-wave excitation is coupled with the lowest-energy TO1 phonon, it must be excited by the electric component of the electromagnetic radiation; at the same time, it has to contribute to dielectric permittivity. Therefore, the excitation seen near 10 meV must be an EM. EMs were previously only identified in single crystals using a thorough polarisation analysis of measured spectra. Here we have determined an EM from unpolarised IR and THz spectra of nanograin ceramics showing its coupling with a TO1 phonon. At the same time, we have shown from INS experiments conducted on powder that the EM in ε-Fe_2O_3 comes from the BZ boundary. The combining of experimental methods in this way provides a guideline for an unambiguous determination of EMs in materials where sufficiently large single crystals for polarised IR and THz measurements are not available.

Figure 2

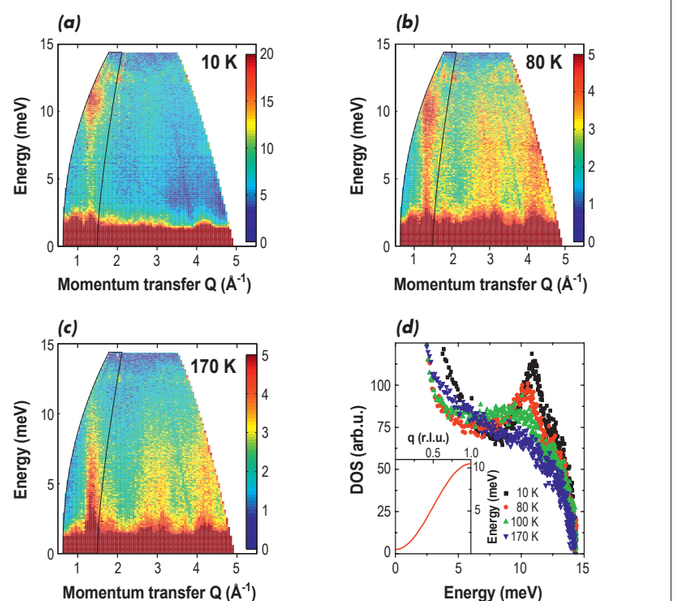

(a), ***(b)***, ***(c)****: Bose-Einstein-factor-normalised INS intensity as a function of momentum Q and energy E transfers for T = 10, 80 and 170 K. Near Q = 1.4 Å^{-1}, a magnon branch with a cut-off energy of ≈ 11 meV can be seen.* ***(d)****: Density of states determined by integrating over the regions marked by black solid lines in* ***(a)***–***(c)***. *Inset of* ***(d)****: Schematic representation of the magnon dispersion branch in reciprocal lattice units.*

Three-axis spectrometer IN14

Chirality of the spin resonance excitation in an unconventional superconductor under magnetic field

Inelastic neutron scattering is a key probe to understand the mechanisms of unconventional superconductivity since it gives access to the magnetic excitation spectrum of these systems, where spin fluctuations are a prime candidate for being involved in the Cooper pair formation. In many such unconventional superconductors, a new excitation named spin resonance emerges in the superconducting phase. By using polarised inelastic neutron scattering under magnetic field, new insight on the resonance of $CeCoIn_5$ is obtained, a significant step toward a better understanding of this mode.

AUTHORS & REFERENCES

S. Raymond and **G. Lapertot** (CEA-INAC/UJF-Grenoble, France)
K. Kaneko (Japan Atomic Energy agency, Japan)
A. Hiess (ESS, Lund, Sweden)
P. Steffens (ILL)

[1] C. Stock *et al.*, Phys. Rev. Lett. 109 (2012) 167207
[2] S. Raymond *et al.*, Phys. Rev. Lett. 109 (2012) 237210
[3] E. Lorenzo *et al.*, Phys. Rev. B 75 (2007) 054418
[4] A. Akbari and P. Thalmeier, Phys. Rev. B 86 (2012)134516

Promises of superconductivity are moderated by important gaps separating technology from basic science in terms of temperature of operation and critical currents achieved. This notwithstanding, the diversity of materials and the understanding of phenomena has been unprecedented in the past decades. The spin resonance is an ubiquitous magnetic excitation that appears in many unconventional superconductors: cuprates, iron pnictides and chalcogenides as well as heavy fermion systems.
This magnetic mode is observed in inelastic neutron scattering experiments below the superconducting transition temperature T_c. It appears at a specific wave-vector for which the superconducting gap changes sign and at an energy of several k_BT_c.

Figure 1

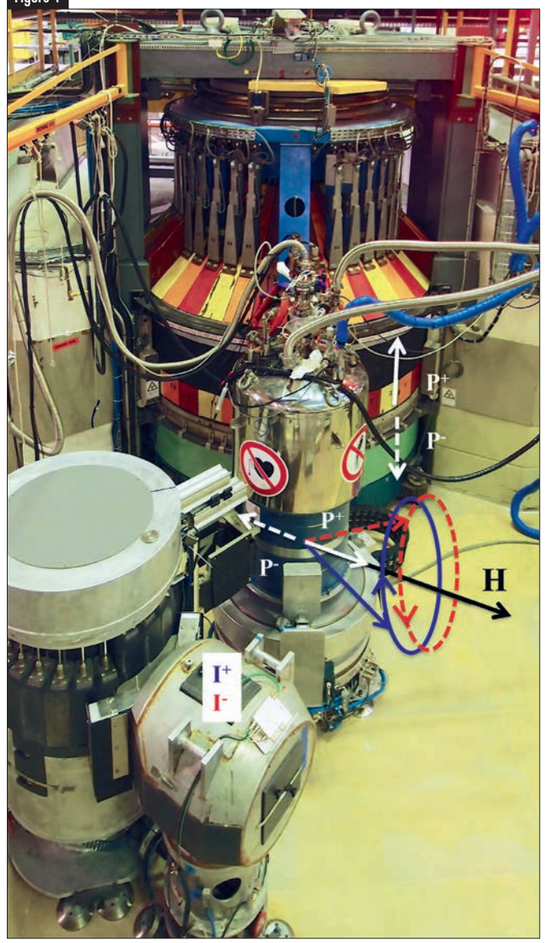

The three-axis spectrometer IN14 with a sketch of the polarised neutron set-up used with a horizontal field magnet. The initial polarisation P^+, respectively P^-, couples with right handed (full blue line) and respectively left handed (dashed red line) spin precession, leading to intensity I^+ and I^-, the chiral response being given by I^--I^+.

While there is no consensus on the origin of such an excitation and its relevance to the pairing mechanism, it provides important information about the superconducting state. Heavy fermion systems, 4f and 5f electron based strongly correlated materials, are particularly well-suited for such studies with expected strong response to a magnetic field, given the intrinsic low energy scales involved in relation to the small values of T_c. $CeCoIn_5$, a heavy fermion superconductor with T_c = 2.3 K, is the first case in which a Zeeman splitting of the spin resonance is evidenced [1]. The study of the spin resonance under magnetic field and using polarised neutrons gives further insight into the anisotropies and degeneracies associated with this mode and therefore on its nature [2].

The measurements were performed on the cold neutron three-axis spectrometer IN14 with the polarised neutron set-up shown in **figure 1**. In this set-up the initial neutron beam is polarised and the polarisation is adiabatically kept toward the sample located in a dilution fridge inside an horizontal field magnet. The field is applied along the scattering vector Q and the polarisation is either parallel (P^+) or antiparallel (P^-) to the horizontal magnetic field. The corresponding scattered intensity measured is I^+ for P^+ and I^- for P^-. With such a set-up, different contributions to the magnetic excitation spectrum can be enhanced or suppressed whereas an unpolarised neutron scattering experiment measures the sum of both contributions [3]. This is due to the so-called chiral correlation function that enters the scattering cross-section for such polarised neutron scattering experiment and that is directly obtained by the difference I^--I^+. In particular, a clockwise spin precession leads to non-vanishing intensity only for P^+ and an anticlockwise precession for P^- (see **figure 1**). A given handedness is therefore associated to a given neutron beam polarisation only.

Figure 2

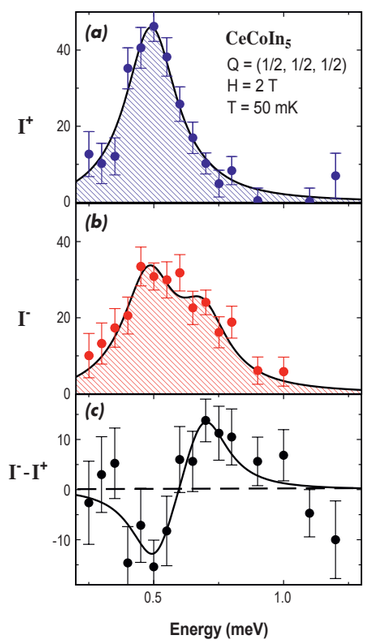

*Magnetic excitation spectrum of the unconventional superconductor $CeCoIn_5$ for Q= (1/2, 1/2, 1/2) at 50 mK and under a magnetic field of 2 T applied along Q for **(a)** polarisation parallel (P^+) to the field, and **(b)** antiparallel to the field (P^-). **(c)** shows the chiral correlation function obtained from the difference I^--I^+. Intensities are given in arbitrary units.*

The spectra obtained for the unconventional superconductor $CeCoIn_5$ at a temperature of 50 mK and for a field of 2 T applied along Q=(1/2, 1/2, 1/2) are shown in **figure 2**. The energy dependence of the signal depends on the initial polarisation indicating the presence of chirality. **Figure 2a** shows the excitation spectrum for P^+ and **figure 2b** the one for P^-. The difference between the two measured intensities, I^--I^+, is shown in, **figure 2c**. This chiral response has similar spectral weight, but with opposite sign, above and below Ω=0.6 meV, which is the zero field resonance energy. The minima and maxima located at Ω-δ and Ω+δ, with $\delta \approx$ 0.08 meV at 2 T, establishes the Zeeman splitting of the resonance, each mode having a different handedness. The peculiar feature is that the symmetry of the chiral contribution **figure 2c** does not reflect the signal in each polarisation channel **figure 2a** and **2b**. At an energy around Ω-δ, both polarisation channels contribute to the scattering while around Ω+δ scattering occurs almost only for the P^- channel. Without any model so far, this asymmetry can be accounted for by the presence of another contribution to the spin dynamics that has no polarisation dependence and therefore no chiral nature. This low energy mode exists on the top of the Zeeman split contribution that exhibits the chirality shown in, **figure 2c**. This possibility may be related to a dominant crystal field anisotropy allowing several kinds of fluctuations (transverse and longitudinal) and such scenario must be addressed by relevant theoretical studies [4].

In summary, two modes of the Zeeman split resonance of $CeCoIn_5$ are observed for different incident neutron polarisation evidencing their chiral nature. An unexpected additional non-chiral contribution must be added in order to account for the asymmetry arising in the individual polarisation channel measurement. This complexity tightens the theoretical scenario for the spin resonance mode. Those are necessary steps for understanding the mechanisms of unconventional superconductivity in view of tailoring new materials in the future.

Reflectometer SuperADAM

Magnetic correlations in multilayers and monolayers of iron oxide nanoparticles

Chemically synthesised magnetic nanoparticles (NPs) are promising materials for the bottom-up approach to nanodevice fabrication [1]. They can be self-assembled in a 2-dimensional (2D) monolayer or in a three-dimensional (3D) multilayer with tunable magnetic and electrical properties. In particular, the interaction between NPs can lead to collective magnetic behaviour manifesting itself in superparamagnetic, superspin-glass, and superferromagnetic states [2]. These states depend on the ordering of the NPs and the type and strength of magnetic interaction between the NPs. We show here that hexagonally ordered spherical NPs with a pure magnetic dipolar coupling can lead to the formation of long-range magnetic order. The understanding of these interactions has implications for data storage media and spintronics devices.

AUTHORS & REFERENCES

D. Mishra, **P. Szary**, **F. Brüssing** and **H. Zabel** (Ruhr University Bochum, Germany)
M.J. Benitez (Ruhr University Bochum, Germany and Max-Planck-Institut, Mülheim, Germany)
O. Petracic (Ruhr University Bochum, Jülich Centre for Neutron Science JCNS and Peter Grünberg Institut PGI, JARA-FIT Forschungszentrum Jülich, Germany)
G.A. Badini Confalonieri (Ruhr University Bochum, Germany and Institute of Materials Science, CSIC Madrid, Spain)
K. Theis-Bröhl (University of Applied Sciences Bremerhaven, Germany)
A. Devishvili (Ruhr University Bochum, Germany and ILL)
A. Vorobiev (Uppsala University, Sweden and ILL)
O. Konovalov (ESRF)
B.P. Toperverg (Ruhr University Bochum, Germany and Petersburg Nuclear Physics Institute, Gatchina, St Petersburg, Russia)

[1] S.A. Majetich *et al.*, ACS Nano 5 (2011) 6081 and A. Dong *et al.*, Nature 466 (2010) 474
[2] O. Petracic, Superlattices and Microstructures 47 (2010) 569
[3] D. Mishra *et al.*, Nanotechnology 23 (2012) 055707

Using spin-coating techniques, we promoted the self-assembly of iron oxide NPs of 20 nm in diameter on silicon substrates. The NPs were dispersed in toluene and separated by oleic acid surfactant. The samples were heat treated at 80°C to evaporate the solvent and annealed at 230°C in vacuum to enhance magnetite as the major phase. **Figure 1** shows SEM images of as-prepared monolayer and multilayer films. The NPs show a hexagonal close-packed arrangement with a long-range structural ordering. This long-range ordering leads to the collective magnetic behaviour of the self-assembled system. The respective measurements were carried out using the SuperADAM instrument at the ILL.

Figure 1

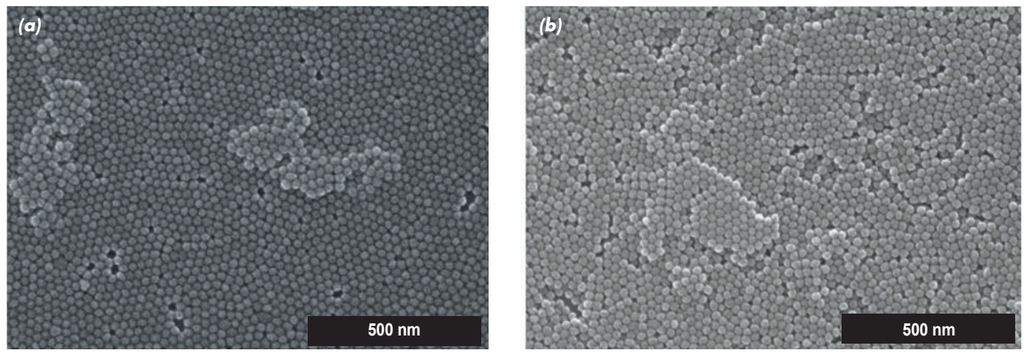

*SEM images of NPs spin-coated on silicon substrate with hexagonal ordering forming **(a)** monolayer and **(b)** multilayer.*

Figure 2 shows the polarised neutron reflectivity from a multilayer sample for up and down polarisation at an applied field of 5 kOe (**a**) and at remanence (**b**), respectively, along with best fits (solid lines). The fitting reveals a 5-layer system with an out-of-plane hexagonal periodicity of 13.5 nm, as confirmed by the Bragg peak (arrow). Furthermore, the fitting reveals several novel features in the multilayer. The nuclear SLD indicates that the out-of-plane NP layering improves from bottom to top, unlike many other self-assembled NP systems.

The fitting also provides insight into the microscopic magnetic structure. The splitting of the reflectivities for up and down polarised neutrons at high fields confirms a finite magnetisation of the multilayer, which is expressed in a finite magnetic SLD, as shown in **figure 2c**, top left panel. At remanence the splitting disappears, which implies that the sample has zero net magnetisation. Surprisingly, the magnetic SLD value, shown in the bottom left panel of **figure 2c**, remains finite and identical to the value at high fields. This can be explained if the system is assumed to have a domain-like structure as shown in the sketch (bottom right panel of **figure 2c**). At the applied field of 5 kOe, the NPs' magnetic moments are aligned mainly along the field axis and a finite magnetisation is observed. When the field is removed, the net magnetisation falls to zero. However, due to strong dipolar interaction between the NPs, their magnetic moments are heavily correlated over microscopic regions. These regions are much smaller than the sample area, but greater than the lateral projection of the neutron coherence length. Within such regions, the NPs' magnetic moments are aligned ferromagnetically forming quasi-domains (shown as brown lines in the bottom right panel) and project a finite magnetic SLD. Arising purely due to dipolar interaction, they are different from usual ferromagnetic domains and have no well-expressed domain walls [3].

In summary, the multilayer shows hexagonal ordering with out-of-plane layering achieved using spin-coating. The structural ordering leads to quasi-domain-like long-range magnetic order mediated by pure dipolar coupling.

Figure 2

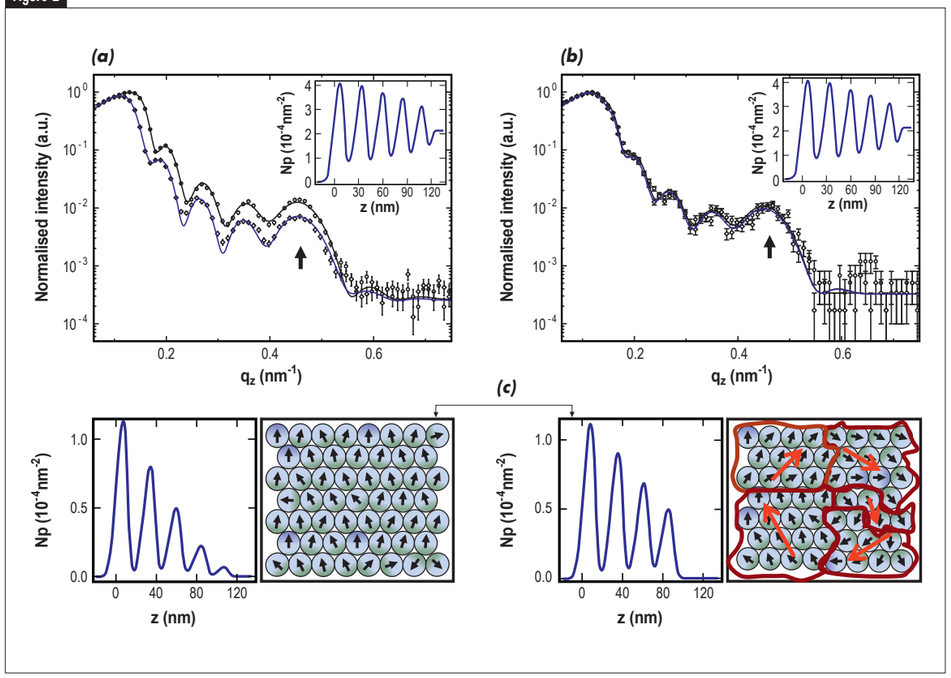

*Polarised neutron reflectivity taken at room temperature and at **(a)** 5 kOe and **(b)** at remanence for two polarisation states, along with best fits. The arrow indicates the Bragg peak of the five-layer stack of NPs. The inset shows the nuclear SLD obtained from fitting. **(c)** Plot of magnetic SLD at 5 kOe (top left panel) and at remanence (bottom left panel). The corresponding sketches of the superspin arrangement at 5 kOe and at remanence are shown in the right-hand panels, respectively. The quasi-domains are highlighted by the brown lines. Figure published in ref [3].*

Single-crystal diffractometer D19

A proton chain in a molecular solid

The movement of water and protons, including transport in confined spaces, is of considerable importance in a number of key areas of science and technology. Water transport can be observed in a wide variety of media from solids, such as zeolites and clays, to living cells, and in various contexts, such as molecular storage materials, catalysis, soil science and many others. Proton migration, which is often related to water transport, is currently of interest in energy applications, while water transport is of particular importance in biology, especially in cell membranes in which sophisticated structures permit the passage of water while blocking ion transport.

L.R. Falvello, **M. Tomas**, **E. Forcen-Vazquez**, **S. Sanz** and **F. Palacio**
(C.S.I.C. - University of Zaragoza, Spain)
G.J. McIntyre (ANSTO, Australia)
S.C. Capelli (ILL)

[1] C.J.T. Grotthuss, Ann. Chim. 58 (1806) 54
[2] S.C. Capelli, L.R. Falvello, E. Forcén-Vázquez, G.J. McIntyre, F. Palacio, S. Sanz and M. Tomás, Angew. Chem. Int. Ed. 52 (50) (2013) 13107
* Front cover of Angewandte Chemie (2013) 13107

A common form of proton migration is the diffusion of water into absorbing materials, either via channels and cavities or via some sort of pathway which involves a proton cascade. When trying to explain electrolysis in water solutions some 200 years ago, Grotthuss already proposed concepts which over time have taken the form of a hopping-reorientation mechanism in which the movement of ionic H^+ is assumed to involve concerted proton "hand-off" from one water molecule to the next in the chain [1]. This type of mechanism has been put forward to explain proton mobility in a number of different processes, very often in solution, but has not always been supported by experimental evidence.

The complete exchange of protium for deuterium on mobile and immobile water molecules in a non-porous crystal of a manganese citrate cubane coordination polymer, $[Mn(H_2O)_6]_{2n}\{[Mn(H_2O)_5]Mn_4(citr)_4[\mu\text{-}Mn(H_2O)_4]\}_n \cdot 8nH_2O$, with geometrical features that are well in line with a Grotthuss "hand-off" chain, has been observed through single-crystal neutron diffraction analysis [2].

When a partially dehydrated crystal of the manganese citrate cubane polymer is exposed to D_2O vapour at room temperature for few hours, all of the 21 H_2O units per polymer link, attached to four independent Mn(II) centres in the form of aqua ligands, and the additional 9 free solvent water sites, become D_2O units.

The primary goal of studying the Mn-containing citrate cubane polymer was to understand the non-destructive, fully reversible single-crystal-to-single-crystal transformation that this non-porous system exhibits upon physical solvent loss and reuptake. The structures of the fully H_2O-hydrated, the dehydrated, and the H_2O-rehydrated compounds were first analysed by single-crystal X-ray diffraction in the home laboratory. The experiments revealed the principal structural changes occurring at the solid-state transformations. However, because of the size of the structure and the small scattering power of hydrogen in X-ray diffraction, the hydrogen atoms of the water molecules could not be located.

Neutron diffraction measurements carried out at 20 K on the thermal neutron single-crystal diffractometer D19 have enabled us to locate the hydrogen atoms in the fully H_2O-hydrated structure and in the D_2O-rehydrated structure. All the H (or D) atomic positions have been identified by neutron Fourier difference maps and fully refined with isotropic displacement parameters. Of the 30 water sites, 8 are found to have 3 hydrogen atoms at bonding distance from the oxygen atom, 2 of which are half-occupied. The fully occupied oxygen forms two chemically perfectly acceptable H_2O units with either of the half-occupied hydrogen atoms. Two additional oxygen atoms are surrounded by four half-occupied hydrogen atoms. Again two water molecules with correct geometry can be formed by the oxygen atom and the two pairs of hydrogen atoms.

The hydrogen-atom disorder implies a superposition of two orientations of water molecules frozen in place at the low temperature of the data collection. The disorder can therefore be interpreted in terms of two chains of double-minimum hydrogen potentials which fit with the two states of a Grotthuss mechanism (**figure 1**). Such a proton chain, or proton wire, allows the transport of hydrogen atoms inside the crystal in a direction parallel to the crystallographic *a*-axis.

The enormous difference in scattering length between protium and deuterium makes neutron diffraction an essential probe for studying proton migration and isotopic substitution phenomena in molecular solids.

Figure 1

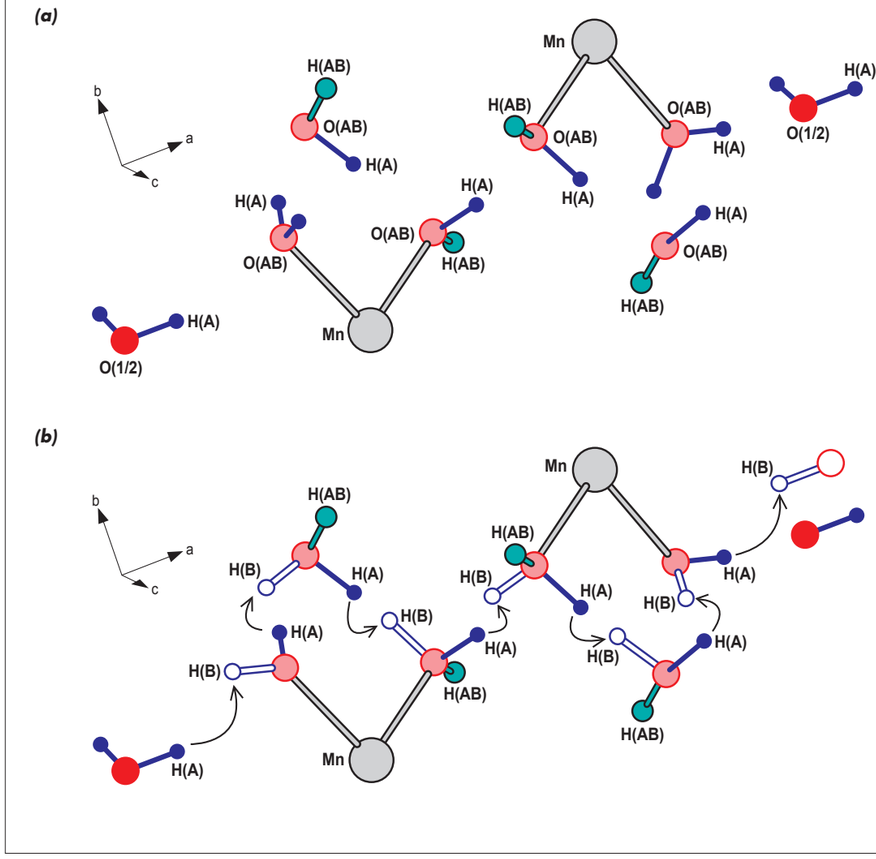

*Schematisation of the Grotthuss hopping mechanism for the hydrogen atoms in the structure of $[Mn(H_2O)_6]_{2n}\{[Mn(H_2O)_5]Mn_4(citr)_4[\mu\text{-}Mn(H_2O)_4]\}_n \cdot 8nH_2O$. **(a)** Starting structure: the hydrogens represented in dark blue are those subjected to the hopping mechanism; **(b)** the arrows indicate the path of the hydrogen atoms in the structure and the open circles the new positions of the hydrogen atoms.*

Single crystal diffractometers D19, D9
Powder diffractometer D1B
Laue diffractometer VIVALDI

Structural and magnetic neutron studies of a molecular multiferroic compound: joining forces across the ILL's neutron diffraction instrument suite

The design of molecular "multiferroic" materials where electric and magnetic order coexist can be achieved by including electrically polarisable guest molecules into a flexible porous host lattice where long range magnetic order resides. Such multifunctional materials have recently aroused much interest with a view to development of new materials with very large magnetoelectric effects [1-4].

AUTHORS & REFERENCES

O. Fabelo and **J.A. Rodríguez-Velamazán** (CSIC-University of Zaragoza, Spain and ILL)
L. Cañadillas-Delgado (CSIC-University of Zaragoza, Centro Universitario de la Defensa de Zaragoza, Spain and ILL)
M.-H. Lemée-Cailleau, **S.A. Mason** and **J. Rodríguez-Carvajal** (ILL)
E. Pardo and **F. Lloret** (University of València, Spain)
J.-P. Zhao and **X.-H. Bu** (Nankai University, Tianjin, China)
V. Simonet and **C.V. Colin** (Institut Néel, CNRS and UJF, Grenoble, France)

[1] H.B. Cui, Z.M. Wang, K. Takahashi, Y. Okano, H. Kobayashi and A. Kobayashi, J. Am. Chem. Soc. 128 (2006) 15074
[2] P. Jain, V. Ramachandran, R.J. Clark, H.D. Zhou, B.H. Toby, N.S. Dalal, H.W. Kroto and A.K. Cheetham, J. Am. Chem. Soc. 131 (2009) 13625
[3] G.-C. Xu, W. Zhang, X.-M. Ma, Y.-H. Chen, L. Zhang, H.-L. Cai, Z.-M. Wang, R.-G. Xiong and S. Gao, J. Am. Chem. Soc. 133 (2011) 14948
[4] J.-C.Tan, P. Jain and A.K. Cheetham, Dalton Trans. 41 (2012) 3949
[5] L. Cañadillas-Delgado, O. Fabelo, J.A. Rodríguez-Velamazán, M.H. Lemee-Cailleau, S.A. Mason, E. Pardo, F. Lloret, J.P. Zhao, X.H. Bu, V. Simonet, C.V. Colin and J. Rodríguez-Carvajal, J. Am. Chem. Soc. 134 (2012) 19772

Neutron diffraction studies have been carried out to shed light on the unprecedented order-disorder phase transition observed in the mixed-valence iron(II)-iron(III) formate framework compound $[NH_2(CH_3)_2]_n[Fe^{III}Fe^{II}(HCOO)_6]_n$. The initial studies were performed using Laue neutron diffraction at the VIVALDI instrument at two different temperatures above and below the transition. The comparison between the two patterns shows the appearance of new Bragg reflections at low temperature, which is a clear sign of a structural phase transition. This nuclear phase transition is associated with an electric phase transition, from paraelectric to antiferroelectric, as corroborated by means of dielectric measurements.

In order to determine the crystal structure in the low temperature phase, a neutron diffraction experiment was carried out at the D19 monochromatic single crystal diffractometer, where the new phase was accurately characterised (see **figure 1**). These results reveal the occurrence of a structural phase transition from *P*-31*c* space group at room temperature to *R*-3*c* space group at low temperature. This phase transition involves small distortions in the rigid $[Fe^{III}Fe^{II}(HCOO)_6]_n$ framework, while a more dramatic change is observed in the dimethylammonium counterions, which are weakly anchored in the cavities. These counterions are disordered at room temperature but become ordered below the phase transition temperature. The length of the *c*-axis in the ordered phase is about three times the length at room temperature, due to the loss of the 3-fold rotation axis that passes through the counterions in the high temperature phase; therefore the three possible equivalent of the dimethylammonium ions observed at high temperature, are split into three well-differentiated positions at low temperature (see **figure 1c**).

Figure 1

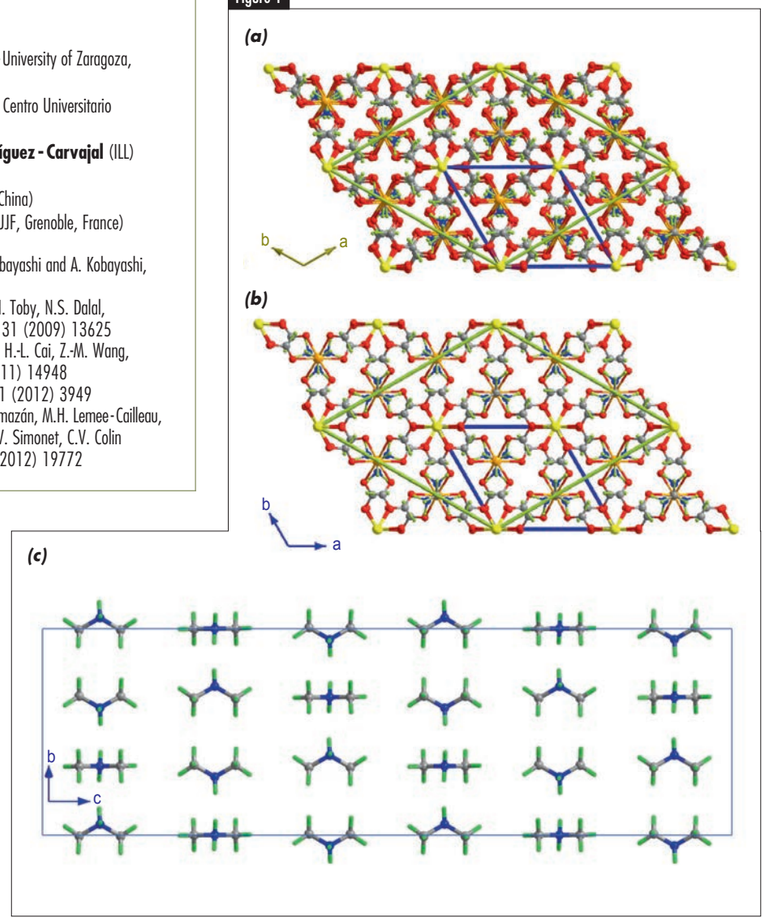

View along c-axis of the high temperature ***(a)*** *and low temperature* ***(b)*** *phases, where the HT and LT unit cells are represented in blue and green, respectively. The symmetry reduction is characterised by a loss of translational symmetry, the space group of the HT phase being P-31c, (a, b, c), while that of the LT phase is its subgroup R-3c but with unit-cell parameters a' = 2a + b, b' = -a + b, c' = 3c.* ***(c)*** *View along the a-axis of the dimethylammonium cation packing in the unit cell in the low temperature phase. Note that the three different positions of the dimethylammonium cations present along the c-axis are due to a screw axis. The metal-organic framework has been omitted from this figure for the sake of clarity.*

Once the crystal structure of the low temperature phase was properly characterised, our objective was to determine the magnetic structure below the ordering temperature (37 K). In order to elucidate the correct magnetic model, a multi-pattern approach based on simultaneous refinement of neutron powder diffraction (instrument D1B) and neutron single-crystal data (instrument D9) was carried out. Among the different magnetic models compatible with the possible irreducible representation, only the magnetic structure shown in **figure 2** gives a solution compatible with the neutron diffraction measurements. The spin moment of the Fe^{III} atoms lies strictly along the *c*-axis while the Fe^{II} atoms have two different components: the main contribution along the *c*-axis, which is coupled antiferromagnetically with the spin moments of the Fe^{III} atoms, and a second one, a small component in the *ab* plane that produces a rotation of the magnetic moments along the *c*-axis. This model produces a ferrimagnetic layered structure, where the magnetic moments are non-compensated along the *c*-axis in agreement with the results previous observed using macroscopic magnetic measurements.

In this work we have determined, using complementary neutron diffraction techniques, the crystal and magnetic structures of the molecular multiferroic $[NH_2(CH_3)_2]_n[Fe^{III}Fe^{II}(HCOO)_6]_n$ compound. The combination of Laue neutron diffraction studies and monochromatic neutron diffraction has allowed us to determine the structural model after an unprecedented order-disorder phase transition.

The order-disorder phase transition is triggered by the occurrence of an extensive network of hydrogen bonds; and neutron diffraction techniques have directly contributed to understand the role of this weak interaction in the physical properties of this material. Finally, the refined magnetic structure below 37K corresponds to a weakly non-collinear ferrimagnetic structure, due to the non-compensation of the magnetic moment of the Fe^{II} and Fe^{III} sites, which are antiferromagnetically coupled.

Figure 2

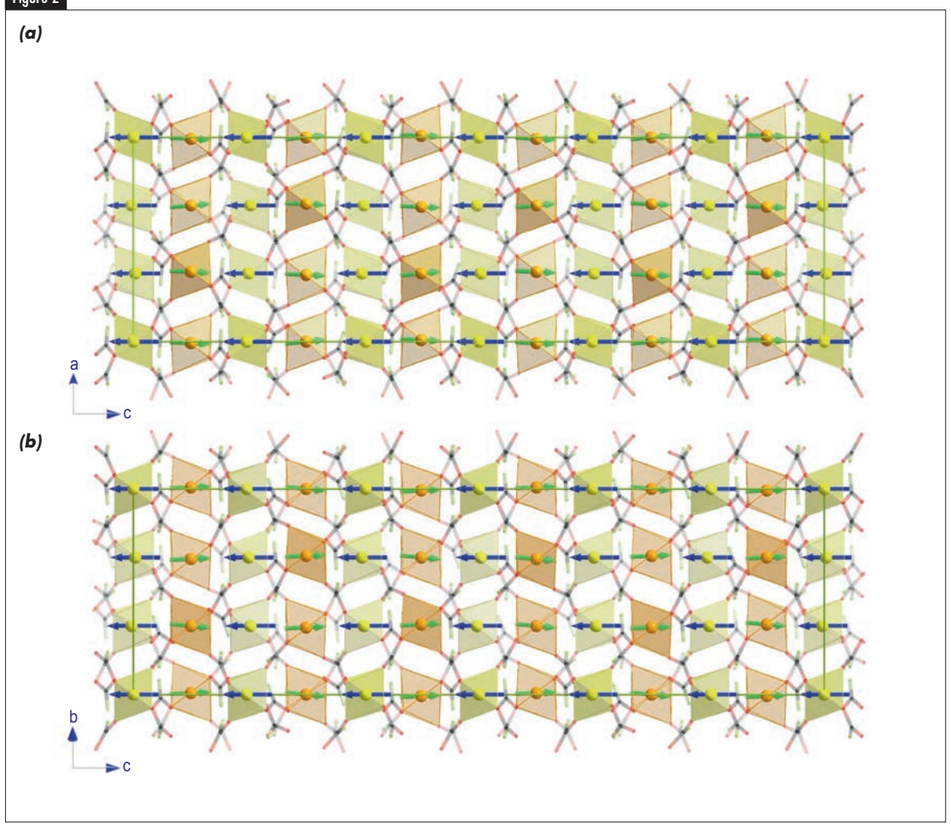

(a) *View along the b-axis of the unit cell of $[NH_2(CH_3)_2]_n[Fe^{III}Fe^{II}(HCOO)_6]_n$ together with the magnetic moment of each Fe^{II} and Fe^{III} site, yellow/blue and orange/green, for nuclear/magnetic structure, respectively.* ***(b)*** *Perspective along the a-axis of the nuclear and magnetic structure of $[NH_2(CH_3)_2]_n[Fe^{III}Fe^{II}(HCOO)_6]_n$, color code as in* ***(a)****. The formate ligands have been represented in transparent mode and the dimethylammonium counterions have been omitted for the sake of clarity.*

High-resolution diffractometer D2B
Powder diffractometer 11-BM
at Argonne National Laboratory

Synthesis and structure determination of $CaSi_{1/3}B_{2/3}O_{8/3}$, a new calcium borosilicate

Boron, alkali and alkaline earth oxides are key additives used to tune properties in technologically important bioactive and optical glass materials. In particular, boron oxide is added to glass compositions (typically silicate-based compositions) in order to optimise the melting and forming stages [1]. This work has led to the identification, synthesis and *in situ* structure determination of a new crystalline calcium borosilicate phase, namely $CaSi_{1/3}B_{2/3}O_{8/3}$, using neutron and X-ray powder diffraction and recent advanced high-resolution solid-state NMR techniques.

AUTHORS & REFERENCES

E. Véron, **M.N. Garaga**, **S. Cadars**, **D. Massiot**, **V. Montouillout**, **G. Matzen** and **M. Allix** (CNRS and University of Orléans, Orléans, France)
D. Pelloquin (National Graduate School of Engineering and Research Center ENSICAEN, Caen, France)
M. Suchomel (Argonne National Laboratory, Argonne, USA)
E. Suard (ILL)

[1] A.K. Varshneya, Fundamentals of Inorganic Glasses (1994)
[2] J.G. Fletcher and F.P. Glasser, J. Mater, Sci. 28 (1993) 2677
[3] G. Oszlanyi and A. Suto, Acta Crystallogr., Sect. A 60 (2004) 134
[4] E. Véron *et al.*, Inorg. Chem. 52 (2013) 4250

In this article, we report the synthesis of $CaSi_{1/3}B_{2/3}O_{8/3}$, a new crystalline compound obtained by crystallisation from a corresponding glass composition using a simple heat treatment. This so-called "X-phase" had been known since the sixties but until now its structure had never been solved. Interestingly, this new compound is located on the tie-line between the $CaSiO_3$ and $Ca_2B_2O_5$ phases in the CaO-SiO_2-B_2O_3 ternary diagram [2], and is only the fourth reported calcium borosilicate oxide phase, despite their importance within the mineralogy, glass and ceramics communities.

To obtain initial crystallographic information, electron diffraction analysis was performed on several $CaSi_{1/3}B_{2/3}O_{8/3}$ crystallites. The reconstruction of the reciprocal space shows an orthorhombic cell with $a \approx 12.1$ Å, $b \approx 5.2$ Å and $c \approx 3.7$ Å, and a space group that is either *Pnam* or $Pna2_1$. No isostructural compound could be found in the ICSD database using these space groups and similar sets of cell parameters.

The crystallographic structure of the calcium borosilicate was then determined *ab initio* using the charge flipping algorithm [3] performed on neutron powder diffraction data collected *in situ* at high temperature. The X-ray scattering of light elements characterised by a low electronic density, such as boron and oxygen, is actually much lower than their neutron scattering power. Moreover, the good contrast between boron and silicon elements using neutrons diffraction (whose scattering cross-sections are 5.24 and 2.17 barn, respectively) allowed us to determine precisely the position of each element within the structure. In order to reduce the absorption by natural abundance of our ^{10}B-containing sample (whose absorption cross-section is 7.10^5 times greater than ^{11}B), a powder sample was prepared from purified commercial products containing only ^{11}B. The absence of ^{10}B made it possible to reduce the acquisition time considerably. Moreover, due to the poor peak shape of the $CaSi_{1/3}B_{2/3}O_{8/3}$ phase at ambient temperature (due to ordering at the nanometric scale, as evidenced by high-resolution transmission electron microscopy [4]), the high-resolution neutron powder diffraction diagram was collected in situ at 650 °C on the D2B diffractometer at the ILL.

At the final stage of structure determination, the crystallographic parameters such as unit cell, atomic positions and site occupancy factors were refined with high levels of precision using the Rietveld method on the neutron diffraction powder diagram (**figure 1**). Due to the high resolution and the high counting level of the data, very good reliability factors ($R_{wp}=3.05$ %, $R_p=2.30$, $\chi^2=1.57$) were obtained. The average long-range structure of the $CaSi_{1/3}B_{2/3}O_{8/3}$ phase consists of an array of linear chains of TO_4 tetrahedra (**figure 2a**) with a mixed composition of 1/3 silicon and 2/3 boron for the *T* sites and a partial occupancy of 2/3 for the bridging oxygen sites (O3, **figure 2b**). From the average structure, the TO_4 tetrahedra appear to be severely distorted, and exhibit large and anisotropic atomic displacement parameters, which indicate deviations from a perfectly ordered structure. The local arrangement, and more especially the Si/B ordering, was then described based on data from ^{29}Si and ^{11}B solid-state Nuclear Magnetic Resonance (NMR) experiments and first-principles calculations.

A one-dimensional (1D) ^{11}B MAS solid-state NMR experiment shed light on the local structure, showing a line-shape characteristic of three-coordinated B sites forming planar BO_3 units, each associated with an oxygen vacancy and thus interrupting the chain. The average TO_4 chain thus consists of an arrangement of SiO_4 tetrahedra and BO_3 planar units, in a 1:2 ratio, and the atomic displacement parameters translate the departure from an ideal chain of tetrahedra. The results of a two-dimensional experiment allowed us to discard the presence of B-O-B chemical bonds. The structure of the calcium borosilicate is thus composed of $Ca_3B_2SiO_8$ (B^{III}-O-Si^{IV}-O-B^{III}) units.

The simplest structural models characteristic of $CaSi_{1/3}B_{2/3}O_{8/3}$ must consist of multiple unit cells of the average structure determined by neutron diffraction. This leads to two possible structures (**figure 2d** and **2e**), which differ in the topology of the chain arrangements. DFT methods then allow (i) the optimisation of the geometry of these two models, and (ii) the computation of their ^{11}B NMR signatures. Remarkably the two models, both involving similar $Ca_3B_2SiO_8$ units (**figure 2d**), yield very similar ^{11}B signatures, both compatible with the observed spectrum. The actual situation is certainly more complex and probably consists of combinations of different topologies of the inter-chain arrangements at the scale of tens of nanometres. Indeed, nanoscale-ordered domains exhibiting super-structures are evidenced by high-resolution electron microscopy images [4].

This study shows the existence of a new calcium borosilicate compound, $CaSi_{1/3}B_{2/3}O_{8/3}$, in the $CaO-SiO_2-B_2O_3$ ternary system that is of considerable interest to both the glass industry and the geology community. The synthesis of this new material was achieved by full crystallisation from glass. Its crystal structure was solved *ab initio* from synchrotron and neutron powder diffraction data collected *in situ* at high temperature. The orthorhombic structure ($Pna2_1$, $a=12.1025(4)$ Å, $b=5.2676(1)$ Å and $c=3.7132(1)$ Å) contains one Ca, one mixed Si/B and three inequivalent O crystallographic sites located on 4*a* Wyckoff positions. The combination of ^{11}B solid-state NMR and DFT calculations suggests that the $CaSi_{1/3}B_{2/3}O_{8/3}$ structure is composed of BO_3-SiO_4-BO_3 units with different arrangements along the [001] direction.

Figure 1

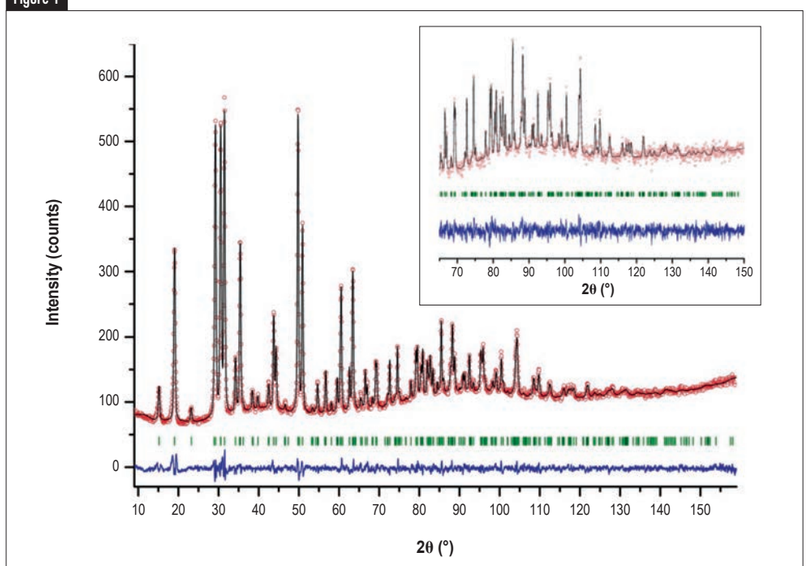

Final Rietveld refinement of neutron powder diffraction data of $CaSi_{1/3}B_{2/3}O_{8/3}$ collected on the high-resolution diffractometer D2B at high temperature ($R_{wp}=3.05\%$, $R_p=2.30\%$ and $\chi^2=1.57$). Observed (red circles), calculated (black line) and difference (blue line) profiles are shown. The set of green vertical lines corresponds to the reflection positions. Enlargement of 70-150° angular range (2θ) is embedded.

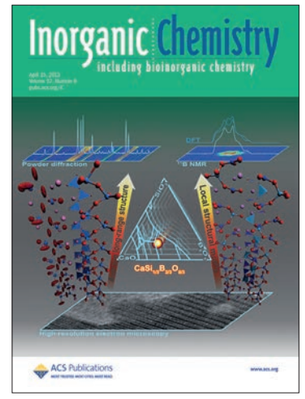

Front cover of Inorganic Chemistry (2013), 52(8).

Figure 2

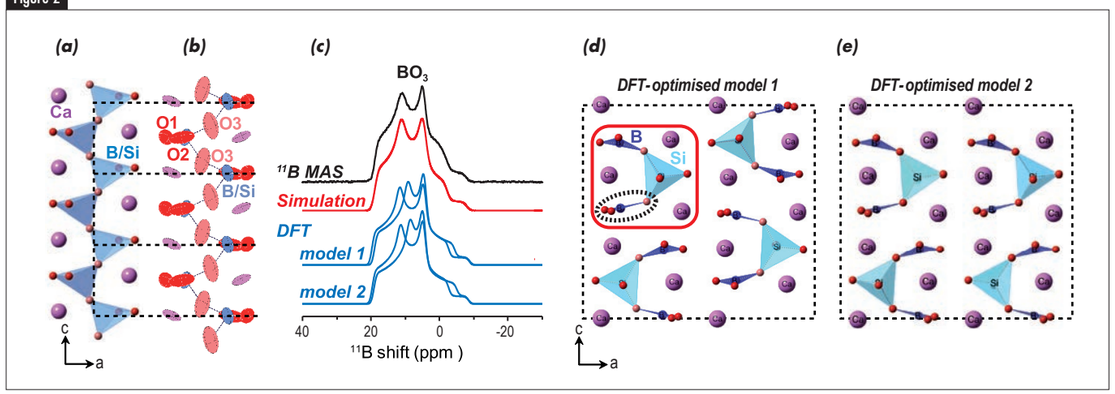

(a) *Chains of distorted TO_4 tetrahedra in the average long-range structure of $CaSi_{1/3}B_{2/3}O_{8/3}$.* ***(b)*** *The local compositional disorder is reflected in the ellipsoids.* ***(c)*** *^{11}B MAS NMR spectrum signing BO_3 units.* ***(d,e)*** *Two DFT-optimised models and their calculated ^{11}B signatures in blue. Both have an identical basic unit highlighted (in red) with a different chain arrangement topology.*

Horizontal reflectometer FIGARO INTER instrument at ISIS

Controlling fluorophore spatial distribution in polymer films for latent fingerprint visualisation

Latent (non-visible) fingerprints are a primary source of forensic evidence, but require physical or chemical treatment to visualise them. Despite a range of such treatments, the success rate is low. Recent work has shown how spatially controlled deposition of electrochromic polymers provides a powerful means of visualising fingerprints in "difficult" scenarios. In a novel extension of this strategy, we have used neutron reflectivity to monitor and optimise a multi-stage interfacial assembly process that yields electroactive films with optical absorption and emission characteristics with the potential for highly sensitive latent fingerprint enhancement

AUTHORS & REFERENCES

R.M. Sapstead, **K.S. Ryder**, **A.R. Hillman** and **C. Fullarton** (University of Leicester, UK)
M. Skoda and **R.M. Dalgliesh** (Rutherford Appleton Laboratory, UK)
E. Watkins, **C. Beebee** and **R. Barker** (ILL)
A. Glidle (Glasgow University, UK)

[1] R.S. Ramotowski (*ed.*), *Advances in Fingerprint Technology*, 3rd edn., CRC Press, Boca Raton (2013)
[2] A.L. Beresford and A.R. Hillman, Anal. Chem., 82 (2009) 483
[3] R.M. Sapstead and A.R. Hillman, Phys. Chem. Chem. Phys., 14 (2012) 8653
[4] R.M. Sapstead, K.S. Ryder, C. Fullarton, M. Skoda, R.M. Dalgliesh, E. Watkins, C. Beebee, R. Barker, A. Glidle and A.R. Hillman, Far. Disc. 164 (2013) 391

The spatial pattern of a fingerprint uniquely identifies an individual. Despite the rise of sophisticated genetic methods, fingerprints are central to criminal investigations and civil identification applications [1]. Indeed, the power of fingerprint evidence is anecdotally recognised in other contexts – DNA "fingerprinting" and the "fingerprint" region of IR spectra. Forensically, most fingerprint evidence derives from latent fingerprints (those for which material exchanged between the finger and the surface is not visible to the eye), but these fingerprints require some means to visualise them. Although diverse reagents have been developed for this purpose - from powders that adhere mechanically to the sticky residue to chemicals that interact with specific components of the residue – the low operational success rate (only ca. 10%) motivates novel approaches.

We have taken a complementary approach to "traditional" methods: instead of targeting the fingerprint residue, which may be depleted or degraded by age or environmental exposure, we use the residue as a template (or "mask") to direct the reagent to the bare surface – the "valleys" between the "hills" of the residue in the cartoon of **figure 1** – producing a negative image of the fingerprint. The surfaces on which we have chosen to operate are metals. Operationally, this corresponds to a range of weapons (guns, bullets, knives), tools (used for entry purposes) and objects of intrinsic value (metal theft). Practically, this allows us to use electrochemical means to drive the deposition process, in our case the polymerisation and deposition of electroactive polymers. Significantly, since only a few nanometres of insulating residue effectively block electron transfer (far less than required by conventional reagents), higher sensitivity is possible. The outcome is illustrated by the polypyrrole-enhanced image on a stainless steel surface of a latent fingerprint that had been degraded by immersion in water for 7 days (**figure 2**). We have taken this further by re-immersion of the object (potentially "evidence") in monomer-free background electrolyte and applying different electrochemical potentials to vary the doping level – and thus colour – of the deposited film, e.g. polyaniline [2] or poly(3,4-ethylenedioxythiophene) [3].

Recognising the sensitivity of fluorescence detection, and indeed its wide forensic exploitation [1], we sought to extend the optical *absorption* strategy above with observations based on *emission*. This requires deposition of a fluorophore-functionalised polymer film. The obvious tactic of polymerising a suitably functionalised monomer resulted in failure; simple considerations based on the relative shapes and sizes of typical monomers (based on aniline, pyrrole or thiophene) and typical fluorophore moieties reveals that geometrical and steric factors will inevitably be problematical. Instead, we devised a strategy (**figure 3**) involving polymerisation of monomers (here, pyrrole-based) functionalised with a labile group (FMOC) small enough to permit polymerisation. Post-polymerisation hydrolysis then results in replacement of the leaving group with solvent. In the dynamic environment of the film, aggregation of these small solvent-filled pockets generates voids large enough to accommodate fluorophores added to the solution; with suitable chemistry, these are bound to the polymer (**figure 3**).

Realising the aspirations of **figure 3** relies upon knowledge and control at each stage of the process of the spatial distributions of the film components: polymer, leaving group, solvent and fluorophore. Neutron reflectivity (NR) is the perfect tool to provide: (i) the content and distribution of solvent, whose presence plasticises the polymer and whose departure creates space for fluorophore; (ii) the efficiency of leaving group expulsion and (iii) the extent of fluorophore functionalisation. There is a delicate balance to be struck. If the solvent content is too low, then fluorophore will not penetrate the film: it will be confined to the outer surface in amounts too low to visualise. If the solvent content is too high, either the film may collapse (ironically, with the same result) or fluorophore will run through to the underlying metal, where quenching will result in low visibility. Between these two extremes, one aims to have fluorophore distributed homogeneously throughout the polymer.

Figure 1

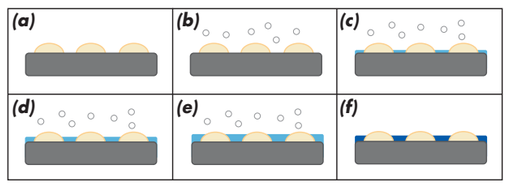

Cartoon illustrating (from side view) the sequence of events in electrochromic polymer enhancement of a latent fingerprint on a metal object: ***(a)*** *fingerprint residue is deposited on the surface;* ***(b)*** *the object ("evidence") is exposed to a solution of monomer;* ***(c)*** *application of a potential to the object initiates polymer formation and deposition selectively on the bare metal surface;* ***(d)*** *the "valleys" between the fingerprint residue "hills" progressively fill;* ***(e)*** *shows overfilling of the "valleys", such that visual discrimination between the hills and valleys is lost;* ***(f)*** *shows the result of transfer of the optimally deposited surface in panel (e) to monomer-free electrolyte and application of a potential to generate a polymer redox state (doping level) giving strong visual contrast against the surface.*

FMOC-functionalised polypyrrole (PyFMOC) was polymerised potentiodynamically ($\nu = 20$ mV s^{-1}) from 10 mM PyFMOC in 0.1 M TBAP / CH_3CN onto Au films supported on quartz blocks. The resulting PPyFMOC polymer films were deprotected using 30% ν/ν piperidine in CH_3CN to yield $PPyNH_2$, which was reacted with 0.01 M Dylight 649 NHS ester (**figure 3**). NR measurements were made on FIGARO (at ILL) and INTER (at ISIS). A crucial aspect of the study was kinetic observation of the hydrolysis process since, in a practical application, this must be optimised.

Reflectivity profiles acquired during PPy-FMOC hydrolysis (to generate the free volume within the film) are shown in **figure 4**. Within each profile, there are fringes with two distinct periodicities. One set is associated with the Au thin film electrode: these are independent of time and, as a consequence of its sharp interfaces, are more evident at higher Q. The other is associated with the polymer film: these fringes stretch out as hydrolysis progresses, corresponding to (partial) film collapse. Detailed fitting of data obtained for a range of contrast scenarios (**figure 5**) was facilitated by two external constraints, namely coulometric assay of the total amount of electroactive polymer (for the data shown, $\Gamma_{PPyFMOC}$ = 20 nmol cm^{-2}) and FTIR spectroscopic verification of FMOC removal and fluorophore binding (via the disappearance and reappearance of a characteristic amide band; see **figure 3**). These spatially integrated insights into "how much?" and "what?" facilitate NR addressing the question "where?" The data revealed that FMOC elution resulted in film shrinkage by ca. 30%, but in an *increase* in solvent volume fraction from 0.41 to 0.60 – an effect of the size of the leaving group. Following polymer relaxation, the solvent volume fraction subsequently fell to 0.52. In relative terms these changes can profoundly affect polymer chain mobility and in absolute terms the replaceable solvent volume fraction permits a high fluorophore population - one fluorophore entity for every ca. five pyrrole monomer units.

Fingerprints play an important role in criminal investigations, security applications and identifications of unknown individuals following natural disasters. The fundamental scientific challenge underlying these societal issues is that successful visualisation of the fingerprint involves observation of *lateral* structure at the centimetre (whole print) to 100 µm (ridge feature size) length scales, but accomplishment of this involves control of *vertical* interfacial chemistry at the nanometre to micrometre scale. We have separately optimised the lateral control of polymer deposition (**figure 2**) and of the *vertical* control of fluorophore functionalisation (**figure 4** and **5**) on a laterally uniform surface. Their combination is the next step. The interplay of (electro)chemistry on different length scales in lateral and vertical directions provides novel challenges to which neutron science will undoubtedly contribute significantly in the near future.

Figure 2

Photograph of a polymer-enhanced fingerprint on a stainless steel surface that was left immersed in water for 7 days before the enhancement treatment, involving electrochemical deposition of polypyrrole.

Figure 3

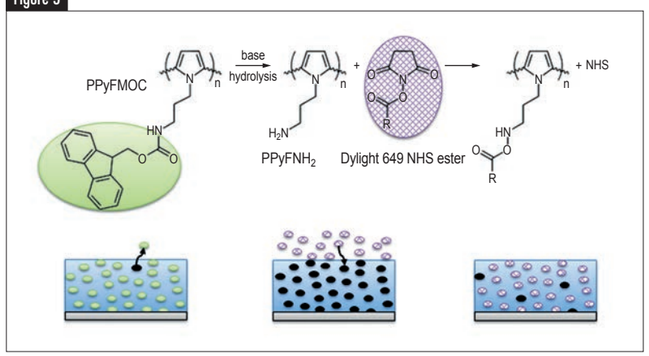

Cartoon representation of (i) PPy-FMOC deposition, (ii) FMOC hydrolysis to create solvent "voids"; (iii) diffusion of fluorophore into voids and attachment to polymer. Stylised ellipsoids (simplistically, of similar size) represent FMOC (pale green), solvent (black) and fluorophore (diamond chequered). (Taken from [4]).

Figure 4

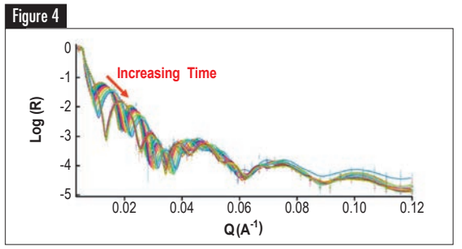

Superimposed reflectivity profiles, R(Q), acquired during piperidine hydrolysis of a PPy-FMOC film supported on an Au electrode and exposed to CD_3CN (to optimise contrast). Profiles acquired at 10 min intervals over a period of 7.5 hours. (Taken from [4]).

Figure 5

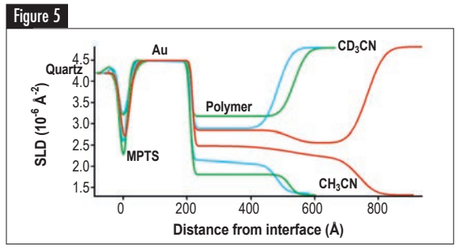

Model fitted scattering length density profiles for a polypyrrole film exposed to h_3-acetonitrile and d_3-acetonitrile at each of the three stages of the process represented in ***figure 3****: nominally PPyFMOC (red traces), $PPyNH_2$ (green traces) and PPy-Dylight (blue traces). (Taken from [4]).*

Liquids and amorphous diffractometer D4

Fragile glass-formers reveal their structural secrets

Calcium aluminates $CaO\text{-}Al_2O_3$ form a significant component of the Earth's mantle and are an important ingredient in several materials having great utility [1]. They are, for example, an integral component of aluminous cement, the glasses have optoelectronic applications in the infra-red spectrum, and the rare-earth doped materials exhibit persistent luminescence. Aerodynamic-levitation with laser-heating allows for the containerless processing of refractory liquid oxides and for the formation of new families of glass forming materials. Here we combine this technique with the method of isotope substitution in neutron diffraction to elucidate the structure of a single levitated droplet of the calcium aluminate $CaAl_2O_4$. The results combined with molecular dynamics simulations reveal key structural modifications on multiple length scales as the liquid forms a glass, findings that may well be applicable to other magma-related materials.

AUTHORS & REFERENCES

J.W.E. Drewitt (University of Edinburgh, UK and CEMHTI-CNRS University of Orléans, France)
L. Hennet (CEMHTI-CNRS University of Orléans, France)
A. Zeidler and **P.S. Salmon** (University of Bath, UK)
S. Jahn (GFZ German Research Centre for Geosciences, Germany)
D.R. Neuville (CNRS-IPGP University of Sorbonne, Paris, France)
H.E. Fischer (ILL)

[1] D.R. Neuville, G.S. Henderson, L. Cormier, and D. Massiot, Am. Mineral. 95 (2010) 1580
[2] C.A. Angell, Science 267 (1995) 1924
[3] J.W.E Drewitt, L. Hennet, A. Zeidler, S. Jahn, P.S. Salmon, D.R. Neuville, and H.E. Fischer, Phys. Rev. Lett. 109 (2012) 235501
[4] G.S. Henderson, G. Calas, and J.F. Stebbins, Elements 2 (2006) 269

Figure 1

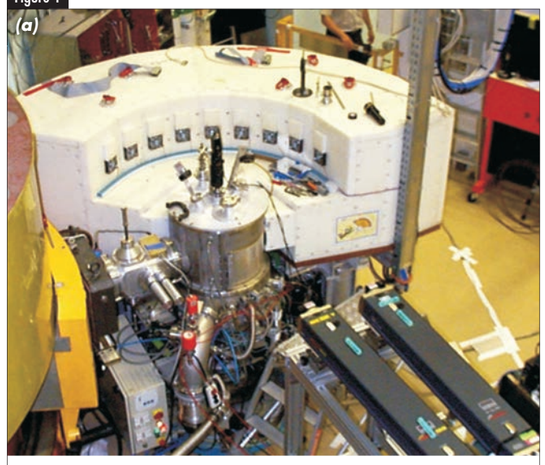

Photograph of the laser heating set-up installed at the neutron diffractometer D4 ***(a)*** *and a schematic of the levitation device mounted in the instrument belljar* ***(b)***.

Liquid calcium aluminates are very fragile glass-forming materials, meaning that their dynamical properties slow-down dramatically with decreasing temperature as the glass transition is approached [2]. The structural complexity, coupled to the high temperatures involved, means that little is known about the processes that take place when glasses are formed.

To tackle this problem, the combined methods of (i) aerodynamic-levitation with laser-heating and (ii) neutron diffraction with Ca isotope substitution were used to investigate the detailed structure of $CaAl_2O_4$ as a liquid at 1973 K and as a glass at room temperature [3]. The ILL diffractometer D4 was employed with the set-up illustrated in **figure 1**.
The levitation method has the advantage that it avoids the use of a container material, thus allowing liquid droplets to be deeply supercooled and new families of glass to be formed. The isotope substitution method is a site-specific structural probe that is well known for giving a clear picture for the structure of liquids and glasses, but its application to aerodynamic-levitation experiments is hindered by the need to use single levitated droplets, typically small spheres of diameter 2.5 mm.

The experimental information was interpreted with the aid of molecular dynamics computer simulations using a polarisable ion model, and the results reveal dramatic and unexpected changes in the material's structure during glass formation.

In the liquid, the aluminium atoms form AlO_4 and AlO_5 structural motifs, and there are significant numbers of threefold coordinated oxygen atoms in so-called tricluster conformations where a single oxygen atom is shared between three AlO_4 tetrahedra.

During glass formation, the AlO_5 units and threefold coordinated oxygen atoms breakdown as the structure reorganises to construct a network of predominantly corner-sharing AlO_4 tetrahedra. This process is accompanied by the formation of branched chains of edge- and face-sharing Ca-centred CaO_x polyhedra that weave through the glass network (**figure 2**).

Glasses formed under high-temperature and high-pressure conditions are often used as proxies for understanding liquids of geophysical importance because they can access structural configurations that crystalline materials cannot reach [4]. The new results show that this can be a dangerous strategy as the process of glass formation in materials such as calcium aluminate is accompanied by a substantial change in nature of the structural configurations. Ultimately, there is no substitute for *in situ* diffraction experiments. The results for the high-temperature liquid from the present work will provide a benchmark for interpreting the structural changes that occur in addition when high-pressures are applied in order to match the conditions experienced by natural magmas in planetary interiors.

Figure 2

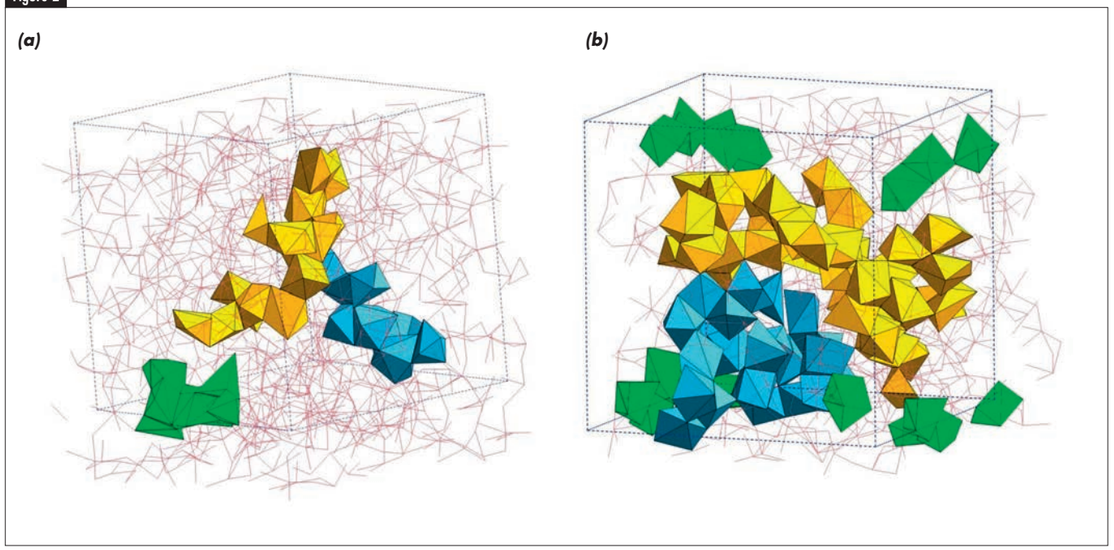

Snapshots from molecular dynamics simulations showing the structure of liquid ***(a)*** *and glassy* ***(b)*** $CaAl_2O_4$. *On quenching the liquid, a reorganisation of Al-centred structural motifs is accompanied by the formation of extended branched chains of edge- and face-sharing Ca-centred polyhedra. Different chains are represented by the connected yellow, blue and green coloured units, and involve many more Ca atoms in the glass than in the liquid.*

High intensity diffractometer D20

Morin transition in hematite (α-Fe_2O_3) under pressure

Hematite is the most important iron-ore and hence of prime importance for our civilisation. It is also known to occur in large quantities on Mars, thereby contributing to the remarkable colour of the 'red planet'. Academic interest in Hematite is due to its spin-flop phenomenon, the famous Morin-transition: when a sample is cooled from ambient temperature, the spin-direction flips at 260 K by 90° without evident change of crystal structure. In recent experiments at ILL the behaviour of the Morin transition was investigated under hydrostatic pressure to 8 GPa. A massive increase by +27 K/GPa is detected, which allows insight into the microscopic origins of the Morin transition.

AUTHORS & REFERENCES

S. Klotz (Pierre et Marie Curie University, Paris, France)
Th. Strässle (Paul Scherrer Institute, PSI, Switzerland)
Th. Hansen (ILL)

[1] F.J. Morin, Phys. Rev., 78 (1950) 819
[2] S. Klotz, Th. Strässle, Th. Hansen, Europhys. Letters 104 (2013) 16001
[3] J.B. Parise *et al.*, Physica B, 385-386 (2006) 391, and references therein
[4] J.O. Artman *et al.*, Phys. Rev. A, 138 (1965) 912

Figure 1

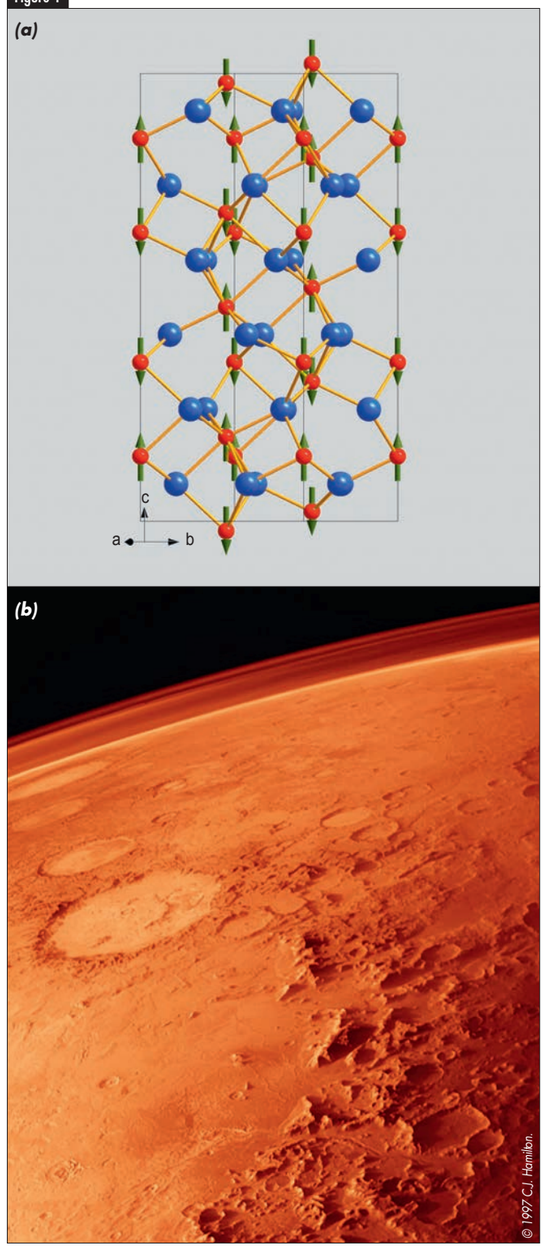

(a) *Structure of Hematite (α-Fe_2O_3, $R\bar{3}c$) with Fe^{3+} spin directions as below the Morin transition T_M. At T_M=260 K the spin direction flips by about 90° into the hexagonal plane.* ***(b)*** *Picture of Mars taken by the Voyager spacecraft. Hematite is believed to be one source of the reddish hue.*

The Morin transition is the textbook example of a spin-flop transition. Hematite is antiferromagnetic with a Néel temperature of 960 K. At low temperature and ambient pressure, the Fe^{3+} moments are aligned along the rhombohedral <111> axis, pointing in opposite directions in adjacent iron-layers, see **figure 1**. At 260 K, the spins flip by 90° into the hexagonal layer. There is also a slight residual canting of the spins by 0.04° which leads to a very small ferromagnetic component.
In recent experiments carried out at ILL, the variation of the Morin transition was investigated under pressure. Such experiments ought to give insight into the microscopic origin of the Morin transition, and spin-flop phenomena in general. To achieve such pressures the group from the University Pierre and Marie Curie (Paris) and the Paul Scherrer Institute (Villigen, Switzerland) used the ILL Paris-Edinburgh pressure cell to compress samples of Fe_2O_3 under strictly hydrostatic conditions up to 8 GPa (80 000 bar).

Figure 2 shows the refined angle of the spin-direction relative to <111> at three different isotherms, as well as the pressure dependence of the internal atomic coordinates. It is seen that the Morin transition shifts dramatically under pressure to higher temperatures. **Figure 3** illustrates the shift of T_M over a pressure range of 5 GPa, giving a massive pressure coefficient of dT_M/dP=+27 K/GPa, which can also be expressed by a 'Grüneisen parameter' $\gamma = -\partial \ln T_M / \partial \ln V = +20$. For comparison, the Grüneisen parameter of Néel temperatures is typically about 3 ('Bloch's 10/3 rule').

Although the pressure dependence of T_M was investigated before, including by several high pressure neutron experiments [3], the ILL study is the first one which carried out the measurements under strictly hydrostatic conditions, thereby avoiding the spurious effects which have been reported before [3] and allowing a meaningful comparison with theory.
The currently accepted understanding explains it by a competition between two contributions to the total anisotropy energy K [4]: the magnetic dipolar anisotropy energy K_{MD}, arising from the dipole interaction of the spins, and the fine structure anisotropy energy K_{FS}, also called the *single ion anisotropy*. At 0 K the two quantities K_{MD} and K_{FS} have opposite sign and cancel each other to within 2 %. Since they follow different temperature dependencies, the total anisotropy energy K changes sign at a temperature where $|K_{MD}(T)| = |K_{FS}(T)|$ which defines the temperature T_M where the spin flop occurs. The ILL measurements give structural parameters which allow the pressure dependence of K_{MD} to be calculated exactly. It turns out that this contribution is negligible, *i.e.* the massive pressure effect observed on T_M is entirely due to the increase of K_{FS}, *i.e.* the change in the splitting of the Fe^{3+} ground state levels.

Figure 2

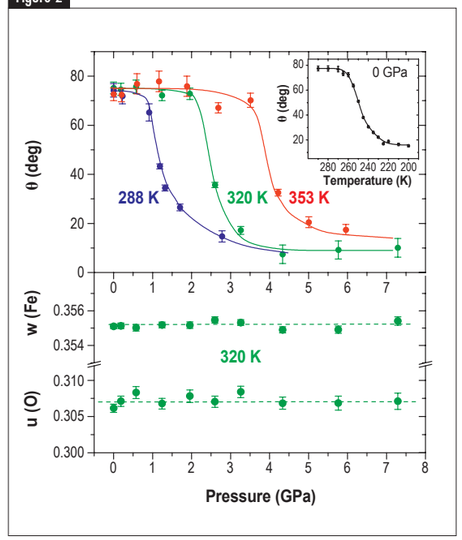

Angle theta between spin direction and <111> axis, for 3 different experiments carried out on D20. Lower panel: pressure dependence of internal atomic coordinates.

Figure 3

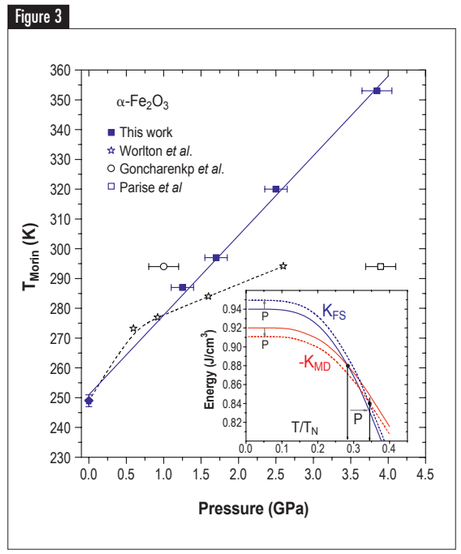

Pressure dependence of the Morin transition, obtained from hydrostatic measurements at ILL compared to previous neutron data [3]. The inset illustrates the shift of T_M from its ambient pressure value by a pressure-induced 1% variation of the anisotropy energies K_{MD} (red) and K_{FS} (blue) at 0 K according to Artman's single ion model [4].

Single-crystal neutron diffractometer D19
Time-of-flight spectrometers IN4 and IN5

Single crystal neutron scattering and *ab initio* calculations reveal the mechanisms of oxide-ionic conduction in modulated structures

Solid-state oxide-ionic conductors are of great current (and greater potential) importance as membrane materials in solid-oxide fuel cells (SOFCs). SOFCs use hydrocarbons and other chemical fuels far more efficiently than any other device, by obtaining electricity directly from their oxidation by O^{2-} ions. They are therefore not subject to the laws of the Carnot cycle, which fundamentally limit the efficiency of thermal power plants to 30–40 %. SOFCs minimise pollutants such as carbon, nitrogen and sulfur oxides, and can use a wide range of fuels – including natural gas, petroleum, coal, biofuels, and hydrogen generated from renewable sources – with efficiencies of up to 85 %.

The key design requirement for SOFC membrane materials is to be impermeable to fuel and oxygen gases under operating conditions, but permeable to oxide ions, which must pass through and react with the fuel. Almost all practical SOFCs still use yttria-stabilised zirconia ($Zr_{1-x}Y_xO_{2-x/2}$, YSZ), which was first demonstrated to meet these criteria in the 1930s. Because YSZ is only a useful ionic conductor at high temperatures (≥ 950 °C), YSZ-based SOFCs require a large power input, suffer from mechanical degradation during thermal cycling, and require the use of high-temperature-stable materials in components such as casings, seals and inter-connects.

One way to reconcile the competing requirements of net chemical stability and local chemical flexibility is to use materials with much more complex structures than YSZ, in which well-ordered regions can act as "scaffolds" supporting wide and continuous channels that become locally disordered in the ionic conducting temperature regime. However, it is difficult to study the structure and dynamics of materials with large and complex unit cells by neutron scattering from conventional polycrystalline (powder) samples. Consequently, such materials remain too poorly understood to be systematically optimised for applications.

These limitations can be overcome to a large extent by applying the same neutron scattering methods to single crystals. In practice, this is rarely done for ionic conducting materials due to the difficulty of obtaining sufficiently large crystals (cm-scale). Furthermore, while much more detailed information can be obtained, the experiments and data treatment are also much more difficult.

We have recently made some progress in this direction, growing large single crystals of a number of oxide-ionic conductors for the first time, and studying them at the ILL. We have been using single-crystal neutron diffraction (SCND) to study their structures, phase transitions, and ionic conduction pathways; inelastic neutron scattering (INS) to investigate the dynamics of ionic conduction in different directions with respect to the crystal lattice; and *ab initio* molecular dynamics (AIMD) calculations to verify and interpret experimental data.

An important class of materials in this context is derived from the high-temperature form of bismuth oxide, δ-Bi_2O_3. This is the best solid-state oxide-ionic conductor known, due to the 25% oxygen vacancies evenly distributed throughout its disordered fluorite-type structure. Pure δ-Bi_2O_3 has never been seriously considered for practical applications due to its limited thermal stability, and the fact that lower-temperature polymorphs eliminate the critical oxygen vacancies. However, the fluorite-type average structure of δ-Bi_2O_3 (along with a significant fraction of its conductivity) can be preserved to room temperature by doping with smaller rare earth or transition-metal cations. These stabilised δ-Bi_2O_3-type phases have genuine technological potential and have been extensively investigated since the 1970's [1–4].

We have a longstanding interest in the complex crystallographic modulations that arise in doped bismuth oxides, which seem to play a key role in stabilising their average δ-Bi_2O_3-type structure. Our results reveal that their complex long-range ordered (modulated) structures create "scaffolds" supporting δ-Bi_2O_3-type channels that are relatively easily disordered, explaining how they retain high oxide-ionic conductivity.

One study [5] concerns the most elegant and effective of these phases, known as Type II, which shows the highest conductivities across the widest ranges of chemical and thermal stability. Type II phases were poorly understood because none of their (3+3)-dimensional "hypercubic" structures (*i.e.* modulated in all 3 directions) has ever been fully determined. With a large (cm-scale) crystal of Type-II Bi_2O_3–Nb_2O_5, grown by refluxing bismuth oxide in a floating-zone furnace, we could collect SCND data on D19 and solve what is by far the most complex and detailed (3+3)-D structure ever determined. The result (**figure 1**) reveals ordered strings of NbO_6 octahedra separating continuous disordered oxygen-deficient channels, explaining its substantially higher conductivity compared to other stabilised δ-Bi_2O_3 phases.

In parallel to the Type II study, we investigated the commensurately ordered superstructure phase $Bi_{26}Mo_{10}O_{69}$ using a combination of INS on IN4 and AIMD calculations [6]. Our results suggest a new explanation for the high oxide-ionic conduction of this phase. The structure is generally supposed to consist of MoO_4 tetrahedra distributed through a δ-Bi_2O_3-type framework, but we show that some Mo atoms have higher coordination numbers than 4; *i.e.*, MoO_5 trigonal bipyramids coexist with MoO_4 tetrahedra. This accounts for the additional oxygen required to achieve the nominal composition (a tetrahedron-only model gives $Bi_{26}Mo_{10}O_{68}$) without invoking a previously proposed unbonded interstitial site, which we show to be energetically unfavorable. In the ionic conducting temperature regime, these MoO_4 and MoO_5 units rotationally disorder. Conduction proceeds by migration of oxide ions from δ-Bi_2O_3-type regions to join MoO_4 units, leaving vacancies that can propagate through the lattice (**figure 2**).

The results of these studies support the conjecture [7] that high ionic conductivity in stabilised δ-Bi_2O_3 phases comes from four structural features: (1) a highly polarisable Bi–O sublattice; (2) dopant cations that can support variable coordination geometry; (3) a superstructure that permits a high degree of rotational freedom to MO_x polyhedra; and (4) a pseudo-cubic ordered superstructure. Such mechanisms probably govern the behaviour of all fluorite-type δ-Bi_2O_3-like phases stabilised by doping with cations that can support flexible coordination environments, notably Nb^{5+}, W^{6+}, and Re^{7+} in addition to V^{5+} and Mo^{6+}.

Another class of oxide-ionic conductor on which we have been working is brownmillerite-type structures, which consist of alternating layers of corner-connected MO_6 octahedra and MO_4 tetrahedra, and can be thought of as oxygen vacancy ordered superstructures of the ubiquitous perovskite-type structure. This creates continuous one-dimensional 'channels' of oxygen vacancies, which are thought to play a role in the transport of oxide ions through the structure. The brownmillerite $Sr_2Fe_2O_5$ displays particularly high oxide ion conductivity in the absence of atmospheric oxygen (>0.1 S cm^{-1} at T > 800 °C) and offers additional advantages of relatively low toxicity and cost.

Some of us together with Paulus *et al.* [8] had previously investigated the nature of oxide ionic mobility in $Sr_2Fe_2O_5$ using INS data collected from polycrystalline (powder) samples, in conjunction with AIMD. We observed quasielastic neutron scattering (QENS) around the Bragg peak, which we ascribed to fast oxygen diffusion, and proposed a model in which dynamics of the apical oxygen atoms (those connecting the octahedral and tetrahedral layers) triggers disorder in the tetrahedral layers. The model can be loosely interpreted as dynamic 'switching' of the orientations of tetrahedra at temperatures as low as 80 °C.

Figure 1

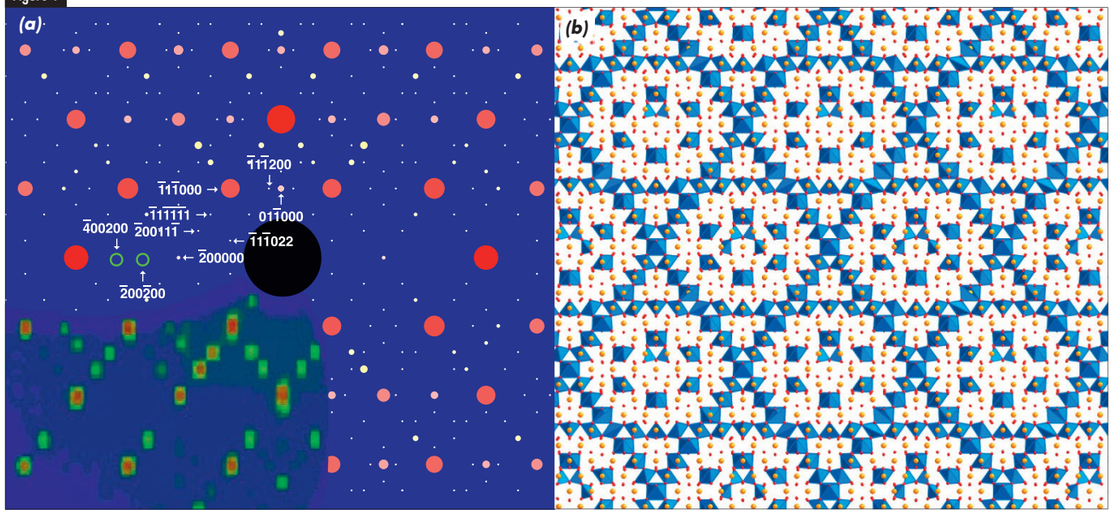

(a) *Single crystal neutron diffraction data (D19) of Type-II Bi_2O_3–Nb_2O_5, overlaid on a schematic representation of the observed Bragg peaks. Selected peaks are indexed. Green circles highlight satellites that are absent due to the d-hyperglide extinction condition.* ***(b)*** *The final refined structure drawn over 8×8×8 fluorite-type subcells. Bi atoms are yellow, O atoms are red, Nb atom-centred polyhedra are blue.*

AUTHORS & REFERENCES

C.D. Ling (Sydney University, Australia)
G. McIntyre (Bragg Institute, Kirrawee, Australia)
M.R. Johnson, **D. Richard**, **S. Rols**, **E. Pellegrini**, **J. Ollivier** and **H. Schober** (ILL)
I.R. Evans (Durham University, UK)

[1] T. Takahashi and H. Iwahara, Materials Research Bulletin 13 (1978) 1447
[2] M. Drache, P. Roussel and J.P. Wignacourt, Chemical Reviews 107 (2007) 80
[3] N.M. Sammes, G.A. Tompsett, H. Nafe and F. Aldinger, Journal of the European Ceramic Society 19 (1999) 1801
[4] K.T. Lee, H.S. Yoon and E.D. Wachsman, J. Mater. Res. 27 (2012) 2063
[5] C.D. Ling, S. Schmid, P.E.R. Blanchard, V. Petricek, G.J. McIntyre, N. Sharma, A. Maljuk, A.A. Yaremchenko, V.V. Kharton, M. Gutmann and R.L. Withers, Journal of the American Chemical Society 135 (2013) 6477
[6] C.D. Ling, W. Miiller, M.R. Johnson, D. Richard, S. Rols, J. Madge and I.R. Evans, Chemistry of Materials 24 (2012) 4607
[7] X. Kuang, J.L. Payne, M.R. Johnson and I.R. Evans, Angwandte Chemie International Edition, SI (2012) 690
[8] W. Paulus, H. Schober, S. Eibl, M. Johnson, T. Berthier, O. Hernandez, M. Ceretti, M. Plazanet, K. Conder and C. Lamberti, *Journal of the American Chemical Society 130* (2008) 16080
[9] J.E. Auckett, A.J. Studer, E. Pellegrini, J. Ollivier, M.R. Johnson, H. Schober, W. Miiller, and C.D. Ling, Chemistry of Materials 25 (2013) 3080

In our latest study on IN5 [9], we used single-crystal samples that allowed a clearer separation of the QENS) part of the INS signal, allowing us to characterise it in detail and providing direct information about the anisotropy of the oxygen ion motions.

We found clear evidence for disordering of the tetrahedral layers at 600 °C, just below the onset temperature for conduction, strongly suggesting that such disordering is a prerequisite for ionic conduction. However, we saw no quasielastic broadening until higher temperatures (750 °C). We also found that the QENS signal is isotropic. AIMD calculations confirmed this interpretation and also showed good agreement for the characteristic time-scale of the oxygen ion dynamics, measured to be 4.2 ps and calculated to be 4.5 ps at 875 °C. This presents a compatible but somewhat simpler picture of ionic conductivity compared to our previous work. It appears that tetrahedral rotations are essentially isotropic, but that they are a precondition for the anisotropic motion that moves oxide ions into the tetrahedral layers from the octahedral layers. This continual but incoherent movement of oxide ions in turn creates conduction pathways and activates long-range diffusion at the interface between layers, which appears to be largely isotropic in two dimensions on the pico-second timescale.

Figure 2

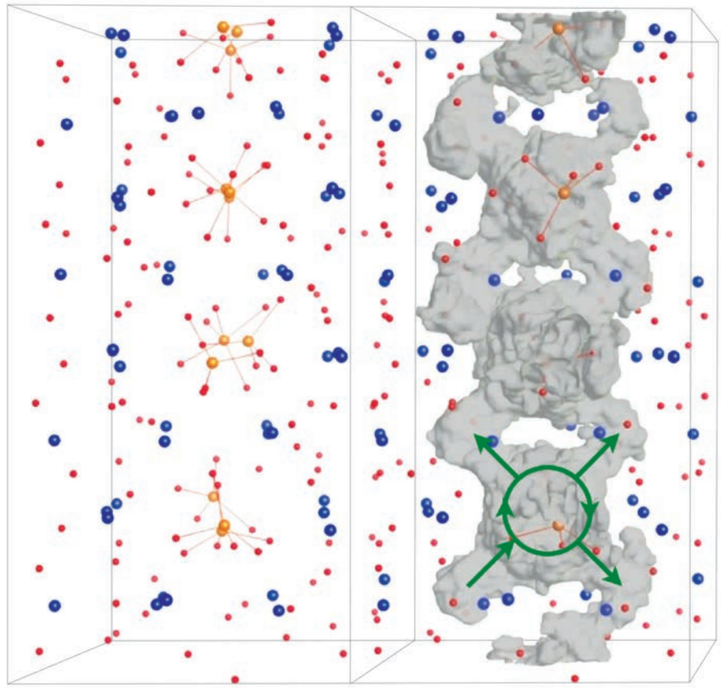

Structure of $Bi_{26}Mo_{10}O_{69}$ in the ionic-conducting temperature regime, from ab initio molecular dynamics calculations. Clouds show the space explored by four oxygen atoms on the edge of a δ-Bi_2O_3-like column, plus four forming a MoO_4 tetrahedron, over the course of 40 ps. Bi atoms are blue, Mo atoms are orange and O atoms are red. The green arrows illustrate the inter-play of rotational and translational diffusion.

These results of all these studies show what can be achieved with a single-crystal sample on modern, high flux, time-of-flight spectrometers, even when measuring the weak scattering from mobile oxide ions (compared to the more usual case of scattering from hydrogen). However, according to our simulations, the length scales we are probing are still only of the order of 1 Å, indicating that local rather than long-range diffusion is being observed. In the context of ionic conduction, it would of course be of more interest to investigate long-range diffusion and look for any associated anisotropy.

Accurate AIMD simulations are still challenging to run on such timescales, given that the spatial extent of the simulation box should ideally be extended beyond that used in this work, and more approximated electronic structure calculation methods should be considered.

Experimentally, however, backscattering and spin-echo spectrometers do extend the dynamical range of neutron scattering to and beyond the nanosecond timescale and new instruments with higher flux (IN16b and WASP) will offer opportunities to extend this work in the near future.

Figure 3

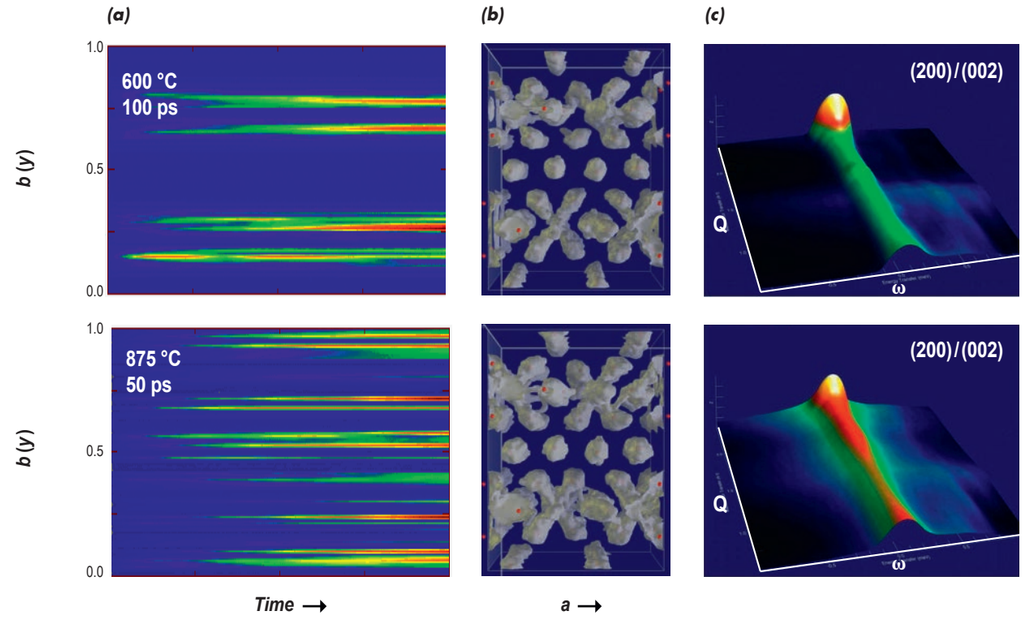

*AIMD and QENS results for $Sr_2Fe_2O_5$ at temperatures below (600 °C) and above (875 °C) the onset of oxide-ionic conduction. **(a)** Colour scales (blue-green-yellow-red) represent increasing mean square displacements (MSDs) of oxygen atoms from the AIMD simulation at each temperature, as a function of their fractional coordinate along the b (layering) axis. **(b)** Clouds represent the space sampled by individual oxygen atoms over the course of each entire AIMD simulation. **(c)** S(Q,ω) plotted on a logarithmic scale.*

Time-of-flight spectrometer IN6

Translational and Rotational diffusion in hot dense water

Water's exceptional behavior mainly derives from the directionality of the hydrogen bond, and from the open geometry of the water molecule. Therefore water represents a paradigm for associated liquids, due to the simplicity of its electronic structure, and the clear influence of the hydrogen bond network in determining the structural properties of the system. The structure of water is now well known for a large portion of the p,T phase diagram [1]. Conversely, knowledge of water dynamics is limited to moderate p,T conditions, in particular for what concerns the diffusive and rotational dynamics [2]. Despite, the diffusion of water at pressures of a few GPa, typical of the transition zone of the Earth's mantle, has strong incidence on the processes governing volcanic eruptions and intermediate-depth seismicity; water diffusion and re-orientation under extreme conditions is essential to characterise new exotic properties, such as the predicted plastic and superionic phases in water, and thus to interpret observations and develop models of planetary interiors, to cite few examples.

AUTHORS & REFERENCES

L.E. Bove, **S. Klotz** and, **A.M. Saitta** (University Pierre & Marie Curie, Paris, France)
Th. Strässle, (PSI, Villigen, Switzerland)
M. Koza (ILL)
J. Teixeira (LLB, CEA Saclay, F-91161 Gif-sur-Yvette, France)

[1] T. Strässle *et al.* , Phys. Rev. Lett. 96 (2006) 067801; Y. Katayama, *et al.*, Phys. Rev. B 81 (2010) 014109
[2] J. Jonas, T. DeFries, and D.J. Wilbur, J. Chem. Phys. 65 (1976) 582; A. Cunsolo, *et al.*, J. Phys. Chem. B 114 (2010) 16713
[3] S. Klotz, Th. Strassle, and L.E. Bove, Appl. Phys. Lett. 103 (2013) 193504; French patent n. 1358938
[4] L. E. Bove *et al.*, Phys. Rev. Letters 111 (2013) 185901
[5] K. Krynicki, C.D. Green, D.W. Sawyer, Faraday Discussions 66 (1978) 199; R. Ludwig, F. Weinhold and T.C. Farrar, J. Chem. Phys. 103 (1995) 6941

Neutrons are the most suited probe to investigate diffusive and re-orientational dynamics in water because of their sensitivity to hydrogen. The quasi-elastic neutron scattering (QENS) technique offers the unique possibility of analysing both atomic and molecular motion on the picosecond timescale and on the scale of atomic distances.

Taking advantage of the new toroidal high pressure chamber of the Paris-Edinburg press, specially conceived for QENS measurements [3], and of the high flux and low background of the time-of-flight (TOF) spectrometer IN6, we measured the self-dynamics of liquid water along isotherms in the 400-450 K range up to ice VII crystallisation (3-3.6 GPa), at pressures one order of magnitude higher than previously studied [2]. An example of the spectra collected along the 400 K isotherm at 0.6 and 1.8 GPa for a selected Q value is shown in **figure 1** [4].

Figure 1

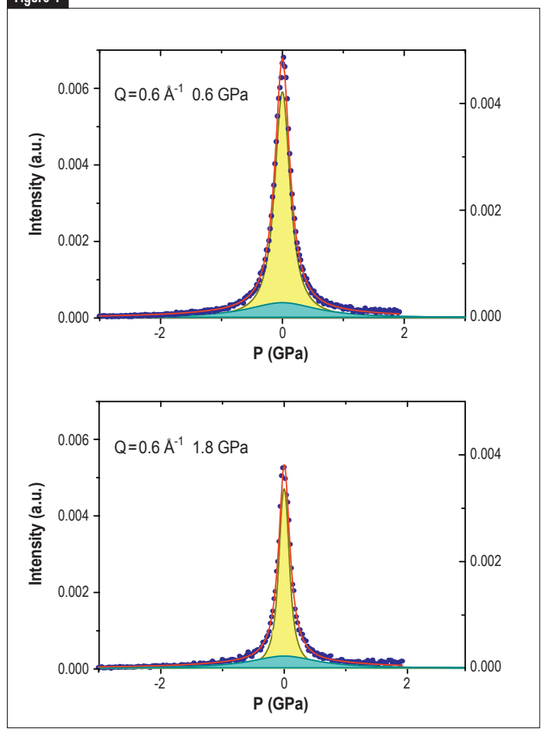

Example of 9-12 h scan collected on water at 400 K at Q = 0.6 Å^{-1} in the HP-QENS set-up of the PE press, on IN6 at ILL, for two pressure values. Data are corrected for background and multiple scattering contributions. Results (red line) of a decoupled roto-traslational fit [4] are compared to the measured intensity (blue dots). The translational and rotational contributions are shown in yellow and cyan, respectively.

Two well distinguished components can be observed: a translational (narrower) and a rotational (broader) contribution from which we extracted [4] the diffusion coefficient (D_T) and the molecular rotational time (t_R), reported in **figure 2**.

We readily see that D_T is strongly reduced under pressure, though its variation is definitively slower than that of shear viscosity (η), reported in the insert. Along the 400 K isotherm, the product $D_T\eta$ is approximately constant at moderate pressures (P: 0.1-1 GPa), while it decreases by a factor 2 in the high-pressure regime. Thus, the Stokes Einstein (SE) relation, $D_T\eta / T = C$, which predicts a constant product of diffusion and shear viscosity at constant temperature is violated [4]. Violation of the SE equation has already been observed in glass forming liquids when approaching the dynamical arrest, *i.e.* in conditions of extremely high viscosity, when dynamical heterogeneities take place. Here we investigated a complementary situation where the viscosity of the system is comparable to that of water at ambient conditions, while a strong density variation (40 %) is produced by pressure.
The observed failure of the SE equation is thus most likely related to the free volume reduction, the consequent enhancement of cage dynamics and the onset of hopping phenomena [4]).
The breakdown of the Debye equation, which establishes a direct relation between the molecular rotational time and the shear viscosity, is still more striking: t_R turns out to be almost pressure independent and translational and rotational dynamics completely decouple under pressure. This unexpected result can be understood relaying on the structural data available for hot dense water [2] and on the mechanism of reorientation of a water molecule in a H-bond network: the first shell of neighbours of a water molecule shows a density-independent O-O distance for the nearest neighbour oxygen atoms, while the radial distribution function of the second coordination shell reveals, instead, a difference between ambient and elevated P-T, associated with the gradual transformation towards a high density configuration (which is totally achieved for pressures higher than 1 GPa at 400 K, see also **figure 2**). Under further compression the number of nearest neighbour oxygen atoms do not change anymore, and as the number and strength of H-bond *per* water molecule remains almost constant [4], t_R turns out to be almost pressure independent.

To summarise, we measured the translational diffusion coefficient and the rotational time of water molecules under unprecedented high-pressure conditions.
We observed a decoupling of the translational and rotational dynamics under pressure.

Our study indicates that the dynamical behaviour of liquid water at 400 K is not that of a simple liquid, and the presence of the H-bond network strongly determines the molecular reorientation. Our results also point out that the use of SE equation or the extrapolation from moderate pressure (P<1GPa) measurements, to quantitatively estimate the diffusion coefficient of water at pressures of several GPa, unreachable experimentally, can lead to erroneous predictions. These conditions are typically found in the transition zone of the Earth mantle, as well as in the subsurface oceans of icy moons, where the knowledge of water diffusion is of great importance to establish reliable geodynamical models. Following our results, a more reliable criterion to predict the diffusion coefficient under these conditions is to consider it constant along the high pressure melting line [4].

Figure 2

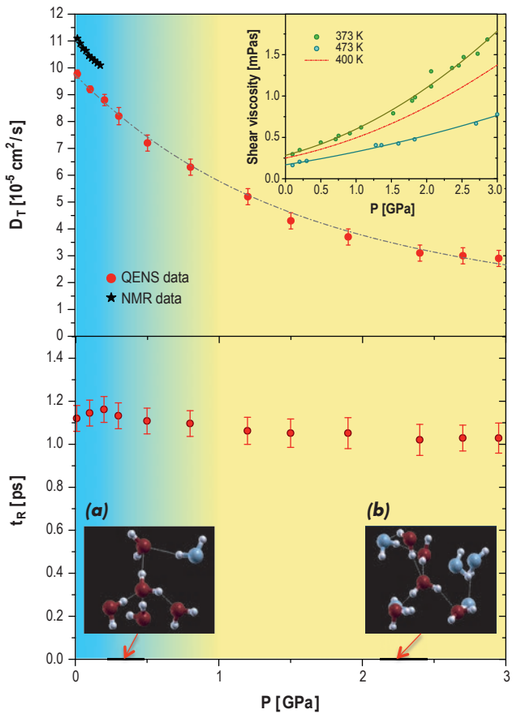

Pressure dependence of the translational diffusion coefficient D_T and of the molecular rotational time t_R along the isotherm 400 K as derived by our QENS experiment. Black stars represent the available low-pressure data [5] on D_T as measured by NMR at 403 K. In the insert we show the shear viscosity dependence on pressure along the 400 K isotherm (red curve), interpolated from data [4] at 373 K (green dots) and at 437 K (cyan dots).
The blue-yellow color boundary indicates the region of collapse of the second coordination shell on the first one [4]. The two simulations snapshots indicate the first neighbours (oxygens in red) and the second neighbours (oxygens in light-blue) of a central water molecule at 0.3 GPa ***(a)*** *and at 2.3 GPa* ***(b)****.*

Liquids and glasses diffractometer D4

Isotopic and isomorphic substitution applied to dilute glassy systems

Bioactive glasses are of great importance for biomedical applications due to their ability to promote bone regeneration. The structural sites present in the glass will be intimately related to their dissolution properties in physiological fluids such as plasma and saliva, and hence to the bioactivity of the material. Detailed structural knowledge is therefore a prerequisite for optimising material design. Here we employ the method of isotopic and isomorphic substitution to unravel the structural role of several key elements.

R.A. Martin (Aston University, UK)
G.J. Cuello (ILL)
J.M. Smith, **R.M. Moss** and **R.J. Newport** (University of Kent, UK)

AUTHORS & REFERENCES

[1] L.L. Hench, J. Mat. Sci. Mat. Med. 17 (2006) 967
[2] N. Miyata, K. Fuke, Q. Chen, M. Kawashita, T. Kokubo, and T. Nakamura, Biomaterials. 25 (2004) 1
[3] R.A. Martin, R.M. Moss, N.J. Lakhkar, J.C. Knowles, G.J. Cuello, M.E. Smith, J.V. Hanna, R.J. Newport, Phys. Chem. Chem. Phys. 14 (2012) 15807
[4] J.M. Smith, R.A. Martin, G.J. Cuello, R.J. Newport, J. Mat. Chem. B. 1 (2013) 1296

Bioactive glasses have the ability to chemically bond to bone and stimulate new bone growth [1]. Consequently they are widely used for a range of biomedical applications including periodontal repair, facial reconstruction and orthopaedic bone grafting. Under physiological conditions these materials dissolve, releasing Ca, P and Si, at a controlled rate which promotes the formation of hydroxyapatite (the mineral component found in teeth and bones). The release rate of these ions is determined by the glass structure and in order to better understand and control these processes a detailed knowledge of the atomic scale arrangement is necessary.

Figure 1

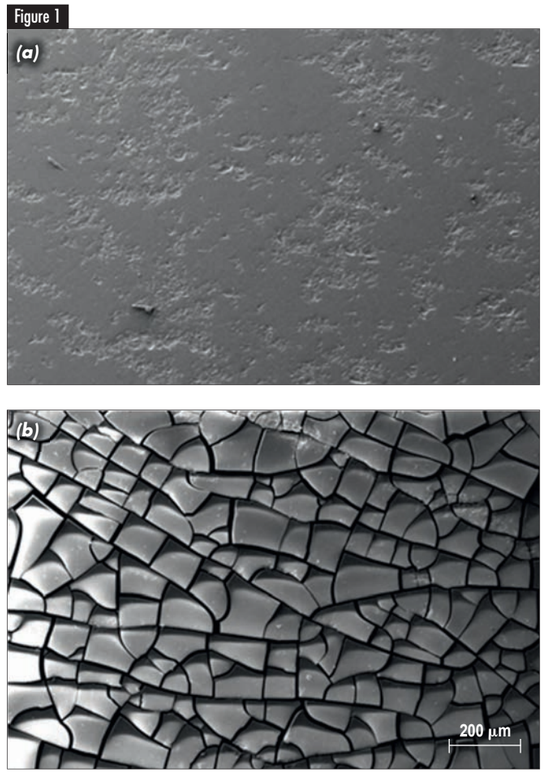

Scanning electron microscopy images of ***(a)*** *Ti-doped bioactive glass surface and* ***(b)*** *the surface after 7 days in culture media.*

However, understanding the structure of glass and the role individual elements play within the glassy matrix is not trivial. Glasses are complex materials that lack long range order or periodicity making it hard to unambiguously determine their local structure. Furthermore glasses of technological or commercial importance typically consist of a large number of components making it difficult to unravel the structure factors of individual elements. In this study we have examined the structure of 45S5 Bioglass® and its derivatives. Bioglass®, $(SiO_2)_{46.1}(Na_2O)_{24.4}(CaO)_{26.9}(P_2O_5)_{2.6}$, is the archetypal bioactive glass and has been used in more than one million bone graft operations [1].

Recently it has been reported that incorporating small concentrations of additional elements into 45S5 may increase bioactivity of these materials. For example, Miyata *et al.* [2] have reported that incorporating titanium to bioactive glasses can improve hydroxyapatite formation. Our laboratory based studies have confirmed that Ti Bioglass® is indeed bioactive and that hydroxyapatite forms on the glass surface (**figure 1**). Other reports have stated that incorporating transition metals such as nickel or cobalt can improve vascularisation, *i.e.*, increase blood vessel formation. However is it not possible to estimate *a priori* the structural role these ions will adopt within the glassy matrix. For example, Ti can form 4-, 5- or 6-fold geometries acting as either a network former or a network modifier; this would have a significant impact on the dissolution and hence bioactivity of the glass. It is difficult to unambiguously determine the co-ordination of Ti from spectroscopic techniques such as XANES. We therefore undertook two experiments to determine the structural role selected elements would adopt when incorporated into Bioglass®.

The first experiment investigated the structure of Ti within Bioglass® using the method of isotopic substitution. Exploiting the scattering length difference between ^{46}Ti and ^{48}Ti meant that by employing difference methods we were able to isolate only those correlations containing Ti. Beside the isotopic substitution, the highly diluted system (less than 1.5% of Ti) makes the task even more difficult. Of these correlations Ti-O occurs at the shortest real-space distance and can easily be resolved from other Ti correlations. This enabled us to determine the fraction of 4- and 6-fold Ti-O present within the glass (**figure 2**). The results showed that Ti occupies a range of environments with a maximum of 40 % being tetrahedrally coordinated [3].

The second experiment employed the method of isomorphic substitution to investigate the structural role Ni and Co adopt when incorporated into bioactive glasses. In an analogous fashion this experiment exploited the scattering difference between natural abundant Ni and Co. The results showed that Ni and Co adopt a significantly different local environment compared to Ti. It was found that two thirds of the Ni (or Co) occupies a five-fold geometry with the remaining third in a tetrahedral environment [4].

In conclusion, we have demonstrated that the methods of isotopic and isomorphic substitution can be applied to dilute glassy systems. The results have shown that first order coordination shells can be determined for systems containing concentrations of less than 1.5 atomic %.

Figure 2

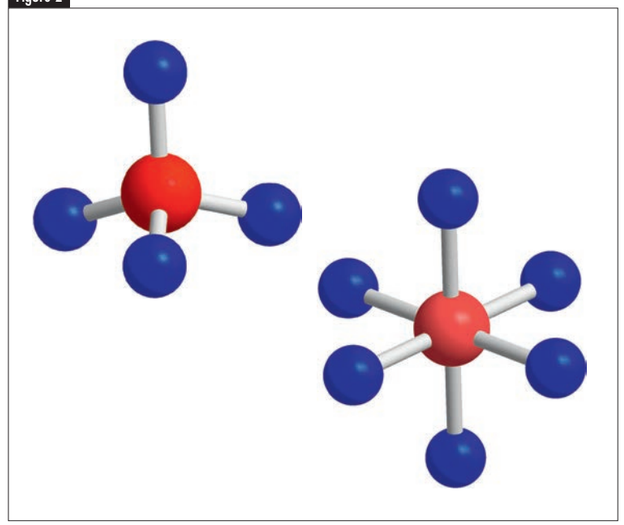

Schematic of tetrahedral (4-fold) and octahedral (6-fold) titanium oxide. The central red spheres represents Ti atoms and the blue spheres represent oxygen atoms.

Brillouin spectrometer BRISP

Collective dynamics of liquid gold: a truly *golden* neutron study combining BRISP measurements and simulations by the Computing for Science group

The propagation of acoustic-like excitations in the form of very-short-wavelength collective motions is a fundamental phenomenon in the physics of liquids. In the recent literature [1] the question has been raised as to whether the behaviour of these excitations differs in metals because of the presence of the conduction electron sea. In fact, until now liquid metals have been described by resorting to models of the dynamic structure factor more complex than those typically employed for other systems. Searching for the possible presence of a "universal" behaviour, we turned our attention to previously unstudied liquid gold.

Like all monatomic systems, liquid gold is a paradigm of simple fluids and is therefore a benchmark for the understanding and modeling of spectroscopic data on the dynamic properties of liquids. In particular, gold (Au) shares with all other fluid metals the property of displaying clear acoustic-like excitations. The dual aim of this experiment was to compare gold's behaviour with that of insulating systems - an extremely challenging exercise due to its high melting temperature and strong neutron absorption – and to perform a simulation study crucial for extending the current experimental kinematic region.
We were able to tackle the technical challenges and important scientific issues associated with liquid gold thanks to the performance levels offered by the Brillouin neutron spectrometer BRISP, an instrument perfectly suited to determining the dynamic structure factor of high-sound-velocity systems at Q values in the inverse nanometre range.
The clean coherent signal from liquid gold (**figure 1**) shows that neutron measurements together with upgraded data analysis can give unexpectedly good results, even with strongly absorbing samples, and that a generalised hydrodynamics model accurately describes the experimental data.

For decades, the microscopic dynamics of fluids has been a canonical field of application of standard simulation techniques. However, in the case of metals, a great incentive for performing such studies has come from the development of *ab initio* methods, much better suited to the treatment of the electronic degrees of freedom. The quality of the neutron data makes a significant comparison with the simulation results possible. The resulting good agreement [2] not only confirms the effectiveness of *ab initio* simulations of metals, but also allows the valuable exploration of collective dynamics at Q values that are difficult to access experimentally. As a result, we have found that an even better description of the dynamics is obtained by analysing the calculated spectra in terms of the more refined viscoelastic model that has proven very efficient in the analysis of collective excitations of non-metallic liquids.

Available dispersion curves and damping rates for the translational collective modes of conducting (*e.g.* Au and Cd) and insulating (*e.g.* CO_2 and CD_4) systems show remarkable similarities, provided the damping-to-frequency ratio z_s/ω_s of sound modes is analysed as a function of the normalised wave vector. **Figure 2** shows this ratio for the four above-mentioned systems properly scaled to the CO_2 values. The results were beyond our expectations. We found a nearly universal behaviour for liquids of different nature, suggesting quite a remarkable picture where collective excitations at meV energies and on a mesoscopic scale, show overall equivalent properties, irrespective of the presence or absence of conduction electrons. The behaviour of liquids at explorable scales thus appears to be dominated by those features of the nucleus-nucleus interaction which are common to both metal and non-conductive systems [1].

AUTHORS & REFERENCES

E. Guarini and **F. Barocchi** (University of Florence, Italy)
U. Bafile (ISC-CNR, Florence, Italy)
A. De Francesco, **F. Formisano** and **A. Laloni** (IOM-CNR c/o ILL)
E. Farhi (ILL)
A. Orecchini (ILL and University of Perugia, Italy)
F. Sacchetti (University of Perugia, Italy)

[1] W. Montfrooij and I. de Schepper, Excitations in Simple Liquids, Liquid Metals and Superfluids, Oxford University Press, New York (2010)
[2] E. Guarini, U. Bafile, F. Barocchi, A. De Francesco, E. Farhi, F. Formisano, A. Laloni, A. Orecchini, A. Polidori, M. Puglini and F. Sacchetti, PRB 88 (2013)104201

Figure 1

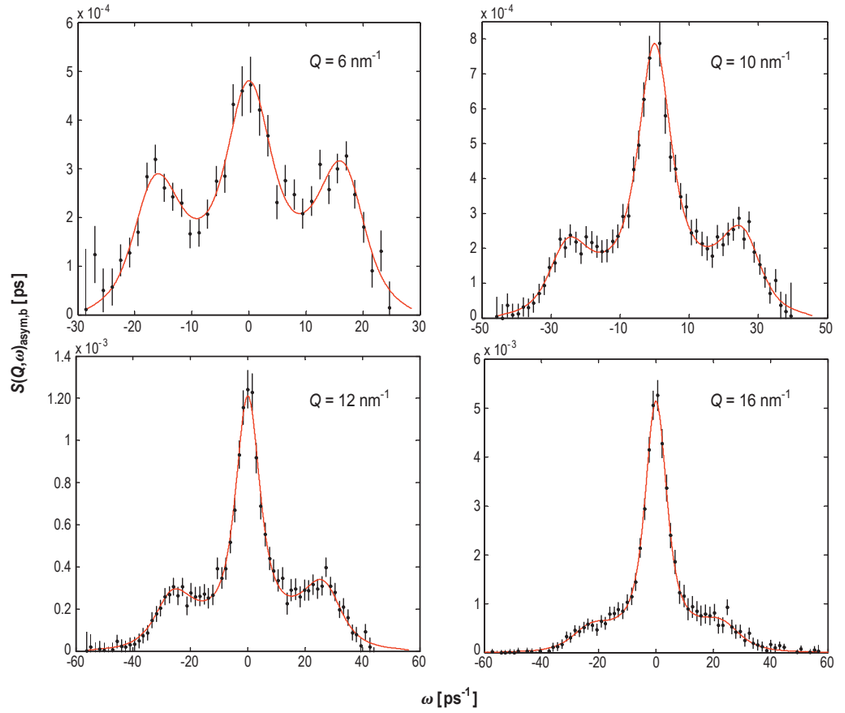

Figure 2

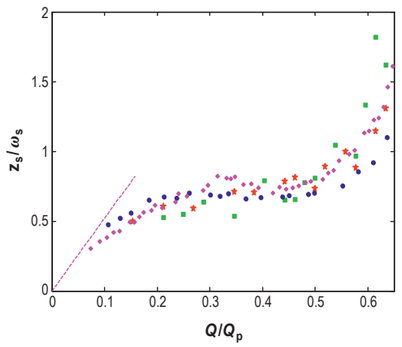

Figure 1 *Dynamic structure factor of gold at different Q values as obtained by the BRISP spectrometer. The fit (solid red line) is a generalised hydrodynamics model accounting for detailed-balance asymmetry and resolution.*

Figure 2 *Ratio of damping to frequency of acoustic excitations for four different liquids. Data for Au (red stars), Cd (green squares) and CD_4 (blue dots) largely follow the same curve as CO_2 (pink diamonds) if multiplied by 3.20, 3.05 and 2.00 respectively. Data are plotted as a function of Q/Q_p where Q_p is the position of the main peak of the static structure factor, with Q_p = 26 nm-1 for Au and Cd, and Q_p = 19 nm^{-1} for CD_4 and CO_2. The dashed line shows the hydrodynamic behaviour of z_s/ω_s for CO_2.*

Small-angle scattering diffractometer D11

Shear-induced macroscopic "Siamese" twins in soft colloidal crystals

Soft materials such as micelles or polymers can form highly ordered crystals which are inherently very susceptible to shear. Large shear strains lead to the formation of macroscopic Siamese twinning in lyotropic fcc crystals formed by block copolymer micelles. The twins exist over the whole gap of the shear cell with the twin boundary located inside the gap. Our experiment indicates that the deformation twinning mechanism is analogous to the plastic deformation of nanocrystalline metals under high shear stress and high deformation rates.

AUTHORS & REFERENCES

S.M. Taheri, **S. Rosenfeldt**, **S. Fischer** and **S. Förster**
(University of Bayreuth, Germany)
P. Bösecke and **T. Narayanan** (European Synchrotron Research Facility - ESRF, Grenoble, France)
P. Lindner (ILL)

[1] S.M. Taheri, S. Rosenfeldt, S. Fischer, P. Bösecke, T. Narayanan, P. Lindner and S. Förster, Soft Matter 9 (2013) 8464

Soft colloidal crystals consist of building blocks such as micelles that interact via soft interaction potentials. The crystalline order tolerates imperfections because the related increase in the potential energy is very small. Hence, the mechanical properties of soft crystals are determined by the number and mobility of defects. This makes them quite different from inorganic crystals. A special defect is the occurrence of twins, where two adjacent crystals share common lattice points in a symmetrical manner such that a twin boundary surface exists between the two crystals. Fcc crystals, which are often found in lyotropic (water soluble) systems, can exist in two different stacking orders of the (111)-planes corresponding to ABCABC (twin A) or ACBACB (twin B) stacking (**figure 1**). Usually, twins or twinned domains occur as small adjacent grains within large multidomain crystals.

With recent progress in instrumentation it has become possible to use sub-millimeter neutron beams to scan through samples with high resolution. Using the instrument D11 and the Bohlin CVO120 HR stress controlled rheometer with a Searle-type quartz shear cell (1 mm gap size) the crystalline structure of a fcc block copolymer was mapped in detail. The samples were constantly sheared until a stationary scattering pattern was developed. Abrupt cessation of shear allowed twin formation. The crystalline structure was scanned with a slitlike neutron beam of 300 µm width at different positions in the gap. The spatial arrangement of set-up and sample is shown in **figure 1**. The radial beam position is parallel to the [111] direction, whereas for the tangential beam position the beam passes parallel to the [110] plane. Additionally the spatial orientation of the unit cells corresponding to both twins is defined. The location of twin B can be obtained from twin A via a rotation around the [111] axis by 60° [1]. In the [111] direction the scattering patterns of both twins are identical and a characteristic 6-fold symmetry is observed. In the [110] direction a 2-fold rotational symmetry of distorted hexagons is obtained in the scattering patterns. This feature allows distinguishing clearly between both twins.

In **figure 2** rheo-small-angle neutron scattering data of a shear oriented fcc phase are shown. The measurements are recorded with a lyotropic micellar phase of a poly(isoprene-b-ethylene-oxides) block copolymer after shear orientation at 500 s^{-1} in the Searle cell of D11. In the radial direction the pattern is characterised by a large number of Bragg peaks corresponding to a fcc crystal. Most of them are caused by the finite domain sizes of the macroscopically oriented crystal and are crystallographically forbidden. As mentioned above the volume ratio of the twins cannot be determined in the [111] direction. The following patterns correspond to different tangential positions and therefore probe the [110] direction of the fcc lattice. In this direction most Bragg spots are allowed. A characteristic feature at the outer gap is the distorted hexagon, with is characteristic for the scattering of twin B. In the center of the gap a regular hexagon with considerable smearing in the horizontal direction occurs. As expected for the twin boundary location both twins occur with equal probability, *i.e.* the twin ratio is 0.5. Inside the gap near the inner rotor the scattering pattern exhibit a hexagon as expected for twin A. Model calculations reveal a twin ration of 0.8 for twin A. Very similar results have been obtained with synchrotron-SAXS experiments at ESRF.

The observation of such macroscopic "Siamese" twins is surprising due to the fact that normally only small twinned domains are reported. The existence of macroscopical twins is explained as follows. At high shear rates in continuous shear the stationary velocity gradient leads to a layer sliding of the closed-packed micellar layers in shear direction ([110]). Abrupt cessation causes locally high stress in the center of the gap. Fast deformation twinning quickly relieves the local stress. The twins grow toward the outer regions until the macroscopic twin is formed. The proposed mechanism is similar to the deformation twinning known for the plastic deformation in metals. Note that this twin formation occurs without breaking the material, a fact that is interesting for crash energy absorption or forging processes.

Figure 1

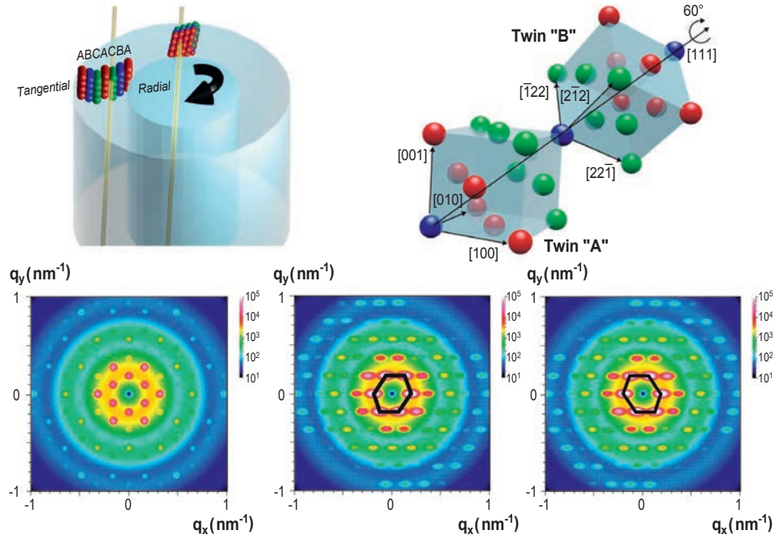

Schematic overview over the spatial arrangement of the instrumental set-up and the configuration twins. Depending on the flow the neutron beam probes the closed-packed (111) planes of the fcc lattice in different spatial orientations. The lines note different beam positions between the radial and the tangential position. Model calculation reveal identical scattering pattern for the radial beam position for both twins (A) but different ones in tangential postion (B, twin B; C, twin A).

Figure 2

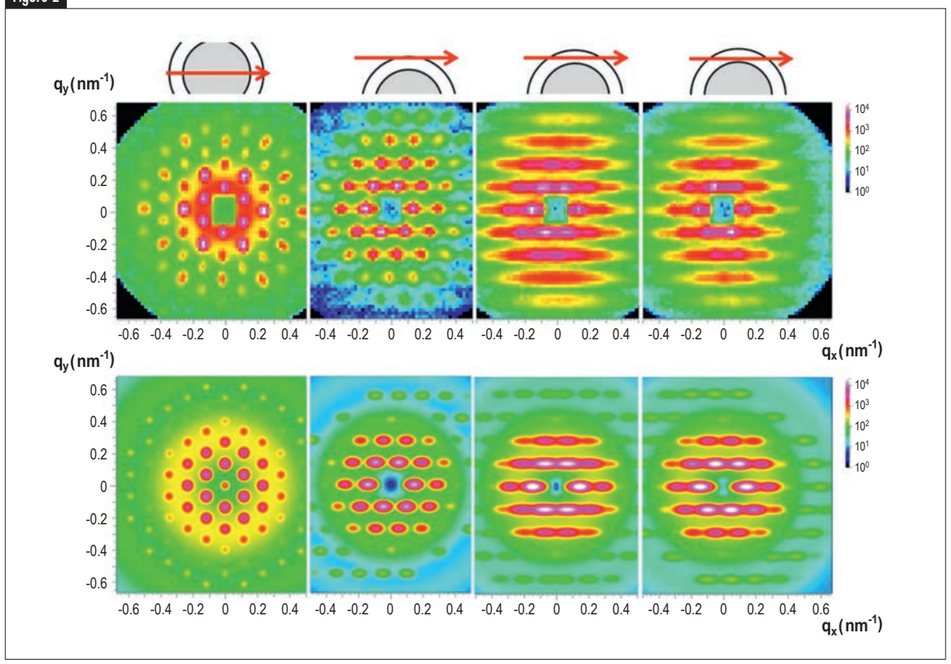

Rheo-SANS data of a shear oriented fcc-phase at 16 wt % poly(isoprene-b-ethylene-oxide) blockcopolymer ($PI_{55}PEO_{170}$). Above the scattering patterns the different positions of the neutron beam for the tangential configuration are indicated. The panels on the bottom show the calculated scattering intensities. For experimental positions with the beam passing through the center of the gap or near to the inner cylinder the resulting peaks are considerably smeared because the beam probes the FCC-lattice and both twins with slightly different orientations due to the curvature of the shear cell. This effect is taken into account in the model calculations (bottom panels).

Horizontal reflectometer FIGARO
Vertical reflectometer D17

Achieving molecular control of bio-adhesive interactions through the design of spacer architecture

Ligand-receptor pairs build lock and key complexes through the formation of specific, non-covalent bonds. They play a crucial role in cell adhesion events that allow the communication, proliferation, differentiation and migration of cells [1]. The quantitative understanding and control of the molecular recognition mechanisms is an important scientific challenge [2], not only in the fields of molecular and cell biology, but also for technological applications as for example in drug delivery [3]. We have built a new class of polymer interfacial structure, named Sliding Anchored Polymers (SAPs), with many new potentially interesting features. SAPs are macromolecules which consist of a ring (mono-cholesteryl cyclodextrin, CD) through which an end-capped polyethylen glycol (PEG) chain is sliding.

AUTHORS & REFERENCES

M. Bauer (CEA, IRAMIS, NIMBE, LIONS, UMR 3299 CEA / CNRS, CEA-Saclay and University of Strasbourg, France)
M. Bernhardt (MPI for Polymer Research, Mainz, Germany)
T. Charitat, **P. Kékicheff** and **C. Marques** (Institut Charles Sadron, University of Strasbourg, France)
C. Fajolles and **J. Daillant** (CEA, IRAMIS, NIMBE, LIONS, UMR 3299 CEA / CNRS, CEA-Saclay, France)
G. Fragneto (ILL)

[1] B. Alberts, A. Johnson, J. Lewis, M. Raff, K. Roberts and P. Walter, *Molecular Biology of the Cell*, Garland, New York (2002)
[2] R. Yerushalmi-Rozen, J. Klein, and L.J. Fetters, *Science*, 263 (5148) (1994) 793
[3] D.D. Lasic and F.J. Martin. *Stealth Liposomes*, CRC Press (1995)
[4] E. Evans and K. Ritchie, *Biophysical journal*, 76(5) (1999) 2439

Our SAPs were obtained by inclusion of a PEG polymer into a cyclodextrin ring modified with a cholesteryl group (**figure 1**), allowing further anchoring into a lipid membrane. By using a wide range of surface probing techniques as Atomic Force Microscopy (AFM), Brewster Angle Microscopy (BAM), Langmuir isotherm, Infra Red Reflection-Absorption Spectroscopy (IRRAS) as well as neutron reflectometry at air/water and solid/water interfaces we have studied the insertion properties of this new class of molecules. Neutron reflectivity experiments were performed at the ILL on both FIGARO and D17 reflectometers. They provided not only structural information on the sliding polymer layers but also guidance for molecular design of the spacer at any stage of the project. In the biological realm, the end-grafted chain has been studied as a mimetic system for the spacers that provide for control of the range and strength of interactions in bio-recognition events promoted by ligand–receptor pairs.

A first series of experiments allowed us to investigate the amphiphilic behaviour of a new Cholesteryl Cyclodextrins and their insertion properties in lipid monolayers and bilayers, before investigating the membrane insertion of SAPs. At first we have shown that the cholesteryl-CD is suitable for anchoring the SAPs at the air-water interface and for insertion into phospholipid monolayers and bilayers. For sufficiently high polymer surface densities they form polymer brushes, which follow the scaling laws predicted by polymer theory. The dense SAP layers display the conventional behavior of end-grafted polymer brushes, in agreement with the theoretical description for grafts of sliding polymers, where asymmetric chain conformations are predicted for high surface densities. Neutron reflectometry allowed us to achieve a detailed understanding of the interfacial properties of SAPs as well as the insertion properties into phospholipid membranes. It is expected that the polymeric chain of the SAPs is able to slide through the CD ring, and the associated modified distribution of chain ends, will translate into a new type of tethered ligand-receptor pairs. The study of such interactions, driven by sliding tethered ligands, could be made *e.g.* by force measurements between two phospholipid bilayers, the first containing SAPs modified with a ligand end-group and the second, opposite bilayer, anchoring a complementary receptor moiety. This project is presently in a phase where we are investigating the adhesive properties and the binding kinetics of model membranes decorated with SAP. A major objective is now to perform Surface Force Apparatus experiments on supported bilayers (ICS, M3 team, P. Kékicheff).

Thanks to neutron reflectivity, a detailed understanding of the insertion properties of this new potential ligand into phospholipid membranes has been obtained. We have demonstrated that the cholesteryl CD is suitable for anchoring the SAPs into phospholipid monolayers and bilayers, forming polymer brushes for sufficiently high polymer surface densities. We believe that the concept of variable spacer length and internal adaptability will open a considerable field of new perspectives. An interesting possibility would for instance be to use diblock copolymers as the spacer, which could provide sensitivity of this technology to environmental conditions such as the pH or the quality of the solvent.

Figure 1

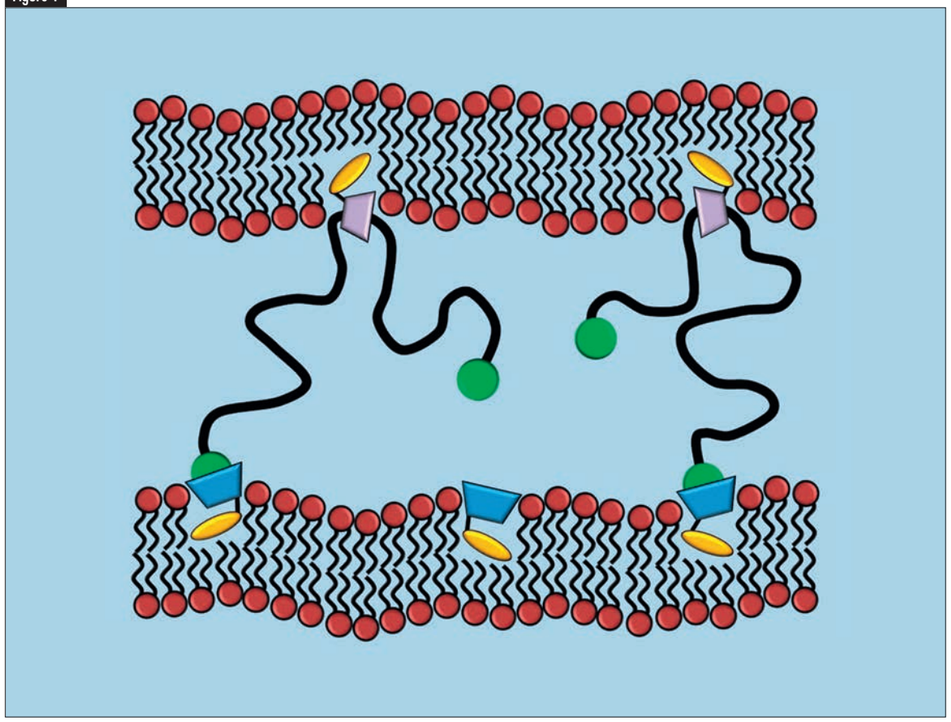

Schematic view of Sliding Anchored Polymer inserted in a supported lipid bilayer and interacting with another one by end-receptor. The SAP is consisting of a polymer (black), an amphiphilic cyclodextrin (cholesteryl group in yellow, alpha_CD in purple) and an end capping group (green) and the corresponding receptor in blue. The model phospholipid membranes which play the role of the insertion matrix is represented.

Figure 2

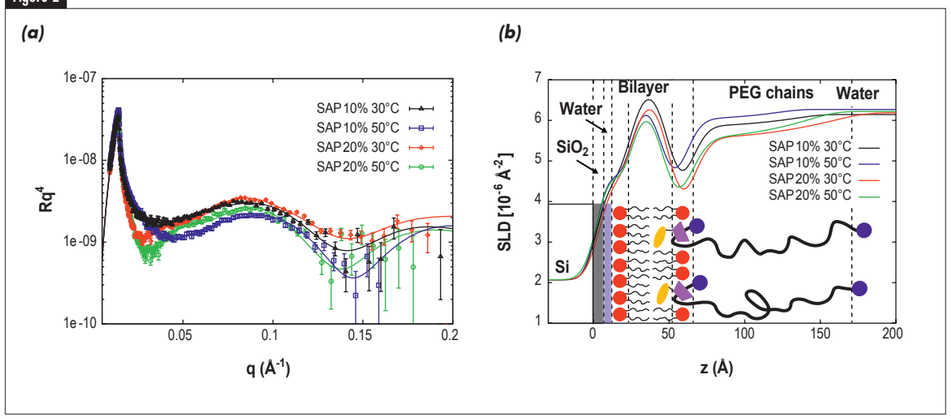

*Neutron reflectivity curves **(a)** and corresponding SLD profiles **(b)** for bilayers with a first layer of pure DPPC and a second mixed layer of SAP-6k/DPPC with different molar ratios of SAP-6k at 30 °C and 55 °C.*

Small-angle scattering diffractometer D22

How do bacteriophages sense the presence of their host?

Bacteriophages, viruses that infect bacteria, are the most abundant and diverse organisms on Earth. They play a crucial role in the ecology, evolution and pathogenicity of bacterial populations from oceans or human intestine, where they also contribute to our immunity [1]. Phages consist of a capsid, containing the phage genetic information, and a tail that allows host recognition. Following binding of the tail tip to the host receptor, the viral genome is injected into the cytoplasm of the bacterium. The biosynthetic host machinery is then hijacked to produce new virions, killing the cell. Phage therapy is becoming an alternative to treat antibiotic-resistant bacterial infections [2], it is thus important to understand the infection mechanisms

AUTHORS & REFERENCES

C. Breyton, **F. Gabel**, **A. Flayhan**, **M. Lethier**, and **C. Ebel** (IBS, Grenoble)
G. Durand (University of Avignon)
P. Boulanger (IBBMC, Orsay)
M. Chami (C-CINA, Basel, Swizterland)

[1] J.J. Barr, R. Auro, M. Furlan, K.L. Whiteson, M.L. Erb, J. Pogliano, A. Stotland, R. Wolkowicz, A.S. Cutting, K.S., Doran, P. Salamon, M. Youle, and F. Rohwer, Proc. Natl. Acad. Sci. U.S.A. 110 (2013) 10771
[2] D. Maura and L. Debarbieux, Appl. Microbiol. Biotechnol. 90 (2011) 851
[3] B. Jacrot, Rep. Prog. Phys. 39 (1976) 911
[4] A.M. Seddon, P. Curnow, and P.J. Booth, Biochim. Biophys. Acta 1666 (2004) 105
[5] C. Breyton, A. Flayhan, F. Gabel, M. Lethier, G. Durand, P. Boulanger, M. Chami and C. Ebel, J. Biol. Chem. 288 (2013) 30763

At the molecular level, phage infection is triggered by the interaction of the Receptor Binding Protein to the bacterial receptor, either a sugar or a protein of the surface of the cell. In the case of the *Escherichia coli*-infecting phage T5 (**figure 1a**), the Receptor Binding Protein pb5 is present as a unique copy located at the tip of the tail. It irreversibly binds FhuA, an outer membrane protein that physiologically transports iron chelated by a siderophore. This interaction is sufficient to induce the opening of the capsid and the perforation of the cell wall by phage tail proteins. By which mechanism is the binding information transmitted to the rest of the phage? To get insights into this question, we have purified both proteins and studied the structure of each protein isolated or within the complex.

Small-angle neutron scattering (SANS) combined with contrast variation and specific deuterium labelling of proteins is a particularly powerful technique to monitor conformational changes undergone by each protein within a complex [3]. The neutron scattering length of the hydrogen nucleus is negative while that of deuterium, and of most of the atoms, are positive. The scattering of a macromolecule is proportional to the square of its contrast with the solvent. The contrast term can be modulated by changing the hydrogen contents of either the macromolecule by deuterium labelling, or of the solvent by adding D_2O. The contrast term may vanish in a buffer containing an appropriate D_2O%, named the contrast match point. Thus, the signal of partners within a protein complex can be selectively highlighted, by deuterating the protein, or suppressed, by performing measurements at its contrast match point. *Ab initio* modeling allows, from the scattering curve, to determine the envelope of a given deuterated protein in the context of a complex, given the others are hydrogenated.

Figure 1

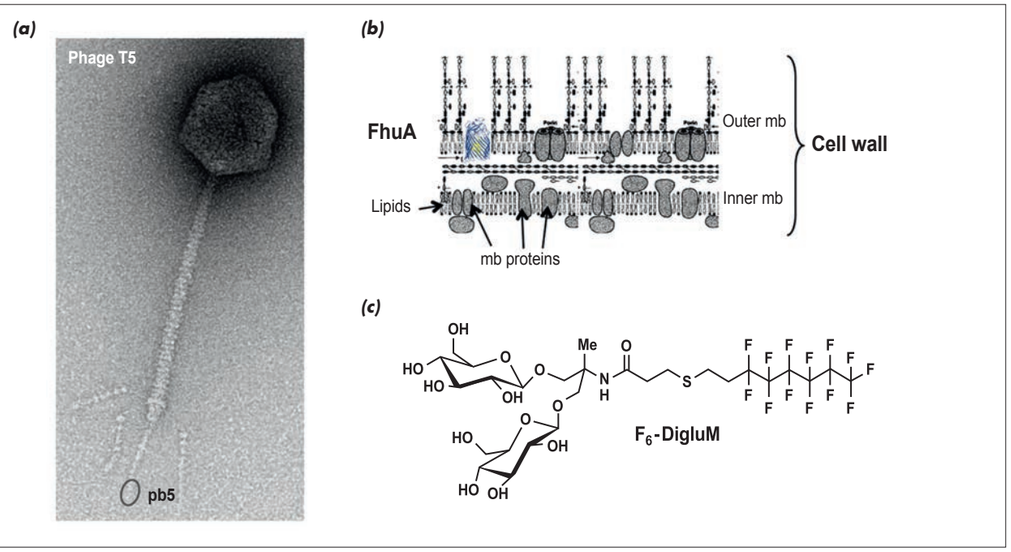

(a) *Electron microscopy image of phage T5. The icosahedral capsid (90 nm diameter) is connected to a long, flexible tail. At its extremity we note three L-shaped fibres that reversibly bind to the saccharides of the outer-membrane, contributing to host recognition, and a straight fibre, at the tip of which is located pb5, the Receptor Binding Protein. Pb5 irreversibly binds to FhuA, a chelated-iron outer-membrane transporter. Diameter of the tail: 12 nm.* ***(b)*** *Schematic representation of a Gram-negative cell wall, composed of the outer-membrane, in which is embedded FhuA, the Receptor of phage T5, the peptidoglycane, and the inner-membrane. A membrane is made up of a lipid bilayer and membrane proteins. The lipids of the outer-membrane, lipopolisaccharids, are grafted with long saccharides molecules on their head groups. mb: membrane.* ***(c)*** *Chemical structure of the F_6-DigluM amphiphile. F_6-DigluM shares with detergents their amphiphilic structure, with a hydrophilic head and a hydrophobic tail.*

Figure 2

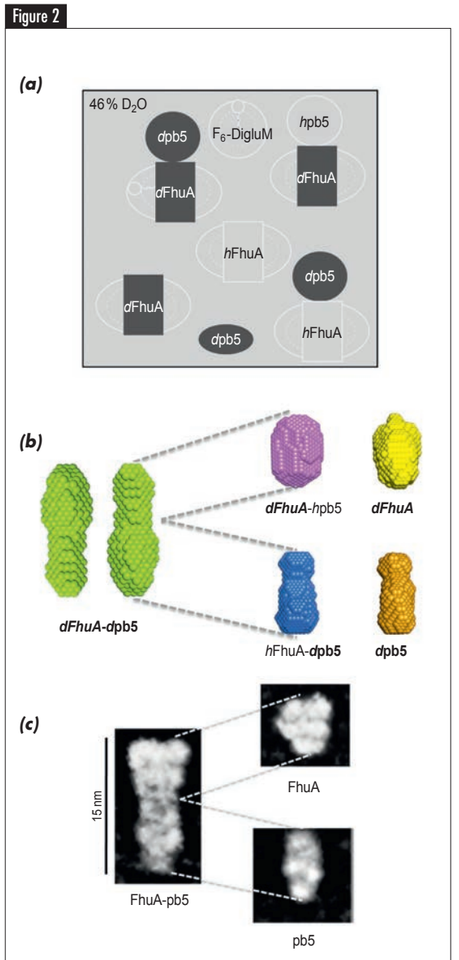

(a) *Small-angle neutron scattering contrast strategy to highlight specific parts of the protein-detergent complexes: deuterated proteins are represented in dark gray. Hydrogenated proteins and the F_6-DigluM micelles are represented in light gray as the 46% D_2O buffer in which they are contrast matched.* ***(b)*** *Ab initio envelopes (at 46% D_2O) of the dFhuA-dpb5 complex and of dFhuA and dpb5 isolated or in the context of the complex (with hpb5 and hFhuA, respectively). Side views.* ***(c)*** *Averaged class of negative stain electron microscopy of the FhuA, pb5 and the FhuA-pb5 complex.*

Purified membrane protein samples are tricky proteins to work with: they are naturally imbedded in a lipid bilayer, and thus comprise a large hydrophobic domain, in contact with the acyl chains of the lipids [4] (**figure 1b**). To extract them from the bilayer and manipulate them in aqueous solution, we use detergents, small amphiphilic molecules that auto-associate in globular aggregates -the micelles, and that come in place of the lipids. Thus, a SANS membrane protein complex sample comprises at least one additional component, the detergent, present as bound detergent and as free micelles. Detergents thus need to be matched in order to obtain structural information from the non-matched protein partner. Fluorinated surfactants share with detergents their amphipathic structure (**figure 1c**). They have been investigated as potential mild surfactants, and we have shown that the contrast match point of F_6-DigluM (46% D_2O) is close to that of most proteins (about 45% D_2O). Most importantly, at its contrast match point, F_6-DigluM is homogeneously matched, which is not usually the case for detergent molecules due to the different chemical composition of the head and tail. These characteristics make F_6-DigluM an ideal candidate for SANS study of solubilised membrane protein complexes: both hydrogenated protein partner(s) and detergent will be matched simultaneously, allowing to focus on deuterated protein partner(s) only.

We have analysed the FhuA-pb5 complex solubilised in F_6-DigluM by SANS. Experiments were performed on D22, thanks to our participation in a local BAG, with the help of the local contacts Phil Callow and Jo Zaccai. A contrast matching strategy (**figure 2a**) was defined to separately resolve each partner alone and within the complex. FhuA low-resolution structure in solution, determined by *ab initio* modeling, is in very good agreement with its crystal structure. It remains unchanged upon formation of the complex. pb5 is shown to be an elongated protein, whose structure, at the resolution of the technique, does not show significant conformational changes upon formation of a complex with FhuA (**figure 2b**). The SANS envelopes of the complex and the individual proteins are in excellent agreement with negative stain single particle electron microscopy (**figure 2c**).

We have previously shown, using biochemical and biophysical methods, that upon binding to FhuA, pb5 undergoes secondary structure conformational changes, β-sheets being formed at the expense of α-helices and random structures. These latter would not be converted into large conformational changes, but could be sufficient to initiate the cascade of signalling events that lead to DNA release and cell wall perforation. We therefore propose that the mechanism of signal transduction from the Receptor Binding Protein to the rest of the phage within phage T5, and thus other siphophages with straight fibres binding protein receptors, is different from that of siphophages binding cell wall saccharides for which structural information is available.

This work was recently published in the Journal of Biological Chemistry [5].

Vertical reflectometer D17

Membrane thickness and the mechanism of action of the short antimicrobial peptide trichogin GA IV

Antimicrobial peptides are natural molecules with a strong antibiotic activity and in most cases kill bacteria by creating pores in their cell membrane (**figure 1**) [1]. They are a promising alternative to traditional antibiotics, which are rapidly and inexorably loosing their effectiveness due to the increasing spread of drug-resistant bacteria. By combining neutron reflectivity data collected on the D17 reflectometer at ILL with molecular dynamics (MD) simulations and activity measurements, we solved a long-standing riddle about the mechanism of pore formation by the peptide trichogin GA IV, which is too short to span the normal thickness of a bilayer. Our findings provide a solid basis for the rational design of a new class of short peptide antibiotics against multidrug-resistant bacteria.

S. Bobone, **G. Bocchinfuso**, **A. Farrotti**, **B. Orioni**, **R. Senesi**,
A. Palleschi and **L. Stella** (University of Rome Tor Vergata, Italy)
Y. Gerelli, **F. Sebastiani** and **G. Fragneto** (ILL)
M. De Zotti, **F. Formaggio** and **C. Toniolo** (University of Padua, Italy)
E. Latter and **J. Penfold** (ISIS, UK)

[1] C.D. Fjell, J.A. Hiss, R.E. W. Hancock and G. Schneider, Nature Rev. Drug Discov. 11 (2012) 37
[2] C. Mazzuca, L. Stella, M. Venanzi, F. Formaggio and C. Toniolo, B. Pispisa, Biophys. J. 88 (2005) 3411
[3] S. Bobone, Y. Gerelli, M. De Zotti, G. Bocchinfuso, A. Farrotti, B. Orioni, F. Sebastiani, E. Latter, J. Penfold, R. Senesi, F. Formaggio, A. Palleschi, C. Toniolo, G. Fragneto and L. Stella, Biochim. Biophys. Acta, Biomembranes 1828 (2013) 1013–1024

Trichogin belongs to the peptaibol family of antimicrobial peptides. Several preliminary data suggested that this peptide might form pores according to a model called "barrel-stave", in which transmembrane oriented peptides aggregate to form a channel [2]. However, trichogin comprises only 10 amino acids, and its helix is about half the normal bilayer thickness. How could such short peptide form transmembrane channels?

Neutrons reflectivity provided the resolution and selectivity needed to answer this question. We performed reflectivity experiments on a planar phospholipid bilayer supported by a silicon crystal and submerged in a water phase, to which increasing trichogin concentrations were added. Deuterated peptide, lipids and water were used in appropriate combinations with the hydrogenated molecules to increase the reflectivity contrast. In **figure 2** the curves of the POPC bilayer in D_2O at the different concentrations of deuterated peptide investigated are compared. Two main features are visible. When trichogin is added, a decrease in reflectivity in the mid-Q region (0.05 – 0.15 $Å^{-1}$) is observed, due to the insertion of the deuterated peptide into the membrane. In addition, the main minimum of the profiles shifts towards higher Q_z values, indicating a thinning of the overall thickness of the deposition. A detailed analysis of these data indeed showed that the peptide inserts in the hydrophobic region of the membrane, reaching a peptide to lipid molar ratio of about 10% (which corresponds approximately to the value needed to form the pores that kill bacteria [2]), and causing a thinning of the tail region from 28 to 21 Å.

MD simulations were in agreement with these findings, and showed that transmembrane-inserted trichogin molecules can cause membrane thinning by interacting with the phospholipid headgroups through electrostatic and H-bonding interactions, enhanced in the low-dielectric constant environment of the hydrophobic membrane core. These interactions lead to thinning by drawing phospholipid headgroups deep into the membrane (**figure 3**). Scattering length density profiles calculated from the simulations were in good agreement with those derived from the experimental data (**figure 2**), conferring a good confidence to the atomic-level picture provided by the MD simulations.

Overall, these data indicate for the first time that a barre-stave mechanism of pore formation is possible for trichogin and for similarly short peptaibols, despite their relatively small size. Our findings are a starting point for the rational design of new peptide-based antimicrobial molecules.

Figure 1

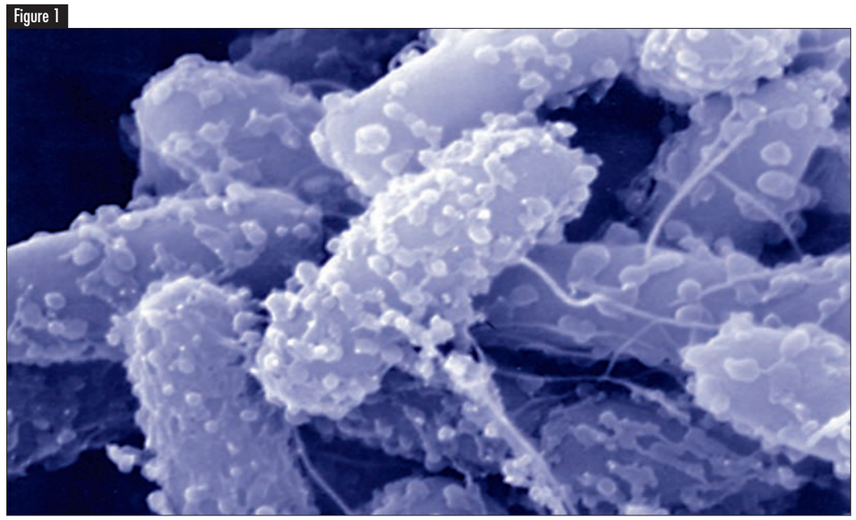

Electron microscopy image of the damage caused to Escherichia coli bacterial membranes by an antimicrobial peptide.

(copyright: Susan Farmer, University of British Columbia. http://www.cmdr.ubc.ca/cool.html).

Figure 2

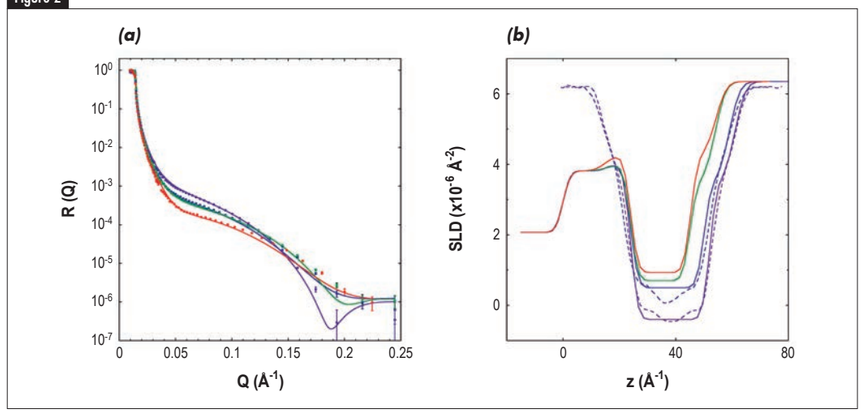

***(a)** Neutron reflectivity profiles for the phospholipid bilayer in D_2O, in the absence of trichogin (violet), and after addition of deuterated peptide, at concentrations 4.5 μM (blue), 15 μM (green), and 30 μM (red).*
***(b)** Neutron scattering length density (SLD) profiles derived from the data in panel A (continuous lines), and calculated from the simulations with 0 (violet) or 8 (blue) trichogin molecules (dashed lines).*

Figure 3

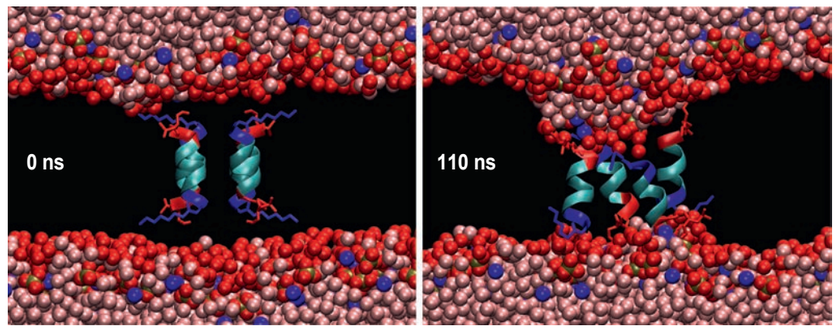

Time evolution of a simulation trajectory with 4 trichogin molecules embedded in the bilayer. P, N and O atoms of phospholipids are shown as gold, blue and red spheres, respectively, while water O atoms are coloured in pink. The acyl chains of the phospholipids are omitted for the sake of clarity. Peptides are represented as ribbons, with the N- and C-termini coloured in blue and red, respectively.

Cover of the 2013 issues of Biochim. Biophys. Acta, Biomembranes, highlighting a figure from this study [3].

Small-angle diffractometer D22
Spin-echo spectrometer IN15

Observing protein cluster phase in concentrated monoclonal antibody solutions

The formation of protein clusters with a preferred finite size is critically important to understand the physics of concentrated protein solutions. Among the many applications, protein clustering plays a key role in controlling the viscosity of therapeutic monoclonal antibodies (mAb) which have been considered the closest thing to "magic bullets" for the treatment of many diseases including cancers. In particular, it is widely speculated that the formation of mAb clusters is responsible for the high viscosity observed for some mAb solutions. This undesired high viscosity is actually one of the main obstacles for the future use of subcutaneous injection for the administration of biopharmaceuticals.

AUTHORS

E.J. Yearly, **P.D. Godfrin**, **T. Perevozchikova** and **Yun Liu**
(Center for Neutron Research, National Institute of Standards and Technology, Gaithersburg, Maryland and University of Delaware, Newark, USA)
H. Zhang (Center for Neutron Research, National Institute of Standards and Technology, Gaithersburg, Maryland and University of Maryland, USA)
P. Falus and **L. Porcar** (ILL)
M. Nagao (Center for Neutron Research, National Institute of Standards and Technology, Gaithersburg, Maryland and Indiana University, USA)
J. Curtisand (Center for Neutron Research, National Institute of Standards and Technology, Gaithersburg, Maryland, USA)
P. Gawande (Theranos Inc., Pal Alto, California, USA)
R. Taingand, **I.E. Zaaraga** (Late Stage Pharmaceutical Development, Genentech Inc., South San Francisco, California, USA)
N.J. Wagner (University of Delaware, Newark DE, USA)

REFERENCES

[1] E.J. Yearley, I.E. Zarraga, S.J. Shire, T.M. Scherer, Y. Gokarn, N.J. Wagner and Y. Liu, "*Small-Angle Neutron Scattering Characterization of Monoclonal Antibody Conformations and Interactions at High Concentrations*", Biophys. J., 105 (2013), 720-731
[2] E.J. Yearley, P.D. Godfrin, T. Perevozchikova, H. Zhang, P. Falus, L. Porcar, M. Nagao, J. Curtis, P. Gawande, R. Taing, I.E. Zarraga, N.J. Wagner and Y. Liu, "*Microstructural origin of anomalously high viscosity in concentrated monoclonal antibody solutions revealed by neutron spin echo*", (2013) submitted.
[3] Y. Liu, L. Porcar, J. Chen, W.-R. Chen, P. Falus, A. Faraone, E. Fratini, K. Hong, P. Baglioni, J. Phys. Chem. B 115 (2011) 7238

However, to date, it has been difficult to directly observe these mAb clusters accurately and quantitatively characterise their microstructure in crowded environments. Many results are still hotly debated in the colloidal community. By combining small-angle neutron and X-ray scattering (SANS/SAXS), neutron spin-echo (NSE), and computer simulations, we have studied two mAbs with small difference in their primary structures to conclusively observe the protein cluster phase with preferred cluster size and establish the relation between the cluster formation and the increased viscosity [1,2].

Despite the small difference in their protein sequences, the two mAbs (denoted as mAb1 and mAb2) have markedly different solution viscosities. The solution viscosity, η, of mAb1 has an anomalously large value of 310 mPa·s at 150 mg/ml compared to many other mAbs that have much smaller viscosity including mAb2 whose viscosity is only 18 mPa·s at 150 mg/ml. Even though the η of mAb1 is not very large in comparison with many other soft materials such as polymer blends and colloidal glass/gel systems, these solution viscosities limit the allowable concentration for bulk manufacturing as well as delivery through thin needles.

The characterisation of the apparent radius of mAb1 and mAb2 at relatively small concentrations (<10 mg/ml) indicates that mAb2 are dispersed as monomers for this concentration range while mAb1 begins forming small clusters. The dynamic light scattering data also show that the apparent hydrodynamic radius of mAb1 proteins increases from that of a monomer at 1 mg/mL to about 1.6 times that of a monomer at 10 mg/mL. The estimated molecular mass of mAb1 clusters at 10 mg/mL is close to that of a mAb1 dimer indicating that dimers may be the dominating species at 10 mg/mL.

To accurately characterise the cluster size at high concentrations, we used neutron spin-echo (NSE) to directly probe the translational self-diffusion coefficient, D_s, of mAb1 samples as a function of concentration, *C*.

It has been shown that mAb2 remains dispersed as monomers in the concentration range studied [1,2]. Therefore, the relative ratio of D_s between mAb2 and mAb1 is an indication of the size of mAb1 clusters relative to a mAb2 monomer. This ratio as shown in **figure 1** is also interpreted as the size of the mAb1 clusters relative to the mAb1 monomer size. Surprisingly, the results in **figure 1** show that once formed at low concentrations (about 10 mg/mL), the cluster size of mAb1 remains almost constant over a large concentration range. This indicates that the clusters in mAb1 solutions have a preferred finite size. This behavior is dramatically different than that of many globular proteins such as lysozyme. Recent study of lysozyme solutions with strong electrostatic repulsion demonstrated that clusters only form at relatively high concentrations and the size of clusters increases with the concentration [3]. Here, the formation of mAb1 clusters shows similarities to micelle formation, which self-assembles into clusters at relatively low concentration but then maintain their size over a range of concentration.

Our computer simulations further show that these clusters likely have an extended open structure and thus, have large effective volume fraction compared to the volume fraction of the monomers. This increase in the effective volume fraction leads to the observed increase in the solution viscosity of mAb1. More importantly, this cluster size can be controlled by the addition of electrolyte such, that a decrease in the solution viscosity is observed along with a decrease of protein cluster sizes. [2] Therefore, the strong correlation of the cluster size and the solution viscosity shows that the formation of small protein clusters is indeed the driving force of the anomalously high viscosity for our mAb solutions.

These measurements were the first to experimentally demonstrate proteins can form clusters of a very small finite size. Additionally the insights gained controlling mAb solution viscosity are useful in the development of mAbs formulations with desired solution properties, which in turn will aid their efficient production and clinical use.

Figure 1

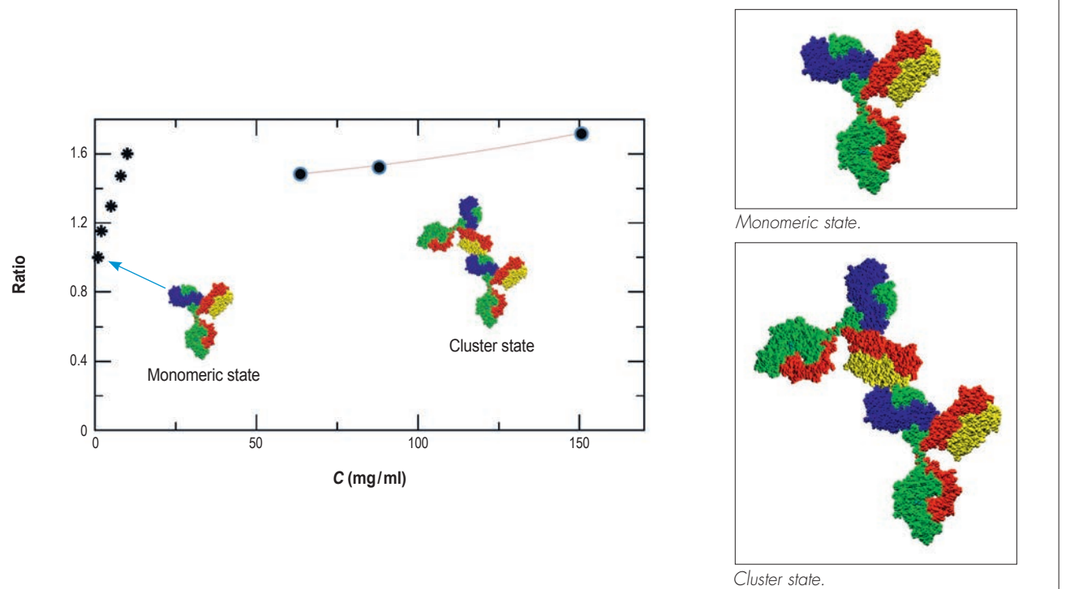

The ratio of the self-diffusion coefficients for mAb2 and mAb1, which is also the ratio of mab1 cluster size relative to its monomer size. The colored mAb protein images are drawn for illustration purposes only.

Backscattering spectrometer IN13

Neutron scattering detects *in vivo* stress in cells

Understanding the genetic and physical aspects of cell response to environmental stress is fundamental in biology because of its importance for survival and the implications in ecological and health issues. Neutron scattering is a promising new tool for the non-invasive study of molecular dynamics in the protein population of living cells. We applied the method at the IN13 instrument at ILL to measure the physical response of microorganisms to thermal stress.

AUTHORS & REFERENCE

G. Zaccai, **J. Peters** and **B. Franzetti** (IBS, UJF, ILL)

[1] V. Marty, M. Jasnin, E. Fabiani, P. Vauclare, F. Gabel, M. Trapp, J. Peters, G. Zaccai and B. Franzetti J. R. Soc. Interface 10 (2013) 20130003

A protein is a chemical polypeptide chain folded into a dynamic three-dimensional structure with biological activity. Protein structure and dynamics are very sensitive to environment. The crowded conditions as well as the presence of extensive molecular interactions that prevail inside a living cell are believed to interfere importantly with protein folding and unfolding processes. It follows that the consequences of environmental stress on the dynamic state of a protein in the cytoplasm could be very different from that measured *in vitro*, under dilute conditions. Neutron scattering has been developed as a method of choice to probe protein dynamics in live cells.

We studied *Halobacterium salinarum* (*Hs*) as a model microorganism and characterised, *in vivo*, the effects of temperature stress on molecular dynamics. *Hs* belongs to the family of the *Haloarchaea*, microorganisms that require high salt concentrations to thrive. **Figure 1** shows a bloom of *Haloarchaea* in the Lac Retba (also known as Lac Rose) in Senegal. The temperature of the lake varies between 20 °C and as high as 50 °C depending on weather, night/day and precipitation that changes the salt concentration. Even though it is not a thermophile (an organism that thrives only in high temperatures) *Hs* can tolerate high temperature stress quite well. This made it possible to explore a range of stress conditions without killing the cells.

Hs cultures were grown in the laboratory at 37°C and normal high salt conditions for the organism, then transferred at the desired stress temperature and cultivated under agitation for a further hour. For the neutron scattering experiment, a paste of live cells was sealed in a gold-plated sample holder (to avoid corrosion by the salt in the suspension) and mounted on the IN13 spectrometer. Whenever a biological sample is examined it is important to verify it has not been denatured during the experiment. Viability tests on the samples, confirmed that the cells survived the stress conditions and were not affected by being enclosed in the sample holder or exposure to the neutron beam (**figure 2**).

As in a billiard ball collision, neutrons bounce off moving nuclei exchanging energy and momentum, so that neutron scattering informs us on the molecular dynamics in the sample. Each neutron spectrometer is sensitive to a particular window in the range of motions. On IN13, the window looks at atomic displacements of the order of 1Å (0.1 nanometres) in 0.100 ns, which corresponds to thermal motions in protein molecules. Atoms in a protein can be seen as being held by springs linking them to their neighbours in the structure. One of the parameters extracted from the neutron scattering data is the mean force constant or resilience (<k> Newtons/metre) of the springs in the protein structures. It is plotted as a function of stress temperature in **figure 3** (right hand axis). The fall in resilience with increasing stress indicated a 'softening' of protein structures, as would occur if there were partial unfolding. A further important control was to make sure that the cells were responding biologically to the imposed thermal stress. Thermosome is a large complex involved in 'housekeeping' for the intracellular protein population, which contributes to cell survival by recycling damaged molecules. Its increased production is one of the genetic responses to stress. Thermosome levels measured in the same samples as a function of stress temperature are in **figure 3** (left hand axis). Note how the genetic response of thermosome accumulation parallels the physical response of decrease in resilience.

The neutron study provided direct insight into the folded state of the proteome (the protein population in the cell) exposed to temperature stress conditions. It established that neutron spectroscopy sensitively detects alterations in the mean molecular dynamics state of the proteome within a living cell in response to environmental changes. Despite the crowded intracellular environment and the induction of protein quality control systems such as thermosome complexes, the dynamic state of a large fraction of the proteome is strongly perturbed under thermal stress. Yet, interestingly, the cells recovered easily when replaced in optimal growth conditions.

Figure 1

Lac Rose in Senegal from the sky showing the harvesting of "fleur de sel" by raking the surface.The colour is due to Haloarchaea growing in the high salt environment.

Figure 2

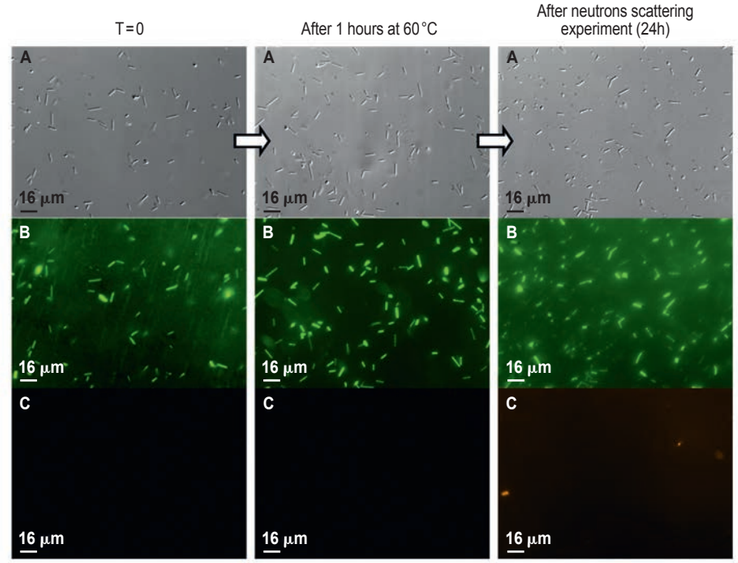

Effect of thermal stress on the viability of Halobacterium salinarum. Cell mortality after heat shock (middle panel) and after the neutron experiment (right hand panel) was assessed by the LIVE/DEAD BacLight kit. A) Differential interference contrast image of the cells. B) Green fluorescence corresponds to viable cells with intact membranes. C) Red fluorescence indicates dead cells. Viability rates were found to be over 95% in all cases. The left hand panel shows the control before stress sets in.

Figure 3

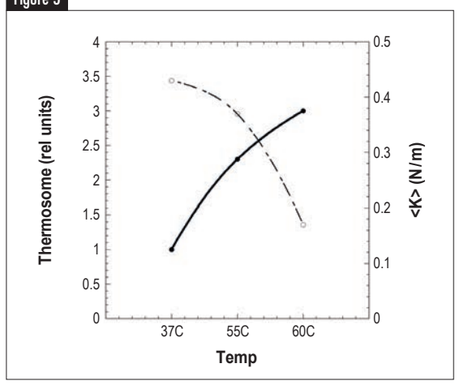

Left axis (black data points): Thermosome accumulation as a function of stress temperature measured by Western Blot (immunodetection) in the samples after the neutron experiment. Right axis (open circle data points): Molecular dynamics resilience in the live cells measured by neutron scattering as a function of stress temperature.

Small-angle diffractometer D22

Snapshots of a jumping gene

DNA transposons are short fragments of DNA capable of jumping from one place to another in a genome, and causing shuffling of the genetic code. A single transposase enzyme promotes this cut-and-paste movement of DNA. Using small-angle neutron scattering (SANS) we have established the shapes of the Mos1 transposase when it is free of DNA and when it is bound to one transposon end, in the early stages of transposition. Our results shed light on the conformational changes occurring in the enzyme that enable the transposon to be cut out from its host.

Transposons make up a large proportion of many genomes (*e.g.*, 45% of the human genome). These genes were originally believed to have no purpose and were described as "junk DNA". However, it is now emerging that transposons are powerful drivers of genetic change; some transposons can move from one place to another within a genome using a simple cut-and-paste mechanism. This DNA rearrangement shuffles the genetic code and can lead to beneficial changes in cells. For example in the human genome, rearrangement of antibody genes enables the immune system to target infection more effectively.

The cut-and-paste property of DNA transposition is now being exploited to develop new biotechnology tools for genetic engineering and gene delivery. One family of transposons – the *mariner/Tc1* family – have proved particularly useful as they are widespread in nature and can jump in a broad range of species, including mammals [1]. Only one protein – a transposase – is required to cut out the transposon and reinsert it elsewhere in the genome. Our aim is to understand how *mariner/Tc1* transposons jump, with particular focus on the transposition pathway of the *mariner* element Mos1 (**figure 1**). By characterising the structures of the protein-DNA complexes between Mos1 transposase and the ends of its transposon, we have gained a deeper understanding of how Mos1 cuts and pastes DNA at the molecular level. These results will help us to engineer the transposase and speed the development of biotechnology applications of transposons.

We used SANS to determine the shape of the Mos1 transposase (a) before it binds to transposon DNA, and (b) when it binds to one transposon end in a single-end complex (SEC2) and before the DNA is cut. We have used the powerful method of contrast variation in SANS [2] to determine the shapes and relative spatial arrangements of the individual components in the protein-DNA complex. Selective masking of either the protein or DNA is achieved simply by altering the ratio of H_2O to heavy water (D_2O) in the solvent. Partially deuterated Mos1 transposase (D-Mos1) was produced for these experiments in the ILL's Life Science Group (the D-LAB). Under the Partnership for Structural Biology the SANS experiments were performed on the instrument D22 at the ILL and small-angle X-ray scattering (SAXS) experiments were performed on the beam line ID14-3 at the ESRF.

The results of SAXS and SANS experiments revealed that in the absence of DNA Mos1 transposase is an elongated homodimer, with a maximum dimension (Dmax) of 185 Å. By comparison, the transposase in the paired-end complex (PEC) crystal structure – at a later stage in the transposition pathway – has a compact crossed conformation [3] with a Dmax of 110 Å. From these data we conclude that the transposase changes shape, either upon binding one transposon end (in SEC2) or after the transposon ends are paired (in the PEC). The results of our contrast variation SANS experiments on SEC2 (**figure 2**) revealed that the transposase-DNA complex is more elongated than the DNA-free Mos1 transposase dimer. Furthermore the DNA component is associated predominantly with one transposase monomer only, and this may allow the other transposase monomer the rotational freedom to drive a change in the shape of the complex.

In conclusion, the similar architectures of the DNA-free transposase and transposase in SEC2 suggest that binding of a pre-formed transposase dimer to the first transposon end occurs without major shape changes in either the protein or the transposon DNA. We propose that these changes occur in the SEC2 to PEC transition, by rotation of one transposase monomer and its capture of the second transposon DNA end.

AUTHORS & REFERENCES

J.M. Richardson (University of Edinburgh, UK)
M. Cuypers and **V.T. Forsyth** (ILL)

[1] I. Ammar, Z. Izsvak, and Z. Ivics, Methods Mol. Biol. 859 (2012) 229
[2] P.A. Timmins and G. Zaccai, Eur. Biophys. J. 15 (1988) 257
[3] J.M. Richardson, S.D. Colloms, D.J. Finnegan, and M.D. Walkinshaw, Cell 138 (2009) 1096
[4] M.G. Cuypers *et al.*, Nucleic Acids Res. 41 (2013) 2020, original publication

Figure 1

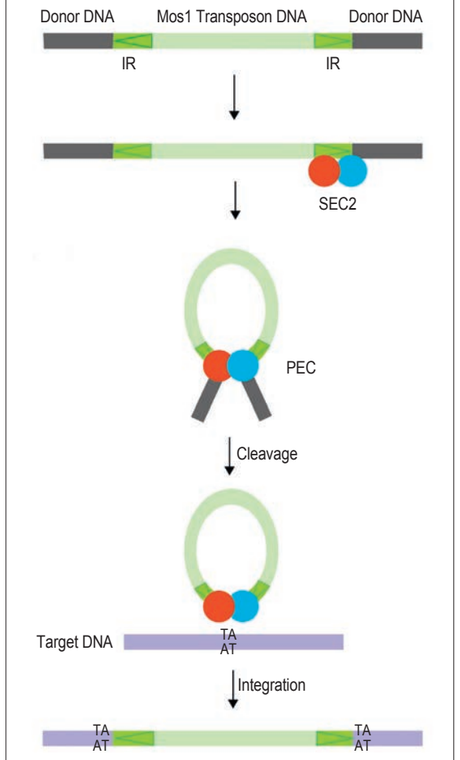

Schematic of cut-and-paste DNA transposition. The 1.3 kB transposon has 28 bp inverted repeats (IR) at either end. A transposase dimer binds to one end forming a single-end complex (SEC2). The transposon is cut from donor DNA in the paired-end complex (PEC). Mariner/Tc1 transposons are pasted in to TA sequences, resulting in signature duplications either side of the inserted transposon.

Figure 2

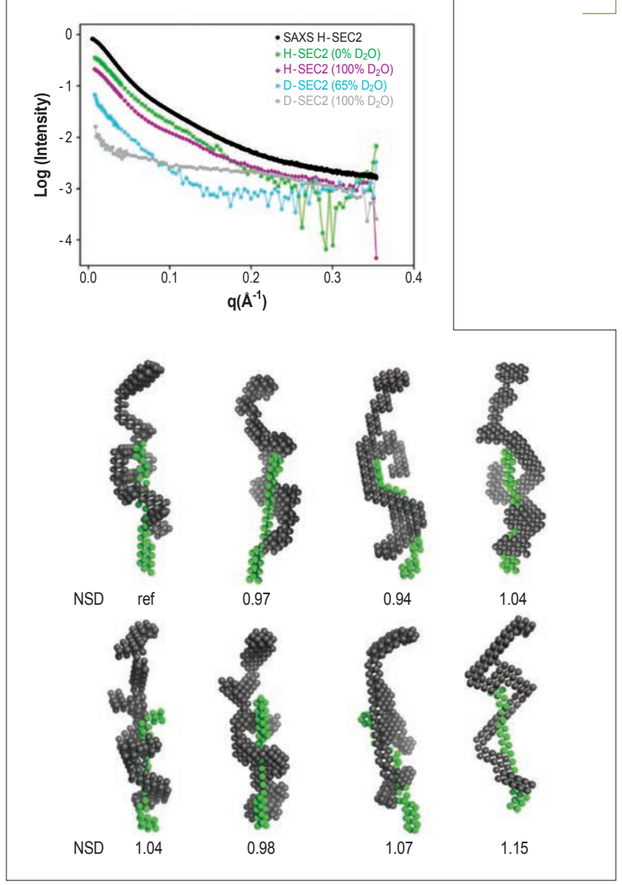

Contrast variation small-angle neutron scattering of SEC2. The solution conformations of SEC2 are shown as a gallery of bead models, containing transposon DNA (green) and a transposase dimer (grey).

Quasi-Laue diffractometer LADI-III

Neutrons show their potential in drug design

Neutrons can provide drug developers with crucial details about the structure and interactions of their pharmaceuticals. After years in the shadow of X-ray based techniques, their use in a crystallographic study of an antiviral drug binding to HIV-1 protease has highlighted how recent technological progress and instrument developments at the ILL are bringing neutrons into line. The successful analysis demonstrates the wealth of new information the combination of these two techniques can provide drug developers going forward.

AUTHORS & REFERENCE

I.T. Weber (Georgia State University, Atlanta, USA)
M.J. Waltman (Los Alamos National Laboratory, New Mexico, USA).
M. Mustyakimov, **P. Langan**, and **A.Y. Kovalevsky**
(Oak Ridge National Laboratory, Tennessee, USA)
M.P. Blakeley (ILL, France)
D.A. Keen (ISIS, UK)
A.K. Ghosh (Purdue University, Indiana, USA)

[1] I.T. Weber, M.J. Waltman, M. Mustyakimov, M.P. Blakeley, D.A. Keen, A.K. Ghosh, P. Langan, and A.Y. Kovalevsky *J Med. Chem.* 56 (13) (2013) 5631

For several decades X-ray crystallography has been routinely used by the pharmaceutical industry to determine how their drugs interact with their protein targets. Nevertheless, a limitation of the technique is that hydrogen atoms are virtually invisible in the X-ray analysis, leaving scientists to speculate on their positions, despite their importance in drug binding through hydrogen bonding. This is where neutrons have an advantage; they allow the positions of all the atoms to be determined including lighter elements such as hydrogen, and therefore neutron crystallography is particularly suited for use in drug discovery and development.

This potential has been acutely demonstrated in a recent study of interactions between a common clinical inhibitor (amprenavir) and HIV-1 protease, an enzyme essential for the replication of the HIV virus, allowing it to break polypeptide chains and create proteins used for viral maturation and the production of new infectious virus particles. After 20 years of analysis with X-rays, results published earlier this year [1] using neutrons provided a more detailed picture than ever before of how an antiviral drug used to inhibit the enzyme actually works. The team were able to identify the position of every hydrogen atom involved in the system, and which were involved in the binding of the inhibitor to the enzyme through hydrogen bonding. Critically the analysis indicated which hydrogen bonds were the weakest and how the binding, and hence the drugs performance could be improved.

This research represents a major step forward for a technique whose application in the field of pharmaceutical R&D has been held back in the past due to various technical challenges. These included the volume of sample crystals that needed to be grown, the length of time it took for the results to be collected, as well as the lack of dedicated instrumentation available around the world where scientists could carry out their studies. During this study the neutron crystallographic experiments were carried out on the LADI-III (quasi-Laue neutron diffractometer) instrument at the ILL where developments in the last decade have addressed the technical challenges allowing crystals as small as 0.05 mm^3 to be analysed, permetting a greater array of studies to be performed.

With the tools for the job, the study was carried out using a 0.2 mm^3 single crystal of HIV-1 protease (deuterated at a level of 85%) with amprenavir bound, and data were collected to 2.0Å resolution.

Figure 1

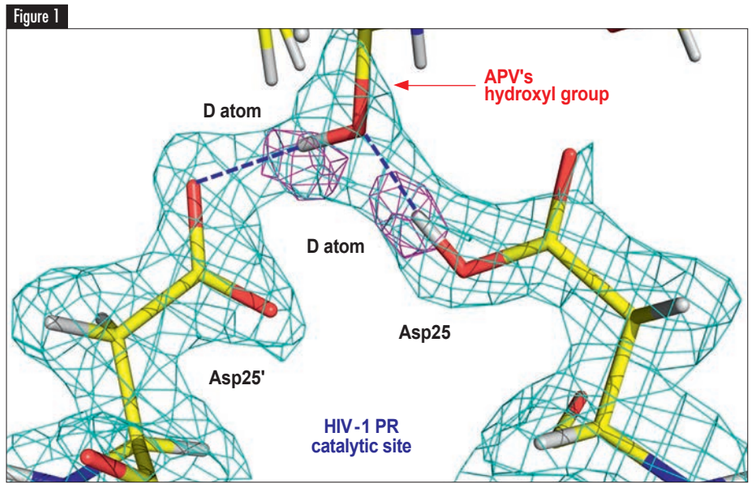

$2F_O$-F_C neutron scattering length density map contoured at 2.3σ (cyan) for the catalytic site showing residues Asp25, Asp25' and the hydroxyl group of amprenavir (APV). Omit difference F_O-F_C neutron scattering length density map contoured at 4.5σ (magenta) shows the locations of D atoms on Asp25 and the drug's hydroxyl group.

Despite its decade of use as a clinical inhibitor, it was only following this first analysis using neutrons that amprenavir's true binding behaviour was revealed, painting a rather different picture to that inferred from the X-ray studies, which had overplayed the importance of several hydrogen bonds. In fact the team suggested the presence of only two strong direct hydrogen bonds between the drug and HIV-1 protease at the catalytic site of the enzyme (**Figure 1**).

The findings present drug designers with a set of new sites to try and improve the drug's chemistry to significantly strengthen the binding, increasing the effectiveness of this and other inhibitors and to reduce the necessary dosages. Suggestions of areas for improvement include replacing weaker water-mediated hydrogen bonds with stronger direct hydrogen bonds to increase the enthalpy of binding. This could be achieved by changing certain functional groups of the drug in order to expel water molecules present in the active site, which at the same time improves the entropy of binding. Another approach would be to increase the strength of the two direct hydrogen bonds by creation of a special type of hydrogen bond known as a 'low-barrier hydrogen bond', in which the proton is equidistant between the donor and acceptor atoms. This can be achieved by lowering the ionisation constant of the hydroxyl group of the drug to make it similar to that of the amino-acids it binds to, via introduction of a strong electronegative atom such as fluorine.

The findings in this latest paper may also help address one of the biggest issues in combating HIV infection - drug resistance. Evolution of the virus over time produces the enzyme variants with weakened binding affinity to an inhibitor, a process that is actually sped up by the introduction of the drugs themselves. One way round this would be to improve the binding of the inhibitor with the main-chain atoms of HIV-1 protease rather than its side-chain atoms, as the main-chain atoms of the enzyme cannot mutate. Before this latest study it was thought the potential for advances in this area were limited because the hydrogen bond interactions with the main-chain atoms were already very strong. However, this has been shown not to be the case, creating a new avenue for the development of HIV pharmaceuticals much less affected by virus evolution and resistance.

X-ray crystallography has played a crucial role in structure-guided drug design for over two decades. Whilst its value to researchers in this field will continue for many years, combining the use of X-rays with neutrons increases the clarity of how drugs interact with their protein targets, providing the pharma industry with a powerful new tool to improve the performance of their products. It's clear that the future of drug design will feature a combination of the two crystallographic techniques that can provide patients with newer more effective medicines to not only battle HIV infection, but for other diseases as well.

Figure 2

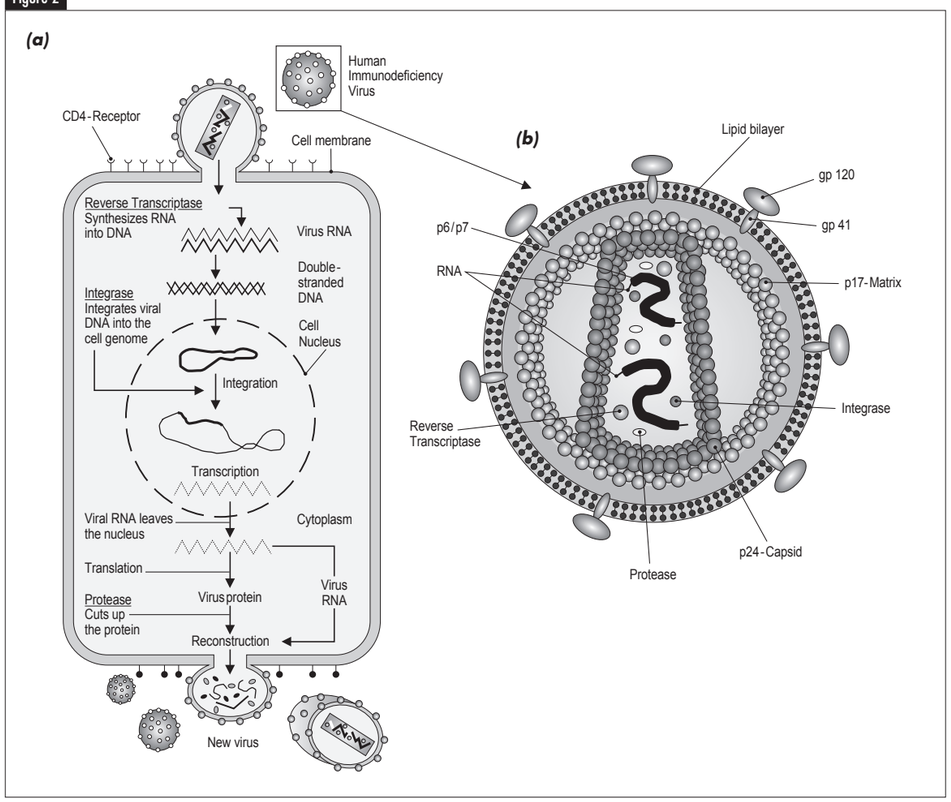

***(a)** The Human immunodeficiency virus (HIV) replication cycle.*
***(b)** The structure of a mature HIV virus particle.*

Picture taken from Wikipedia, the free encyclopedia.

Vertical reflectometer D17

Effect of functionalised gold nanoparticles on floating lipid bilayers

The development of novel nano-engineered materials poses important questions regarding the impact of these new materials on living systems. Possible adverse effects must be assessed in order to prevent risks for the health and the environment. On the other hand, a thorough understanding of their interaction with biological systems might also result in the creation of novel biomedical applications [1].

A key issue in making use of nanoparticles (NP) for biomedical purposes is understanding of their interaction with cells beyond the designated functions. Since the first contact that all nanomaterials will always have with any living organism is through the cell membrane, this study focuses on the interaction of a particular class of NP with model cell membranes.
Many recent studies have addressed the interaction between nanoparticles and membranes. Besides size, shape, ligand structure, and composition, the way in which biological cells take up nanoparticles is significantly affected by the nanoparticles' surface charge [2]. While cationic nanoparticles are thought to enter the cell by membrane diffusion, anionic nanoparticles probably insert through endocytosis, that is a process whereby the plasma membrane folds inward to bring substances into the cell without passage thorough the membrane.

To provide insight into the fate of gold nanoparticles (AuNPs) and their impact on cell membrane integrity, we analysed the interaction of two classes of AuNPs with single component model membranes. For this purpose, we brought two nanometer diameter AuNPs functionalised with cationic [N, N, N-trimethyl (11-mercaptoundecyl) ammonium] and anionic (mercaptoundecanoic acid) surface ligands into contact with single-component zwitterionic DSPC (1,2-distearoyl-sn-glycero-3-phosphocholine) bilayers. As model membrane, we chose a system composed by a solid supported double lipid bilayer, in which the second bilayer floats 20-30 Å above the first one and bypasses the interaction between the first lipid bilayer and the substrate. Our choice gives access to a highly hydrated, fluctuating bilayer that represents a membrane system with dynamic properties comparable to biological membranes and is greatly relevant for the examination of the influence of AuNPs on lipid membrane structure and integrity.

There are several advantages by using the neutron reflectivity technique for this kind of study. Neutrons have a weak interaction with matter because they are not charged and perturb soft matter systems very little. They are deeply penetrating and therefore ideal probes for buried interfaces. Last, but not least, with the use of isotopic substitution, we can vary the contrast between different regions of the system, highlighting the scattering of each component of the system. For example, in our systems this allows us to distinguish between the density variation in the bilayers due to solvent and/or NPs penetration. All these signatures of neutrons allow us a structural determination at a resolution not reachable with any other technique.

In agreement with previous experimental and theoretical results, we could confirm in the presented neutron reflectometry experiments that the charge of the AuNPs indeed affects the way nanoparticles interact with lipid bilayers. The AuNPs functionalised with cationic head groups penetrate into the hydrophobic moiety of the lipid bilayers and cause membrane disruption at an increased concentration. Furthermore, they tend to pass through the fluid phase of the lipid membrane and remain embedded in the hydrophobic moiety of the floating bilayer [3].
By a precise modeling of the reflectivity data, we could quantify the amount of AuNPs that remain embedded in the lipid bilayers. **Figure 2** shows the reflectivity profile obtained by measuring a pristine lipid membrane and a lipid membrane in the presence of the AuNPs, from which we calculated the scattering length density profile of our stratified system and obtained precise information about the thickness, roughness, composition and hydration of the bilayers. The analysis of the profile indicates that the cationic AuNPs only penetrate the first bilayer. Fitting models that included AuNPs in the supported bilayer or excluded the presence of AuNPs from the complete bilayer system were not compatible with the data.
In contrast, the AuNPs functionalised with anionic head groups did not enter but seemed to impede the destruction of the lipid bilayer at an alkaline pH. They did not have the tendency to penetrate the lipid membrane, but rather interact with its surface.

Overall, this study shows that the nature of AuNP–lipid membrane interaction depends on the AuNP surface charge. Further studies that focus on the AuNP concentration and size, as well as lipid bilayer surface charge and composition are necessary to elucidate further parameters influencing the nanoparticle–cell membrane interaction and their consequences on the membrane structure and integrity. This knowledge is crucial to effectively design safe nanoparticles for biomedical applications and also to define practices and procedures for the secure handling of nanoparticles in general. The information obtained might influence the strategy for a better nanoparticle risk assessment based on a surface charge evaluation and contribute to nano-safety considerations during their design.

Figure 1

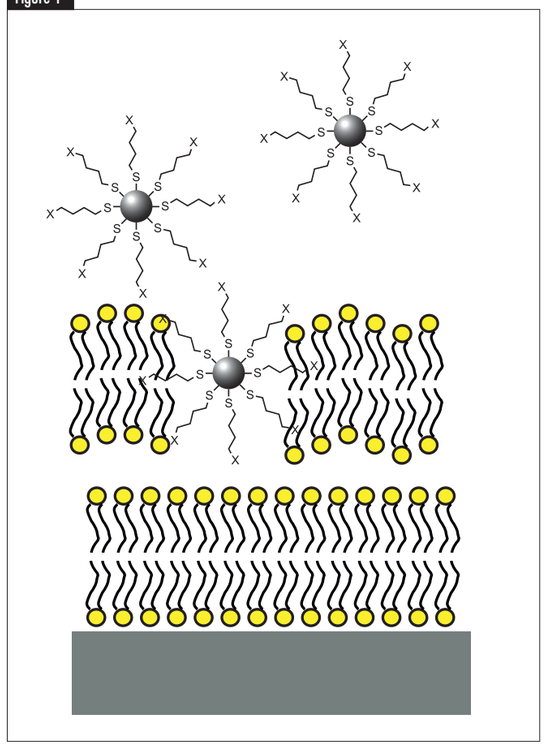

Schematic representation of functionalised nanoparticles interacting with a lipid system.

Figure 2

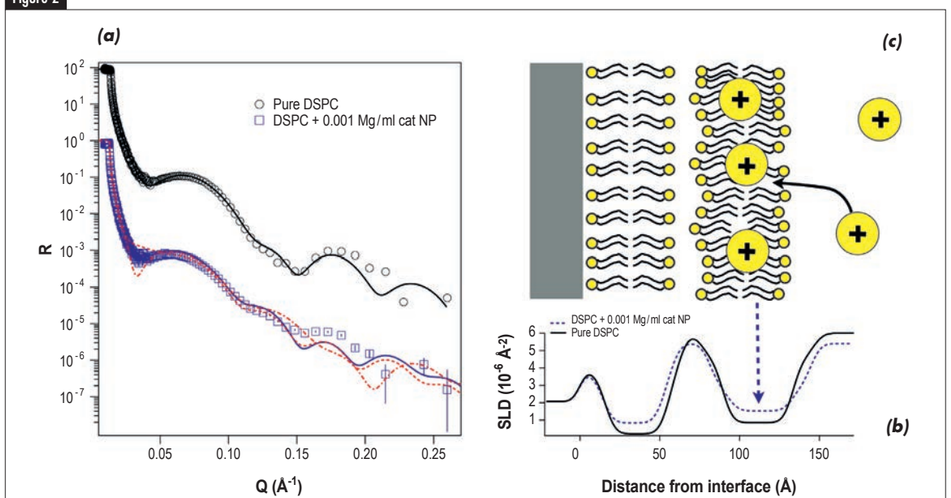

Reflectivity profiles of the DSPC bilayers system measured in the pristine form and in the presence of 0.01 mg ml^{-1} cationic Au NPs nanoparticles at 25°C. The reflectivity profile of the pure DSPC double bilayer is offset. Continuous black and blue lines are the best fits to the measured data. The red lines represent the results of the fitting models that include the presence of the cationic Me3NAu NPs also in the supported bilayer (dash) and the absence of NPs in the lipid bilayers (dashed dotted line). ***(b)*** *SLD profiles of the sample are extracted from the fits to the measurements. Thanks to measurements performed at different contrasts we can distinguish between the effect of solvent penetration and NPs inclusion in the bilayers.* ***(c)*** *The sketch shows structural details deduced from the fitting parameters of the reflectivity curves.*

AUTHORS & REFERENCES

M. Maccarini (TIMC / IMAG, Grenoble, France)
S. Tatur (University of Illinois, Chicago, USA)
R. Barker and **G. Fragneto** (ILL)

[1] Y.-C. Yeh, B. Creran and V.M. Rotello, Nanoscale 4 (2012) 1871
[2] C. M.Goodman, C.D. McCusker, T. Yilmaz, and V.M. Rotello, Bioconjugate Chem. 15 (2004) 897
[3] S. Tatur, M. Maccarini, R. Barker, N. Nelson and G. Fragneto, Langmuir 29 (2013) 6606

Polarised cold neutron beam facility PF1B

EXILL, a campaign of measurements devoted to nuclear spectroscopy

The combination of a well collimated, intense cold-neutron beam available at the instrument PF1B and a highly efficient Germanium detector array made a unique nuclear structure physics campaign possible. The measurements were devoted to prompt γ-ray spectroscopy of stable nuclei and of medium-heavy mass neutron-rich isotopes produced in neutron induced fission. For two full reactor cycles both, stable and fissile targets (^{235}U and ^{241}Pu), were irradiated.

A. Blanc, **M. Jentschel**, **U. Köster**, **P. Mutti** and **T. Soldner** (ILL)
G. de France (GANIL, Caen, France)
J.M. Regis (IKP Cologne, Germany)
G. Simpson (LPSC, Grenoble, France)
C.A. Ur (INFN Padova, Italy)
W. Urban (Faculty of Physics, University of Warsaw, Poland)

[1] M.A.C. Hotchkis *et al.*, Nucl. Phys. A 530 (1991) 111
[2] I. Ahmad and W.R. Phillips, Rep. Prog. Phys. 58 (1995)1415
[3] W. Urban *et al.*, Phys. Rev. C, 85 (2012) 14329
[4] W. Urban *et al.*, JINST, 8 (2013) P03014
[5] J. Simpson *et al.*, Acta Phys. Hung., 11(2000)159
[6] C. Rossi Alvarez, Nucl. Phys. News, 3 (1993)
[7] H. Mach *et al.*, Nucl. Instr. and Meth. A, 280 (1989) 49
[8] J.M. Régis *et al.*, Nucl. Instr. and Meth. A 622 (2010) 83
[9] J.M. Régis *et al.*, Nucl. Instr. and Meth. A 684 (2012) 36
[10] J. Jolie, Eur. Journ. Phys. A Conf. Ser., in press

THE PHYSICS CASE

The usefulness and feasibility to study fission products with High Purity Germanium (HPGe) detector arrays has been demonstrated in the past by experiments with spontaneous fission sources such as ^{252}Cf and ^{248}Cm [1,2,3]. Neutron induced fission (with isotopes ^{235}U and ^{241}Pu) yields a very effective way to produce and study low-lying states of neutron-rich nuclei in the mass range A ~ 85-160, specifically in the scientifically interesting and so far unknown doubly magic regions of ^{78}Ni and ^{132}Sn. The population of entire isotope chains allows a systematic study of the prediction power of the nuclear shell model. Moreover, due to their doubly magic structure, they form waiting points along the r-process nucleosynthesis path. The elementary abundances at waiting points is highly enhanced since the decay time of the unstable isotope is longer as a consequence of the increased stability of the nuclear structure. Further motivation comes from experiments focusing on the radiative neutron capture (n,γ) reaction itself. The non-selectivity of the capture process populates a large majority of the low spin excitations. This gives access to very rich and detailed spectroscopic information of isotopes close to the line of stability.
The high interest in the campaign is demonstrated by 120 scientific visitors from 18 laboratories submitting more than 80 different proposals and actively participating in the data taking.

THE EXILL CAMPAIGN

Experiments with HPGe detector clusters in combination with a neutron beam were so far limited to very small collections of up to 8 detectors only [4]. Within the EXILL campaign for the first time a large HPGe array has been installed around a highly collimated cold-neutron beam with a flux of 10^8 n.s^{-1}.cm^{-2} at the target position. During the campaign 19 different samples with stable isotopes with capture cross section from 0.02 to 61000 barns (7 orders of magnitude range!) have been used. Furthermore, fissile isotopes such as ^{235}U and ^{241}Pu have been also irradiated.
In the high efficiency configuration the detector array consisted of 10 EXOGAM [5] clover detectors from GANIL (France), 2 clover detectors from ILL and 6 GASP [6] coaxial Ge detectors from LNL (Italy). A second configuration consisted of 8 EXOGAM clovers combined with 16 $LaBr_3$ scintillator detectors from the FATIMA collaboration [7]. This configuration profits from the excellent time resolution of the scintillators (below 200 ps) allowing lifetime measurements of nuclear states.
The signals from the detectors were fed into a digital data acquisition system consisting of 100 MHz digitizer modules which allowed both, energy and time information, to be recorded. The time signals from the $LaBr_3$ scintillator detectors were processed using analogue electronics. All data were recorded in a triggerless mode to preserve a maximum of information and resulting in about 60 TB of stored raw data.

ANALYSIS METHOD AND QUALITY OF DATA

Fission produces different nuclei as fragments of the fission process. At least one fragment must be identified in order to interpret the data. In the EXILL campaign this is done via known characteristic γ-rays, which are used to search for further γ-rays within a certain time window (coincidence). These other rays provide new information on the fission fragment. These can be the energies of unknown transitions within the same de-excitation path or the lifetime of intermediate nuclear states. This technique typically requires at least 3 γ-rays to be detected in coincidence. Therefore the sensitivity of the experiment depends highly on the efficiency, the energy resolution and the granularity of the detector array. The full EXILL array had a total detection efficiency of 6% at 1.3 MeV and consisted of in total 72 individual detector channels.

The experiment produced data during 95% of the total beam time. Depending on the particular fission yield the data from spontaneous fission sources were substantially improved, which gives access to new isomers and decay schemes. For example in the case of ^{92}Rb the statistical gain is in the order of 30.

In **figure 2** we show the example of a γγ-coincidence matrix of the reaction ^{155}Gd(n,γ)^{156}Gd illustrating the quality of spectra obtained in the experiment. In the fast timing configuration, the EXOGAM detectors were used to select the fragment of interest and the $LaBr_3$ scintillators give the lifetimes via a start/stop γ–ray detection [8]. Recently, this method was optimised [9] yielding an accuracy for lifetime determination of 5 ps. This has been demonstrated with a ^{152}Eu source and the ^{48}Ti(n,γ)^{49}Ti radiative capture reaction during the EXILL campaign.

A shared effort is presently ongoing in the sorting and analysis of the enormous data set. Despite the number of people involved several years of work lie ahead for this collaboration. First physics results from (n, γ) measurements have already been presented at conferences [10].

Figure 1

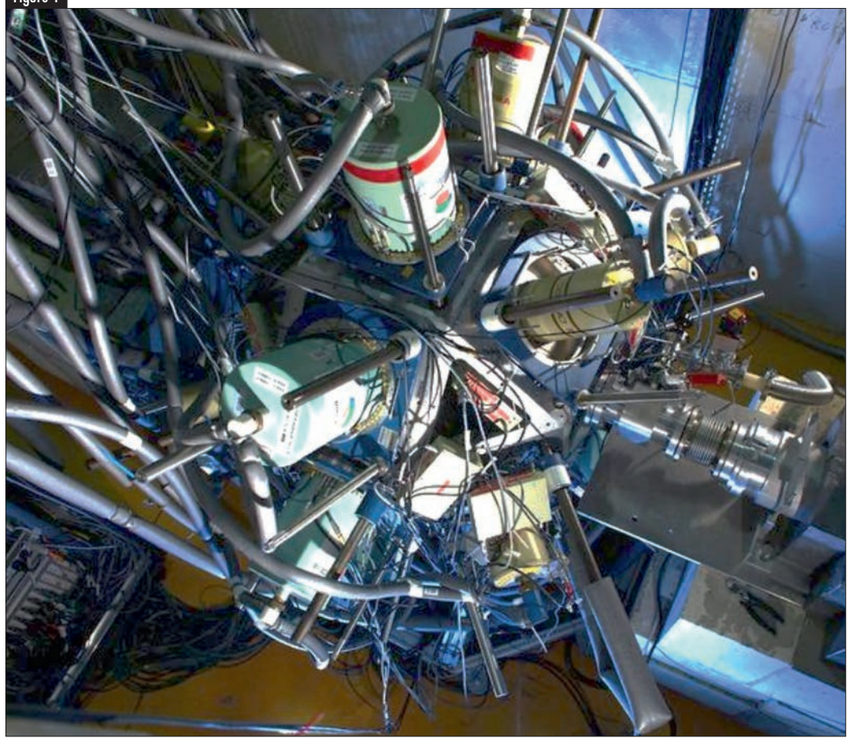

The EXILL high efficiency configuration installed at PF1B.

Figure 2

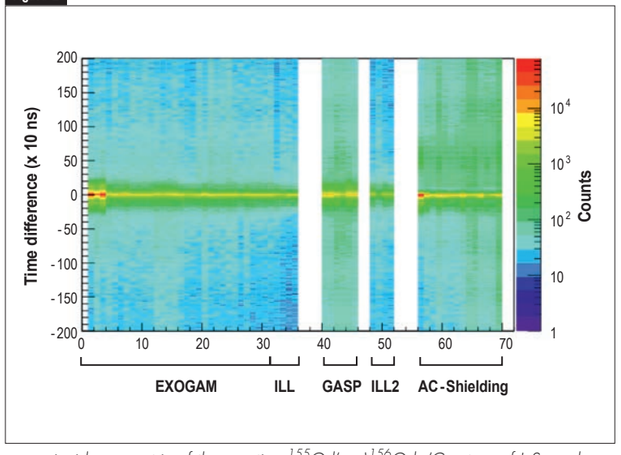

γγ-coincidence matrix of the reaction ^{155}Gd(n,γ)^{156}Gd. (Courtesy of L.Sengele, IPHC Strasbourg).

Ultra-cold neutron facility PF2

MONOPOL – A travelling-wave magnetic neutron spin resonator for tailoring polarised neutron beams

Since the early 1960s it is known that spin resonance in undulatory static magnetic fields allows for wavelength-selective spin flip of polarised neutrons. Implementing a novel travelling-wave technique, we have developed this concept towards a resonator which does not only allow to monochromatise the neutron beam but also to chop it into a sequence of pulses short enough for time-of-flight applications. The outstanding performance of such a resonator which was optimised for very cold neutrons could be demonstrated successfully at the PF2-VCN beam line.

AUTHORS & REFERENCES

E. Jericha, **Ch. Gösselsberger**, and **G. Badurek**
(Atominstitut, Vienna University of Technology, Austria)
P. Geltenbort (ILL)

[1]] G.M. Drabkin, Sov. Phys. JETP 16 (1963) 282
[2]] Ch. Gösselsberger *et al.*, Physics Procedia 42 (2013) 106

As shown already in the 1960s [1], the combination of a static vertical and a spatially alternating horizontal magnetic field constitutes an NMR-like system for polarised neutron beams, with the peculiarity that for given spatial period and strength of the vertical field each neutron creates its own '*resonance*' frequency according to its individual speed. Clearly, when placed between two polarising neutron mirrors such a resonator acts as neutron monochromator. The conventional design of such a resonator employs a thin meander-shaped metal conductor foil where each turn of the foil defines a single resonator element. Increasing the number of such elements improves the achievable wavelength resolution but evidently increases also the length of the resonator. Neutron pulses may be generated by switching the foil supply current on and off with the consequence that the achievable minimum pulse length is defined by the overall resonator length.

However, in our novel '*travelling wave*' technique the undulatory resonator field is applied in synchronisation with the resonant neutron pulse during its passage through each of the consecutive resonator elements. As a consequence, the minimum pulse length is defined only by the length of a single resonator element and hence be up to two orders of magnitude shorter than in the conventional mode. The experimental realisation of this novel technique, which allows for a complete decoupling of wavelength and time resolution, is a major step towards the development of electronically tuneable neutron monochromators and choppers of utmost flexibility. As additional feature, the concept can be applied across the complete thermal and cold neutron spectrum.

We have built a resonator composed of 48 elements (**figure 1**), each consisting of a 11.6 mm thick prismatic single-turn coil made of a 0.1 mm aluminium sheet and fed by an individually controllable current source which can be switched on and off within about 1 microsecond. This resonator was tested at the PF2-VCN beamline with a polychromatic beam of very cold neutrons, polarised and analysed by a pair of Fe/SiGe-based supermirrors. We established 'Dark-field' conditions by inverting the neutron polarisation over the complete incoming neutron spectrum by means of a broad-band current sheet spin flipper. Spectral analysis was performed by employing a single-disk chopper with about 5 ms opening time when operated at 10 Hz repetition rate (chopper-detector distance: 2.7 m). The blue symbols in **figure 2** represent the incoming VCN spectrum obtained with the resonator and the current sheet flipper switched off. Activating both results in the spectrum represented by the red symbols. The effect of spatial neutron spin resonance is clearly seen from the reduced spectral width of the detected neutron distribution (which is of course the result of a convolution of the actual spectrum with the transmission function of the disk chopper). Indeed, its width is dominated by the chopper opening time, while the wavelength resolution of the resonator is fully compatible with the theoretical value of 3% for a resonator consisting of 48 elements.

With this resonator we have realised at PF2-VCN the first travelling wave spin resonance at a white neutron beam ever (**figure 3**). Due to the fast switching time of our current sources the magnetic field is switched on practically instantaneously for the slow neutrons. Each resonator element has been activated for a certain time interval only (1.5 and 10 ms, respectively). Now, the resonator itself acts as a neutron beam chopper which is able to create neutron pulses of arbitrary length. As a clear advantage, the travelling wave mode produces much sharper neutron pulses than the conventional mode. Eventually this might be of value for novel ESS instrumentation.

ACKNOWLEDGEMENT

We acknowledge the vital contributions of T. Oda and M. Hino from Kyoto University to the experimental set-up and of S. Baumgartner, B. Berger, and R. Raab who performed their master theses on this project.

Figure 1

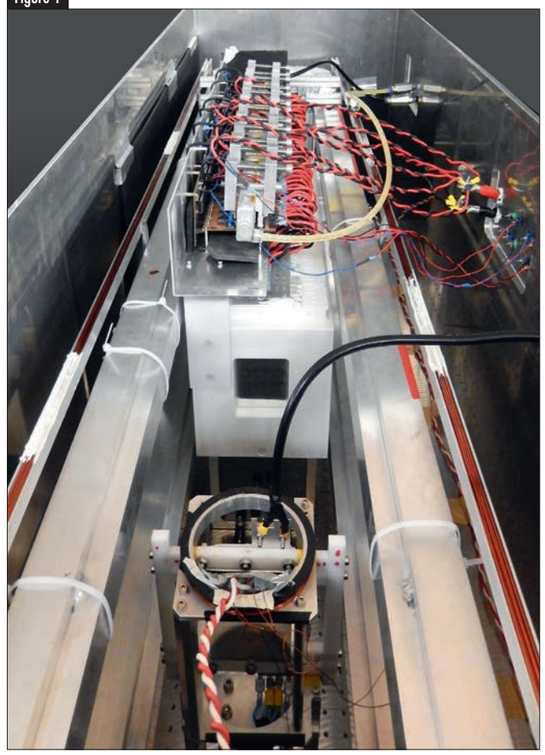

Up-stream view of the experimental set-up: the resonator with 48 individual elements is shown together with the individual supply lines from the current sources on its top. A broad-band current sheet spin flipper for polarisation inversion of the neutron beam can be seen in the foreground. The complete experiment has been placed in a He atmosphere to reduce neutron scattering and suppress VCN absorption.

Figure 2

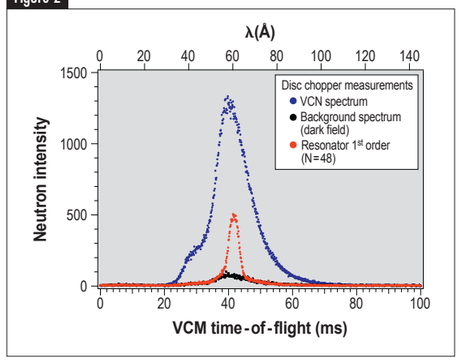

Time-of-flight spectra of the VCN beam as measured by means of a mechanical single-disk chopper: blue symbols show the total spectrum when the resonator is turned off, red symbols the combined effect of the neutron resonator and the broad-band spin-flipper; black symbols indicate the neutron background due to non-ideal neutron polarisers when the resonator is turned off.

Figure 3

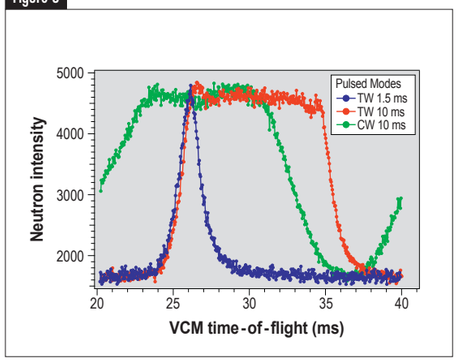

Tailoring the temporal structure of the neutron beam by pulsed operation of the resonator. The typical time scale for VCN is milliseconds. In the novel travelling wave (TW) mode the edges of the pulses are considerably sharper than in conventional mode (CM) where the resonator is switched on and off as a whole.

Analysis of the multiferroicity in the hexagonal manganite $YMnO_3$

Magnetoelectric material are actively studied, since they allow the cross control of magnetic and electric properties with possible applications in electronic devices. $YMnO_3$ is a prototype magnetoelectric compound presenting a coupling between the polarisation (P), dielectric constant (ε) and the magnetic order. Until recently its magnetic state and magnetoelectric coupling order parameters were the subject to controversies. We analysed neutron scattering, magnetisation, polarisation, dielectric constant, second harmonic generation (SHG) experiments and proposed a comprehensive model resolving the apparent contradiction between all these experimental results. The strength of theory is also to predict new properties. We showed that the long search for a reversal of the magnetic order by a switch of the polarisation is vain, since the later couples to P^2 and is thus insensitive to the polarisation sign. If such compounds are not fit to switch the magnetisation with an electric field, they however can be used to switch antiferromagnetism with an intense magnetic field, providing memories resilient to magnetic fields.

AUTHORS & REFERENCES

M.-B. Lepetit (ILL and Institut Néel, CNRS, Grenoble, France)
K. Singh, **N. Bellido** and **J. Varignon** (CRISMAT, CNRS-ENSICAEN, Caen, France)
C. Simon (ILL)
S. Pailhès (LLB and IML University Claude Bernard Lyon I, Villeurbanne, France)
A. De Muer (LNCMI, CNRS-UJF, Grenoble, France)

[1] K. Singh, M.B. Lepetit, C. Simon, N. Bellido, S. Pailhès, J. Varignon and A. De Muer, J. Phys. Condens. Matter 25 (2013) 416002
[2] E.F. Bertaut and M. Mercier, Phys. Letters 5, 27 (1963); E.F. Bertaut, R. Pauthenet and M. Mercier, Phys. Letters 7 (1963) 110
[3] A. Muñoz *et al.*, Phys. Rev. B 62 (2000) 9498
[4] P.J. Brown and T. Chatterji, J. Phys. Condens. Matter 18 (2006) 10085
[5] D. Fröhlich *et al.*, Phys. Rev. Letters 81 (1998) 3239; M. Fiebig *et al.*, Phys Rev. Letters 84 (2000) 5620
[6] S. Pailhès *et al.*, Phys. Rev. B 79 (2009) 134409

The magnetic transition of $YMnO_3$ occurs around T_N=74 K. Neutron diffraction measurements [2–4] showed that the structure is antiferromagnetic (AFM) with moments in the ab-plane. Following Bertaut *et al.* [2], Muñoz *et al.* [3] proposed for the antiferromagnetic order the totally symmetric (Γ_1) solution of the $P6_3cm$ group, pictured as V_1 in **figure 2**. More recently, a neutron diffraction and polarimetry analysis performed at ILL [4] showed that the ac/bc-mirror planes are lost and that the magnetic order should rather be, either a combination of V_2 and V_1 ($P6_3$ group), or of W_1 and W_2 ($P6'_3$ group). Finally, in a SHG experiment, Fröhlich *et al.* concluded to a very different order (W_2) associated with the $P6'_3cm'$ magnetic group [5]. Let us note that, while Bertaut *et al.* [2], and Muñoz *et al.* [3] performed a full symmetry analysis, Brown and Chatterji [4], as well as Fiebig *et al.* [5] only considered the Γ_1 solution of the tested symmetry groups. One should however remember that while P behaves as the density matrix and thus belongs to the Γ_1 representation, the magnetic order (spin part of the wave-function) can belong to any of the irreducible representations of the magnetic symmetry group.

We performed additional measurements: P and ε versus temperature and magnetic field, as well as precise magnetic measurements on a SQUID magnetometer at low magnetic field. Indeed, S. Pailhès observed in a non-polarised neutrons scattering experiment, a Bragg peak that was associated with a ferromagnetic (FM) component [6]. After carefully checking out the possibility of magnetic impurities, we confirmed the existence of such a component.

Figure 1

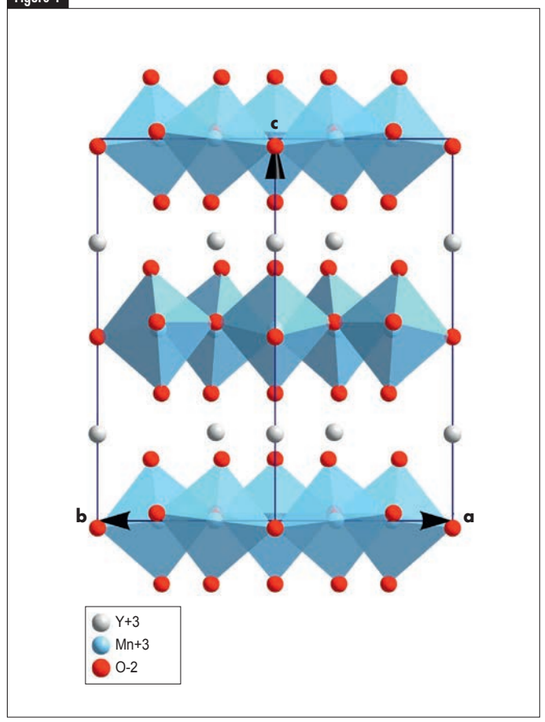

Schematic representation of the $YMnO_3$ compound.

Let us summarise what we learned from the analysis of experimental facts.

- ε and the AFM Bragg peak intensity present similar temperature dependence, showing the existence of a magneto-electric coupling between the AFM and the ferroelectric (FE) orders.
- ε does not diverge at T_N, excluding a linear magnetoelectric coupling. Therefore, the AFM and FE (polarisation) order parameters cannot be in the same representation and thus the magnetic order cannot be in the Γ_1 representation of its group.
- There is a weak FM component along the *c*-axis. Let us notice that the effect of the spin-orbit on a V_1 magnetic order would induce such a component.
- AFM and FM orders are not linearly coupled, since they present different temperature behaviors at T_N.

Can we find a model able to account for all those experimental facts plus the SHG results?

The answer is yes if one abandons the ac/bc-mirror planes. Indeed, we showed that only one magnetic group is compatible with these requirements, the $P6'_3$ group (first guessed by Brown and Chatterji [4]), however not associated with the Γ_1 representation (W_1+W_2), but with V_1 plus a small component of V3 (Γ_4 representation).

We also showed that the SHG selection rules, associated with the $P6'_3$ group and V_1+V_3 magnetic order, predict a magnetic contribution to the in-plane component of the susceptibility, but not to the out-of-plane ones, in full agreement with the experimental data [5].

Finally we derived the long saught Landau theory for the magnetic phase transition. For it to be fully consistent, the transition must be driven by three order parameters: the AFM order (S^2 principal order parameter), and two secondary ones, the change in polarisation and the magnetisation.
The Landau equations are fully compatible with all the above experimental requirements, but also retrieve other experimental results such as the decrease in the polarisation at T_N or the linear relation between ε(T) and S^2(T).

The strength of theory is also to predict new properties. In the present case we showed that the long search for a reversal of the magnetic order by a switch of the polarisation is vain, since both magnetic orders couple to P^2 and are thus insensitive to its sign. On the contrary, the AFM and FM orders are switched simultaneously. For applications, this type of system cannot be used to switch the magnetisation with an electric field, but rather to switch antiferromagnetism with an intense magnetic field, providing memories resilient to magnetic fields.

Figure 2

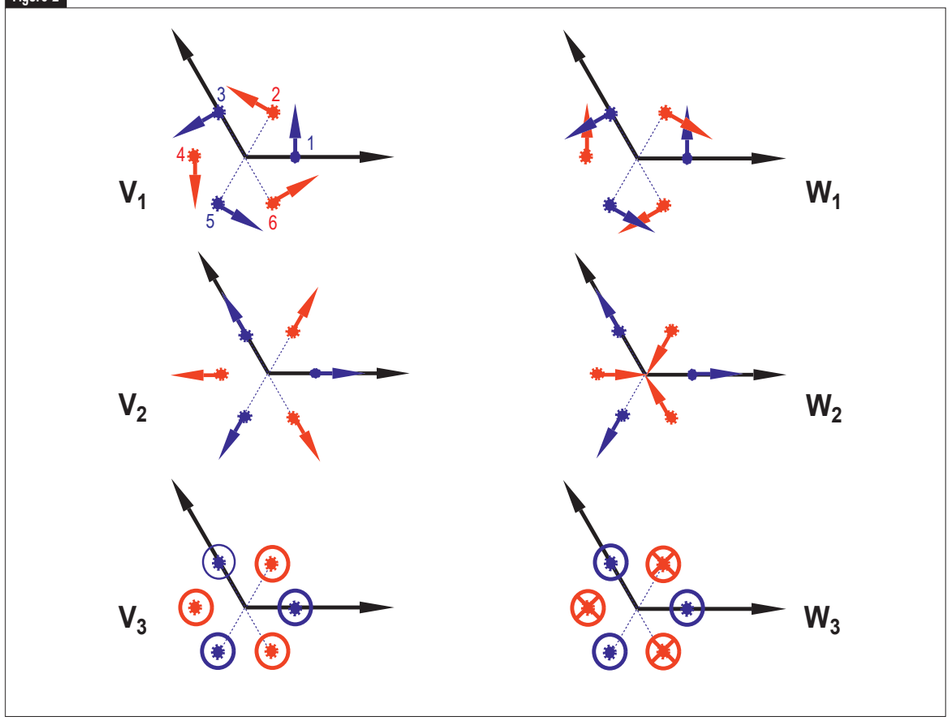

$YMnO_3$ possible AFM orders. The blue Mn sites are in the z=0 layer and the red sites in the z=1/2 layer.

THE ENDURANCE PROGRAMME

After the great success of the Millennium Programme, a new initiative to continue to upgrade ILL instruments and scientific infrastructure is being planned: the Endurance programme is built on the solid foundation and experience gained during the work carried out over the past years. The recently produced ILL 20/20 Endurance brochure [1] presents the detailed plan for the programme, which is shortly summarised in this article.

The ILL has led the world in neutron science for almost 40 years – a remarkable record that has been achieved by offering best-in-class instruments served by the brightest neutron source, and by attracting many of the most talented neutron scientists and technical staff to work with us. This, in turn, has meant that the instrument suite has had to evolve continuously by exploiting new technology – much of it developed in-house – to redefine the limits of what is measurable and offer new scientific opportunities.

The latest such development, stretching over more than a decade, is the Millennium Programme, which has delivered an increase of more than a factor of 25 in average instrument brightness for less than one year's budget. This has not only enabled us to increase the number of experiments and thus users that we can support, but has also opened up completely new avenues of science.

Recent achievements include the first *in situ* measurement of the structure of a fluid as it passes through a microfluidic cell, thus providing direct insights into key manufacturing processes. Also observed for the first time is the relaxation of magnetisation in single crystals of a single-molecule magnet, which has provided unique information relevant to its potential for data storage and quantum computing. However, there is still great potential to improve our facilities further by upgrading those instruments not yet boosted by the Millennium Programme.

The Endurance programme is dedicated to improving the performance, fitness and long-term potential of the ILL instrument suite. To achieve its scientific goals and open up new science, a challenging technical programme is being implemented to manage the design and construction of up to seven future world-leading instruments. In addition, seven existing instruments will be extensively modernised and four existing neutron guides completely re-designed.

The Endurance instrument vision cannot be separated from two ambitious companion programmes: NESSE – a vision for future sample environments, and BASTILLE – a new approach to data treatment. These will be put in place during the Endurance programme.

THE CHARTREUSE AND VERCORS ENSEMBLES

The existing four neutron guides concerned by these projects were installed just over 40 years ago. Their replacement by state-of-the-art neutron distribution systems will provide optimal experimental areas for four new instruments and will boost the performance of four other refurbished ones. The new guide systems will provide additional capabilities for the implementation of instruments that are under evaluation following the Scientific Council advice (Phase II), as well as better neutron beams for technical instruments used for advanced R&D on detectors and neutron optics.

In both the Vercors and Chartreuse projects (see **table 1**), a typical gain factor of two to four is expected from the guides installed upstream of each instrument depending on the instrument acceptance of the beam divergence.

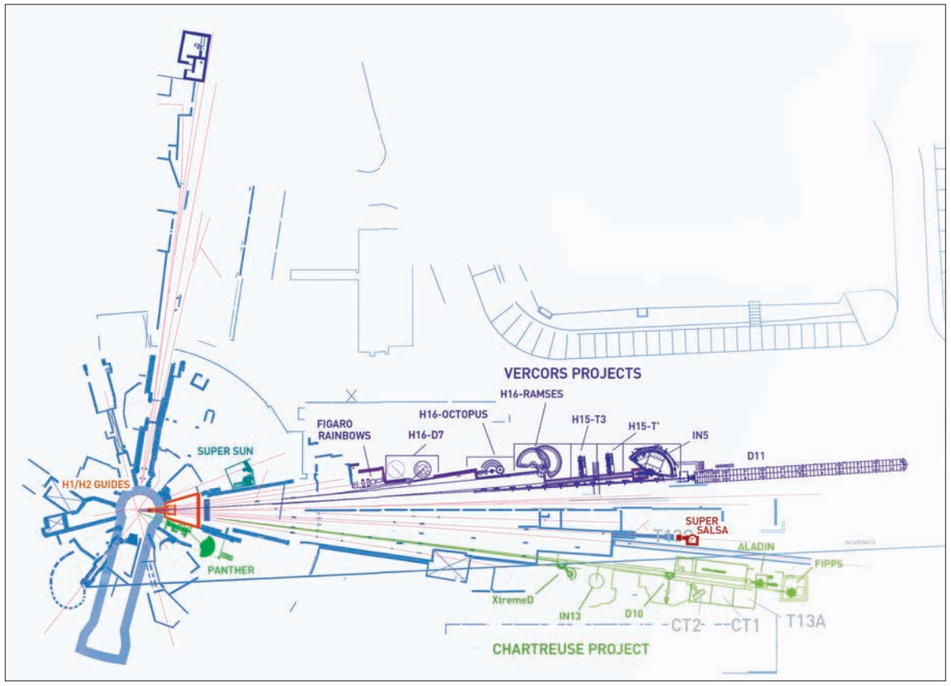

The position of the instruments once the entire programme (Phase I and Phase II) is completed.

Table 1

CHARTREUSE NEUTRON GUIDE H23 – H24	VERCORS NEUTRON H15 – H16
XtremeD: a dedicated guide will provide the high-intensity beam required	Ramses will take the place left by the IN6 decommissioning.
FIPPS: a dedicated area and casemate are provided	RAINBOWS–FIGARO: installation of the RAINBOWS and GISANS option on FIGARO.
D10: higher neutron flux for the upgrade of one of the ILL's most productive instruments.	IN5: extension of its incoming spectrum to shorter wavelengths and minimisation of the fast-neutron background.
IN13 (CRG): the modernised guide will provide the input for a refurbishment already investigated some years ago.	D7: better performance by optimising the sample–monochromator distance and an in-guide polarised beam.
FURTHER INSTRUMENTS: PHASE II PROJECTS UNDER EVALUATION	
ALADIN: a dedicated guide section will provide the required pure white beam.	OCTOPUS: the new outline of the H15–H16 guides will provide a position for this instrument.
TECHNICAL INSTRUMENTS	
T13 A/C: R&D for neutron optics. CT1/2: R&D for neutron detectors.	Irradiation facility: industrial applications T3: R&D for neutron optics (coating).

Instrument sites to be provided by Vercors and Chartreuse projects.

AUTHOR & REFERENCE

H. Schober (ILL)

[1] The pdf of the brochure can be downloaded from http://www.ill.eu/quick-links/publications/

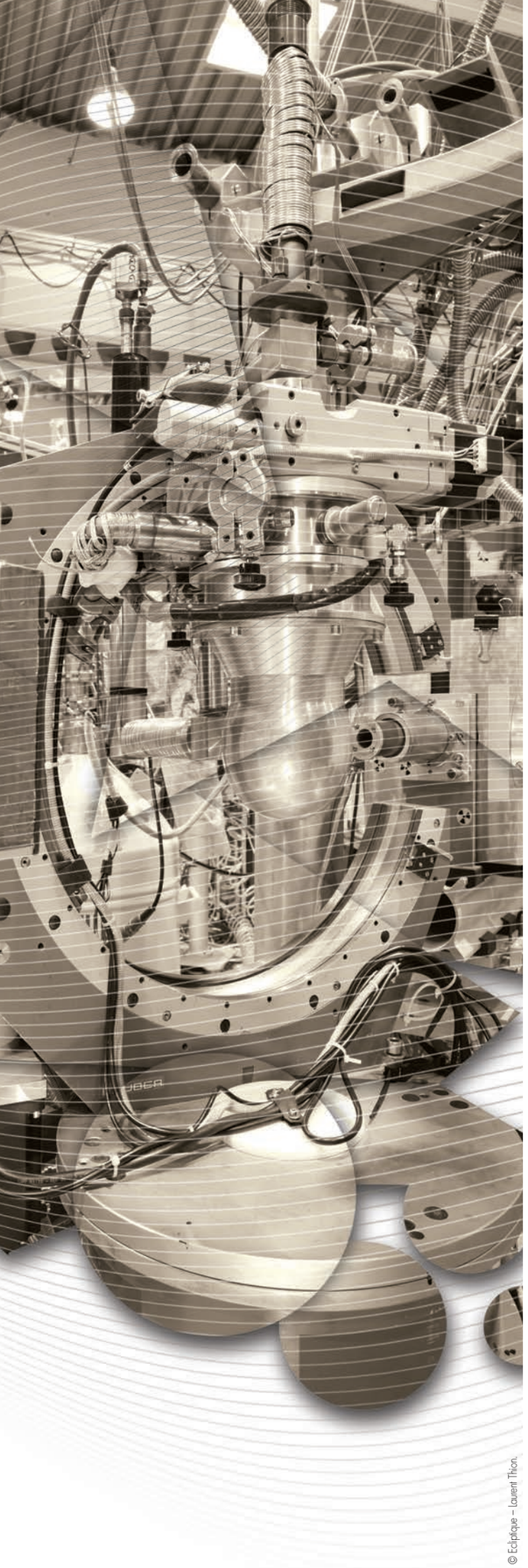

MILLENNIUM PROGRAMME
TECHNICAL DEVELOPMENTS

I have no doubt the Institute will remain at the cutting edge of neutron technology for at least the next decade.

The Millennium Programme has played a major role in enabling the ILL to retain its position as world leader in neutron science. Involving a total investment of 91 M€ over the period 2001-2014, the programme represents an extremely important part of the joint undertaking by the Associates and the Scientific Members to support the ILL's modernisation efforts.

As it approaches the end of this first phase of modernisation work, the ILL is beginning to take full advantage of the enormous benefits the Millennium Programme has brought in terms of science and user service. The instruments D33, LADI, IN11, IN12, D11, IN1-LAGRANGE, D17 and IN4 have all either been completely rebuilt or have benefited from a new guide, making it possible to improve instrument performance considerably with respect to flux, resolution and background. The CRG IN12 is now quite simply the best cold neutron three-axis spectrometer in the world. LADI is having a major impact in the field of structural biology. The spin-echo instrument IN11 has increased its flux considerably, thanks to its new guide. And last but not least, IN1-LAGRANGE now offers the chemistry user community an outstanding spectrometer which complements UV and IR spectrometers for the materials community.
In 2013, the backscattering spectrometer IN16B was commissioned and we are waiting for the first results to be compared to those of our competitors. The time-of-flight massive dynamic Q range small-angle diffractometer D33 is now fully operational; the first publications from this instrument are expected in the near future.
2014 will see the completion of ThALES - the ILL equivalent of the IN12 three-axis spectrometer - and the replacement of the H5 guide, which will deliver neutrons to IN15, D22, D16, SuperADAM and the future instrument WASP.

Work on preparing the next phase of the ILL modernisation programme, known as Endurance, is under way (see article on *p.74*). This new initiative began with the ILL 2020 Vision user meeting, which was held back in September 2010 and was attended by representatives of the user community. The programme has since been further developed in collaboration with the ILL's Scientific Council and the Instrument Subcommittee at various meetings over the course of the past few months. Endurance, which sets the scene for the next decade and continues the momentum of the Millennium Programme, has three important components: guides, instruments and infrastructure. In addition, in close cooperation with other research centres, data acquisition, processing and analysis will be also part of Endurance. Over the coming months, the teams of the Projects and Techniques Division (DPT) will be working with the Science Division on preparing the details of this ambitious project.

The DPT is also heavily involved in innovation. In the framework of a project supported by the European Commission and involving a number of other European large-scale infrastructures, the ILL is one of the first research centres to have implemented a scientific data policy that is perfectly in line with European guidelines in terms of the valuation of and access to scientific data. In the field of detectors, monochromators and guide alignment technologies, the ILL is at the forefront of innovation in neutron technologies. Polarisation analysis is another of the ILL's strengths, as can be seen from the regular requests we receive to supply our technology to other facilities (a detector for LLB Saclay, France, a monochromator for SNS, USA, polarisation analysis for ISIS, UK, and ANSTO, Australia). The Institute is leading efforts to develop a new boron-based technology for detectors, and other neutron facilities are also beginning to show an interest in implementing our data acquisition software NOMAD. All these projects clearly demonstrate the excellent neutron technology expertise available at the ILL.

In the coming years, the teams at the ILL will have to face the challenge of continuing to lead the world in neutron technology in the context of increasingly limited budgetary resources compared to those available to our competitors. In the past, the ILL has proved on many occasions that it is capable of meeting such challenges and I have no doubt that we will do so once again and that the Institute will remain at the cutting edge of neutron technology for at least the next decade.

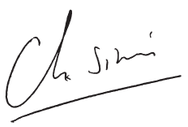

Charles Simon
Associate Director

Millennium Programme 2013

In 2013, work on the Millennium Programme was again extremely intense. The commissioning of the new backscattering spectrometer IN16B was completed and the instrument welcomed its first users. Progress was made with the construction of the new ILL three-axis spectrometer ThALES, which is due to be completed in 2014 and hopes to become the best instrument in its category. However, the bulk of the work being carried out during the long 2013-2014 shutdown is devoted to the guide hall ILL22 and its cold neutron guide H5, which will feed IN15, D22, D16, CRYOEDM, SuperADAM, a free position and WASP.

AUTHOR

C. Simon (ILL)

The commissioning of the backscattering spectrometer IN16B was completed in time for the arrival of its first users. The new and extremely challenging phase transformer is working perfectly and six full-size analysers are in the process of being installed.

The three-axis spectrometer **ThALES**, developed in collaboration with Charles University of Prague and with the support of our Spanish Scientific Member, will be constructed in the reactor hall. **Figure 1** shows the present state of the space reserved for this instrument, which we hope will prove to be the best in its category.

The bulk of the work scheduled for the long reactor shutdown (August 2013 - June 2014) is devoted to the **guide hall ILL22**, which will house IN15, D22, D16, CRYOEDM, SuperADAM, a free position and WASP, and its **guide H5**. The building has been extended, a new cooling system has been built for IN15 and WASP, and the guide itself is being completely rebuilt to increase the neutron flux on the instruments and reduce the background on the detectors. D16 will also benefit from no longer being positioned behind a monochromator, which was damaging for its performance. Each new instrument will have its own cabin for experimentalists.
To date, the building is finished (but still empty), the cooling system is ready and the casemates for the guides are under construction (**figure 2**). One of the major challenges facing the ILL teams in 2014 will be the construction of the H5 guide, which has a rather complex structure making it possible to optimise the flux on every instrument in the guide hall.

The wide-angle spin-echo machine **WASP** is due to be delivered in 2016. One important aspect of this instrument is the construction of the polarisation analyser, which is described in detail later in this report. The guide and the primary spectrometer are under construction. The primary cooling circuit and the supply network are ready to provide power and cooling to the giant precession coil, which is currently under construction (to be delivered early 2015).

The high-resolution spin-echo instrument **IN15** will also be completely rebuilt, with new precession coils which will take advantage of the power and cooling circuits mentioned earlier. The instrument will also benefit from the fact that there are no magnetic structures in the reconstructed guide hall. This will make it easier in future to tune the phase of the instrument and should increase the resolution in time.

2013 was a year of transition for the ILL's Millennium Programme, marking the start of a lot of new work. 2014 will be a year of achievements, with the delivery of guide hall ILL22 and its instruments.

Figure 1

The "hole" in the reactor hall, which will house the three-axis spectrometer ThALES.

Figure 2

Current state of the almost empty guide hall ILL22.

The upgraded IN12 instrument: a powerful cold neutron three-axis spectrometer

Following the completion of the H14 project and the extension of guide hall ILL7, the cold neutron three-axis spectrometer IN12 is back to successful user operation again. The primary spectrometer of IN12 has been upgraded over the last two years and the instrument has been moved to a new position.

The last two cycles in 2012 were used to commission and test new components. A gain in flux of about an order of magnitude at the sample position has been achieved compared to the previous instrument and IN12's wavelength range now extends far into the "warmish" region. The upgraded IN12 therefore retains its position as one of the best cold three-axis spectrometers in the world.

AUTHORS

K. Schmalzl and **W. Schmidt** (Jülich Centre for Neutron Science, Germany)
S. Raymond and **B. Vettard** (CEA Grenoble, France)
T. Brückel (Jülich Centre for Neutron Science and PGI, Germany)

The new experimental area of IN12.

Three-axis spectrometers (TAS) have been an essential part of a reactor's instrument suite since the very beginnings of neutron research. The study of dynamics and elementary excitations (low energy excitations in the case of cold neutron TAS) allows insight into fundamental processes in modern materials. In recent years, substantial progress has been made in particular in neutron optics and many TAS have implemented new components to improve their performance. With the refurbishment of the H14 guide system at the ILL, IN12 has also upgraded its primary spectrometer, giving the instrument a new lease of life.

As the previous position of IN12 is now occupied by D33, IN12 has moved to the Chartreuse side of the guide hall ILL7, about 115 m away from the cold source. IN12 is now located at an end position on a newly installed guide with m=2 coating. This means there is more divergence in the guide than was previously the case. To compensate for the curvature of the guide, the outer side is coated with m=2.4. The guide widens vertically from 105 mm to 140 mm to match the mosaicity of the new monochromator crystals. To be able to focus on small spots (1-2 cm^2) at the sample position, we use the virtual source concept: the last 8 m of the guide focus horizontally down from 45 to 20 mm in width. At the focusing guide-end, the coating increases to m=3.2. To optimise the transport of the neutrons to the sample position, we use a new double-focusing PG monochromator, comprising 11 x 11 crystals, with a total size of 16 x 20 cm. A velocity selector in the guide ensures a clean beam, preventing higher order reflections from the monochromator and reducing the background at the sample position. Directly behind the velocity selector, a guide changer with a normal guide element and a polarising cavity guarantees an easy-to-use polarisation set-up.

Thanks to this upgrade, the new IN12 can now access incident wavelengths from 1.4 to 6.3 Å, corresponding to a k_i of 1 up to about 4.8 $Å^{-1}$, and incident energies from 2 up to about 42 meV. In this way, the wavelength range extends into the thermal region compared to the old IN12, where we were limited to a wavelength of 2.3 Å in the cold wavelength range (**figure 1**). The same figure also shows a gain in flux of about a factor of 10 for a typical wavevector of 2 $Å^{-1}$. Overall we have also doubled the accessible Q-range. A scan performed with the same sample at the old and the new IN12 and then fitted in the same way confirms this gain in flux (**figure 2**).

An important feature is the availability of polarised neutrons. The guide changer with the polarising cavity is simple to use and results in a flipping ratio at the sample position of 20 – 27, depending on the wavelength used.

One definite advantage of the upgraded IN12 is its high flux, giving us more and better results. However, the higher energy transfers that are now achievable and the larger accessible Q-range also open up new possibilities which were not available with the previous instrument. With this upgrade, IN12 has become a modern and powerful instrument. Following its shutdown at the end of 2010 and after 2 years of upgrade work, the new IN12 successfully restarted user operation at the end of 2012.

IN12 is operated by the Forschungszentrum Jülich as a CRG-B instrument at the ILL in collaboration with the CEA Grenoble. Our thanks go to the engineers and technicians from Jülich as well as from the ILL who contributed to the success of this upgrade project.

Figure 1

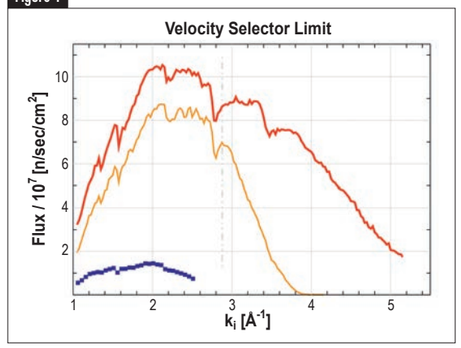

Neutron flux measurements performed in 2012 for the new IN12 with the double-focusing monochromator (red) and velocity selector (orange), compared to the old IN12 (blue).

Figure 2

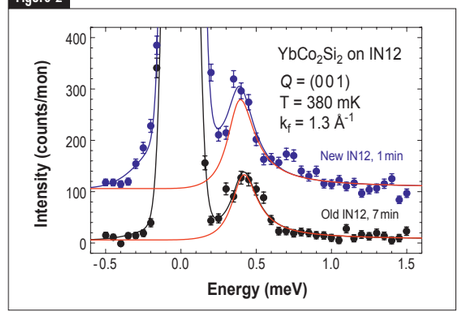

Old vs. new IN12: Measurement of the same sample shows a gain for the integrated inelastic peak intensity by a factor of 9-11. (Spectra show the same background and are shifted in intensity by about 100 counts. Sample courtesy of O. Stockert, MPI Dresden).

Co/Ti supermirror analyser with large detector area coverage for WASP

At the ILL, m=2.8 Co/Ti supermirrors are manufactured on a large scale for polarising neutrons. Over the last four years, more than two thousand mirrors have been successfully produced with the aim of constructing the world's largest analyser for the new spin-echo instrument WASP. For the commissioning of the instrument in 2015, we expect to complete the production of 3330 mirrors to cover the first 90° of the analyser angle.

P. Courtois, **T. Bigault**, **V. Gaignon**, **A. Vittoz** and **G. Delphin** (ILL)
D. Bourgault (Néel Institute, CNRS, Grenoble, France)

[1] P. Fouquet, B. Farago, K.H. Andersen *et al.*, Rev. Sc. Instr. 80 (2009) 095105
[2] J.R. Stewart, P.P. Deen, K.H. Andersen, H. Schober, J.F. Barthelemy *et al.*, Journ. Appl.Cryst. 42 (2009) 69

Ferromagnetic Co/Ti supermirrors provide an opportunity to build efficient spin analyser devices for cold neutron instruments. They consist of alternating layers of cobalt and titanium with graded thicknesses varying from 50 Å to 600 Å, deposited on a glass or silicon substrate. A Co/Ti supermirror only reflects the neutron spin component that is parallel to the magnetic field applied to the mirror (the spin-up component). Spin-down neutrons are not reflected but are transmitted into the layers. To absorb the transmitted neutrons before they reach the substrate, an anti-reflecting layer of Gd/Ti is introduced between the supermirror and the substrate. Such absorbing layers make it possible to maximize the angular and wavelength range for the spin-up neutrons.

Co/Ti supermirrors with anti-reflecting layers will be used to build the large polarisation analyser for the new spin-echo instrument WASP. The analyser design, based on Schärpf-type C-shaped benders and described in [1], is inspired by the design of the D7 analyser upgrade [2]. With a total area of 636 m^2, which is equivalent to the area of 3 tennis courts, it is composed of 8800 m=2.8 Co/Ti supermirrors, double-side coated on borated float glass. The full-scale analyser covers a large solid angle of 0.197 steradians for a horizontal scattering angle of 240°. The new instrument WASP will be equipped with the largest neutron-spin analyser in the world!

Supermirrors are produced at the ILL using the magnetron sputtering machine Pi (**figure 1**). An m=2.8 Co/Ti supermirror consists of 500 layers of Co/Ti and 41 layers of Gd/Ti. Multilayers are deposited on 0.2 mm-thick glass substrates by DC magnetron sputtering at a low argon pressure of approximately 10^{-3} mbar. The substrate dimensions of 254 x 141 x 0.2 mm^3 were chosen to fit the instrument geometry and to maximise the number of substrates coated per process, making it possible to produce 12 one-side coated supermirrors per day.

Figure 1

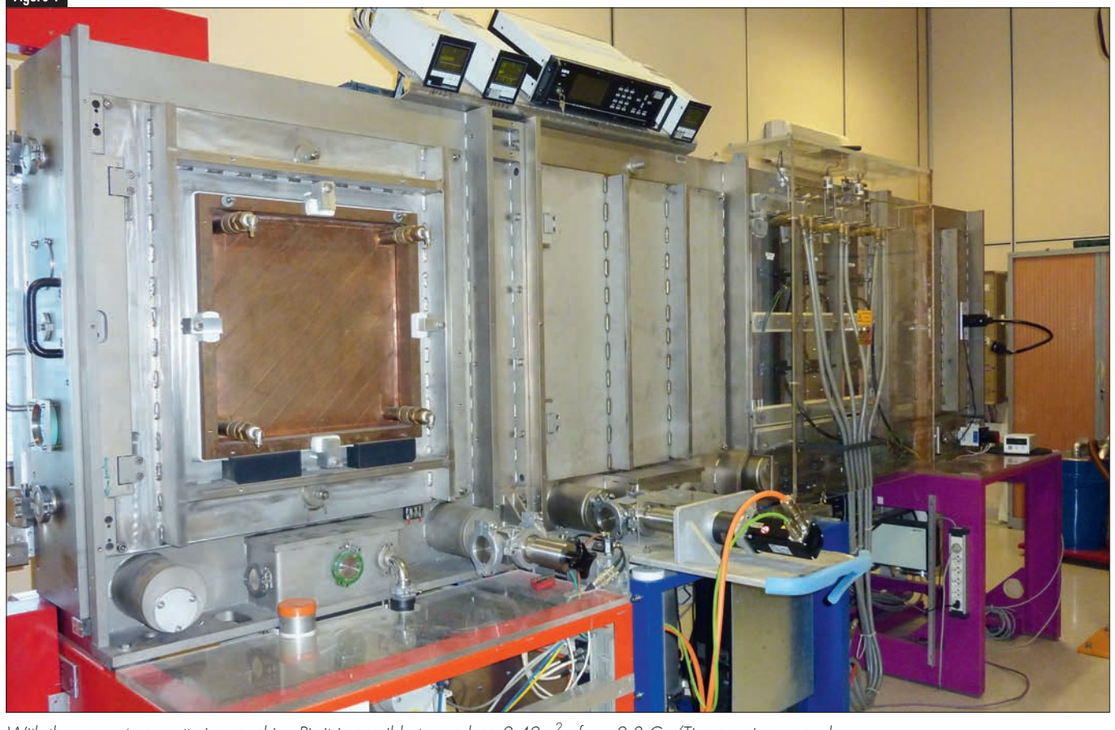

With the magnetron sputtering machine Pi, it is possible to produce 0.42 m^2 of m=2.8 Co/Ti supermirrors per day.

The magnetic properties of m=2.8 Co/Ti supermirrors were investigated using a vibrating sample magnetometer at the CNRS, Grenoble (**figure 2**). The easy axis of magnetisation is parallel to the direction of the substrate movement during the deposition process. Such measurements indicate that an external magnetic field of at least 40 mT must be applied on the mirror in order to reach magnetic saturation.

Each production batch is checked using the ILL neutron reflectometer T3 at a neutron wavelength of 7.5 Å. **Figure 3** shows the performance of a typical supermirror produced recently for the WASP project. With a neutron reflectivity of the spin-up component of better than 70 % and polarisation efficiency higher than 90 %, these Co/Ti supermirrors demonstrate high performances for polarisation analysis.

After neutron characterisation, the mirrors will be mounted into special cassettes, which hold them with a bending radius of about 7 m (**figure 4**) and a spacing of 1 mm between adjacent mirrors. Each cassette contains 37 mirrors and corresponds to a horizontal scattering angle of analysis of 1° from the sample position. The cassettes will then be installed in a suitable magnetic device which provides a magnetic field strong enough to maintain full magnetisation of the supermirrors [1].

Today enough mirrors have been produced to cover about 55° of the analyser. To facilitate operations and improve the reliability of the process, a new programmable logic controller was installed on the Pi machine in 2013. As a direct result, we expect to increase the production rate by 20% in the coming years. Instrument commissioning is due to take place at the end of 2015, with 90° of analyser coverage.

Figure 2

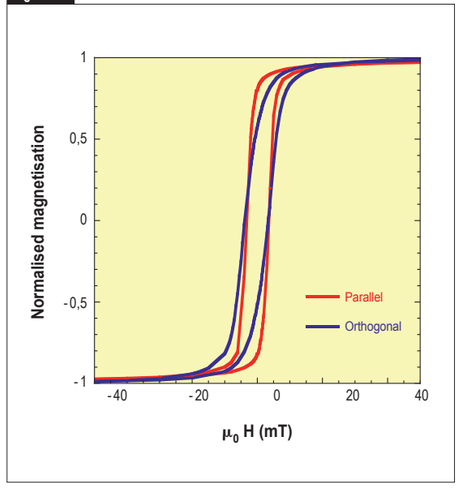

Magnetic hysteresis of a typical m=2.8 Co/Ti supermirror measured parallel and orthogonal to the direction of the substrate movement during the sputtering process.

Figure 3

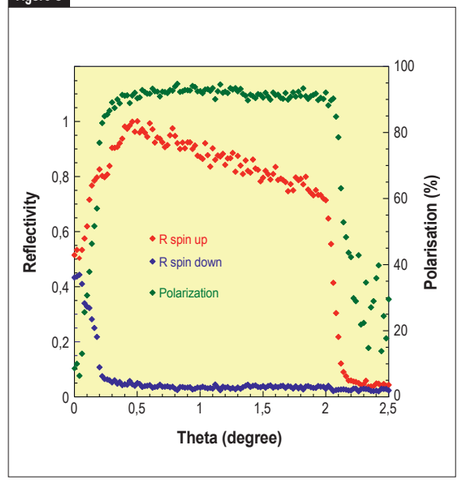

Typical neutron reflectivity with spin parallel and antiparallel to the magnetic field applied to the mirror and resulting polarisation of an m=2.8 Co/Ti supermirror. The measurements were performed on T3 at a wavelength of 7.5 Å.

Figure 4

An individual analyser cassette contains 37 mirrors and covers an angle of 1°.

0.1 K closed-cycle four-circle dilution cryostat on D10

The full determination of magnetic ground states is a key point in understanding the fundamental properties of magnetic materials. The determination of the magnetic structure factors requires access to the three dimensions of reciprocal space using single-crystal four-circle geometry. A four-circle dilution cryostat that avoids the influence of gravity by using a capillary dilution chamber was developed [1,2] for experiments below 2 K. This system, where the sample was cooled down to 110 mK by a gravity-insensitive dilution refrigerator, was successfully used on D10 for several years. However, it did present certain disadvantages: autonomy was limited to a few days, the re-distillation of the ^{3}He was done off-site, and temperature stability was difficult to maintain when rotating the phi shaft. To overcome these difficulties, a completely new closed-cycle dilution cryostat providing four-circle diffraction accessibility has been developed.

THE GRAVITY-INSENSITIVE DILUTION SYSTEM

A dilution refrigerator is commonly used to reach very low temperatures. In the so-called mixing box, where the cooling power is available, the two phases of the ^{3}He-^{4}He mixture are separated by gravity, the lighter ^{3}He-rich phase being above the heavier ^{3}He-poor phase. For applications where the system has to support a random position on the earth or even for space applications, a gravity-independent dilution refrigerator can be made by directly mixing the two isotopes in narrow capillaries.

For D10, in order to cope with the 4-circle geometry, we adopted the original system that was developed for space applications and successfully used in the Planck mission [3]. In a conventional dilution system, only the ^{3}He isotope circulates. The interface between the concentrated and the diluted phases is localised by gravity within the mixing chamber. In our cryostat, we apply the closed-cycle dilution refrigerator principle. The key idea of the dilution process is to inject and mix both helium isotopes through two capillaries in a Y-junction, and to recover the mixture through a third capillary.

At low temperature (< 0.1 K), the dilute phase has a finite solubility of ^{3}He of 6.6 %. If the ^{3}He concentration exceeds this value, not all ^{3}He is diluted and some stays in the ^{3}He-rich phase, forming ^{3}He droplets. In this design, the ^{3}He-rich phase droplets fill the cross-section of the capillaries, where the capillary forces play the role of gravity.

THE ISOTOPE MIXTURE SEPARATION SYSTEM

Once mixed in the dilution refrigerator, the ^{4}He and ^{3}He are pumped at low pressure and processed in the isotope separation system. The continuous separation process is still based on conventional dilution at about 0.8 K, where the ^{3}He concentration in the vapour is about 95%. In this process, originally developed for space applications [4], the ^{4}He is extracted by a fountain pump exploiting the unique superfluid properties of this isotope. The fully automated gas-handling system shown in **figure 2** was developed in order to operate the isotope separation system. The flows required for the dilution refrigerator (**figure 1**) are regulated by two mass flow controllers (about 20 cc/min ^{3}He and 40 cc/min ^{4}He). The gases are then recompressed to the required dilution-refrigerator inlet pressure of about 2 bar.

Figure 1

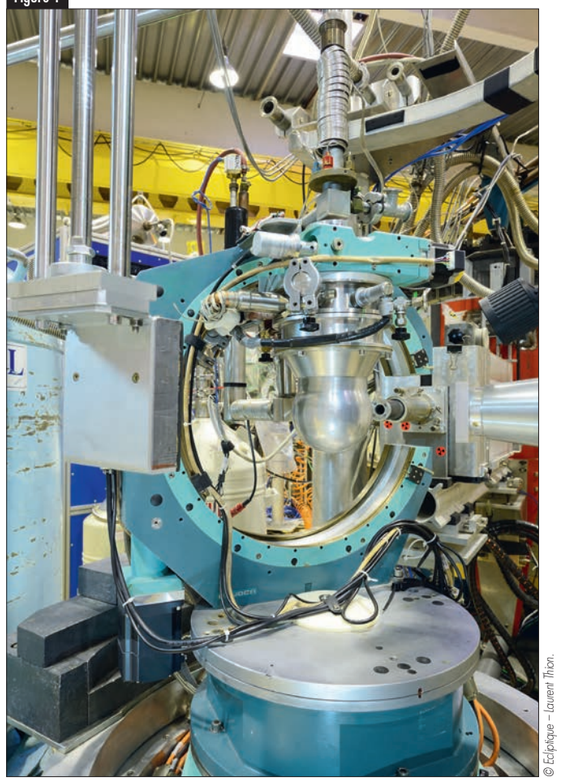

© Ecliptique – Laurent Thion.

Photo of the dilution refrigerator mounted on the cradle of D10.

FIRST RESULTS

The new system was commissioned in 2013 and three diffraction experiments were conducted on problems requiring access to more than one plane of reciprocal space at temperatures below 1.6 K. One of the investigations performed was the study of the long-range order in bond-disordered spin ½ antiferromagnetic Heisenberg chains. $Cu(C_5H_5N)_2Cl_2$ belongs to the family of S=1/2 chain compounds, where bond disorder, due to a small random variation in the Cu-X-Cu bond angle, leads to a random singlet phase. This phase is crucial for superexchange interactions between Cu^{2+} ions. The magnetic ground state was studied in order to understand this bond disorder. The $Cu(C_5H_5N)_2Cl_2$ compound presents an incommensurate antiferromagnetic state below T_N=1.15 K with a propagation vector k=[½ 0.4 ½]. A set of magnetic and nuclear Bragg reflections was measured during the allocated beamtime.

As shown in **figure 3**, the new dilution system is capable of maintaining a base temperature of 107 mK while rotating the sample. Thanks to this excellent temperature stability, it was possible to measure the temperature dependence of the magnetic reflection and determine a magnetic transition at T_N = 1.15 K (**figure 4**).

ACKNOWLEDGMENTS

We would like to thank M. Thede and E. Ressouche for providing their preliminary results.

Figure 3

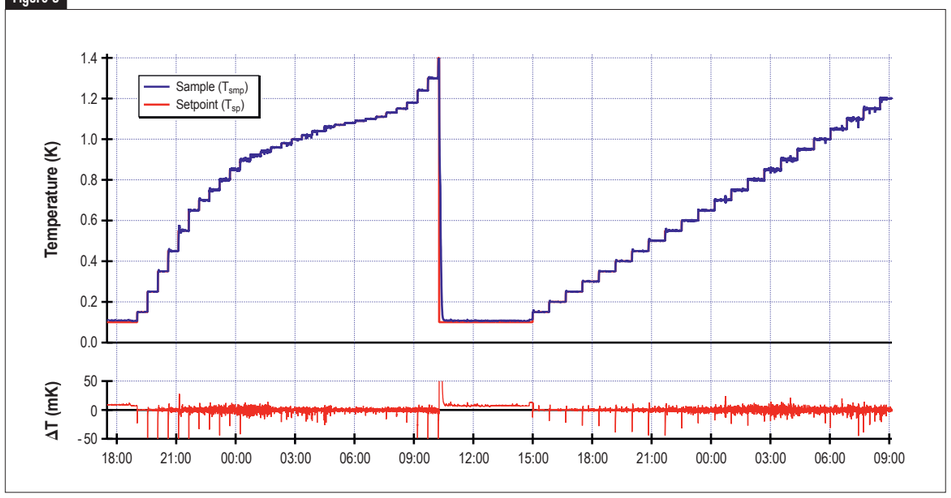

Temperature stability of the new closed-cycle dilution system over several days. The inset shows temperature steps performed during the experiment.

Figure 2

© Ecliptique – Laurent Thion.

Photo of the complex automated gas-handling system of the closed-cycle dilution system on D10.

Figure 4

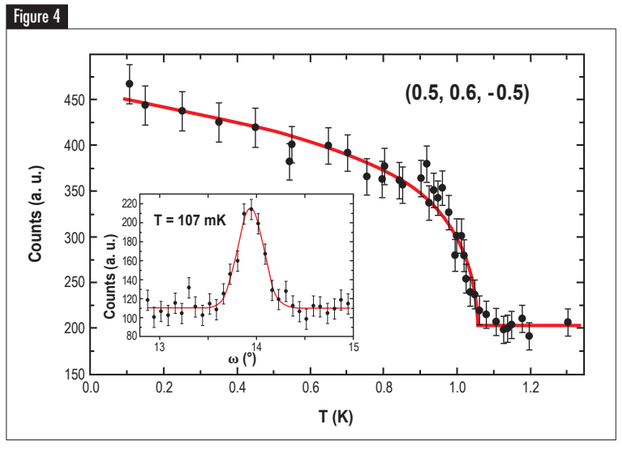

Temperature dependence of the (0.5 0.6 -0.5) magnetic reflection.
***Inset:** omega scan of the reflection measured at 107 mK.*

AUTHORS & REFERENCES

J. Allibon, **N. Belkhier**, **P. Decarpentrie**, **E. Lelièvre-Berna**, **P. Martin**, **B. Ouladdiaf** and **X. Tonon** (ILL)
Ph. Camus, **G. Donnier-Valentin**, **G. Garde**, **Y. Launay** and **O. Tissot** (Institut Néel, CNRS, Grenoble)

[1] A. Benoît and S. Pujol, Physica B 169 (1991) 457
[2] A. Benoît, M. Caussignac, and S. Pujol, Physica B 197 (1994) 48
[3] S. Triqueneaux, L. Sentis, Ph. Camus, A. Benoit and G. Guyot, Cryogenics 46 (2006) 288
[4] Ph. Camus *et al.*, "*Status of the Closed-Cycle Dilution Refrigerator Development for Space Astrophysics*", LTD-15 conf. proc. (2013), accepted for publication in JLTP

Slow-neutron mirrors from holographic nanoparticle-polymer composites

Neutron optics and the neutron scattering and spectroscopy methods into which it has evolved have long been key techniques for fundamental and condensed-matter physics. In view of the number of existing neutron research centres and the effort put into these and forthcoming facilities, it is essential that neutron-optical techniques be further developed alongside more well-established methods. To push this development forward, we have introduced holographic nanoparticle-polymer composite gratings of unprecedented quality and efficiency as optical elements for slow neutrons.

Neutron optics theory is based on the one-particle Schrödinger equation, which contains the optical potential for a particular material or, equivalently, the neutron refractive index at a certain neutron wavelength. Provided we can tune the value of the refractive index for neutrons and provided we can also imprint refractive-index structures on to materials, diffractive neutron-optical elements become feasible.

A simple one-dimensional grating structure - periodically modulated along a single direction - can be characterised by a modulated refractive index.

The most common grating structures in neutron optics are probably crystals, which are used in a variety of devices, such as monochromators, wavelength analysers, polarisers and beam splitters for neutron interferometry. However, for cold and very cold neutrons, the grating period of crystals is usually much too small. As an alternative, artificial structures are used that offer a wide range of production processes and available materials (see for instance [1-3]). In addition to techniques such as sputter-etching and lithography, artificial grating structures can also be produced by optical holography, where signal and reference light beams are superposed at the position of a photosensitive recording material held between two glass slides, as shown in **figure 1**. This superposition results in a periodic light-intensity pattern in the recording material which modulates the density of a one of its ingredients, for example via an intensity-dependent photo-polymerisation process. The resulting hologram can be used as neutron diffraction grating (**figure 2**).

We use nanoparticle-polymer composites as recording materials. The embedded nanoparticles have an average core diameter of about 13 nm with a size distribution of approximately ± 5%. The nanoparticle sol is dispersed in a (meth)acrylate monomer. A photoinitiator is added to enable the monomer to polymerise on illumination with light.

Figure 1

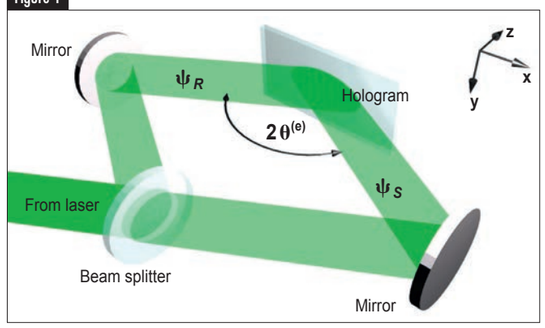

Two coherent-plane s-polarised light waves (signal and reference beams ψ_S and ψ_R, respectively) are superposed to interfere within the recording material. Each beam encloses the (external) incidence angle $\theta^{(e)}$ with the sample surface normal. The resulting light-intensity pattern therefore exhibits a sinusoidal modulation with a period Λ proportional to the light wavelength and inversely proportional to sin $\theta^{(e)}$.

Before recording, the photoinitiator, the monomer and the nanoparticles are homogeneously distributed in the sample material. Thanks to the photoinitiator, the light-intensity pattern triggers polymerisation in the bright sample regions. This process consumes monomers,which diffuse from dark to bright regions. As a consequence, the nanoparticles move from bright to dark regions, producing an approximately sinusoidal nanoparticle-concentration pattern, which acts as neutron diffraction grating.

One major advantage of nanoparticle-containing materials is their optical quality and versatility [4], due to the wide range of possible isotopes that can be embedded to select the value of the refractive index. For instance, holographic gratings with superparamagnetic nanoparticles could potentially be used as polarising beam splitters for cold neutrons. Due to the interplay of nuclear and magnetic interactions, such gratings could act as mirrors for one neutron spin state, while being virtually transparent for the other.

Figure 3 shows the results of neutron diffraction experiments carried out at the very cold neutron beam port of PF2 with free-standing NP-polymer film gratings. Here, the glass plates used for preparation and recording are coated with silane so that they can be easily removed from the surface of the polymer sample after recording, thus reducing incoherent scattering and neutron absorption.

This type of free-standing film grating with a periodicity of 0.5 µm, 100 µm thickness and 20 vol% SiO_2 nanoparticle concentration was shown to exhibit 90% reflectivity, *i.e.* mirror-like behaviour, for a neutron wavelength of about 4.1 nm [5].

Figure 2

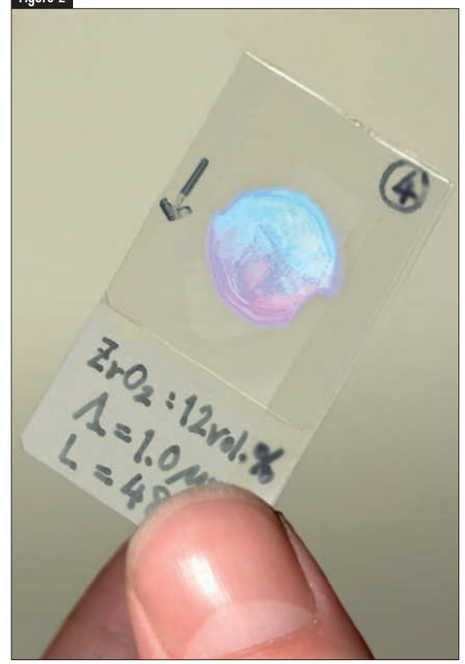

Holographic ZrO_2 nanoparticle-polymer composite grating diffracting light from a lamp. The grating periods and thickness typically range from 300 to 1000 nm and from 50 to 150 µm, respectively. The sample diameter ranges from 1 to 3 cm. The long-term mechanical stability of the holograms over several years has been confirmed by regularly checking the properties of samples with light.

Figure 3

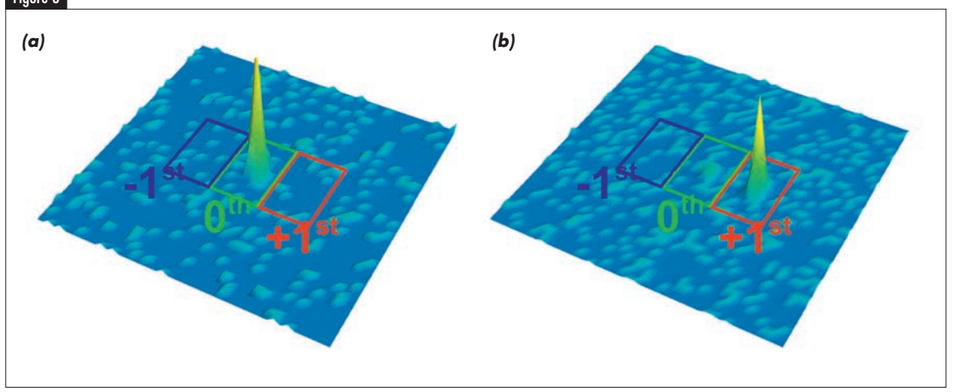

(a) *Detector image of the diffraction pattern of a free-standing SiO_2-nanoparticle film grating far from the Bragg angle θ_B (as given by $\lambda = 2\Lambda \sin\theta_B$). The neutron beam is transmitted.* ***(b)*** *The same grating rotated to the Bragg angle θ_B. Fulfilling the Bragg condition, the grating diffracts nearly all the intensity to the +1st diffraction order, thus exhibiting mirror-like reflectivity [5].*

AUTHORS & REFERENCES

J. Klepp and **M. Fally** (University of Vienna, Austria)
P. Geltenbort (ILL)
C. Pruner (University of Salzburg, Austria)
Y. Tomita (University of Electro-Communications, Tokyo, Japan)

[1] H. Rauch and S.A. Werner, Neutron Interferometry, Clarendon Press, Oxford, UK (2000)
[2] F. Pfeiffer, C. Grünzweig, O. Bunk, G. Frei, E. Lehmann and C. David, Phys. Rev. Lett. 96 (2006) 215505
[3] M. Trinker, E. Jericha, R. Loidl, and H. Rauch, Nucl. Instrum. Methods A 586 (2008) 124
[4] N. Suzuki, Y. Tomita, and T. Kojima, Appl. Phys. Lett. 81 (2002) 4121
[5] J. Klepp, C. Pruner, Y. Tomita, K. Mitsube, P. Geltenbort and M. Fally, Appl. Phys. Lett. 100 (2012) 214104

A digital constant fraction discriminator for fast timing studies in the picosecond range

Over the course of two reactor cycles, the EXILL measurement campaign provided the ideal test bench for the development of a new digital constant fraction discriminator implemented in a dedicated FPGA. The new hardware offers a fast algorithm for determining on-line the arrival time of an event with a time resolution in the tenth-of-a-picosecond range. The results obtained with our new digital electronics are comparable to those from equivalent analogue systems.

AUTHORS & REFERENCES

P. Mutti, **E. Ruiz-Martinez**, **T. Mary**, **J. Ratel** and **F. Rey** (ILL)

[1] CAEN, http://www.caen.it (2010)
[1] J.M. Régis *et al.*, Nucl. Instr. and Meth. A 622 (2010) 83

WHY A DIGITAL CONSTANT FRACTION DISCRIMINATOR?

Thermal or cold neutron capture on different fissioning systems is an excellent method for producing a variety of very neutron-rich nuclei. Since neutrons at these energies bring to the reaction just enough energy to produce fission, the fragments remain neutron-rich due to negligible neutron evaporation, thus allowing detailed nuclear structure studies on exotic nuclei. The de-excitation of nuclear excited states takes place on a timescale ranging from a few femtoseconds to up to several nanoseconds or more. Although longer lifetimes can be measured using fast digitizers with sampling frequencies of 1 or 2 GHz, it is more complex to obtain time resolution in the picosecond range. The conventional approach consists of using a number of analogue constant fraction discriminators (CFD) to determine the start and stop pulses, and time-to-amplitude converters (TAC) to measure the time difference between them. It is easy to see how the complexity of the setup together with instabilities in the analogue electronics might produce errors in the time determination

THE DIGITAL APPROACH

The incentive for designing a digital CFD is the possibility of producing very accurate pulse-time information. In the ideal case, this signal is precisely related in time to the occurrence of an event, thus eliminating the amplitude-dependent time walk. In order to provide an alternative to the standard analogue approach, we have developed a new real-time digital CFD system. The goal was to maintain the excellent performances of the TAC, capable of time resolution in the 10 ps range. Our design, which is fully implemented in hardware, does not add any dead time to the acquisition chain. The system consists of two main elements: a number of digitizers to match the required number of channels and a digital CFD card providing a real-time CFD algorithm for timing accuracy. A CAEN V1751 (8 channels, 10 bits, 1 GS/s) waveform digitizer [1] samples the analogue signal from the detector. Since the digitizer has several memory buffers for the trigger signals, the acquisition can take place without any loss of events, irrespective of their frequency and distribution, at least until the readout rate allows the buffer memory to be emptied. Each channel has an SRAM memory buffer with independent read-write access divided into 1 to 1024 buffers of programmable size. The board houses a daisy-chain optical link capable of transferring data at 80 MB/s. The digital CFD board, shown in **figure 1**, consists of a VME64X-configurable high-density I/O connection carrier board based on the latest Xilinx Virtex-6T FPGA and including 1 GB of DDR3 shared memory. The board is the result of a joint development project between the company loXoS in Switzerland and the ILL. Using the board's edge-to-edge interconnection solution, which provides full PCB front-end area utilisation, we are able to communicate with the optical link of the digitizers using the CAEN proprietary protocol CONET2 and to read out the data stored in the circular buffers of the flash ADC at a very high event rate. The main purpose of the digital CFD board is to perform a specific CFD algorithm on the sampled pulse shape to obtain accurate timing in the ps range. In this way, only the digitizer's time-stamp and the calculated event arrival time are stored in the event-mode data flow, thus reducing considerably the amount of recorded data.

Figure 1

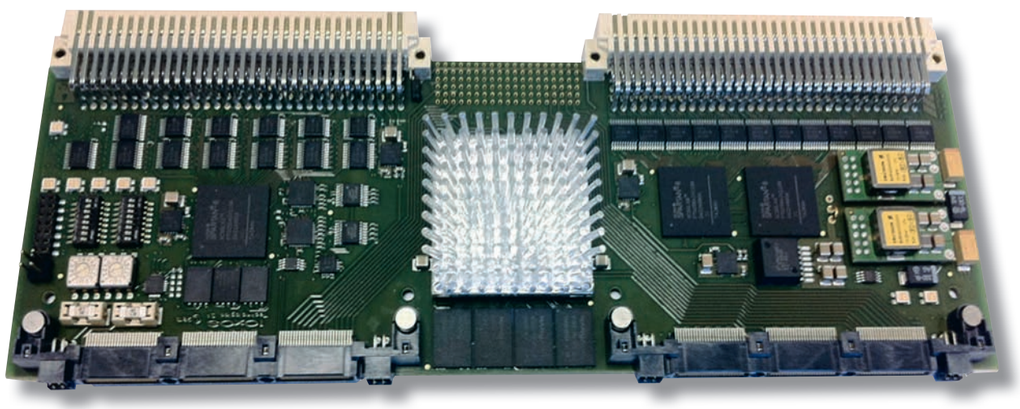

The digital CFD board, a joint development project between the Swiss company loXoS and the ILL.

FIRST RESULTS

The left part of **figure 2** shows the results obtained using a pulse generator to reproduce the detector pulses. By sending the same pulse into two different channels of the acquisition chain, it was possible to evaluate the intrinsic time resolution achievable with the adopted electronics and CFD algorithm. After tuning the algorithm's parameters, we obtained a dispersion of 14 ps. The second part of the test was performed using a ^{22}Na radioactive source placed between two $LaBr_3$(Ce) detectors. An energy window centred on the 511 keV annihilation line was used to select the relevant events from the background to avoid random coincidences. As the two γ-lines are emitted at the same time, no lifetime contribution is expected in the time distribution. The latter therefore represents a direct measurement of the intrinsic time resolution of the system. The right part of **figure 2** depicts our results with a FWHM of the time distribution of about 400 ps, which includes all uncertainties concerning the scintillator and photomultiplier, electronics and setup geometry. These results are compatible with those in [2] obtained with an analogue system.

Figure 2

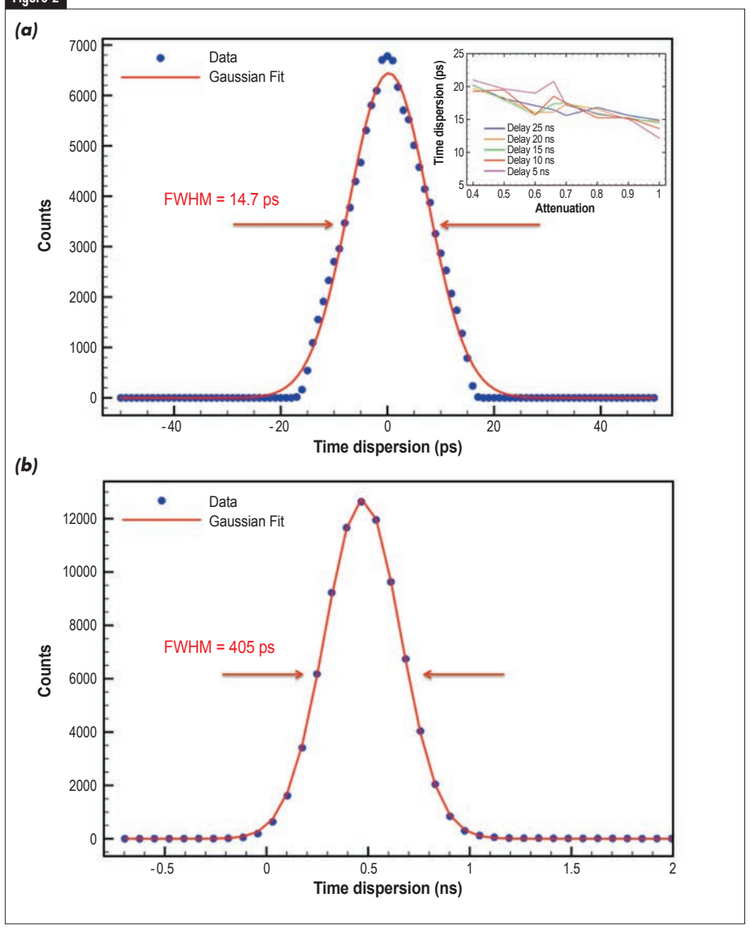

Time dispersion obtained using a pulse generator in two different channels of the acquisition chain ***(a)*** *and with two $LaBr_3$(Ce) detectors facing a ^{22}Na radioactive source* ***(b)***.

USER PROGRAMME

USER AND BEAMTIME STATISTICS

INSTRUMENT LIST

The ILL User Support team is dedicated to helping all visiting researchers to make the most of its facilities. If you are coming to the ILL to carry out experiments, the User Office is here to give you the organisational and administrative support you need to successfully perform your experiments.

Neutron beams and instrument facilities are free of charge for proposers of accepted experiments. Scientists affiliated to the Institute's member countries will also, in general, be assisted with necessary travel and daily subsistence for a limited period.
The User Support Team makes all arrangements for accommodation and will process claims for expenses after you have completed your experiment.

If you would like more information about the Institute's facilities, application for beamtime, user support and experimental programme, please visit our web-site.

http://www.ill.eu/users

USER PROGRAMME

AUTHOR

G. Cicognani (ILL)

THE ILL USER CLUB

All administrative tools for our scientific visitors are grouped together and directly accessible on the web, thanks to the User Club. All information is presented in a user-friendly environment. After having logged in with your own personal identification[1], you will have direct access to all the available information which concerns you. Users with particular responsibilities have privileged access to other tools, according to their role. The ILL User Club includes the electronic proposal and experimental reports submission procedures, and electronic peer review of proposals. Additional electronic services have also been put in place: acknowledgement of proposals, subcommittee results, invitation letters, user satisfaction forms and so on.

PROPOSAL SUBMISSION

There are different ways of submitting a proposal to the ILL:

- Standard submission – twice a year – via the Electronic Proposal System (EPS).
- Long-Term Proposals – once a year – via the Electronic Proposal System (EPS).
- EASY access system (EASY) throughout the year.
- Director's Discretion Time (DDT) throughout the year.
- Special access for proprietary research and industrial users.

Submission of a standard research proposal

Applications for beamtime should be submitted electronically, via our Electronic Proposal Submission system (EPS), available on the User Club web-site. Proposals can be submitted to the ILL twice a year, usually in February and in September. The web system is activated two months before each deadline. Submitted proposals are divided amongst the different colleges (see ***box below***) according to their main subject area.
Proposals are judged by a Peer Review Committee of the Subcommittees of the ILL Scientific Council. Subcommittee members are specialists in relevant areas of each College and they evaluate the proposals for scientific merit and recommend to the ILL Management the award of beamtime to the highest-priority proposals.

Before the meeting, the subcommittee receives a report on the technical feasibility and safety of a proposed experiment from the appropriate College at the ILL. Two proposal review rounds are held each year, approximately eight weeks after the deadline for submission of applications.

There are normally 4 reactor cycles a year, each of which lasts 50 days. Accepted proposals submitted by February will receive beamtime in the second half of the year and those submitted by September, in the first half of the following year. More detailed information on application for beamtime and deadlines is given on our website at
http://www.ill.eu/users/applying-for-beamtime/

THE ILL SCIENTIFIC LIFE IS ORGANISED INTO 10 COLLEGES

College 1	Applied Metallurgy, Instrumentation and Techniques
College 2	Theory
College 3	Nuclear and Particle Physics
College 4	Magnetic Excitations
College 5A	Crystallography
College 5B	Magnetic Structures
College 6	Structure and Dynamics of Liquids and Glasses
College 7	Spectroscopy in Solid State Physics and Chemistry
College 8	Structure and Dynamics of Biological Systems
College 9	Structure and Dynamics of Soft-Condensed Matter

Easy Access System

The Easy Access System (EASY) grants diffraction beamtime to scientists from ILL member countries, who need a rapid structural characterisation of samples and data analysis. Access is open all year long, and it does not go through the ILL standard proposal round and consequent peer review system.
The system offers one neutron day per cycle, on 4 instruments (D1A, D2B, D16 and OrientExpress) to perform very short experiments at room temperature. The users will not be invited to the ILL, but will send their samples to one of two designated ILL scientists, who will be responsible for the measurements and sample radiological control. The ILL will ship back the sample once the measurement is finished. You can apply for EASY beamtime on the Visitors Club. More information is available at
http://club.ill.eu/cvDocs/EASY_Guidelines.pdf

Long-Term Proposals

Users from ILL member countries can also apply for extended periods of beamtime, by submitting a Long-Term Proposal (LTP). Its purpose is to facilitate the development of instrumentation, techniques or software – which could be beneficial to the ILL community as a whole - through the award of beamtime over several cycles. The total amount of beamtime that may be allocated to LTPs on any particular instrument is capped at 10%, and beamtime is not awarded to LTPs to perform science beyond essential testing.

LTPs can be submitted once a year at the autumn proposal round using the specific LTP application form. The primary criterion for acceptance of a LTP is the excellence of the science that it will ultimately enable. The length of LTP projects is expected to be 3 years typically, with continuation approved at the end of each year, based on an annual report; a final report is also required at the end of the project. More details are given at
http://www.ill.eu/users/applying-for-beamtime/

Submission of a proposal to the Director's Discretion Time

This option allows a researcher to obtain beamtime quickly, without going through the peer-review procedure. DDT is normally used for 'hot' topics, new ideas, feasibility tests and to encourage new users. Applications for Director's Discretion Time can be submitted to the Head of the Science Division, Prof. Helmut Schober, at any time.

Experimental reports

Users are asked to complete an experimental report on the outcome of their experiments. The submission of an experimental report is compulsory for every user who is granted ILL beamtime. Failure to do so may lead to rejection in case of application for beamtime for a continuation proposal.
All ILL experimental reports are archived electronically and searchable via the web server as PDF files (under ***http://dub.ill.eu/cv/***). Experimental reports for experiments performed in 2012 are included in the CD-ROM of this year's Annual Report.

COLLABORATIVE RESEARCH GROUP INSTRUMENTS

The ILL provides a framework in which Collaborating Research Groups (CRGs) can build and manage instruments at the ILL to carry out their own research programmes. CRGs represent a particularly successful form of long-term international scientific collaboration. They are composed of scientists from one or two research disciplines, and often multinational, carrying out a joint research programme centred around a specific instrument. CRGs enjoy exclusive access to these instruments for at least half of the beamtime available. The CRGs provide their own scientific and technical support and cover the general operating costs of these instruments. If there is demand from the user community and the resources are available, the beamtime reserved for ILL can be made accessible to users via the subcommittees.

There are currently three different categories of CRG instruments:

- CRG-A in which the external group leases an instrument owned by the ILL. They have 50% of the beamtime at their disposal and for the remaining 50% they support ILL's scientific user programme.
- The CRG-B category owns their instrument and retains 70% of the available beamtime, supporting the ILL programme for the other 30%.
- Finally, CRG-C instruments are used full time for specific research programmes by the external group, which has exclusive use of the beam.

SUPPORT LABORATORIES

The opportunities we offer to our users extend beyond the privileges of access to the world's leading suite of neutron instruments. The ILL - in collaboration with the ESRF and other institutes - is actively responding to the needs of scientists unfamiliar with neutron techniques and in need of training and support facilities. New support facilities have been already set up on the ILL site. For more information see the chapter "More than simply neutrons", *p.106*.

ACCESS FOR INDUSTRIAL USERS

Besides academic research, ILL's instruments are used by a wide range of industries from pharmaceutical and chemical companies to materials and process engineering, energy and environment sectors. Neutron techniques are of particular interest in the industrial context as they provide unique and essential informations at the atomic and molecular level.

The Business Development Office (BDO) is the single point of contact for industry to use ILL neutrons scattering instruments. The Business Development Office will match the needs of industrial customers, direct them towards the best technique and scientists and takes care of the administrative procedures. The BDO will provide to industrial customers a fast proprietary access and confidentiality under specific contract giving access to any of the world leading scientific instruments of the ILL. The BDO may also set dedicated R&D partnerships for technological research with consortium including academic and industrial partners.
Contact: Jérôme Beaucour, ***beaucour@ill.eu***

[1] *If you are not yet registered in the Visitors Club and you wish to join it, you can register directly at* ***http://club.ill.eu/cv/***

USER AND BEAMTIME STATISTICS

THE ILL USER COMMUNITY

The ILL welcomed 1269 users in 2013, including 290 from France, 226 from Germany and 216 from the UK (**figure 1**). Many of our visitors were received more than once (for a total of 1767 user visits).

We value feedback from our users as an indicator of how well our facility is fulfilling their needs and to initiate actions when this is not the case (**figure 2**).

The User Satisfaction Form is a means of finding out what our users think of the facility. Users who have just finished an experiment at the ILL are asked to complete the questionnaire on the User Club and give us their views on different topics. User comments are made available to managers for their information and actions when appropriate. User feedback rate was about 65 % in 2013.

INSTRUMENTS

The instrumental facilities at the ILL are shown in the schematic diagram on page 98. Besides the 28 ILL instruments, there are 9 CRG-instruments (marked with an asterisk *):

- Powder diffractometers: D1B*, D2B, D20, SALSA.
- Liquids diffractometer: D4.
- Polarised neutron diffractometers: D3, D23*.
- Single-crystal diffractometers: D9, D10.
- Large scale structures diffractometers: D19, LADI.
- Small-angle scattering diffractometers: D11, D22, D33.
- Low momentum-transfer diffractometer: D16.
- Reflectometers: SuperADAM*, D17, FIGARO.
- Diffuse scattering and polarisation analysis spectrometer: D7.
- Three-axis spectrometers: IN1-LAGRANGE, IN8, IN12*, IN14, IN20, IN22*.
- Time-of-flight spectrometers: BRISP*, IN4, IN5, IN6.
- Backscattering and spin-echo spectrometers: IN11, IN13*, IN15, IN16B.
- Nuclear physics instruments: PN1, PN3.
- Fundamental physics instruments: PF1, PF2, S18*.

LADI and IN15 have a special status, since they are joint ventures of the ILL with other laboratories: in the case of LADI with EMBL and for IN15 with FZ Jülich and HZB Berlin.
Cryo-EDM is a CRG-C instrument and is not available as a 'user' instrument.
Details of the instruments can be found on the web at
http://www.ill.eu/instruments-support/instruments-groups/

Figure 1

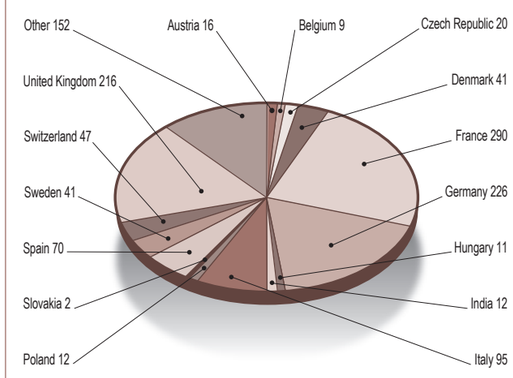

National affiliation of ILL users in 2013.

Figure 2

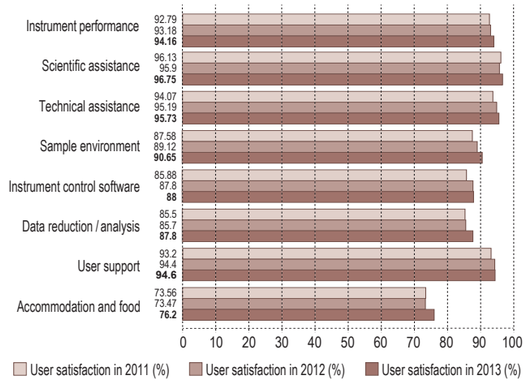

User satisfaction survey results for 2013, compared with those obtained in previous years.

BEAMTIME ALLOCATION AND UTILISATION FOR 2013

During 2013, the reactor operated for about 3 cycles - representing 139 days of neutrons (see ***Reactor Operation, p.102***). The accumulated backlog on most instruments combined with the long shutdown (started in August 2013 and scheduled to end 25 June 2014), led the ILL management to decide that no subcommittees were held in 2013. As a consequence all cycles in 2013 were allocated during the panel meeting held in November 2012, which saw as a consequence a new record in demand.

Overall, the Subcommittees of the Scientific Council examined 834 proposals requesting 5880 days for 2013, out of which 553 proposals received beamtime, allocating 3174 days of beamtime on the different instruments. A total of 603 experiments were scheduled. The distribution of accepted proposals amongst the different research areas and colleges is given in **figure 3**.

In 2013, the member countries of the ILL were: France, Germany, UK, Austria, Belgium, the Czech Republic, Denmark, Hungary, Italy, Poland, Slovakia, Spain, Sweden, Switzerland and India.

Table 1 gives the beamtime distribution amongst the different member countries (request and allocation in 2013). In calculating the statistics of beamtime per country, the attribution is based on the location of the laboratory of the proposers, not their individual nationality. For a proposal involving laboratories from more than one member country, the total number of days is divided amongst the collaborating countries, and weighted by the number of people for each country. Local contacts are not counted as proposers except when they are members of the research team.
The beamtime requested by and allocated to scientists from ILL, ESRF or EMBL is allocated to the member countries according to a weighting system based on the fractional membership of the country of the institute concerned. When a proposal involves collaboration with a non-member country, the allocated time is attributed entirely to the collaborating member country (or countries), and weighted by the number of people for each member country. Proposals for which all proposers are from non-member countries therefore do not appear in this table. This explains why the total number of allocated days differs from **table 2**.

Figure 3

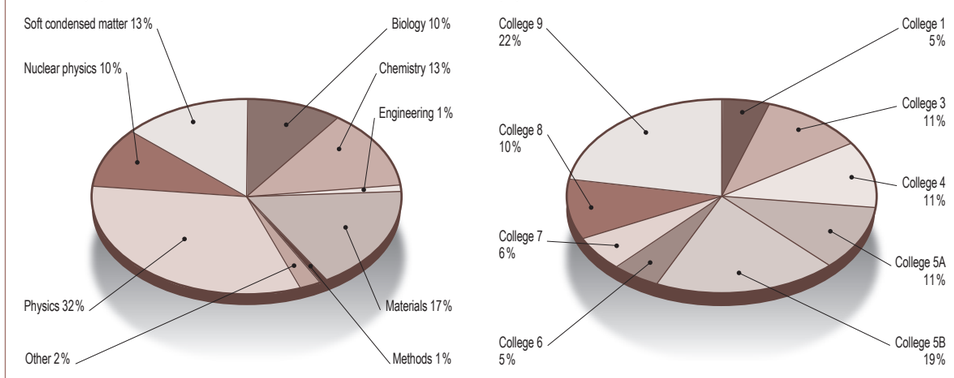

*Beamtime allocation in 2013: distribution amongst the different research areas **(a)** and colleges **(b)**.*

Table 1

Country *	Requested days	Requested in %	Allocated days	Allocated in %	Allocated days	Allocated in %
			Before national balance		After national balance	
AT	146.61	2.55	62.39	1.98	62.53	1.98
BE	24.79	0.43	16.84	0.53	16.94	0.54
CH	246.63	4.29	143.89	4.56	132.57	4.19
CZ	48.42	0.84	18.81	0.60	18.87	0.60
DE	**1528.90**	**26.57**	**798.90**	**25.29**	**814.65**	**25.77**
ES	278.24	4.83	157.03	4.97	158.57	5.02
FR	**1514.79**	**26.32**	**878.54**	**27.81**	**871.12**	**27.55**
HU	30.18	0.52	19.16	0.61	19.22	0.61
IN	226.49	3.94	67.98	2.15	57.65	1.82
IT	321.14	5.58	191.13	6.05	172.07	5.44
PL	66.23	1.15	21.26	0.67	25.56	0.81
SE	176.86	3.07	100.35	3.18	100.06	3.16
SK	14.80	0.26	3.98	0.13	3.94	0.12
UK	**1127.14**	**19.58**	**675.85**	**21.40**	**704.81**	**22.29**
Total	***5755.16***	***100.00***	***3158.78***	***100.00***	***3161.78***	***100.00***

Distribution amongst the Associate and Scientifi-Member countries of beamtime requested and allocated in 2012 during the Subcommittees of the Scientific Council.

Proposals from purely non-member countries do not appear in this table, therefore the total request and allocation is different in table 2.

** Only member countries.*

USER AND BEAMTIME STATISTICS

A more complete view of beamtime use is given in **table 2**. Request and allocation of beamtime as well as the number of scheduled experiments refer to standard submissions to the subcommittee meetings. The effective number of days given to our users takes into account also Director's Discretion Time and CRG time for CRG instruments.

INSTRUMENT PERFORMANCE

Table 2 also gives a summary of instrument performance for 2013. For each cycle, a record is kept of any time lost from the total available beamtime and the reasons for the lost time are analysed for all the instruments. The table gives a global summary for the year.

Overall 4184 days were made available to our users in 2013 on ILL and CRG instruments, which represents about 78.5% of the total days of operation. 220 days were used by ILL scientists to carry out their own scientific research. About 19% of the total beamtime available on the ILL instruments was allowed for tests, calibrations, scheduling flexibility, minor breakdowns recuperation and student training.

Beam days delivered for science in 2013 amount to 4404 (used for users and internal research).
In 2013, 432 out of 5327 days were lost due to various malfunctions, which represent about 8 % of the total available beamtime. The breakdown by reasons for beamtime losses is shown in **figure 4b**.

Detailed comments on the larger beamtime losses (above 25 days) are as follows:

- IN5 lost 18 days during the first cycle and 15 days during the second one, because of chopper and chopper electronics failures.
- On PN1, the entire first cycle was lost since no target change could be made: an end-switch contact/cable of the sample changer was damaged during the VS maintenance in the shutdown. The problem was recognised during the first target change, but no repair intervention was possible in the primary casemate during reactor operation.
- GAMS-5 lost 24 days because the AV-system and the He-Ne laser frequency stabilisation were broken; in addition it could not work for 12 days during the second cycle because the antivibrational system was not stable.

Figure 4

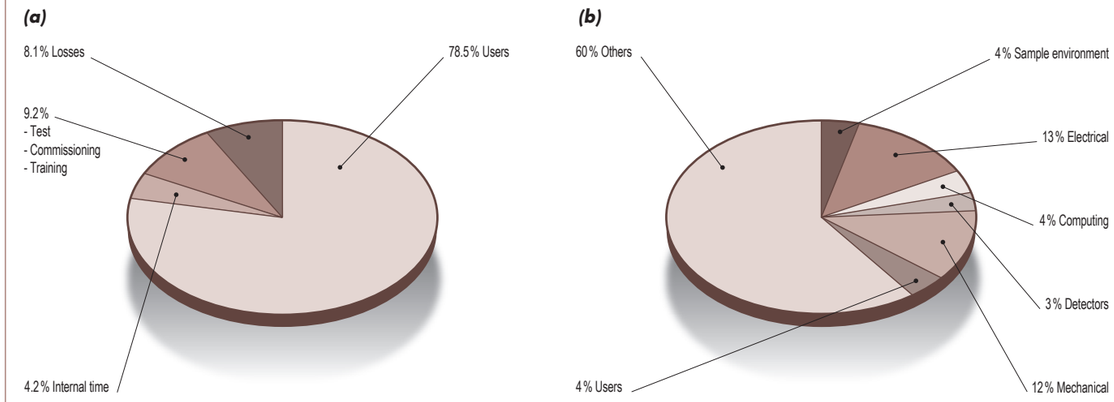

(a) *Use of ILL beamtime* ***(b)*** *Reasons for beamtime losses.*

Table 2

REQUEST, ALLOCATION AND INSTRUMENT PERFORMANCE FOR 2013

Instrument	Days requested	Days allocated*	Number of scheduled experiments	Available days	Days used for users**	Days lost	Days for commissioning/ test/training	Days for internal research
BRISP	**74**	**33**	**3**	**139**	**118**	**8**	**13**	**0**
D1B	**58**	**56**	**21**	**139**	**125**	**5**	**8**	**1**
D10	147	106	15	139	124	0	15	0
D11	135	77	43	139	94	7	37	1
D16	112	71	16	139	91	2	22	24
D17	155	82	24	139	111	5	12	11
D19	138	106	16	139	124	3	11	1
D2B	135	102	43	139	122	3	6	8
D20	144	84	31	139	112	4	2	21
D22	187	58	25	139	106	9	19	5
D23	**45**	**35**	**5**	**139**	**132**	**0**	**7**	**0**
D3	100	100	13	139	117	13	9	0
D33	139	93	29	139	100	5	25	9
D4	92	34	7	66	50	5	4	7
D7	136	105	17	139	119	3	15	2
D9	160	80	14	139	95	6	22	16
FIGARO	144	106	32	139	116	10	13	0
IN1-LAGRANGE	105	51	10	73	49	8	13	3
IN11	156	106	13	139	109	3	10	17
IN12	**38**	**14**	**3**	**139**	**116**	**4**	**17**	**2**
IN13	**102**	**57**	**10**	**139**	**131**	**2**	**5**	**1**
IN14	236	111	15	139	125	2	8	4
IN15	225	67	10	139	114	4	12	9
IN16	252	100	18	139	96	3	14	26
IN16B				45	29	4	3	9
IN20	132	88	10	139	118	5	7	9
IN22	**92**	**31**	**5**	**139**	**136**	**3**	**0**	**0**
IN4	155	100	22	139	111	10	9	9
IN5	253	94	21	139	92	39	3	5
IN6	159	96	22	139	134	2	2	1
IN8	122	85	14	139	100	6	28	5
LADI	107	29	8	139	100	12	27	0
PF1B	1081	505	36	139	136	3	0	1
PF2/5	88	73	2	139	105	16	18	0
PN1	153	70	7	139	81	55	2	
PN3 - GAMS 5	89	61	4	139	82	47	10	0
PN3 - GAMS 6	14	14	1	139	0	94	45	0
SALSA	90	60	12	139	105	7	14	13
SUPERADAM	**130**	**34**	**6**	**139**	**132**	**3**	**4**	**0**
S18	**28**	**28**	**1**	**139**	**127**	**12**	**0**	**0**
Total	***5880***	***3174***	***603***	***5327***	***4184***	***432***	***491***	***220***
Percentage of the total available beamtime					***78.50%***	***8.10%***	***9.20%***	***4.10%***

Beamtime request/allocation (via standard subcommittees and Director Discretion Time (DDT) together) by instrument and instrument performance.CRG instruments are in brown.

** 'days allocated' refers to only those days reviewed by the subcommittees (i.e., excluding CRG days and DDT).*
*** 'days used' refers to the total number of days delivered to users (i.e., including CRG days for CRGs and DDT).*

PF2 consists of different set-ups where several experiments are running simultaneously. The values given are averages for these positions.
D4 and IN1 share the same beam port and cannot be run simultaneously.

INSTRUMENT LIST - DECEMBER 2013

ILL INSTRUMENTS

D2B	powder diffractometer	operational
D3	single-crystal diffractometer	operational
D4 (50% with IN1)	liquids diffractometer	operational
D7	diffuse-scattering spectrometer	operational
D9	single-crystal diffractometer	operational
D10	single-crystal diffractometer	operational
D11	small-angle scattering diffractometer	operational
D16	small momentum-transfer diffractometer	operational
D17	reflectometer	operational
D19	single-crystal diffractometer	operational
D20	powder diffractometer	operational
D22	small-angle scattering diffractometer	operational
D33	small-angle scattering diffractometer	operational
FIGARO	horizontal reflectometer	operational
IN1- LAGRANGE (50% with D4)	three-axis spectrometer	operational
IN4	time-of-flight spectrometer	operational
IN5	time-of-flight spectrometer	operational
IN6	time-of-flight spectrometer	operational
IN8	three-axis spectrometer	operational
IN11	spin-echo spectrometer	operational
IN14	three-axis spectrometer	operational
IN16	backscattering spectrometer	operational
IN20	three-vaxis spectrometer	operational
PF1	neutron beam for fundamental physics	operational
PF2	ultracold neutron source for fundamental physics	operational
PN1	fission product mass-spectrometer	operational
PN3 - GAMS	gamma-ray spectrometer	operational
SALSA	strain analyser for engineering application	operational
VIVALDI	thermal neutron Laue diffractometer	on hold

CRG INSTRUMENTS

BRISP	Brillouin spectrometer	CRG-B operational
CRYO EDM	installation for the search for the neutron electric dipole moment	CRG-C operational
D1B	powder diffractometer	CRG-A operational
D23	single-crystal diffractometer	CRG-B operational
GRANIT	gravitation state measurement	CRG operational
IN12	three-axis spectrometer	CRG-B operational
IN13	backscattering spectrometer	CRG-A operational
IN22	three-axis spectrometer	CRG-B operational
SuperADAM	reflectometer	CRG-B operational
S18	interferometer	CRG-B operational

JOINTLY FUNDED INSTRUMENTS

LADI (50%)	Laue diffractometer	operated with EMBL
IN15	spin-echo spectrometer	operated with FZ Jülich and HZB Berlin
GRANIT	gravitation state measurement	operated with LPSC (UJF, CNRS)

TEST AND CHARACTERISATION BEAMS

CT1, CT2	detector test facilities
CYCLOPS	Laue diffractometer
TOMOGRAPHY	neutrography
OrientExpress	Laue diffractometer
T3	neutron optics test facility
T13A, C	monochromator test facility
T17	cold neutron test facility

INSTRUMENT LAYOUT JANUARY 2014

INSTRUMENT LAYOUT - JANUARY 2014

Neutron guide hall / ILL 22

Reactor operational level (D)

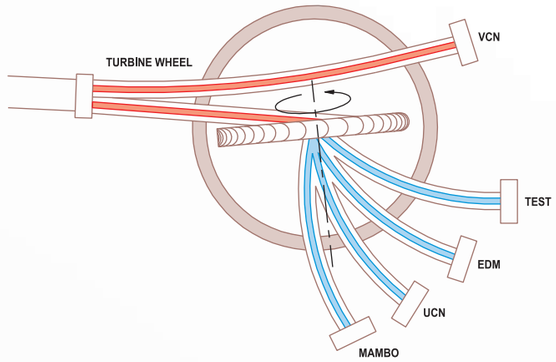

Reactor hall / Inclined guide H4

Neutron guide hall / ILL 7 - Vercors side (WEST)

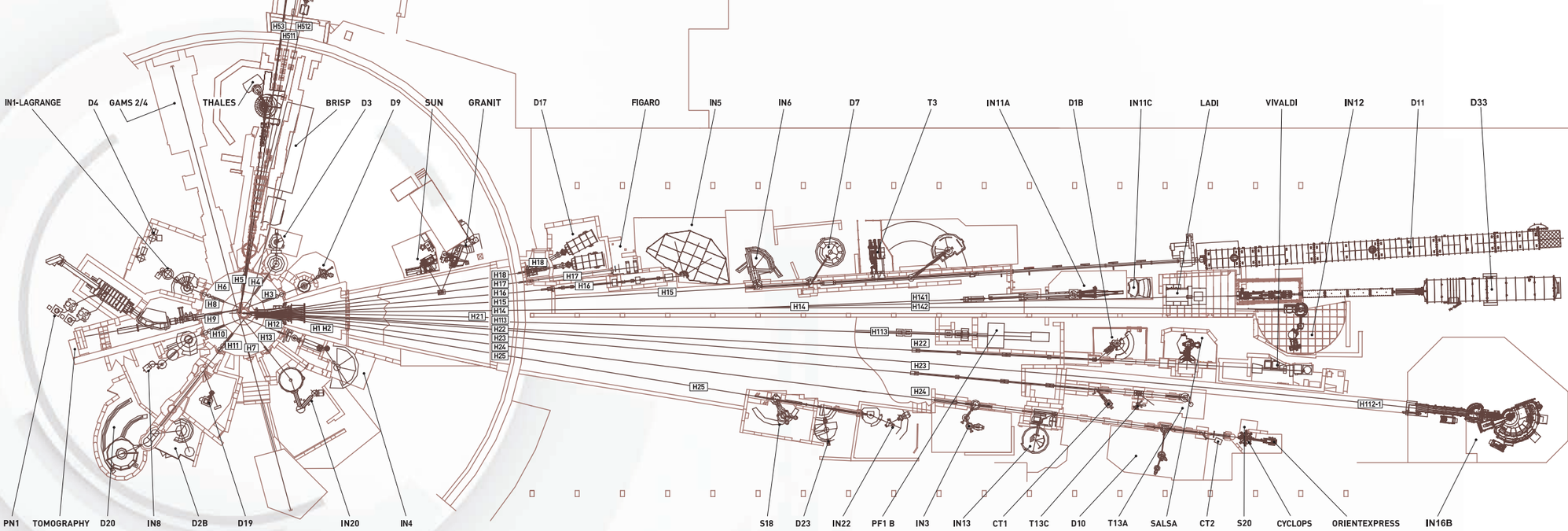

Reactor hall ILL 5 / Experimental level (C)

Neutron guide hall / ILL 7 - Chartreuse side (EAST)

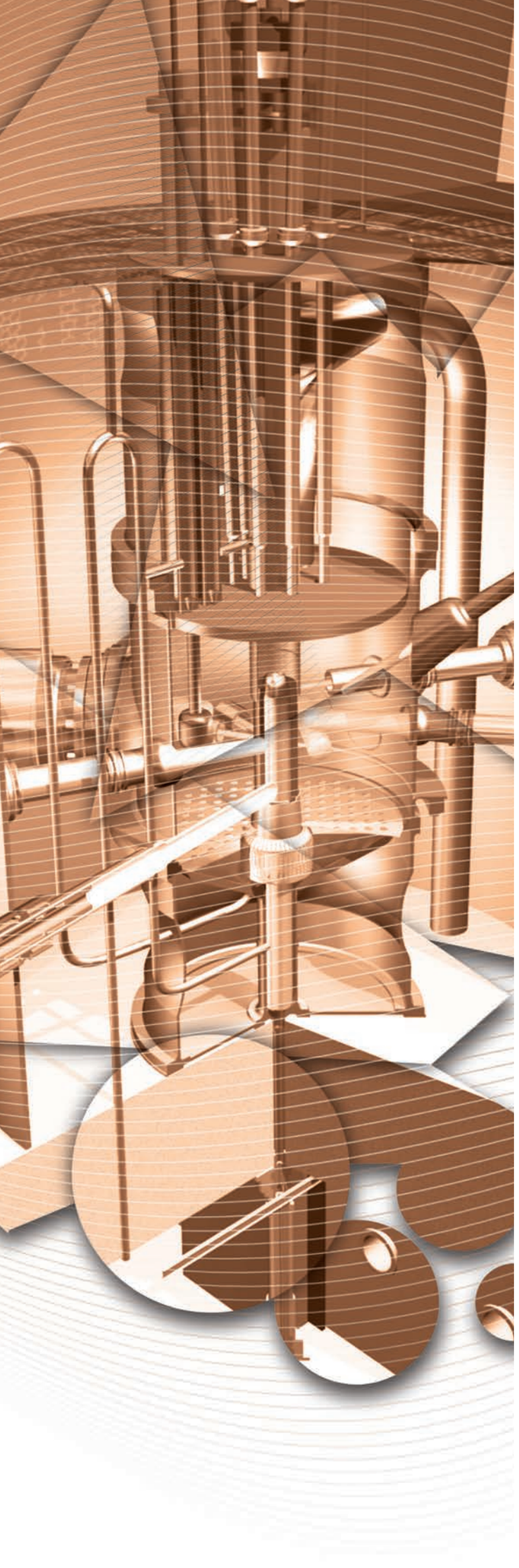

"I would like to stress the importance and quality of the safety evaluation report you submitted on 15 September 2011. It corresponded well to the specifications and enabled an analysis to be performed of the robustness of your installations and of your plans for improvements."
The french Nuclear Safety Authority (ASN).

This ILL High Flux Reactor (HFR) produces the most intense neutron flux in the world: 1.5×10^{15} neutrons per second per cm^2, with a thermal power of 58.3 MW. The reactor operates on 50-day cycles, with each cycle of operation followed by a shutdown period during which the fuel element is changed and a number of checks are carried out. Occasional longer shutdowns allow for equipment maintenance and upgrades. There are normally 4 reactor cycles per year, supplying 200 days of neutron flux for scientific use.

Following the nuclear accident at Fukushima, Japan, the french Nuclear Safety Authority (the ASN) decided to launch additional safety assessments on all French nuclear bases (INBs), including the ILL. This additional safety review has an impact on the Institute and affects its budget over the next years.
The studies performed by the Reactor Division teams analysed the behaviour of the ILL reactor under extreme conditions: the earthquake scenarios envisaged would have caused major damage to a town like Grenoble and would have led to the failure of all the dams on the river Drac, leaving the centre of town under 10 metres of water. On 15 September 2011 ILL submitted the results of its analyses to the IRSN (*Institut de Radioprotection et de Sûreté Nucléaire) and the ASN (Autorité de Sûreté Nucleaire*). On 16 November the permanent group of experts for nuclear reactors replied with its conclusions: the ILL's proposals have been completely accepted. The precise plan of work has been well received by the ASN. On 6 August 2012 the ASN wrote as follows to the ILL:

"First of all, I would like to stress the importance and quality of the safety evaluation report you submitted on September 15, 2011. It corresponded well to the specifications and enabled an analysis to be performed of the robustness of your installations and of your plans for improvements."

Since 2012 we have been putting these plans into operation. You will probably know that a major seismic reinforcement programme (the "Refit Programme") was carried out at ILL, ending in 2007. Unsurprisingly, the 2011 studies demonstrate the robustness of the reactor against maximum expectable earthquake conditions. However, cumulated with the possibility of the loss of the 4 dams upstream on the river Drac, it has been decided to reinforce elements traversing the reactor containment and to build a new emergency reactor control room from which all the emergency safety circuits can be controlled by the crisis-management teams. The building housing this control room has already been built.

The reinforcement work is programmed over 5 years (from 2012 to 2016) and should have no major impact on the ILL user programme. Its total cost was originally estimated at 12 M€. Following an ASN decision of 6 December 2013 and the studies it requires, the cost is now estimated at 15 M€. The additional work now required involves the installation of a new reactor electronics room, modifications to the ILL4 office building to minimise any movement during an earthquake, and the replacement of the air intake building.

Hervé Guyon
Head of Reactor Division

AUTHORS

H. Guyon and **J. Tribolet** (ILL)

Three reactor cycles were planned in 2013 and 139 days of scientific activity were provided overall (see **table 1**).

THE KEY REACTOR COMPONENTS PROGRAMME

In order to ensure reactor safety and reliability over the next few years the Reactor Division has been running the "Key Reactor Components programme", whose aim is essentially to ensure that the most important parts within the reactor are regularly replaced and improved. The programme started in 2005 and will continue until at least 2017, the date of the next ten-year safety review of our installations.

The main operations planned under this programme are:
- the replacement of the beamtubes,
- an upgrade of the out-of-pile part of the horizontal cold source, including its instrumentation and control system,
- manufacture of the hafnium safety rods,
- upgrade of the control systems on the safety circuits,
- procurement of backup cells for the cold sources,
- the construction of the new heavy water management building and heavy water exchange installations (for the deliveries from Canada of 40 m^3 of fresh heavy water for the reactor, with the removal of the tritiated heavy water).

CONSEQUENCES OF THE POST-FUKUSHIMA SAFETY ASSESSMENT

The investigations carried out in 2011 and the subsequent discussions with the safety authority's expert groups in November successfully demonstrated that:
- the ILL has significant safety margins available with respect to the risk of a design-basis earthquake,
- the loss of a single safety function would never result in an acute escalation of the danger (cliff-edge effect),
- the loss of both reactivity and the confinement would never result in a major escalation of the danger (cliff-edge effect),
- there are always at least two major barriers in place to prevent and mitigate the accidents to be feared,
- fusion under water would never result in a cliff-edge effect.

To comply with requirements following the Safety Assessment, the ILL must ensure that it is equipped with a "hard core" safety system, by
- completing its installation of the emergency core reflood system and seismic depressurisation circuit,
- and installing a groundwater supply system, a complementary emergency rod-drop system, and a new emergency reactor control room.

This programme of work has been defined and is progressing well:
- test drills have been carried out to define the dimensions of the 2 wells required to guarantee a long-term water supply,
- the structural engineering work for the new control room is finished - the building is dimensioned to resist an earthquake on the Belledonne fault of 7.3 on the Richer scale, and the breach of the 4 dams on the Drac river. The ground floor of this building now accommodates the heavy water unit used for handling the transfers of heavy water between the ILL and Canada.

ILL received the safety authorities' decision and instructions on this programme of work on 6 December 2013. The authorities have validated our studies, but require additions to the "hard core" system - a new reactor electronics room and reinforcements limiting potential movement of building ILL 4 in the event of an earthquake, as well as the replacement of the air intake building.

WINTER SHUTDOWN 2013/2014

This is a shutdown planned to last from 9 August 2013 to 25 June 2014, with a particularly ambitious work schedule. The programme includes work on the key reactor components and on the projects specified in the authorities' recent instructions following our Safety Assessment; we will also be performing numerous maintenance operations. As we are keen to avoid a second long shutdown before 2016, we will also be preparing the ground for operations to be performed later in the framework of the Safety Assessment.

MAIN WORK CARRIED OUT IN 2013

Maintenance operations:
- dispatch of 6 spent fuel elements to La Hague,
- testing of 2 spare 'cooling stop' pumps on the heavy water circuit,
- homogenisation of the ion exchange resins of the primary circuit and reactor pools, to ensure that the active resins generated over the last 20 years meet ANDRA's waste conditioning criteria,
- modifications to the reactor protection circuit,
- inspections of the cold sources' and gaseous decay tanks' (nuclear pressure equipment),
- replacement of the upper part of a safety rod,
- maintenance on the control rod mechanism,
- major maintenance on the main diesels.

Work on the Key Reactor Components:
- manufacture of a prototype hafnium safety rod (currently produced using a silver-indium-cadmium alloy),
- replacement of the IH3 beamtube, withdrawal of the H13 beamtube, dismantling of the interior of the H5 beamtube (the replacement of the H6/H7 beamtube used under helium pressure is therefore postponed 3 years),
- construction of the heavy water building, in less than one year, together with its technical installations. This ensured that we were able to take in 20 m^3 of clean heavy water from Canada for the reactor's primary circuit and send off 10 m^3 of heavy water in return. Technical problems at one of the Canadian installations led to an interruption in these operations, which will now be continued at the end of March 2014.

Work following the post-Fukushima Safety Assessment:
- installation of bearing piles to secure the work on buildings connecting with the reactor,
- construction of the buildings (ILL 5E and 5F),
- piercing of reactor containment penetrations and fitting bridges for the circuits and cables of the "hard core" system,
- installation of lighting and scaffolding in the space within the twin walling of the reactor containment.

Table 1

Cycle no.	Start of cycle	End of cycle	Number of days of operation	Number of days scheduled	Number of unscheduled shutdowns
168	19.02.13	06.04.13	49	49	0
169	29.04.13	13.06.13	42.1	45	1
170	25.06.13	09.08.13	45	45	0
Total			***136.1***	***139***	***1***

RADIOACTIVE WASTE AND EFFLUENTS

The ILL's activities in 2013 generated waste and effluents respecting the regulatory limits applicable to our installation, as follows:

Evacuation of radioactive waste	Quantity
Decay bin (60 l)*	0
5 m^3 pre-concreted crate (low and intermediate level waste)	0
5 m^3 crate (low and intermediate level waste)	9
5 m^3 crate (very low level waste)	3
200 l drums of oil	3
200 l drums of "incineratable" (laboratory waste)	0
HDPE drums 120 l (laboratory waste)	0
30 l cylinders (liquid)	0

** Waste stocked in these decay bins is still quite active and does not meet ANDRA's specification for intermediate-level waste.*

Gaseous effluents	Released in 2013 (TBq)
Tritium	12
Rare gas	0.86
Carbone 14	0.46
Iodine	0.00000086
Aerosols	0.00000011

Liquid effluents	Released in 2013 (TBq)
Tritium	0.24
Carbone 14	0.00025
Iodine	0.00000084
Other activation products	0.00011

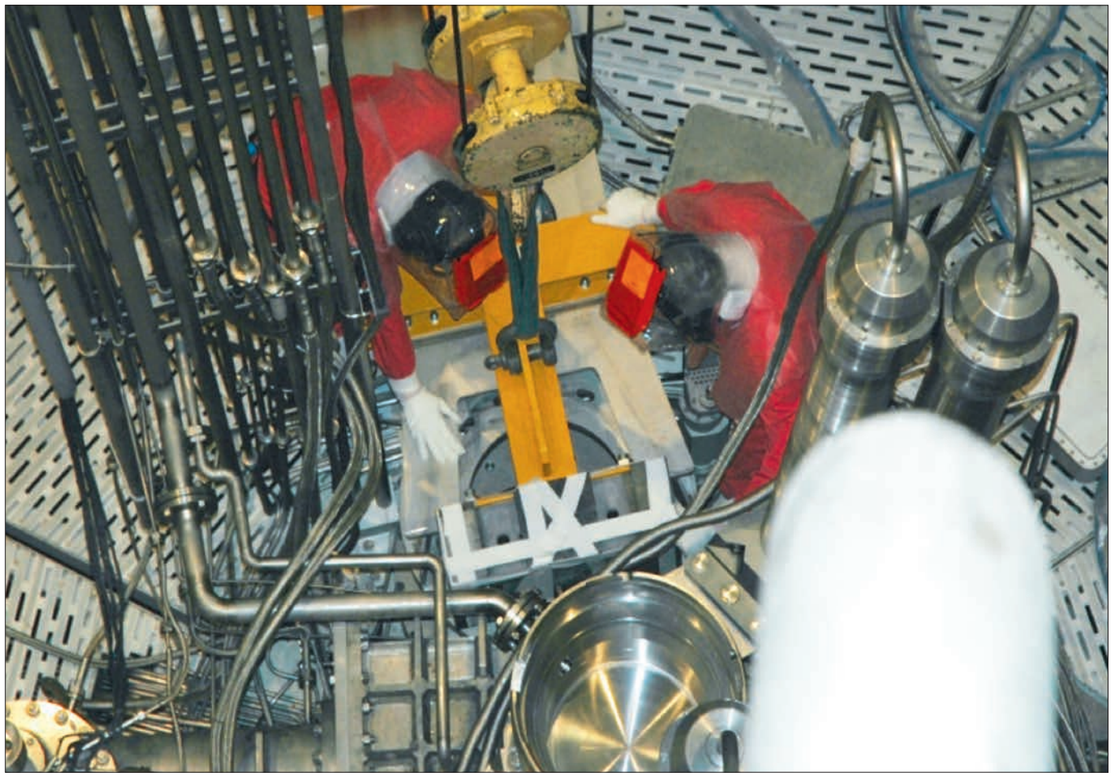

Inserting the CRU (emergency reflood circuit) into the reactor vessel.

THE EPN-CAMPUS

SCIENTIFIC SUPPORT LABORATORIES

The ILL is firmly committed not only to build high-performance instruments but also to offer the best scientific environment to the user community.

In order to maintain their ranking on the international scene, European research institutes must optimise their resources and develop synergies at every level.

The ILL is firmly committed not only to build high-performance instruments but also to offer the best scientific environment to the user community and it has established successful collaboration with neighbouring institutes over the years. After the successful Partnership for Structural Biology, we have now launched a Partnership for Soft Condensed Matter.

In parallel, the ILL and the ESRF have been working on plans to transform our joint site into a research campus – the European Photon and Neutron science campus, or EPN-campus for short - with a truly international reputation, and launched an ambitious project to extend the facilities already offered by our international site. The new scientific and technological installations will be complemented with other more general improvements, such as a new Science Building, a new site entrance, a dispatch and reception platform, a bigger restaurant and internal roadways.

In addition, the ILL has teamed up with the other institutes located on the Polygone scientifique science park (where our Institute is located) for the GIANT partnership, a project which aims to develop our neighbourhood into a world-class science and technology park. The GIANT project aims to develop Grenoble's Polygone Scientifique into a world-class science and technology park.

THE EPN-CAMPUS

THE SCIENCE BUILDING

The new Science Building provides 5 000 square metres of floor space across five levels – four floors of offices and labs etc. and one technical floor. In 2013 the construction was achieved and the first people started to move in their new premises. The building provides a number of platforms for promoting the complementary aspects of neutron and synchrotron techniques (*p.108*), and collectively enhance the visibility of ILL and ESRF in different research fields ranging from Soft Matter to Materials Science to Technology.

Several shared ESRF and ILL initiatives are hosted in the building including:

- The common library
- The theory group
- The Partnership for Soft Condensed Matter
- The common chemistry laboratories

In addition, the ESRF Business Development Office and the ILL Industrial Liaison Office will provide a unique contact point for industry. Further laboratories for sample characterisation and manipulation offer state-of-the art complementary techniques to neutrons and X-rays.

THE IBS NOW ON SITE

2013 saw the arrival on the EPN campus of the IBS, the *Institut de Biologie Structurale*. The IBS is a French national research institute with 240 members of staff, including 181 scientists: researchers, teacher-researchers, engineers and technicians… It has five main fields of activity, three being biological in focus; the other two aiming at the development of new technical approaches:

- Immunity and host-pathogen interactions
- Fundamental intracellular processes
- Limits of life
- Membrane proteins
- New methodologies for integrated structural biology.

In practice many of the protein and other molecules studied at IBS play an important role in life processes. A better knowledge of the mechanisms at play could lead to the development of new medicines.

We could cite as examples research into HIV virus entry mechanisms, or the resistance of bacteria to antibiotics and the design of new antibiotics, amongst many others.

As IBS director, Dr Eva Pebay-Peyroula, said: "The EPN campus, with its 4th generation synchrotron source and high-flux neutron source, provides unique facilities for a structural biology institute. The IBS needs these for its research and integrates their capabilities into its programme of development. In return, the IBS brings with it complementary techniques for the site, such as high-field NMR and electron microscopy. These are tools providing an excellent complement to the neutron and X-ray facilities".

More information on these can be found on the IBS's website:
http://www.ibs.fr/science/axes-thematiques/

GRENOBLE AND THE FUTURE

The Grenoble Innovation for Advanced New Technologies partnership, or '**GIANT**', is forging dynamic new links between higher education, research and industry, to foster technological breakthroughs for the future. The city of Grenoble has been supporting the project with the construction of a new 250 hectare town quarter in the neighborhood of ILL.

A tram line is also being extended, with a new terminus which will serve the ILL well, as it will be only 300 metres from the future site entrance. It will take ca 10 mins to go from ILL to Grenoble railway station and 15 mins to the town centre.

The current plans are for the tram to be up and running for the end of 2014.

The Institut de Biologie Structurale (IBS) is now on the EPN campus.

The new Science Building.

SCIENTIFIC SUPPORT LABORATORIES

PARTNERSHIP FOR SOFT CONDENSED MATTER

Year 2013 saw an ever increasing demand for using the complementary techniques available in the ILL Soft Matter Lab and a considerable success in terms of publications including samples prepared and characterised in this lab. The new chemistry lab responsible, David Heß has largely contributed to the running and maintenance of the instrumentation and work is in progress to upgrade the available tools when moving to the Science Building. A new group has been created, the Soft Matter Science & Support group, that includes responsibilities for the chemistry and PSCM labs and initiatives. A new scientist has been hired, Yuri Gerelli, for filling the duties of ILL PSCM coordinator.

By early 2014, the PSCM will be able to host up to 20 scientists and technicians both internal and from Collaborative Partners laboratories working in the new Science Building of the joint ESRF/ILL campus. In these laboratories, scientists will be able to prepare experiments with highly complex self-assembled and non-equilibrium soft matter systems in fields related to nanotechnologies, life sciences, environment as well as renewable energy. Activities within the PSCM initiative in 2013 have included the start of negotiations with a number of laboratories, potential Collaborative Partners as well the organisation of a workshop to attract industrial partners.

Users wishing to use the facility in conjunction with neutrons or synchrotron radiation measurements should indicate this when submitting their request for beamtime.

Further details can be found at

http://www.ill.eu/instruments-support/labs-facilities/pscm/

PARTNERSHIP FOR STRUCTURAL BIOLOGY

The Partnership for Structural Biology (PSB) contains a powerful set of technology platforms that are contributed by the various partner institutes (ILL, ESRF, EMBL, IBS, and the unit for host-pathogen interactions). These platforms include advanced capabilities that complement the powerful neutron scattering facilities available to ILL users: synchrotron X-rays, electron microscopy, NMR, high-throughput methods (soluble expression and crystallisation), and a range of biophysical techniques such as isothermal calorimetry and surface plasmon resonance. A joint SANS/SAXS platform has been developed and there is also strong connectivity and collaboration between the ILL and ESRF crystallography groups involved in structural biology and related industrial efforts. The aim of the PSB is to enhance the interdisciplinary capabilities of each of the facilities co-located on the site. Further details are provided on its website ***http://www.psb-grenoble.eu/***. The Carl-Ivar Brändén building (CIBB), is the principal focus for the PSB and its partner organisations.

DEUTERATION LABORATORY

ILL's Life Science Group is located within the CIBB and contains the Deuteration Laboratory platform (D-LAB). The group is involved in a wide variety of externally funded programmes that exploit the capabilities of the PSB as well as promoting interdisciplinary structural biology (see ***http://www.ill.eu/PSBLS***). The group also has a number of programmes for method development relating to sample preparation and data collection using crystallography, SANS, fibre diffraction and dynamics; it is therefore of central importance to the activities of biological work relating to all of the ILL instrument groups

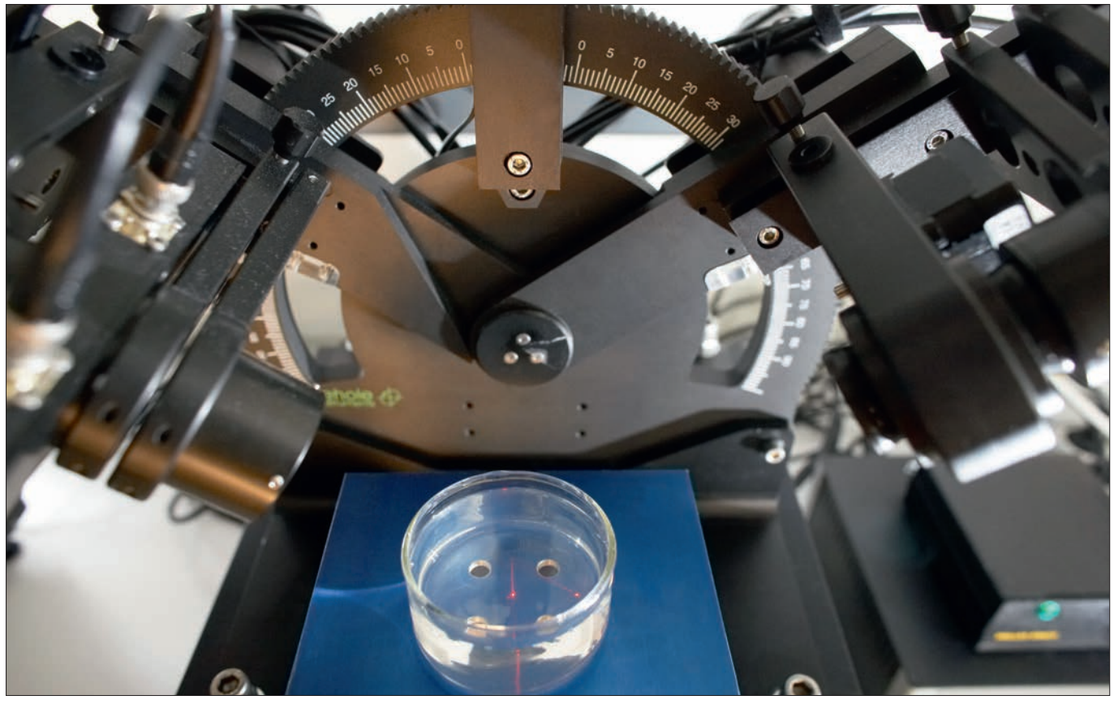

The phase modulated ellipsometer in the Partnership for Soft Condensed Matter (PSCM) has been used for the provision of complementary laser reflection data to support publications resulting from neutrons studies at the air/water interface on FIGARO over the last few years.

MATERIALS SCIENCE SUPPORT LABORATORY

The joint ILL-ESRF Materials Science Support Laboratory provides a range of support to our users, from advice with experiment proposals to advanced sample metrology. In particular, the Laboratory works with users to optimise the experimental methodology before the start of an experiment. This takes the form of standardised specimen mounting, digitisation of samples, definition of measurement macros and liaising with the instrument responsible. It is recommended that users arrive at the ILL a day or two prior to the start of an experiment to enable these off-line preparations to be performed. More information may be found on the MSSL's website

http://www.ill.eu/sites/mssl/

C-LAB

The Computation-Lab offers support to ILL users for atomistic simulations using classical and *ab initio* methods. Typical applications for simulations are structure, phonons and (some) magnetism in crystals and structure and dynamics in (partially) disordered systems ranging from liquids and glasses to macro/bio-molecular systems.

As samples become more complex, simulations can provide key, complementary information that will help to interpret experimental data and understand how systems behave. Scientists and thesis students at the ILL benefit from the software, hardware and expertise of the C-Lab and users can benefit via their local contacts. In order to improve access to simulations for users, they are now able to request simulation support for their neutron scattering experiments on the official ILL proposal forms by ticking the appropriate box. In 11 proposal rounds since Autumn 2007, there have been 390 requests, at an average of 35 requests per round, with the last round being a record with 55 requests. For more information see ILL News N.47, June 2007 & N. 50, June 2009

http://www.ill.eu/html/quick-links/publications/ill-news/

The Materials Science Support Laboratory (MSSL) has moved into the Science Building and is already in use. Here the precision saw and polishing equipment.

Sergio Garcia Martinez, the technician of the Materials Science Support laboratory, changing the touch probe of the dimensional coordinate measuring machine.

FACTS AND FIGURES
ORGANISATION CHART

To provide practical and efficient expertise in areas as varied as the ILL's human resources, purchasing and finance, legal support, building construction and maintenance.

2013 was a key year for the ILL. It was the year that saw the completion of the vast majority of the Millennium Programme projects and the start of work programmed for the exceptional long shutdown. At the same time the scientific and technical teams were making major progress on preparations to launch the Endurance Programme, an enterprise to ensure that ILL continues to drive the world's science forward in the ILL's particular domain. The high point of the year, however, was surely the signature of the Fifth Protocol to the ILL's Intergovernmental Convention. The Associates' extension of the Convention sent a strong message of confidence to the ILL's staff and user communities, confirming the Associates' commitment to the Institute for the next ten years at least.

The Administration Division's role is to contribute to this mission by providing practical and efficient expertise in areas as varied as the ILL's human resources, purchasing and finance, legal support, building construction and maintenance.

As usual, the Human Resources Service played an important role in the negotiations with the trade unions in 2013. Some of these negotiations concerned the long reactor shutdown and its consequences for staff (internal transfers to strengthen certain services, external transfers to allow scientists in particular to organise exchanges with other centres). There were also the mandatory annual negotiations to be held (on the 2013 salary levels for example) and negotiations imposed by legislative change (France's new *contrat de génération* and changes in retirement conditions, etc.).

In addition the Service assisted in achieving an agreement acceptable to the entire ILL staff on the mutualised obligatory health insurance scheme. This scheme covers not only the staff classed as Active but also those who have retired from the Institute but who wish to continue to be insured under the system and are prepared to pay the monthly subscription.

The Human Resources Service has also been addressing the question of the national balance of staff at the Institute. Following discussions with our Associates we have taken measures to attract more applications from candidates in the Associates' and Scientific Members' countries. It is clearly in the ILL's interest to maintain a healthy diversity of nationalities, not only amongst the scientists but also amongst the technical and administrative staff. These measures should hopefully bear fruit in the years to come.

Finally on staff issues, we attach particular importance to seeking to resolve the difficulties in pension entitlement experienced by staff whose careers have led them to serve in different countries and who are disadvantaged by the lack of harmonisation in pension legislation.

The Finance and Purchasing Service continued, with habitual intensity, to deliver the multifarious services for which it is responsible. It completed a major upgrade of its integrated management software; the new functions now available will further improve the management of the ILL's budget, accounts and purchasing. The Service now needs to focus on improving the tools available to support decision-making at ILL, for the Management Board in particular. Its Purchasing Group was very busy in 2013, following the significant increase in the number of calls for tender to be issued, as a result of additional and complementary safety measures, the work to be performed during the long shutdown, and the impressive building programme under way. I should add that the Purchasing Group had, together with ILL's other services, been tasked with improving our funders' return on investment. This requires improving the national balance of purchasing contracts awarded to the Associate and Scientific Member countries for those goods and services available on markets not subject to inhibitive regulation or monopoly.

The action taken in this direction together with our purchasing advisors in the partner countries has resulted in a reasonable improvement in industrial return for Germany and the UK, as well as for some of our Scientific Members. We will be continuing with these efforts in the future.

In 2013 our Building and Site Maintenance Service brought the main projects to a successful conclusion. Of these it is the Science Building which stands out in particular, funded by local authority investment (Région Rhône-Alpes, Grenoble-Alpes Métropole, and the city of Grenoble). The aim of this building, which we share with the ESRF, is to foster scientific collaboration. Its presence and facilities will open up scientific partnerships between the ILL's Associate or Scientific Member countries, as well as with the ESRF's Members and Scientific Associates. Similarly, the arrival on the EPN Campus of the IBS during the course of the year will further enhance the potential for collaboration. On the technical side, the SAE staff also oversaw the completion of the new ILL 5D building, designed to house our new heavy water facilities and an additional reactor control room. At the same time they were busy with the ILL 22 guide hall: the old instruments were dismantled and the hall made ready to receive the new ones.

All of this activity has its legal underpinnings… the signature of the Fifth Protocol in particular of course, but also the renewal of the contracts with the Scientific Members, an operation requiring frequent exchange and negotiation by our legal staff with the different countries involved. The negotiations advanced well and the contracts should be signed in the first few months of 2014.

The Administration Division staff were as competent and committed as ever in 2013, and more than happy to contribute with skills and professionalism to the ILL's adventure.

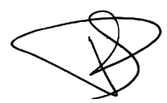

Manuel Rodriguez Castellano
Head of Administration

FACTS AND FIGURES

STAFF ON 31/12/2013

- 497 people, including 62 scientists and 38 thesis students.
- 338.5 French, 44.5 German, 42.5 British, 44 Scientific Member countries and 27.5 others.

Country		%
France	338.5	68.11
Germany	44.5	8.95
United Kingdom	42.5	8.55
Scientific Member countries	44	8.85
Others	27.5	5.53
Total	*497*	*100*

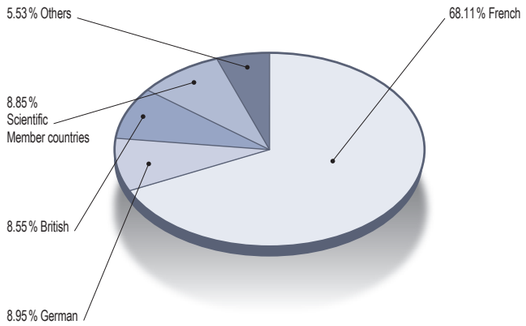

REVISED BUDGET 2013: 100.448 M€ (excluding taxes)

Income	M€	%
Income from Associates*	63.180	62.90%
Income from Scientific Members	20.539	20.45%
Own income	2.322	2.31%
Carry-forward from 2012	6.761	6.73%
Contribution from local autority	6.776	6.75%
HEU reserve	-0.350	-0.35%
Cash flow	1.220	1.21%
Total	*100.448*	*100.00*

** Including Fukushima expenses, Millennium Programme & additional nuclear taxes.*

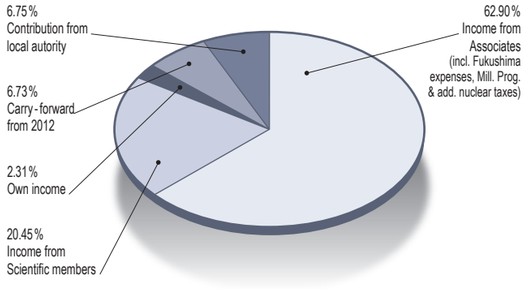

Expenditure	M€	%
Staff costs	44.650	44.45%
Operating costs	15.775	15.70%
Investment costs	28.310	28.18%
Fuel cycle	11.713	11.66%
Total	*100.448*	*100.00*

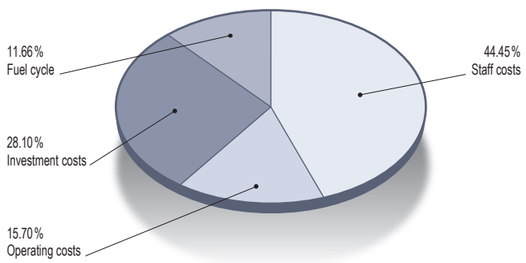

PURCHASING STATISTICS (Figures to end September 2013)

Expenditure	M€	%
France (non-captive market)	14.39	59.34%
Germany	4.08	16.82%
United Kingdom	1.77	7.30%
Scientific Members	1.33	5.48%
Others	2.68	11.05%
Total	*24.25*	*100.00*
France captive/market	12.23	-
Total captive + non-captive	*36.48*	*-*

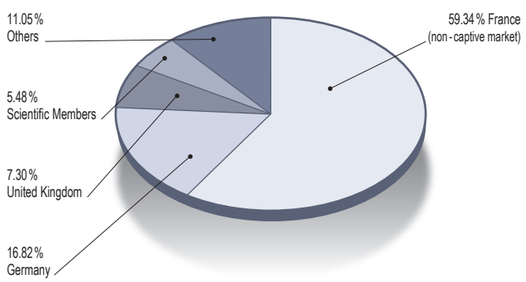

NAME

Institut Max von Laue - Paul Langevin (ILL).

FOUNDED

17 January 1967.
Intergovernmental Convention between France, Germany and UK (19/07/1974).

ASSOCIATES

France
Commissariat à l'Energie Atomique et aux Energies Alternatives (CEA).
Centre National de la Recherche Scientifique (CNRS).

Germany
Forschungszentrum Jülich (FZJ).

United Kingdom
Science & Technology Facilities Council (STFC).

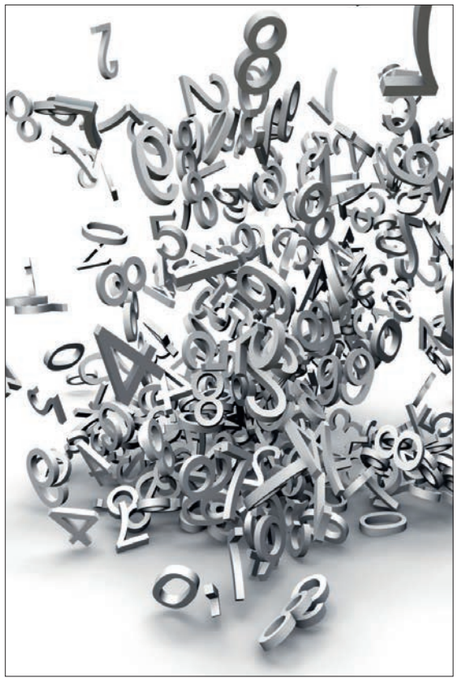

COUNTRIES WITH SCIENTIFIC MEMBERSHIP

Spain
MINECO Ministerio de Economia y Competitividad.

Switzerland
Staatssekretariat für Bildung und Forschung (SBF).

Italy
Consiglio Nazionale delle Ricerche (CNR).

CENI (Central European Neutron Initiative)
Consortium composed of:
- Austria: Österreichische Akademie der Wissenschaften.
- Czech Republic: Charles University of Prague.
- Hungary: Research Institute for Solid State Physics and Optics (RISP) / Budapest on behalf of the Hungarian Academy of Sciences (MTA).
- Slovakia: Comenius University Bratislava.

BELPOLSWENI
(BELgian POLish SWEdish Neutron Initiative)
- Belgium: Belgian Federal Science Policy Office (BELSPO).
- Sweden: Swedish Research Council (SRC).
- Poland: Polish Academy of Sciences.

India
Bhabha Atomic Research Centre (BARC).
Interim scientific membership 01/01/2011 - 31/12/2014.

SUPERVISORY AND ADVISORY BODIES

- Steering Committee, which meets twice a year.
- Subcommittee on Administrative Questions, which meets twice a year.
- Audit Commission, which meets once a year, and statutory Auditor.
- Scientific Council with 9 Subcommittees, which meets twice a year.

REACTOR

58 MW, operating about 3 cycles in 2013 (139 days).
(with cycles of 50 days).

EXPERIMENTAL PROGRAMME

- 603 experiments (allocated by subcommittees) on 28 ILL - funded and 9 CRG instruments.
- 1269 visitors from 46 countries.
- No proposal round in 2013.

ORGANISATION CHART IN 2013

REVIEW PANELS
(Chairs)

APPLIED METALLURGY, INSTRUMENTATION AND TECHNIQUES
D. Hughes (WMG, University of Warwick, UK)

NUCLEAR AND PARTICLE PHYSICS
W. Korten (CEA Saclay, France)

MAGNETIC EXCITATIONS
E. Blackburn (Birmingham University, UK)

CRYSTALLOGRAPHY
R. Walton (Warwick University, UK)

MAGNETISM
R. Kremer (MPI Stuttgart, Germany)

STRUCTURE AND DYNAMICS OF LIQUIDS AND GLASSES
D. Holland-Moritz (Institute of Materials Physics in Space, Cologne, Germany)

SPECTROSCOPY IN SOLID STATE PHYSICS AND CHEMISTRY
D. Djurado (CEA Grenoble, France)

STRUCTURE AND DYNAMICS OF BIOLOGICAL SYSTEMS
C. Cardin (Reading University, UK)

STRUCTURE AND DYNAMICS OF SOFT-CONDENSED MATTER
J. Cabral (London Imperial College, UK)

SCIENTIFIC COUNCIL
Chair: C.C. Wilson

STEERING COMMITTEE
Chair: J. Pinton

SUBCOMMITEE ON ADMINISTRATIVE QUESTIONS (SAQ)
Chair: J. Hahn

DIRECTOR
A. Harrison

DIRECTOR'S SERVICES

- HEAD OF HEALTH PHYSICS — J. Tribolet
- SAFETY ENGINEER — G. Rochex
- MEDICAL SERVICE — M. Falanga
- RISK MANAGEMENT — X. Fargues
- COMMUNICATION — G. Cicognani, F. Vauquois (Press Officer)

SCIENCE DIVISION
H. Schober (Associate Director)

- SENIOR ILL FELLOWS — J. Zaccai, G. Fragneto
- NUCLEAR and PARTICLE PHYSICS GROUP — O. Zimmer
- SCIENTIFIC COMPUTING — M. Johnson
- DIFFRACTION GROUP — L. Chapon
- SCIENTIFIC COORDINATION and USER SUPPORT — G. Cicognani
- LARGE-SCALE STRUCTURE GROUP — R. Cubitt
- JOINT ILL/ESRF LIBRARY — V. Teissier
- THREE-AXIS SPECTROMETER GROUP — J. Kulda
- SOFT MATTER SCIENCE AND SUPPORT — G. Fragneto
- TIME-OF-FLIGHT, HIGH RESOLUTION GROUP — B. Farago
- LIFE SCIENCES — T. Forsyth
- THEORY GROUP — T. Ziman

PROJECTS and TECHNIQUES DIVISION
C. Simon (Associate Director)
R. Gähler (Deputy)

- NEUTRON DISTRIB., MECHANICS — J. Beaucour
- INSTRUMENT CONTROL — P. Mutti
- IT SERVICES — J.F. Perrin
- NEUTRON OPTICS — P. Courtois
- DETECTORS — B. Guérard
- ADVANCED NEUTRON ENVIRONMENT — E. Lelièvre-Berna
- PROJECTS AND CALCULATIONS OFFICE — Y. Calzavara

REACTOR DIVISION
H. Guyon
B. Desbrière (Deputy)

- SHIFT TEAMS, SITE SECURITY — L. Brayer
- ELECTRICITY and ELECTRONICS — L. Pacallet
- MECHANICAL SERVICES — F. Fréry

ADMINISTRATION DIVISION
M. Rodriguez-Castellano

- FINANCE and PURCHASING — Ph. Guérin
- PERSONNEL and HUMAN RES. — R. Mulot
- BUILDING and MAINTENANCE — P. Cogo

ILL WORKSHOPS AND SCHOOLS IN 2013

21 JANUARY 2013
EXILL collaboration meeting.

23-25 JANUARY
Flipper 2013, International Workshop on Single-Crystal Diffraction with Polarised Neutrons.

18-22 MARCH
ADD 2013, Analysis of Diffraction Data in Real Space.

25-27 MARCH
NPPatLPS 2013: ESS Science Symposium on Neutron Particle Physics at Long Pulse Spallation Sources .

6-10 MAY
EMBO Practical Course 2013
(Small-angle neutron and X-ray scattering from proteins in solution).

29 MAY
"Les carrières des femmes en science vers l'équité"
(sponsored by ILL)

5-6 JULY
Dynamics of Molecules and Materials-II.

9 JULY
NMI3 Industry workshop 2013.

12-13 OCTOBER
ILL Open Days.

18-23 NOVEMBER
FullProf School-2013.

28 NOVEMBER
Bragg symposium: Crystallography for life.

Short reports on the ILL workshops can be found on the ILL News (December 2013 issue)
http://www.ill.eu/top-links/publications/ill-news/

Workshops websites can be found at
http://www.ill.eu/news-events/past-events/

ILL CHRONICLE 2013

25 FEBRUARY-15 MARCH
HERCULES 2013 - Higher Education Research Course for Users of Large Experimental Systems.

28 MARCH
Clip session of the ILL PhD students.

21-22 MARCH
Meetings of the ILL Scientific Council.

26-27 MARCH
Visit of the German committee for research, educational and technology impact assessment.

4 APRIL
Visit of the Swedish Research Council.

14-15 MAY
Meeting of the Subcommittee on Administrative Questions (SAQ).

26-27 JUNE
Meeting of the Steering Committee in Lyon.

1 OCTOBER
Visit of Dr. J. Yeck, Chief executive, Director General ESS AB, Dr. Ch. Quitmann, Director MAX-IV and Prof. P. Ericksson, Vice Chancellor of Lund University.

15-16 OCTOBER
Meeting of the Subcommittee on Administrative Questions (SAQ).

28 OCTOBER
Visit from Luxemburg delegation, Prof. J. Kreisel and Dr. A. Michels.

7-8 NOVEMBER
Meetings of the ILL Scientific Council.

28-29 NOVEMBER
Meeting of the Steering Committee in Grenoble.

A YEAR IN PHOTOS

VISITS AND EVENTS

1

2

3

4

5

6

7

8

9

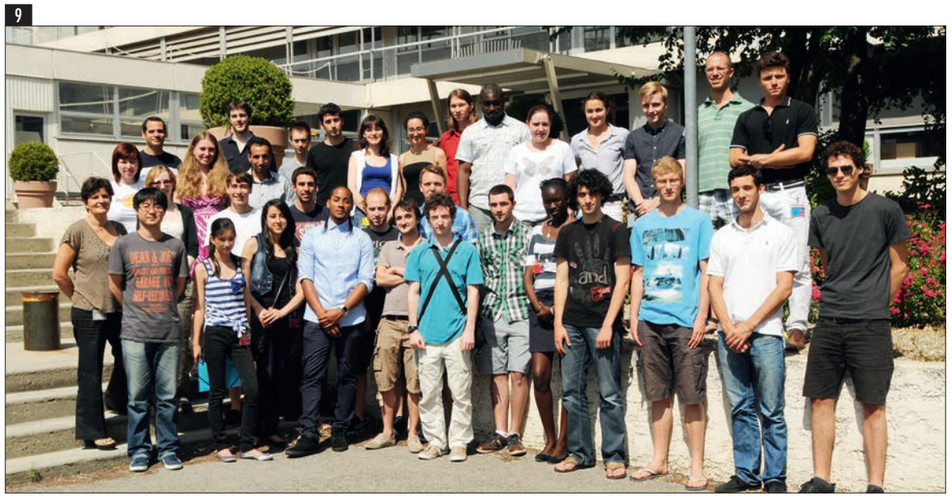

1 - *The ILL has a new British Director General, Bill Stirling (right), who took over his role from Andrew Harrison on 1 January 2014.*

2 - *Participants to the EXILL collaboration meeting on 21 January.*

3 - *Helmut Schober accompanying a delegation of the Swedish Research Council on a visit of the ILL on 4 April.*

4 - *Karin Schmalz (first on the left) and Ralf Schweins (second from the left) accompanying members of the German committee for research, educational and technology impact assessment, on a visit of the facility on 27 March.*

5 - *The ILL Scientific Council members at their meeting in November.*

6 - *Giuseppe Zaccai (IBS, center) has won the prestigious Walter Hälg for his consistent and outstanding work in neutron scattering with a long-term impact on scientific and/or technical neutron scattering.*

7 - *The three ILL directors welcome the visit from Luxemburg delegation on 28 March: Prof. J. Kreisel (center) and Dr. A. Michels (first from the right).*

8 - *Clip session of the ILL PhD students on 28 March.*

9 - *The ILL summer trainees with Anita Schober (first on the left, Human Resource service).*

LONG SHUTDOWN

From 9 August 2013 to June 2014, the ILL reactor is shut down. During this period, a number of major projects have been scheduled. Some are part of the modernisation programme; others are the result of the complementary safety assessment performed by the ILL following the accident at Fukushima.

The main operations planned during the shutdown are: the installation of the new instrument ThALES and the major upgrade of another four (SuperADAM, D16, D22, IN15); the replacement of two beam tubes - H13 and IH3 - and the replacement of almost all the H5 guides (see *p. 98 - 99*).

1

2

3

4

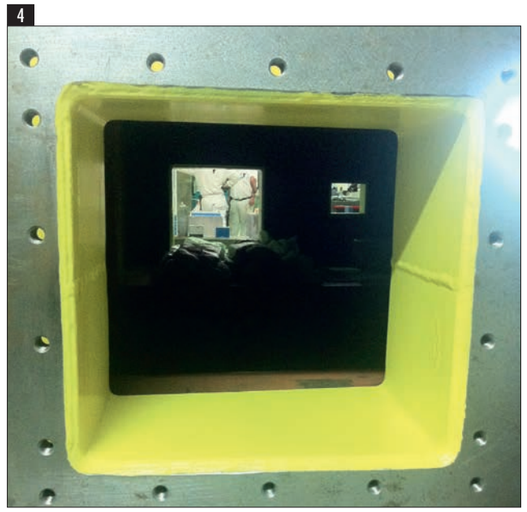

5

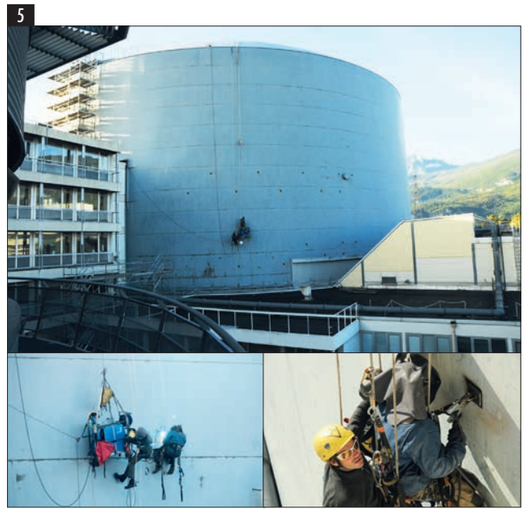

1 - *The emptied ILL7 guide hall, a few weeks after the reactor shutdown.*

2 - *The newly finished extension of the ILL22 guide hall.*

3 - *The new "Poste de commandement secondaire" (emergency/secondary reactor control room), built following the post-Fukushima new safety regulations.*

4 - *View into the reactor, from the ILL22 guide-hall, after removal of the H512 guide.*

5 - *Installation of the scaffolding needed for the connection of the PCS to the new seismic control room.*

OPEN DAYS

The ILL staff welcomed the Grenoble public to the site during the Open Days on 12 and 13 October.

1

2

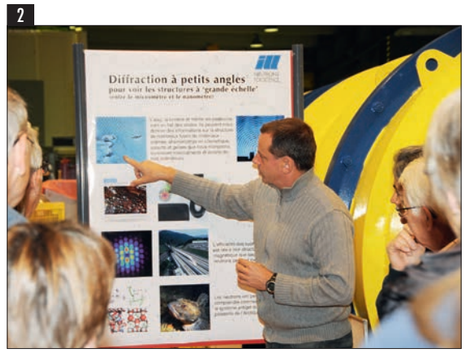

3

4

5

1 - *Philip Gutfreund explaining the principle of diffraction.*

2 - *Bob Cubitt describing the science done on the small-angle scattering machines.*

3 - *Bernard Frick on IN16B.*

4 - *Simon Baudoin during a cryo-demo.*

5 - *Virginie Guérard, Alain Filhol and Françoise Vauquois enjoying their lunch-break.*

A YEAR IN PHOTOS

HAPPY USERS

1
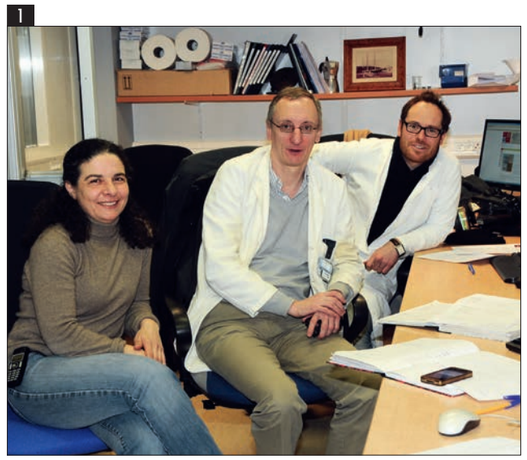

2
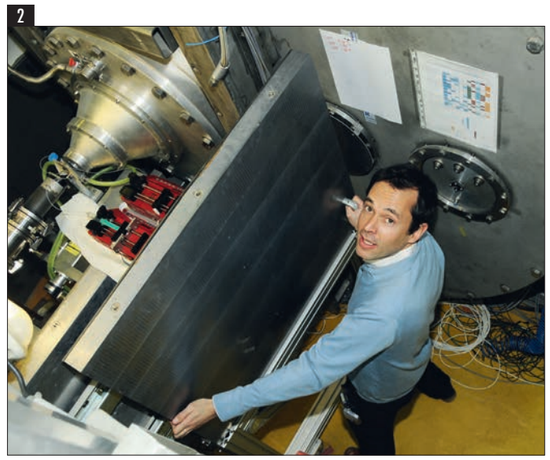

3


4
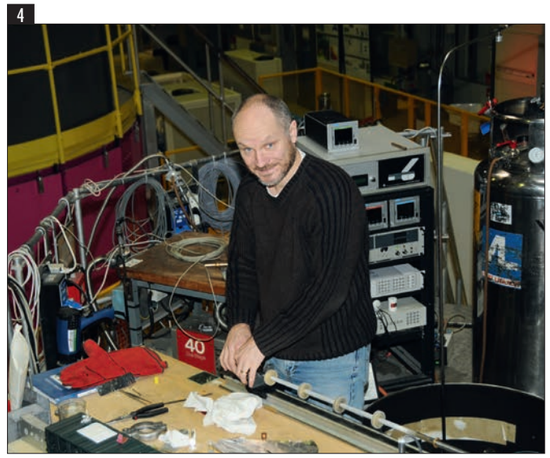

5


6


7
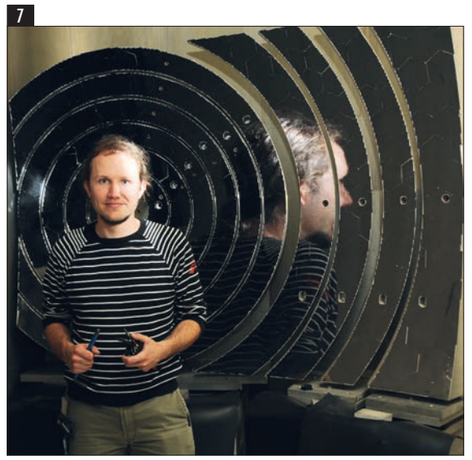

8
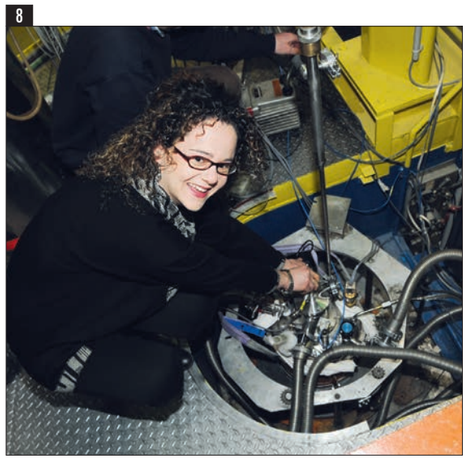

9


10
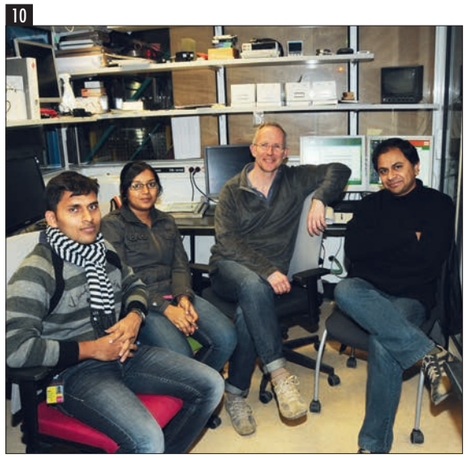

1 - *Giovanna Fragneto (left, ILL senior fellow and head of Soft Matter Science and Support group), Jean Daillant (centre, director of Soleil) and Florent Malloggi (right, CEA) performing a pioneering neutron reflectometry experiment to probe co-polymer layers at flat oil/water interfaces with a new concept for a liquid/liquid sample cell benefitting from a microfluidic set-up.*

2 - *Joao Cabral (Imperial College, London), regular ILL user and new member of the ILL Scientific Council, setting up his experiment.*

3 - *Jacques Ollivier (ILL scientist, left) with Bertrand Toudic (University of Rennes and new member of the ILL scientific council) and Mariana Verezhak (master student at the University of Rennes), searching for the signature of some specific transition in an incommensurate intercalation compound on D10.*

4 - *Andrew Wildes, D7 instrument scientist, mounting a sample on the cryostat stick.*

5 - *Patrick Guenoun (left, Head of the Lions group, CEA, Saclay) and Lucie Besnard (right, PhD student in the same group) during their experiment on FIGARO.*

6 - *Thomas Sottmann (in the back, Koeln university) and three of his students on D22.*

7 - *Marcus Appel, ILL PhD student, on IN16.*

8 - *Maria Tsoutsouva (ESRF) mounting an ammonium perchlorate sample on IN10, during this year's HERCULES practical on "Neutron backscattering".*

9 - *Patrick Judeinstein (LLB), Gerard Gebel (CEA Grenoble) and Govind Prajapati (CEA/INAC/SPRAM/PCI Grenoble) on IN16B.*

10 - *Mark Johnson (second from the right) talking with Soumit S. Mandal, Rikhia Ghosh and Aninda Jiban Bhattacharyya (Indian Institute of Science, Bangalore) about simulations of proteins in nanotubes.*

PUBLICATION IN 2013

In 2013, the ILL received notice of 587 publications by ILL staff and users.
They are listed in the CD-ROM of this year's Annual Report.

THE DISTRIBUTION BY SUBJECT IS AS FOLLOWS

Applied Physics, Instrumentation and Techniques	45
Biology	59
Crystallography	99
Liquids and Glasses	30
Magnetic Excitations	54
Magnetic Structures	88
Materials Science and Engineering	40
Nuclear and Particle Physics	47
Theory	6
Soft Matter	78
Spectroscopy in Solid State Physics and Chemistry	41

ILL PHD STUDENTSHIPS

PhD students at ILL in 2013*	45
PhD theses completed in 2013	7

** Receiving a grant from ILL.*